Technische Universität München

On phase-space representations of spin systems and their relations to infinite-dimensional quantum states

---

Bálint Koczor

Vollständiger Abdruck der von der Fakultät für Chemie der Technischen Universität München zur Erlangung des akademischen Grades eines

Doktors der Naturwissenschaften

genehmigten Dissertation.

Vorsitzender:

Prof. Dr. Klaus Köhler

Prüfer der Dissertation:

1. Prof. Dr. Steffen J. Glaser
2. Prof. Dr. Bernd Reif
3. Prof. Dr. Maurice A. de Gosson (Universität Wien)

Die Dissertation wurde am 27.11.2018 bei der Technischen Universität München eingereicht und durch die Fakultät für Chemie am 07.01.2019 angenommen.

Declaration

I hereby declare that the content of my thesis is original work and is based on the following publications, which have already been submitted to or planned to be submitted to scientific journals:

- B. Koczor, F. vom Ende, M. A. de Gosson, S. J. Glaser, R. Zeier: *Phase Spaces, Parity Operators, and the Born-Jordan Distribution.* arXiv preprint 1811.05872

- B. Koczor, R. Zeier, S. J. Glaser: *Continuous phase spaces and the time evolution of spins: star products and spin-weighted spherical harmonics.*
  J. Phys. A (2019) **52**, 055302. DOI: 10.1088/1751-8121/aaf302
  arXiv preprint 1808.02697

- B. Koczor, R. Zeier, S. J. Glaser: *Continuous phase-space representations for finite-dimensional quantum states and their tomography.* arXiv preprint 1711.07994

- B. Koczor, R. Zeier, S. J. Glaser: *Time evolution of coupled spin systems in a generalized Wigner representation.*
  Ann. Phys. (to be published) DOI: 10.1016/j.aop.2018.11.020
  arXiv preprint 1612.06777

Date:

_____

_____

List of publications

- B. Koczor, F. vom Ende, M. A. de Gosson, S. J. Glaser, R. Zeier: *Phase Spaces, Parity Operators, and the Born-Jordan Distribution.*
  to be submitted to Comm. Math. Phys. (2018) arXiv preprint 1811.05872

- B. Koczor, R. Zeier, S. J. Glaser: *Continuous phase spaces and the time evolution of spins: star products and spin-weighted spherical harmonics.*
  J. Phys. A (2019) **52**, 055302. DOI: 10.1088/1751-8121/aaf302
  arXiv preprint 1808.02697

- B. Koczor, R. Zeier, S. J. Glaser: *Continuous phase-space representations for finite-dimensional quantum states and their tomography.*
  submitted to Phys. Rev. A (2018) arXiv preprint 1711.07994

- B. Koczor, R. Zeier, S. J. Glaser: *Time evolution of coupled spin systems in a generalized Wigner representation.*
  Ann. Phys. (to be published) DOI: 10.1016/j.aop.2018.11.020
  arXiv preprint 1612.06777

- B. Koczor, J. Rohonczy: *A novel pulse scheme for multiple quantum excitation, SFAM to enhance the sensitivity of MQMAS experiments.* Solid State Nucl. Magn. Reson. (2016) 74-75, 1-9. DOI: 10.1016/j.ssnmr.2016.02.001

- B. Koczor, I. Sedyó, J. Rohonczy: *An alternative solution for computer controlled tuning and matching of existing NMR probes.* J. Magn. Reson. (2015) 259, 179-185. DOI: 10.1016/j.jmr.2015.08.017

- B. Koczor, J. Rohonczy: *PIC microcontroller based external fast analog to digital converter to acquire wide-lined solid NMR spectra by BRUKER DRX and Avance-I spectrometers.* Solid State Nucl. Magn. Reson. (2015) 66, 21-28.
  DOI: 10.1016/j.ssnmr.2015.02.002

Abstract

Classical phase spaces have been widely applied in physics, engineering, economics or biology. In this thesis, phase spaces of quantum systems are considered, which have become a powerful tool for describing, analyzing, and tomographically reconstructing quantum states. We provide a complete phase-space description of (coupled) spin systems including their time evolution, tomography, large-spin approximations and their infinite-dimensional limit, which recovers the well-known case of quantum optics. Finally, Born-Jordan distributions of infinite-dimensional quantum systems are described.

Zusammenfassung

Titel: Zu Phasenraumdarstellungen von Spinsystemen und ihren Beziehungen zu unendlichdimensionalen Quantenzuständen

Klassische Phasenräume finden in Physik, Ingenieurwesen, Wirtschaft und Biologie vielfältige Anwendungen. In dieser Arbeit werden Phasenräume von Quantensystemen betrachtet, die ein leistungsstarkes Werkzeug für die Beschreibung, Analyse und tomographische Rekonstruktion von Quantenzuständen bilden. Wir geben eine vollständige Phasenraum-Beschreibung von (gekoppelten) Spinsystemen, einschließlich ihrer Zeitentwicklung, Tomographie, Näherungsformeln für große Spins und ihren unedlich-dimesionalen Grenzfall, der dem wohlbekannten Fall der Quantenoptik entspricht. Schließlich werden Born-Jordan-Verteilungen von unendlich-dimensionalen Quantensystemen beschrieben.

Acknowledgments

First of all, I would like to thank Professor Steffen Glaser for being an extremely supportive supervisor. Meeting him in Zürich and having an inspiring discussion with him encouraged me to join his group and to explore the new, open questions that later constituted my PhD topic. His excitement for finding new challenges and devotion to solving them have been particularly motivating.

I would also like to thank Dr. Robert Zeier for co-supervising my projects. His questions, remarks and endless support in improving manuscripts contributed greatly to reaching the final form of our publications.

I would like to use this as an opportunity to thank Professor Maurice de Gosson for motivating me to seek out new connections between different fields. His books have greatly inspired me.

I highly appreciated the help of Frederik vom Ende whose remarks and challenging questions contributed to the mathematical precision of our work.

I would like to thank Dr. Thomas Schulte-Herbrüggen for the sparkling conversations and for his useful pieces of advice.

I would also like to thank the Glaser group for their hospitality and for creating a good working environment. In particular, thanks to: Frau Martina Heinemann and Dr. Raimund Marx for their aid in official and administrative matters; to David Leiner and to Amit Devra for the friendly conversations that we usually shared with Michael Tesch, Quentin Ansel and Thomas Heydenreich.

Finally, I wish to thank my fiancée, Zsuzsanna Benda, for her loving support and her unlimited encouragement.

Szüleimnek és Nagyszüleimnek

Contents

CHAPTER 1

Introduction

The phase-space formulation of quantum mechanics has a long history. This unquestionably started with the ground-breaking idea of Eugene Wigner from 1932 [262]. In his work, Wigner proposed a quasi-probability distribution for a spinless quantum particle over a classical phase space, which established a direct bridge from the well-known classical world to the shortly before discovered quantum world.

In this regard, classical phase spaces have a much longer and tangled history [198] and date back to the early 1800's. The concept of a classical phase space evolved from the 1838 mathematical work of Liouville [177]. Jacobi recognized this work and used it in the context of classical mechanics [137] in 1842. In particular, he established the connection between Liouville's theorem of conservation in a phase space and Hamilton's formulation of mechanics from 1834 [125]. Liouville's conservation law was then adapted by Boltzmann in his 1871 paper on the kinetic theory of gases. However, the modern concept of a phase space became widespread only later, along the works of Ehrenfest [81], Rosenthal [216] and Plancherel [208]. Since then, phase spaces have been applied in various fields of physics, engineering, economics or biology. In fact, James Gleick calls phase space "one of the most powerful inventions of modern science" in his popular book on chaos theory [109].

Using modern notation, the state of a classical-mechanical system is uniquely characterized by its coordinate x and momentum p variables [163, 20]. The set of all possible values (x, p) is called a phase space, and every point (x, p) in a phase space therefore uniquely characterizes a particular state of the system. The time evolution is then determined by a

Hamiltonian $H(x,p,t)$, which is a function of phase-space coordinates and can also depend on time. In particular, an arbitrary phase-space function $f(x,p,t)$ evolves according to

$$\frac{\mathrm{d}f}{\mathrm{d}t} = \frac{\partial f}{\partial t} + \{H,f\} \qquad \text{with} \quad \{H,f\} \coloneqq \frac{\partial H}{\partial p}\frac{\partial f}{\partial x} - \frac{\partial H}{\partial x}\frac{\partial f}{\partial p}, \tag{1.1}$$

where $\{\cdot,\cdot\}$ denotes the Poisson bracket [163, 20]. For example, substituting the arbitrary phase-space function with coordinate $f = x$ or momentum $f = p$ variables recovers Hamilton's equations of motion [163, 20]. However, f can represent more general functions, such as the probability density $\rho_c(x,p)$. This function assigns a probability $\rho_c \geq 0$ to the neighborhood of each point (x,p) in a phase space, i.e., to possible states of the system. This probability density is central in statistical mechanics and its well-known equation of motion $\frac{\partial \rho_c}{\partial t} = -\{H,\rho_c\}$ essentially describes the flow of a phase-space fluid due to Liouville's theorem [163, 20]. A quantum mechanical analogue, the so-called density operator was introduced by von Neumann in 1927 [255], at the time when quantum mechanics was still under development. Dirac adapted this concept in his 1930 book, *The principles of quantum mechanics* with the following introduction [76]

> *"... There exists a corresponding density ρ in quantum mechanics, having properties analogous to the above. It was introduced by von Neumann. Its existence is rather surprising in view of the fact that phase space has no meaning in quantum mechanics, there being no possibility of assigning numerical values simultaneously to the q's and p's."* (P. A. M. Dirac, 1930)

The strong analogy between the classical probability density $\rho_c(x,p)$ in phase space and the density operator ρ is reflected by their formally identical equations of motion. In particular, the density operator evolves according to the von Neumann equation $i\frac{\partial \rho}{\partial t} = [\mathcal{H},\rho]$, but note that both ρ and $\mathcal{H}$ are Hilbert-space operators and $[.,.]$ is their commutator.

Quantum mechanics, during its initial mathematical formulation between 1925-26, was first described in terms of infinite-dimensional matrices by Heisenberg [129] and in terms of differential equations by Schrödinger [231]. Dirac later showed [76] that these two descriptions are equivalent and are two particular choices of a more general mathematical framework, called a Hilbert space. In modern notation, Hilbert-space formulation of quantum mechanics represents physical observables of coordinate x and momentum p as operators $\hat{x}$ and $\hat{p}$. These operators in fact define mappings between elements of a Hilbert space. The state of a quantum mechanical system is expressed as a density operator ρ and the Hamiltonian as well corresponds to an operator $\mathcal{H}$, which describes time evolution. In general, any physical observable f is represented as an operator $\hat{f}$ which defines a particular mapping between Hilbert-space elements and this construction does not resemble the classical description in spirit at all. Moreover, determining phase-space coordinates (x,p) of a quantum state is not possible due to the uncertainty principle, i.e., the commutator of operators $[\hat{x},\hat{p}] = i\hbar$ is non-zero. However, Wigner showed that one must not conclude that *"phase space has no meaning in quantum mechanics"* [76].

In his 1932 paper [262], Eugene Wigner proposed a revolutionary approach to describe quantum mechanics consistently with the classical phase-space picture. This approach is logically autonomous and independent from the Hilbert-space formulation, however, it is equivalent to that. The state of a quantum system is described by its Wigner function $W_\rho(x,p)$, which uniquely corresponds to a density operator ρ, i.e., there is a one-to-one mapping between the two. This Wigner function $W_\rho(x,p)$ is an analog of the classical $\rho_c(x,p)$, however, it can have negative values and it is therefore a quantum mechanical generalization of the non-negative phase-space probability density $\rho_c(x,p)$.

More than a decade later Gronewold [118] and Moyal [195] showed that the Wigner function indeed provides a complete description of quantum mechanics and its equation of motion corresponds to a generalization of the Poission bracket, called the Moyal bracket. This Moyal bracket is the phase-space equivalent of commutators and is based on the so-called star product, refer to Section 3.3.1. Moreover, mapping a density operator to its Wigner function is just the inverse procedure of the so-called Weyl quantization [259, 260, 261] which assigns a Hilbert space operator to a classical phase-space function.

There are, however, infinitely many ways to describe quantum mechanics in phase-space using generalizations of the Wigner function. These were introduced by Cohen in the 1960's as convolved derivatives of the Wigner function and led to a development of so-called coherent-state representations [51, 50, 11, 10] and associated quantization schemes. Most importantly, the s-parametrized distributions are Gaussian convolved variants of the Wigner function which reproduce the well-known special cases of the Husimi Q ($s = -1$), Wigner ($s = 0$) and Glauber P ($s = 1$) functions. Wigner's original approach and its variants describe a non-relativistic, spinless quantum particle in phase space which can, however, be applied to various other scenarios that correspond to the same underlying Heisenberg-Weyl symmetry group. In particular, phase-space approaches have been widely adapted in the context of pseudo-differential operators and time-frequency analysis [113, 111, 116, 60], and the s-parametrized family of distribution functions have played a central role in developing a quantum theory of light [107]. In both cases phase space is a 2-dimensional plane and underlying symmetries correspond to the Heisenberg-Weyl group.

A general framework was introduced by Berezin [28, 29] and Bayen [25, 26] for extending Wigner's original approach and their analogs to quantum systems with more general symmetry groups, i.e., with phase spaces beyond a Euclidean plane. Since then, generalized coherent states for various Lie groups have been developed and have been applied in mathematics and physics [205, 99, 13, 30]. Most importantly, coherent states for the spherical phase space of single spins J were introduced by Arecchi [18] and this approach was utilized in [7] to obtain a coherent-state representation, the Q function of spins. This coherent-state representation was later extended to the Wigner function [253] and to the full s-parametrized family of distributions [47] of a single spin J via the axiomatic construction of Stratonovich [242, 243]. These single spin Wigner functions have found many applications since then [150, 152, 156, 248] and are relevant in various experimental scenarios, refer to Chapter 2.

In the current work, spherical phase spaces of spin systems are considered and the full family of s-parametrized distribution functions is constructed using parity operators. These

naturally incorporate the well-known distribution functions of Cahill and Glauber [51, 50] in the large-spin limit. A complete description of their time evolution is provided, including their tomographic reconstructions and relations amongst them. For a detailed introduction to single spins refer to Section 2.1.1. This phase-space description is extended to the overarching scenario of distinguishable, coupled spin systems, their time evolutions and visualizations in Chapter 3. Note that there exist a plethora of phase-space descriptions for coupled spin systems, refer to Sections 3.3.3, 3.3.4 and 3.3.6, however, the current construction has several advantages: it reflects underlying symmetries of the spin system, incorporates infinite-dimensional phase spaces in the large-spin limit and allows for natural visualizations. Moreover, methods for calculating approximate phases-space distribution functions and their time evolutions efficiently are developed in Chapter 4. These results are useful for spin systems with large J and the approximations become exact in the limit $J \to \infty$ and reproduce the well-known case of Wigner's original approach and its corresponding variants. These star-product methods rely on so-called spin-weighted spherical harmonics which were introduced by Newman and Penrose in the context of general relativity. Their formalism is adapted in Chapter 4 for describing exact and approximate time evolutions of spin systems.

Finally, infinite-dimensional quantum systems and their generalized phase-space distributions are considered in Chapter 5. In particular, parity operators are introduced, quantum-mechanical expectation values of which give rise to a general class of phase spaces. New results are obtained for the case of Born-Jordan distributions and a matrix representation of its parity operator is derived that can be calculated efficiently. These results can directly be applied to bosonic quantum systems, such as in quantum optics.

This thesis is based on the manuscripts [159, 160, 161, 158] and main results are summarized in the following.

Main results contained in Chapter 2

Result 2.1: The full class of s-parametrized phases-spaces are defined for a qudit with $d = 2J+1$ or equivalently for a single spin J in terms of rotated parity operators. This construction naturally incorporates the well-known s-parametrized distribution functions of quantum optics in the large-spin limit.

Theorem 2.1: The large-spin limit formula of the parity operators from Result 2.1 recovers the parity operators from quantum optics.

Result 2.2: Transformations between particular s-parametrized phase spaces are described. These transformations are Gaussian-like spherical convolutions with the spin-up state. This is the finite-dimensional equivalent of the Gaussian convolution from quantum optics which is recovered in the large-spin limit

Theorem 2.2: Spin-up state distribution functions of a qudit or single spin J, used for the convolution in Result 2.2, recover their infinite-dimensional counterparts as Gaussian functions in the large-spin limit.

Result 2.3: A general tomography formula is obtained for the s-parametrized distribution functions. This tomography scheme is the finite-dimensional equivalent of the 'direct measurement' technique in quantum optics and recovers that in the large-spin limit.

Section 2.5.5: A tomography formula is proposed that relies on spherical Radon transforms. This is a finite-dimensional equivalent of the optical homodyne tomography and recovers that in the large-spin limit

Main results contained in Chapter 3

Result 3.1: Results from Chapter 2 are extended to coupled spins. In particular, the Wigner function of N coupled, distinguishable qudits or spins J is defined.

Theorem 3.1: The Wigner function from Result 3.1 is generalized to the s-parametrized phase spaces of N coupled spins J. This construction is based on rotated parity operators from Result 2.1. These general phase spaces satisfy the Stratonovich postulates from Appendix B.3.2, transform naturally under arbitrary local rotations and recover quantum optics in the large-spin limit (as N coupled modes of the electromagnetic field).

Result 3.2: An exact, differential star product is developed for the Wigner function of a single qubit or spin $1/2$ (the general case of a single qudit or single spin J is treated in Chapter 4).

Result 3.3: The exact, differential star product is obtained for the Wigner function of N coupled, distinguishable qubits or spins $1/2$. Its properties are then discussed in detail (the general case of qudits or spins J is obtained in Chapter 4).

Corollary 3.1: The explicit form of Result 3.3 is detailed for $N = 2$ qubits or spins $1/2$.

Corollary 3.3: The explicit form of Result 3.3 is detailed for $N = 3$ qubits or spins $1/2$.

Result 3.4: The explicit and exact differential equation of motion is obtained for the Wigner function of N coupled, distinguishable qubits or spins $1/2$ (the general case of qudits or spins J is discussed in Chapter 4).

Corollary 3.2: The simplified form of Result 3.4 is discussed for $N = 2$ qubits or spins $1/2$

Corollary 3.4: The simplified form of Result 3.4 is discussed for $N = 3$ qubits or spins $1/2$

Corollary 3.5: The equation of motion for N coupled, distinguishable qubits or spins $1/2$ from Result 3.4 reduces to the classical Poisson bracket if the system Hamiltonian contains at most pairwise interactions.

Additional material contained in Chapter 3

Section 3.4: Example time evolutions are calculated for simple spin systems. The resulting high-dimensional Wigner functions are visualized using the PROPS representation and their three-dimensional plots.

Section 3.6: Further examples are calculated for spin systems up to $N = 3$ including entanglement generation in phase space.

Section 3.7: Connections to alternative or related characterizations are discussed. These include, e.g., the angular momentum differential operator or quaternions and their quaternionic products.

Main results contained in Chapter 4

Proposition 4.1: Spin-weighted spherical harmonics were introduced by Newman and Penrose in the context of general relativity. An approximation formula is proposed for the corresponding spin weight raising and lowering operators.

Proposition 4.2: Spin-weighted spherical harmonics are relevant in the context of spin phase-space representations. An approximation formula is proposed using spin weight raising and lowering operators. This approximation naturally recovers the case of quantum optics in the large spin limit.

Result 4.1: Exact star products for Glauber P and Husimi Q functions of a qudit or single spin J are obtained based on spin weight raising and lowering operators.

Result 4.2: Approximate star products for P and Q functions are derived using Proposition 4.2. These approximations become exact and recover their infinite dimensional counterparts as quantum optics in the large-spin limit.

Result 4.3: Differential operators are obtained in terms of spin weight raising and lowering operators. These differential operators are useful for transforming between different s-parametrized phase-space distributions of a qudit or single spin J.

Result 4.4: Approximations of the differential operators from Result 4.3 are obtained using Proposition 4.2. These approximations become exact and reproduce the infinite-dimensional formalism in the large spin limit.

Result 4.5: Star products for arbitrary s-parametrized phase-space distribution functions of a qudit or single spin J are derived.

Result 4.6: Approximations of the star product from Result 4.5 are derived using Proposition 4.2. These approximations become exact and reproduce their infinite-dimensional counterparts in the large spin limit.

Section 4.11: Exact and approximate time evolutions of qudits or single spins J are discussed. Their equation of motion is obtained using star products.

Section 4.12: A method based on star products and their approximations is proposed for efficiently calculating s-parametrized phase-space distribution functions of qudits or spins J.

Section 4.13: Star products and time evolutions of the s-parametrized phase spaces of N coupled qudits or spins J are established. In particular, the coupled qubit or spin-$1/2$ star product from Result 3.3 is generalized to arbitrary J while extending the star product formalism from Result 4.5 to N coupled qudits or spins J.

Main results contained in Chapter 5

Definition 5.3: Generalized distribution functions are defined for planar phase spaces in the form of quantum-mechanical expectation values of displaced parity operators, such as in quantum optics.

Theorem 5.1: Quantum-mechanical expectation values of the parity operators in Definition 5.3 define distribution functions as the Cohen class. These phase-space representations are therefore related to the Wigner function via a convolution with the so-called Cohen kernel θ.

Section 5.6.2: Parity operators are Weyl quantizations of their corresponding Cohen convolution kernels θ.

Section 5.6.3: Parity operators for important, well-known distribution functions are summarized along with their operator norms and spectral decompositions in Sec 5.7.2.

Theorem 5.2: The explicit action and the operator norm of the parity operator is derived which defines Shubin's τ-parametrized distributions.

Theorem 5.3: The parity operator for Born-Jordan distributions is derived in the form of a weighted average of displacement operators.

Theorem 5.4: The Born-Jordan parity operator is equivalently a weighted average of squeezing operators. These squeezing operators are widely used in quantum optics and describe a non-linear optical transformation.

Proposition 5.2: The Born-Jordan parity operator is a bounded operator on the Hilbert space of square-integrable functions.

Theorem 5.5: The Born-Jordan parity operator admits a generalized spectral decomposition.

Theorem 5.6: The matrix representation of the Born-Jordan parity operator is calculated in the number-state basis.

Conjecture 5.1: An efficient, recursion-based computation scheme is proposed for calculating the matrix representation of the Born-Jordan parity operator.

Section 5.9: Born-Jordan distributions are calculated for simple, bosonic quantum systems and are juxtaposed with corresponding Wigner and Husimi Q functions.

CHAPTER 2

Continuous phase-space representations for finite-dimensional quantum states and their tomography

2.1 Foreword to Chapter 2

This chapter is based on the manuscript [160] and discusses continuous phase-space representations for single spins with new results on their relations, large spin limits and tomographic reconstructions. Building on previous works on Wigner functions [253, 47, 78] and on s-parametrized phase-space representations [7, 47] for a single spin J, we obtain significant, new results for the overarching theme of spin phase-space representations. In particular, we define these distribution functions as expectation values of rotated parity operators in analogy to the infinite-dimensional case (see Chapter 5), which is then naturally recovered in the large-spin limit. We show that all members of the s-parametrized family of phase-space representations are related to each other via a Gaussian-like convolution. Multiple examples are provided to illustrate and visualize the resulting phase-space functions and underlying concepts. We finally describe the experimental tomographic reconstruction of the full class of s-parametrized distribution functions which is practically relevant for current experimental methods. The basic concept of a single spin J and its applications are first introduced in a preliminary section (Section 2.1.1).

2.1.1 Preliminary: single spin J

A single spin, which is often called a qudit, has been widely used in various fields of physics in different contexts. Here, we give a short summary of its mathematical properties and its relation to other physical systems.

Spin operators $\mathcal{J}_x$, $\mathcal{J}_y$ and $\mathcal{J}_z$ in general are generators of the group $\mathrm{SU}(2)$ via the commutation relations $[\mathcal{J}_j, \mathcal{J}_k] = i \sum_l \epsilon_{jkl} \mathcal{J}_l$ for $j, k, l = x, y, z$ and ϵ_{jkl} is the Levi-Civita symbol, refer to, e.g., [192, 223]. A qudit, or equivalently a single spin J is a quantum mechanical system, the state space of which is identified with a $d = 2J+1$-dimensional Hilbert space. The eigenvalue equation in this d-dimensional Hilbert space

$$\mathcal{J}_z|Jm\rangle := m|Jm\rangle \qquad \text{with} \quad m \in \{-J, -J+1, \ldots, J\} \tag{2.1}$$

follows from the basic commutation relations, which also allow to derive matrix representations of spin operators[1], refer to Chapter 3.5 in [223]. Rotation operators in the form $e^{-i\phi\mathcal{J}_z} e^{-i\theta\mathcal{J}_y} e^{-i\psi\mathcal{J}_z}$ are irreducible representations of the group $\mathrm{SU}(2)$ in this d-dimensional Hilbert space, and define the Wigner-D matrix elements via [192, 223]

$$\langle Jm_1|e^{-i\phi\mathcal{J}_z} e^{-i\theta\mathcal{J}_y} e^{-i\psi\mathcal{J}_z}|Jm_2\rangle := D^j_{m_1 m_2}(\phi, \theta, \psi). \tag{2.2}$$

Numerous physical systems can be modeled by a qudit or spin. Atomic nuclei studied in magnetic resonance spectroscopy, especially in the solid state [96], often include spins with J larger than $1/2$. In particular, certain atomic nuclei, such as $^7\mathrm{Li}$ or $^{23}\mathrm{Na}$, couple with external electric field due to their spins larger than $1/2$ and therefore allow for experimentally determining the electric field quadrupole tensor. There are various other applications of single spins. These are mostly based on mapping a subset of all available states of a quantum system to states of a qudit or spin. We recollect two of the most important applications in the following.

2.1.1.1 Qubits in symmetric states

We will now introduce a mapping between symmetric states of a system of N coupled qubits or spins-$1/2$ and states of a single spin J, refer to [241]. Recall that a single qubit is a two-level system, its state space corresponds to a two-dimensional Hilbert space $\mathcal{H} := \mathbb{C}^2$ and its spin operators are defined via the matrices

$$I_x := \tfrac{1}{2}\begin{pmatrix} 0 & 1 \\ 1 & 0 \end{pmatrix}, \qquad I_y := \tfrac{1}{2}\begin{pmatrix} 0 & -i \\ i & 0 \end{pmatrix}, \quad \text{and} \quad I_z := \tfrac{1}{2}\begin{pmatrix} 1 & 0 \\ 0 & -1 \end{pmatrix}, \tag{2.3}$$

which are generators of the group $\mathrm{SU}(2)$ via the commutation relation $[I_j, I_k] = i \sum_l \epsilon_{jkl} I_l$ with $j, k, l = x, y, z$ and ϵ_{jkl} is the Levi-Civita symbol [61]. Every state $|\psi\rangle \in \mathcal{H}$ in Hilbert

[1] Deriving matrix representations is via raising and lowering operators $\mathcal{J}_\pm := \mathcal{J}_x \pm i\mathcal{J}_y$ and their consequent commutation relations $[\mathcal{J}_z, \mathcal{J}_\pm] = \pm\mathcal{J}_\pm$. One can calculate the action of raising and lowering operators $\mathcal{J}_z\mathcal{J}_\pm|Jm\rangle = (m \pm 1)\mathcal{J}_\pm|Jm\rangle$ using their commutators, and therefore $\mathcal{J}_\pm|Jm\rangle \propto |Jm \pm 1\rangle$. Proportionality factors similarly follow from commutation relations, refer to Chapter 3.5 in [223] for a detailed derivation.

space can be expressed as a linear combination $|\psi\rangle := c_0|0\rangle + c_1|1\rangle$, where basis states are the column vectors $|0\rangle := (0,1)^T$ and $|1\rangle := (1,0)^T$. State space of N coupled spins is spanned by a direct product of the individual Hilbert spaces, which results in the Hilbert space $\mathbb{C}_{2^N}$ of dimension 2^N. Dimensionality of this space is exponentially large in the number of coupled spins. Orthonormal basis states are usually denoted as $\{|10\dots0\rangle, |01\dots0\rangle, \dots, |00\dots1\rangle\}$, and let us now consider the symmetric subspace of this exponentially large state space.

Let us consider basis states with the first n qubits in state $|1\rangle$ and the last $N-n$ qubits in state $|0\rangle$ as $|1_1, 1_2, \dots, 1_n, 0_{n+1}, \dots, 0_n\rangle$ where $n = 0, \dots, N$. For a fixed value of n, there are $p := \binom{N}{n}$ distinct permutations of qubits which redistribute positions of zeros and ones, but leave the overall number of zeros and ones invariant. We define permutation invariant basis states for N qubits as a normalized superposition of all permutations as

$$|Nn\rangle := \frac{1}{\sqrt{\text{numb. all perm.}}} \sum_{l \in \{\text{all perm.}\}} P_l \, |1_1, 1_2, \dots, 1_n, 0_{n+1}, \dots, 0_N\rangle \tag{2.4}$$

$$= \frac{1}{\sqrt{p}} \sum_{k=1}^{p} P_k \, |1_1, 1_2, \dots, 1_n, 0_{n+1}, \dots, 0_N\rangle, \tag{2.5}$$

where P_l permutes qubit subspaces and $\{P_k\}$ is the set of all $p = \binom{N}{n}$ distinct permutations of the spin subspaces for a fixed n. Collective angular-momentum operators in the following form by definition commute with permutations

$$J_x := \sum_{n=1}^{N} I_{n,x}, \qquad J_y := \sum_{n=1}^{N} I_{n,y}, \qquad J_z := \sum_{n=1}^{N} I_{n,z}, \tag{2.6}$$

where $I_{n,x}, I_{n,y}, I_{n,z}$ are embedded spin-$1/2$ operators and act on the n-th spin. For example, $I_{2,y}$ acts on the 2nd spin as $\mathrm{Id}_2 \otimes I_y \otimes \mathrm{Id}_2 \cdots \otimes \mathrm{Id}_2$ where Id_2 is the 2×2 identity operator. Using that commutators $[I_{n_1,j}, I_{n_2,k}] = 0$ vanish if $n_1 \neq n_2$, one can show that collective spin operators are also generators of the group $\mathrm{SU}(2)$ via the commutation relations

$$[J_j, J_k] = \sum_{n_1,n_2=1}^{N} [I_{n_1,j}, I_{n_2,k}] = \sum_{n=1}^{N} i \sum_{l} \epsilon_{jkl} I_{n,l} = i \sum_{l} \epsilon_{jkl} J_l. \tag{2.7}$$

Permutation invariant basis states from (2.4) span an $N+1$-dimensional subspace of the exponentially large Hilbert space of N qubits, and the eigenvalue equation from (2.1) is satisfied by the collective spin operator J_z

$$J_z|Nn\rangle = (N/2 - n)|Nn\rangle \leftrightarrow \mathcal{J}_z|Jm\rangle = m|Jm\rangle \qquad \text{for } n = J - m \in \{0, 1, \dots, N\}. \tag{2.8}$$

One can therefore uniquely map these states via $|Nn\rangle \leftrightarrow |Jm\rangle$ to basis states of a single qudit of dimension $d = N + 1$, or equivalently, to a single spin J with $J = N/2$. Matrix representations of collective spin operators in this $N + 1$-dimensional subspace are equivalent to matrix representations of spin operators and follow [2] from the commutation relations

[2] The derivation is via raising and lowering operators $J_\pm := J_x \pm J_y$, which satisfy their usual commutation relation and therefore $J_z J_\pm |Nn\rangle = (N/2 - n \pm 1)\mathcal{J}_\pm |Nn\rangle$. This allows for calculating matrix representations of J_x, J_y, J_z, which are indeed identical to matrix representations of $\mathcal{J}_x, \mathcal{J}_y, \mathcal{J}_z$ in their respective bases.

in (2.7). The strict correspondence $J_x, J_y, J_z \leftrightarrow \mathcal{J}_x, \mathcal{J}_y, \mathcal{J}_z$ results in a one-to-one mapping between the two physical systems, for example, Figure 2.1 depicts the (generalized) W state [79] of $N = 2J$ permutationally symmetric qubits, which is represented as a single qudit state. Many important quantum states belong to this family of permutationally symmetric qubit states which include, e.g., a family of maximally entangled states [241, 250, 178]. Moreover, experimental spin-like systems of indistinguishable qubits are commonly represented as qudits, these include, e.g., atomic ensembles [188, 122], Bose-Einstein condensates [17, 132, 199, 240, 176, 214, 228, 126, 244], or trapped ions [166, 40, 193], and the states $|Nn\rangle$ are often referred to as symmetric Dicke states [75].

2.1.1.2 Angular-momentum representation of bosons

We will now introduce the so-called Schwinger model of angular momentum, following [234, 223]. Let us consider a quantum system, which consists of two boson fields. Their joint state space is described by the Hilbert space $\ell^2 \otimes \ell^2$ of infinite-dimensional vectors [234, 223]. Joint number states $|n_a n_b\rangle := |n_a\rangle \otimes |n_b\rangle$ span an orthonormal basis and satisfy the eigenvalue equation

$$a^\dagger a\,|n_a n_b\rangle = n_a |n_a n_b\rangle, \qquad b^\dagger b\,|n_a n_b\rangle = n_b |n_a n_b\rangle \tag{2.9}$$

of the usual annihilation and creation operators, which are defined to satisfy the commutation relations $[a, a^\dagger] = 1$, $[b, b^\dagger] = 1$ and other commutators, such as $[a, b^\dagger] = [b, a^\dagger] = 0$, vanish.

Let us now introduce angular momentum operators, which are composed of annihilation and creation operators and therefore act on the state space of the two-mode oscillator

$$L_z := a^\dagger a - b^\dagger b, \qquad L_+ := a^\dagger b \quad \text{and} \quad L_- := b^\dagger a. \tag{2.10}$$

The usual Cartesian form is obtained via the linear combinations $L_x = (L_+ + L_y)/\sqrt{2}$ and $L_y = -i(L_+ - L_y)/\sqrt{2}$. One can show that these operators satisfy the angular momentum commutation relations as $[L_j, L_k] = i \sum_l \epsilon_{jkl} L_l$ with $j, k, l = x, y, z$ and the eigenvalue equation yields

$$L_z |n_a n_b\rangle = (a^\dagger a - b^\dagger b)|n_a n_b\rangle = (n_a - n_b)|n_a n_b\rangle. \tag{2.11}$$

Most importantly, the subspace spanned by the orthonormal states $\{|n_a n_b\rangle, n_a + n_b \text{ is fixed}\}$ forms a Hilbert space of dimension $n_a + n_b + 1$ and one has a strict correspondence between the states $|n_a n_b\rangle \leftrightarrow |Jm\rangle$ with the $J \leftrightarrow (n_a + n_b)/2$ and $m \leftrightarrow (n_a - n_b)/2$ and between the operators $L_x, L_y, L_z \leftrightarrow \mathcal{J}_x, \mathcal{J}_y, \mathcal{J}_z$.

This mapping has been commonly used to represent a two-mode optical system that contains a fixed number $n_a + n_b$ of photons in the two modes. These systems include polarization states of the electromagnetic field or optical interferometry [44, 156, 55].

2.1.2 Additional results

This subsection details proofs of results from the manuscript [160]. In particular, Theorem 2.1 considers the s-parametrized spin parity operator M_s from Result 2.1 and establishes the large spin limit of its matrix representation. This theorem ensures that phase-space representations from Result 2.1, as expectation values of this parity operator, recover their infinite-dimensional counterparts from quantum optics in the large spin limit. Theorem 2.1 is a generalization of, and uses techniques from the proof in [16], which considered the special case of Wigner functions, i.e., $s = 0$.

Theorem 2.1. *Let us denote diagonal matrix elements of the parity operator from* (2.1) *as* $[M_s]_{nn} := \langle J, J-n|M_s|J, J-n\rangle$*, using the index* $n = 0, 1, \dots 2J$*, which is defined relative to the spin-up state with* $m = J - n$*. These matrix elements converge to their infinite-dimensional counterparts* $[\Pi_s]_{nn}$ *with* $-1 \leq s < 1$ *as*

$$\lim_{J\to\infty} [M_s]_{nn} = \lim_{J\to\infty} \frac{1}{R} \sum_{j=0}^{2J} \sqrt{\tfrac{2j+1}{4\pi}} (\gamma_j)^{-s} [\mathrm{T}_{j0}]_{nn} = [\Pi_s]_{nn}. \tag{2.12}$$

Here, matrix elements of the limiting parity operator $[\Pi_s]_{nn}$ *from* (2.15) *have the explicit form (refer to* (5.28) *and Eq. 19 in [194])*

$$[\Pi_s]_{nn} := \langle n|\Pi_s|n\rangle = 2(-1)^n \frac{(1+s)^n}{(1-s)^{n+1}} \tag{2.13}$$

in the number state basis $|n\rangle$*, refer to Appendix A.1 for a proof.*

The following theorem considers phase-space representations of the spin up state and their convergence to the corresponding infinite-dimensional counterparts as Gaussian functions, refer to Figure 2.4. These phase-space functions are used to define smoothing convolutions in Result 2.2 which translate between different s-parametrized distributions.

Theorem 2.2. *Using the arc-length parametrization* $\alpha = \sqrt{J/2}\,\theta\, e^{-i\phi}$ *from Section 2.5, the* s*-parametrized phase-space representation of the spin up state* $F_{|JJ\rangle}(\Omega, s)$ *converges to its infinite-dimensional counterpart, i.e., to the vacuum state* $F_{|0\rangle}(\Omega, s)$*. In particular, we obtain for* $s < 1$ *that*

$$\lim_{J\to\infty} [F_{|JJ\rangle}(\Omega, s)] = F_{|0\rangle}(\Omega, s) = \tfrac{2}{(1-s)} \exp[\tfrac{2}{(s-1)}|\alpha|^2] \tag{2.14}$$

refer to Appendix A.2 for a proof.

2.1.3 List of Symbols in Chapter 2

symbol	description
J	spin number: related to dimension $d = 2J + 1$
d	dimension of the quantum system (and of Hilbert space) with $d = 2, 3, \ldots$
ρ	quantum state as a density operator (positive semidefinite and unit trace)
$F_\rho(\Omega, s)$	s-parametrized phase-space distribution function of a quantum state ρ
Ω	abstract phase-space coordinate: can be α, (x, p), (θ, ϕ) etc.
s	parameter, which interpolates between Glauber P ($s = 1$) Wigner ($s = 0$) and Husimi Q ($s = -1$) functions
P_ρ	Glauber P function: abbreviated notation for $F_\rho(\Omega, 1)$
W_ρ	Wigner function: abbreviated notation for $F_\rho(\Omega, 0)$
Q_ρ	Husimi Q function: abbreviated notation for $F_\rho(\Omega, -1)$
$\mathcal{D}(\Omega)$	displacement operator: irreducible, unitary representation of the group $\mathrm{H}_3/\mathrm{U}(1)$ its parametrization Ω spans a planar phase space
α	phase-space coordinate of the complex plane parametrization
$\lvert 0\rangle$	vacuum state of the quantum-harmonic oscillator
$\lvert\alpha\rangle$	coherent states of the quantum-harmonic oscillator (also denoted by $\lvert\Omega\rangle$)
Π	usual parity operator: reflects phase-space coordinates $\Pi\lvert\alpha\rangle = \lvert-\alpha\rangle$
Π_s	s-parametrized parity operator for infinite-dimensional systems
$\delta^{(2)}(\alpha)$	two-dimensional delta distribution
θ	polar rotation angle
ϕ	azimuthal rotation angle
$\mathcal{R}(\Omega)$	rotation operator: irreducible, unitary representation of the group $\mathrm{SU}(2)/\mathrm{U}(1)$ its parametrization Ω spans a spherical phase space via $\mathcal{R}(\theta, \phi) = e^{i\phi\mathcal{J}_z} e^{i\theta\mathcal{J}_y}$
$\mathcal{J}_z$	z component of the angular momentum operator of a spin J
$\mathcal{J}_y$	y component of the angular momentum operator of a spin J
$\lvert Jm\rangle$	angular momentum eigenkets as $\mathcal{J}_z\lvert Jm\rangle = m\lvert Jm\rangle$ with $m \in \{J, \ldots, -J\}$
$\lvert JJ\rangle$	spin-up state as $\mathcal{J}_z\lvert JJ\rangle = J\lvert JJ\rangle$
R	radius of the spherical phase space with $R := \sqrt{J/(2\pi)}$
a	arc length on the sphere relative to the north pole with $a = \theta R = \theta\sqrt{J/(2\pi)}$
M_s	s-parametrized parity operator for finite-dimensional systems
Y_{jm}	spherical harmonics of rank j and order m
T_{jm}	tensor operators of rank j and order m
T_{j0}	tensor operators of order 0: can be represented as diagonal matrices
γ_j	rotation invariant coefficients: real numbers, which depend only on the rank j
$C^{jm}_{j_1 m_1, j_2 m_2}$	Clebsch-Gordan coefficients of angular momentum
$[A]_{m_1 m_2}$	matrix representation of an operator as $[A]_{m_1 m_2} := \langle Jm_1\lvert A\rvert Jm_2\rangle$
$p_m(\Omega)$	Stern-Gerlach probability of measuring eigenstate m after a rotation Ω
M_s^R	parity operator, which corresponds to the spherical Radon transform of $F_\rho(\Omega, s)$
$P_j(0)$	Legendre polynomial at point $x = 0$
$W_{\lvert m\rangle}$	Wigner function of the eigenstate $\lvert m\rangle$

2.2 Summary

Continuous phase spaces have become a powerful tool for describing, analyzing, and tomographically reconstructing quantum states in quantum optics and beyond. A plethora of these phase-space techniques are known, however a thorough understanding of their relations was still lacking for finite-dimensional quantum states. We present a unified approach to continuous phase-space representations which highlights their relations and tomography. The infinite-dimensional case from quantum optics is then recovered in the large-spin limit.

2.3 Introduction

Phase spaces provide both theoretically and experimentally useful ways to visualize and analyze abstract states of infinite- and finite-dimensional quantum systems. A plethora of phase-space representations are known [227, 266, 232, 62], including the Glauber P, Wigner, and Husimi Q function, each of which has provided insights in quantum optics, quantum information theory, and beyond. Phase spaces have also played an essential role in characterizing the quantum nature of light and became a natural language for quantum optics due to the seminal work of Glauber [106, 107, 50], also clarifying their interrelations in terms of Gaussian convolutions. Beyond quantum optics, phase spaces are conceptually invaluable and provide a complete description of quantum mechanics. They mirror and naturally reduce to classical phase spaces in the limit of a vanishing Planck constant [118, 195, 25, 26, 28, 29]. Phase-space techniques and their associated quantizations [259, 260, 261] have been widely applied in the context of harmonic analysis and pseudo-differential operators [113, 111, 116, 59, 60]. In this work, we focus on *finite-dimensional* quantum states, for which phase-space methods have been explored only to a lesser extent.

Recent advances in experimentally creating entangled quantum states for spins or spin-like systems, such as atomic ensembles [188, 122], Bose-Einstein condensates [17, 132, 199, 240, 176, 214, 228, 126, 244], trapped ions [166, 40, 193], and light polarization [44, 156, 55], have been in certain cases illustrated with phase-space techniques and therefore call for a more profound understanding of these tools with regard to finite-dimensional quantum states. To this end, we present a general approach to continuous phase spaces for spins which clarifies their interrelations by conveniently translating between them, while emphasizing the connection to the infinite-dimensional case from quantum optics. We do not consider discrete phase spaces such as the one proposed by Wootters [263], see also [170, 101, 92] and references therein.

Phase-space representations have become crucial in the tomographic reconstruction of infinite-dimensional quantum states [171, 227]. The optical homodyne tomography reconstructs the quantum state of light by directly measuring the planar Radon transform of the Wigner function [237, 171]. Also, the Husimi Q function [135] has been experimentally measured for various systems [40, 122, 244, 141, 82, 8, 44]. We detail how to tomographically reconstruct a class of finite-dimensional phase-space representations.

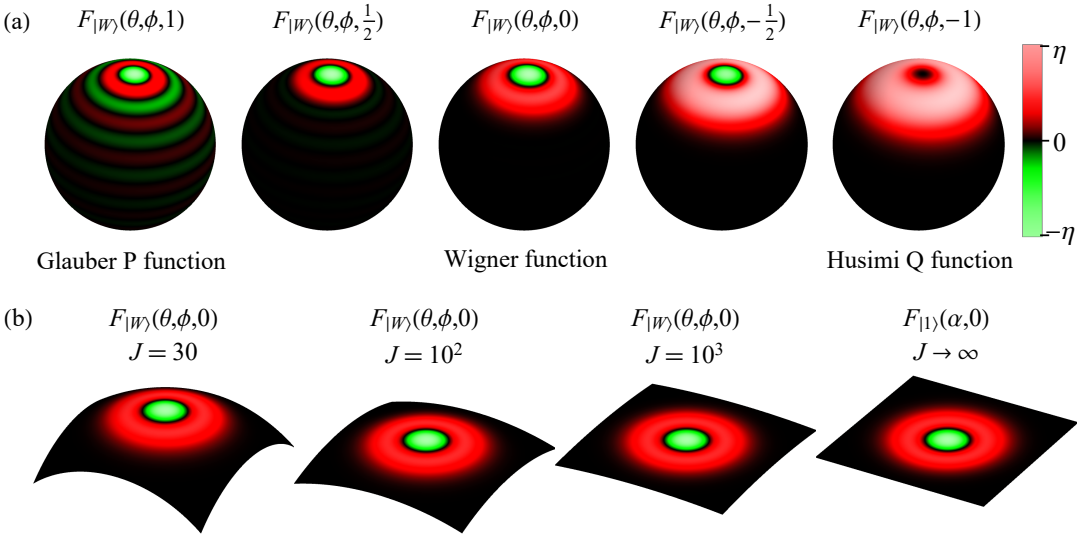

Figure 2.1: (a) s-parametrized phase-space representations $F_{|W\rangle}(\theta,\phi,s)$ for particular values $s \in \{1, 1/2, 0, -1/2, -1\}$ of a (generalized) W state $|\mathrm{W}\rangle$ for a single spin with $J = 10$, or equivalently the symmetric Dicke state $|J, J-1\rangle$ of $2J$ indistinguishable qubits with a single Majorana vector pointing to the south pole and $2J-1$ vectors pointing to the north pole. A decreasing s (left-to-right) smearing out $F_{|W\rangle}(\theta,\phi,s)$ is interpreted as a Gaussian-like convolution. Red (dark gray) and green (light gray) represent positive and negative values, respectively. The brightness reflects the absolute value of the function relative to its global maximum η. (b) Spherical Wigner functions $F_{|W\rangle}(\theta,\phi,0)$ for increasing J approach their planar counterpart, i.e., the single-photon state $F_{|1\rangle}(\alpha,0)$ (see Section 2.4). Identical coordinate patches with $-1.2 \le x, y \le 1.2$ have been used, where $x = R\sin\theta\cos\phi$, $y = R\sin\theta\sin\phi$ in the first three plots and $x = \Re(\alpha)$, $y = \Im(\alpha)$ in the last one. (For the plots in (b), methods from [161] to efficiently approximate phase-space representations for large J have been applied, refer to Section 4.12 for details about this approximation.)

In this work, we develop a general and unified description of continuous phase-space representations for quantum states of a single spin with arbitrary, integer or half-integer spin number J (i.e. a qudit with $d = 2J+1$), which is simultaneously applicable to experimental bosonic systems consisting of indistinguishable qubits [75, 241, 250, 178]. A single qudit can be identified with a bosonic system consisting of $2J$ indistinguishable qubits: Figure 2.1 depicts a quantum state of a single qudit (i.e. a single spin J) corresponding to a (generalized) W state [79] (i.e. Dicke state) of $2J$ indistinguishable qubits (see also Sec. III A of [241] for an explicit map and Chap. 3.8 of [223] or [234] for links to the second quantization). In particular, we address the following fundamental open questions related to finite-dimensional phase-space representations (e.g., Glauber P, Wigner, and Husimi Q): (a) How can they be systematically defined to naturally recover the infinite-dimensional case of quantum optics in the limit of large J? (b) How can they be transformed into each other? (c) How can their experimental tomographic approaches be formulated in a unified way?

In the current work, we present answers to these questions for the full class of (finite-dimensional) s-parametrized phase-space representations with $-1 \le s \le 1$. Our approach relies on rotated parity operators and thereby significantly simplifies earlier work (such as [47] and particular cases discussed in [7, 78]). It also extends [130, 153, 248, 221, 222] in the case of single spins (and bosonic systems consisting of indistinguishable qubits) to

all s-parametrized phase spaces. In addition to a deeper theoretical knowledge connecting planar and spherical phase spaces, the insights provided here will also guide practitioners to design innovative experimental schemes, such as the tomographic reconstruction of phase-space representations. Before discussing finite-dimensional quantum states, we first review important properties of the infinite-dimensional phase spaces from quantum optics.

2.4 Summary of infinite-dimensional phase-space representations

Let us recall the s-parametrized phase-space distribution function [50, 194, 171, 113] (where $-1 \leq s \leq 1$)

$$F_\rho(\Omega, s) = \mathrm{Tr}\left[\, \rho\, \mathcal{D}(\Omega) \Pi_s \mathcal{D}^\dagger(\Omega)\right] \tag{2.15}$$

as the expectation value of the parity operator Π_s (*vide infra*) transformed by the displacement operator $\mathcal{D}(\Omega)$, which acts on coherent states via $\mathcal{D}(\Omega)|0\rangle = |\Omega\rangle$ [99]. Here, $|0\rangle$ denotes the vacuum state and Ω fully parametrizes a phase space with either the variables p and q or the complex eigenvalues α of the annihilation operator [106, 171].

Different parity operators Π_s lead to different distribution functions $F_\rho(\Omega, s)$. The Q function $Q_\rho = Q_\rho(\Omega) := F_\rho(\Omega, -1)$ arises from the parity operator Π_{-1} whose entries are given by $[\Pi_{-1}]_{nn} := \delta_{n0}$ [194] in the number state representation [171]. Similarly, the Wigner function $W_\rho := F_\rho(\Omega, 0)$ is determined by $[\Pi_0]_{nn} = 2(-1)^n$ [194], which inverts phase-space coordinates via $\Pi_0|\Omega\rangle = |-\Omega\rangle$ [113]. The P function $P_\rho := F_\rho(\Omega, 1)$ is singular for all pure states [50], and the entries of its parity operator Π_1 diverge in the number-state representation [194]. The discussed representations are considered in the upper part of Figure 2.2. An example is given by the vacuum state $|0\rangle$ whose Wigner function $W_{|0\rangle} = 2e^{-2|\alpha|^2}$ is a Gaussian distribution. The respective Q function $Q_{|0\rangle} = e^{-|\alpha|^2}$ is a Gaussian of double width and the P function is the two-dimensional delta function $P_{|0\rangle} = \delta^{(2)}(\alpha)$.

We now recollect how to transform between phase-space representations with Gaussian convolutions [50, 171]. Two phase-space distribution functions $K(\Omega)$ and $F(\Omega)$ can be combined using their convolution [171]

$$[K * F](\Omega) = \int [\mathcal{D}^{-1}(\Omega) K(\Omega')] F(\Omega')\, \mathrm{d}\Omega', \tag{2.16}$$

which corresponds to a multiplication in the Fourier domain. Convolution of a distribution function $F_\rho(\Omega, s)$ with the vacuum-state representation $F_{|0\rangle}(\Omega, s')$ results in the phase-space distribution function

$$F_\rho(\Omega, s{+}s'{-}1) = F_{|0\rangle}(\Omega, s') * F_\rho(\Omega, s) \tag{2.17}$$

of type $s{+}s'{-}1$. A convolution $P_{|0\rangle}(\Omega) * F(\Omega) = F(\Omega)$ with the P function $P_{|0\rangle}$ acts as identity operation, while a convolution with the Gaussians $W_{|0\rangle}$ or $Q_{|0\rangle}$ blurs out $F_\rho(\Omega, s)$. This Gaussian smoothing is widely used in image processing and allows us to transform different phase-space representations into each other [171] as in the upper part Figure 2.2. For example, the non-negative Q function $Q_\rho = W_{|0\rangle} * W_\rho$ is obtained from the Wigner

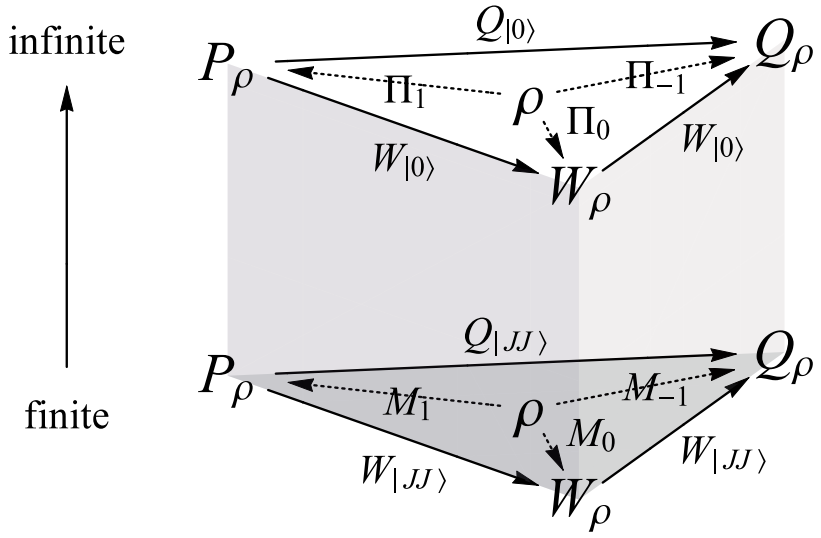

Figure 2.2: Phase-space representations W_ρ, Q_ρ, P_ρ of *infinite*- or *finite*-dimensional density operators ρ as expectation value of parity operators Π_s or M_s [dashed arrows], see Equation 2.15 or Equation 2.18. Transformed by Gaussian smoothing with $W_{|0\rangle}$, $Q_{|0\rangle}$ or reversibly with $W_{|JJ\rangle}$, $Q_{|JJ\rangle}$ [solid arrows], see Equation 2.17 or Equation 2.24.

function W_ρ by convolution with $W_{|0\rangle}$; the negative regions in W_ρ are therefore bounded by the variance $1/4$ of $W_{|0\rangle}$ [171].

2.5 Phase-space representations for spins

2.5.1 Definition of phase-space representations for spins

We now establish a consistent formalism for s-parametrized phase-space representations ($-1 \leq s \leq 1$) for quantum states of single spins, which in the limit of an increasing spin number J converges to the just discussed infinite-dimensional case. The continuous phase space $\Omega := (\theta, \phi)$ can be completely parametrized in terms of two Euler angles of the rotation operator $\mathcal{R}(\Omega) = \mathcal{R}(\theta, \phi) := e^{i\phi\mathcal{J}_z} e^{i\theta\mathcal{J}_y}$, where $\mathcal{J}_z$ and $\mathcal{J}_y$ are components of the angular momentum operator [192]. The rotation operator $\mathcal{R}(\Omega)$ replaces the displacement operator $\mathcal{D}(\Omega)$ and maps the spin-up state $|JJ\rangle$ to spin coherent states $|\Omega\rangle = \mathcal{R}(\Omega)|JJ\rangle$ [205, 18, 78, 99]. This leads to a spherical phase space, whose radius is set to $R := \sqrt{J/(2\pi)}$.

Result 2.1. *For a density operator ρ of a single spin J, the s-parametrized phase-space representation [cf. Equation 2.15]*

$$F_\rho(\Omega, s) := \mathrm{Tr}\left[\,\rho\,\mathcal{R}(\Omega) M_s \mathcal{R}^\dagger(\Omega)\right] \tag{2.18}$$

is the expectation value of the rotated parity operator

$$M_s := \frac{1}{R}\sum_{j=0}^{2J}\sqrt{\tfrac{2j+1}{4\pi}}(\gamma_j)^{-s}\,\mathrm{T}_{j0}, \tag{2.19}$$

which is a weighted sum of zeroth-order tensor operators.

The diagonal tensor operators $[\mathrm{T}_{j0}]_{mm'} = \delta_{mm'}\sqrt{(2j{+}1)/(2J{+}1)}\,C^{Jm}_{Jm,j0}$ of order zero [209] have been applied in Equation 2.19, and they can be specified via the Clebsch-Gordan coefficients $C^{Jm}_{Jm,j0}$ [192] where $j \in \mathbb{N}\cup\{0\}$ and $m, m' \in \{-J, \ldots, J\}$. We also use the coefficients $\gamma_j := R\sqrt{4\pi}(2J)!\,[(2J{+}j{+}1)!\,(2J{-}j)!\,]^{-1/2}$. With increasing spin number J, the parity operators M_s converge to the infinite-dimensional operators Π_s in Equation 2.15, while rotations transform into translations along the tangent of a sphere [16, 18, 78, 155]. The phase-space representations in Equation 2.18 fulfill the Stratonovich postulates [242, 7, 253, 47, 159]; an s-parametrized version is given in Ref. [47]. Prior results [130, 153, 248, 221, 222] using rotated parity operators are extended for single spins to all s-parametrized phase spaces. For Wigner functions, our definition conforms to Sec. VI of [222] but differs from Eq. (8) in [248]. The latter can be identified as a linearly shifted Q function $aQ_\rho - b$, and it relaxes the postulate $\mathrm{Tr}(AB) = \int_{S^2} F_A(\Omega,0)F_B(\Omega,0)\,\mathrm{d}\Omega$. We consider in this work only spherical rotations (even for qudits) which yield spherical phase spaces, forgoing general rotations [153, 249, 248, 221]. Generalizations to coupled spins are known in the Wigner case [98, 248, 221]; our methods in [159] are also applicable.

We further highlight how the approach of Result 2.1 connects to earlier work. An equivalent form of the s-parameterized phase-space representation in Equation 2.18 has been previously determined in Eq. (5.28) of [47] (up to a global factor) as

$$F_\rho(\Omega, s) = \mathrm{Tr}\left[\,\rho\,\Delta_s(\theta,\phi)\right], \quad \text{with} \quad \Delta_s(\theta,\phi) := \tfrac{1}{R}\sum_{j=0}^{2J}\sum_{m=-j}^{j}(\gamma_j)^{-s}\,\mathrm{T}_{jm}[\mathrm{Y}_{jm}(\theta,\phi)]^* \tag{2.20}$$

using the kernel $\Delta_s(\theta,\phi)$. The work of [46, 47] builds on the particular cases of $s \in \{-1, 0, 1\}$ obtained in [253]. Along similar lines, the pioneering work of [7] proposed spherical-harmonics expansions (see Eq. (3.15) in [7]) for spin phase-space representations

$$F^{(\Omega)}_\rho(\theta,\phi) = \sum_{j=0}^{2J}\sum_{m=-j}^{j} c^{(\Omega)}_{jm}\,\mathrm{Y}_{jm}(\theta,\phi), \tag{2.21}$$

which are indexed by $\Omega = \Omega_{jm}$ and use the coefficients $c^{(\Omega)}_{jm} = \mathrm{Tr}\,[\rho\,\mathrm{T}^\dagger_{jm}]/\Omega_{jm}$. For s-parametrized phase spaces, one has $\Omega = \Omega_{jm} = R\gamma_j^s$. Note that [7] established the explicit

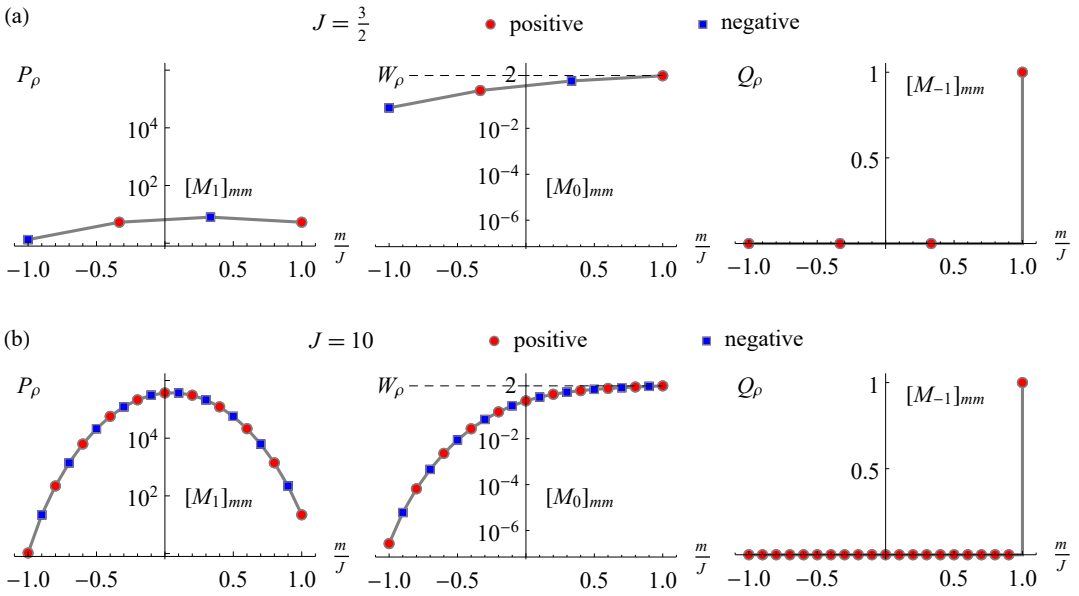

Figure 2.3: Parity-operator entries $[M_s]_{mm}$ corresponding to Equation 2.19 [and equivalently the Stern-Gerlach reconstruction weights in Equation 2.25] for a single spin J shown for the P function P_ρ, the Wigner function W_ρ, and the Q function Q_ρ.

form of Ω_{jm} only for Husimi Q functions, i.e., $s = -1$. The case of Wigner functions ($s = 0$) has been discussed in [78]. Note that the tensor-operator components T_{jm} can be explicitly given as $[\mathrm{T}_{jm}]_{m_1 m_2} = \sqrt{(2j+1)/(2J+1)}\, C^{Jm_1}_{Jm_2,jm} = (-1)^{J-m_2}\, C^{jm}_{Jm_1 J,-m_2}$ using Clebsch-Gordan coefficients and $m_1, m_2 \in \{J, \ldots, -J\}$ [192, 47, 33, 87].

By using rotated parity operators, the approach of Result 2.1 has important conceptual advantages when compared to Equation 2.20 and Equation 2.21. First, Result 2.1 separates the dependence on the parameter s in the parity operator from the rotations. Second, Equation 2.18 naturally transforms in the large-spin limit into the infinite-dimensional case discussed in Equation 2.15 by replacing rotations $\mathcal{R}(\Omega)$ with displacements $\mathcal{D}(\Omega)$. Third, the above mentioned tensor operators and spherical-harmonics decompositions are averted and the rotations $\mathcal{R}(\Omega)$ can be efficiently calculated via the Wigner D-matrix [246, 89]. Finally, the particular form given in Result 2.1 enables us to develop a general tomography formula as discussed in Section 2.5.4 below.

Particular cases of Result 2.1 are considered in the lower part of Figure 2.2. The Q function specifies the expectation value of rotated spin-up states, where $[M_{-1}]_{mm} := \delta_{mJ}$ (right of Figure 2.3), and its zeros are the so-called Majorana vectors [252, 44, 36]. The Wigner function determines the expectation value of the rotated parity operator M_0. The matrix entries $[M_0]_{mm}$ are shown in the middle of Figure 2.3, highlighting their infinite-dimensional limit of ± 2 for $m/J \approx 1$ [16]. The matrix entries $[M_1]_{mm}$ for the parity operator of the P function are shown in the left panel of Figure 2.3, including their rapid divergence in the large-spin limit.

Further exploring the infinite-dimensional limit of large J, the phase-space representation

$$F_{|JJ\rangle}(\theta, s) := \frac{1}{R^2} \sum_{j=0}^{2J} \sqrt{\tfrac{2j+1}{4\pi}} (\gamma_j)^{1-s}\, \mathrm{Y}_{j0}(\theta) \tag{2.22}$$

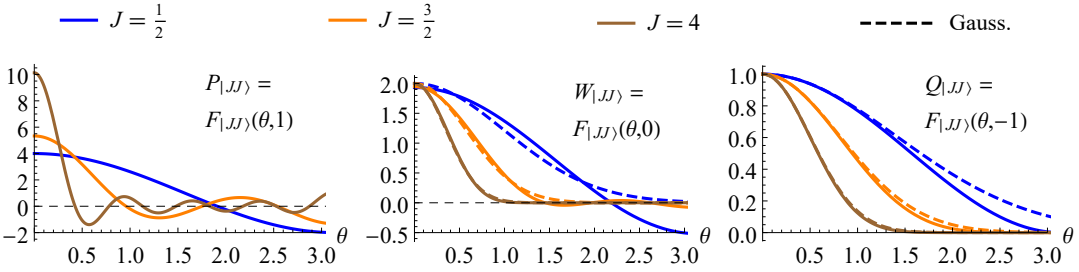

Figure 2.4: Phase-space representations $F_{|JJ\rangle}(\theta, s)$ of the spin-up state $|JJ\rangle$, c.f. Equation 2.22. As J increases, $Q_{|JJ\rangle}$ and $W_{|JJ\rangle}$ rapidly converge to the Gaussian distributions $Q_{|0\rangle}$ and $W_{|0\rangle}$ (dashed line); $P_{|JJ\rangle}$ slowly approaches the delta function $P_{|0\rangle} = \delta(\Omega)$.

of the spin-up state (i.e. the ground state with least uncertainty) is easily expanded into a weighted sum of axially symmetric spherical harmonics $\mathrm{Y}_{j0}(\theta)$. The examples $Q_{|JJ\rangle}$, $W_{|JJ\rangle}$, and $P_{|JJ\rangle}$ are plotted in Figure 2.4 as functions of the angle θ. Even though the Gaussian width of $F_{|JJ\rangle}(\theta, s)$ shrinks in terms of θ with increasing J, $F_{|JJ\rangle}(\theta, s)$ converges to the Gaussian $F_{|0\rangle}(\Omega, s)$ related to the infinite-dimensional vacuum state if parametrized by the relevant arc length $a := \theta R = \theta\sqrt{J/(2\pi)}$ (Figure 2.1/(b) illustrates the sphere-to-plane transition in the infinite-dimensional limit).

For example, $Q_{|JJ\rangle}$ can be shown to be equal to the Wigner D-matrix element $|D^J_{JJ}|^2 = \cos(\theta/2)^{4J}$, and it converges rapidly with increasing J to the Gaussian $Q_{|0\rangle}(\alpha) = e^{-|\alpha|^2} = e^{-a^2\pi} = e^{-J\theta^2/2}$ using the phase-space coordinate $\alpha = \sqrt{\pi}ae^{-i\phi}$ [205, 18]. Similarly, $W_{|JJ\rangle}$ rapidly converges to the normalized Gaussian $W_{|0\rangle} = 2e^{-2|\alpha|^2} = 2e^{-2a^2\pi} = 2e^{-J\theta^2}$ of the vacuum state. The P function $P_{|JJ\rangle}(\theta) := \tilde{\delta}(\Omega)$ is the spherical $sinc$ function, i.e., a truncated version of the spherical delta function $\delta(\Omega) := \delta(\theta)\delta(\phi)/\sin\theta$ (where the tilde projects onto the physical subspace of spherical harmonics with rank $j \leq 2J$ [103]), which by definition approaches the delta function in the large-spin limit $\delta(\Omega) := \sum_{j=0}^{\infty}\sqrt{(2j+1)/(4\pi)}\,\mathrm{Y}_{j,0}(\Omega)$. Qualitative similarities between certain finite- and infinite-dimensional Wigner functions were already highlighted in [78]. But this connection is clarified in our formulation by emphasizing the large-spin convergence for all of the s-parametrized phase spaces.

2.5.2 Spherical convolution

To translate between the different spherical phase-space representations in the lower part of Figure 2.2 (which can be done reversibly assuming arbitrary precision), we define the convolution [cf. Equation 2.16]

$$[K * F](\Omega) := \int_{S^2} [\mathcal{R}^{-1}(\Omega)K(\Omega')]F(\Omega')\,\mathrm{d}\Omega' \tag{2.23}$$

via a spherical integration where $\mathrm{d}\Omega' = R^2\sin\theta'\mathrm{d}\theta'\,\mathrm{d}\phi'$. First, the kernel function $K(\Omega')$ is rotated by $\mathcal{R}^{-1}(\Omega)$ to $K(\Omega'-\Omega)$, which is then projected onto the distribution function $F(\Omega')$ via a spherical integral. The kernel function $K(\Omega')$ has to be axially symmetric due to the so-called Funk-Hecke theorem [117, 147]. The spherical convolution is a multiplication in the spherical-harmonics domain, and substituting spherical harmonics into Equation 2.23

yields $\mathrm{Y}_{j'0} * \mathrm{Y}_{jm} = R^2\sqrt{4\pi/(2j+1)}\,\mathrm{Y}_{jm}\,\delta_{jj'}$. This allows us to transform between different spherical phase-space representations:

Result 2.2. *The convolution of a phase-space distribution function $F_\rho(\Omega, s)$ with the phase-space representation $F_{|JJ\rangle}(\Omega, s')$ of the spin-up state results in a type-$(s{+}s'{-}1)$ distribution function [cf. Equation 2.17]*

$$F_\rho(\Omega, s{+}s'{-}1) = F_{|JJ\rangle}(\theta, s') * F_\rho(\Omega, s). \tag{2.24}$$

The pioneering work of [7] proposed spin phase-space representations in the form of expansions into spherical-harmonics [refer to Equation 2.21] and defined their relations using integral transformation kernels (see (3.19) in [7]). Result 2.2 clarifies that these relations are indeed spherical convolutions, in complete analogy with the infinite-dimensional case considered in quantum optics. The particular form of Equation 2.24 has not been formally described in the literature before. Some convolution properties were detailed for *discrete*, planar phase spaces in [48, 202]. We want to also stress that spherical convolutions have efficient implementations [145, 257].

In the infinite-dimensional limit of an increasing spin number J, Equation 2.24 turns into Equation 2.17. We emphasize that the convolution transformation in Equation 2.24 is reversible (assuming arbitrary precision) for general parameters $s, s' \in \mathbb{R}$ (as the coefficients γ_j in Equation 2.22 are non-zero). Also, a convolution $P_{|JJ\rangle}(\theta) * F(\Omega, s) = F(\Omega, s)$ with the P function $P_{|JJ\rangle}(\theta)$ acts as an identity operation, just as in the infinite-dimensional case. The Wigner function W_ρ can be transformed into the non-negative Q function $Q_\rho = W_{|JJ\rangle} * W_\rho$ by Gaussian-like smoothing, cf. Figure 2.1. Consequently, the negative regions of W_ρ are bounded by the variance $\propto 1/4$ of $W_{|JJ\rangle}$, similar as for infinite-dimensional phase spaces. Result 2.2 completes our characterization of how to transform between spherical phase-space representations as illustrated in Figure 2.2.

2.5.3 Examples of phase-space functions

Figure 2.5 depicts phase-space representations of typical finite-dimensional quantum states. The P, Wigner, and Q functions are shown in a triangular arrangement along with their corresponding convolution kernels, which generate the spherical convolutions from Equation 2.24 between edges of the triangle.

In Figure 2.5/(a), we consider the quantum state of a single spin J corresponding to the $2J$-qubit GHZ state $|\mathrm{GHZ}\rangle = (|0\rangle^{\otimes 2J} + |1\rangle^{\otimes 2J})/\sqrt{2} = (|JJ\rangle + |J,{-}J\rangle)/\sqrt{2}$ consisting of a quantum superposition of the two symmetric Dicke states given by the spin-up and spin-down state (which can be identified with a $2J$-photon NOON state). This GHZ state factorizes up to permutations into a product of its Majorana vectors $\bigotimes_k |v_k\rangle$ [252, 36], where $|v_k\rangle$ is a single-qubit state with Bloch vector v_k. These Majorana vectors correspond to zeros of the Q function and point to the edges of a regular n-gon, see $Q_{|\mathrm{GHZ}\rangle}$ in Figure 2.5/(a). The zeros of

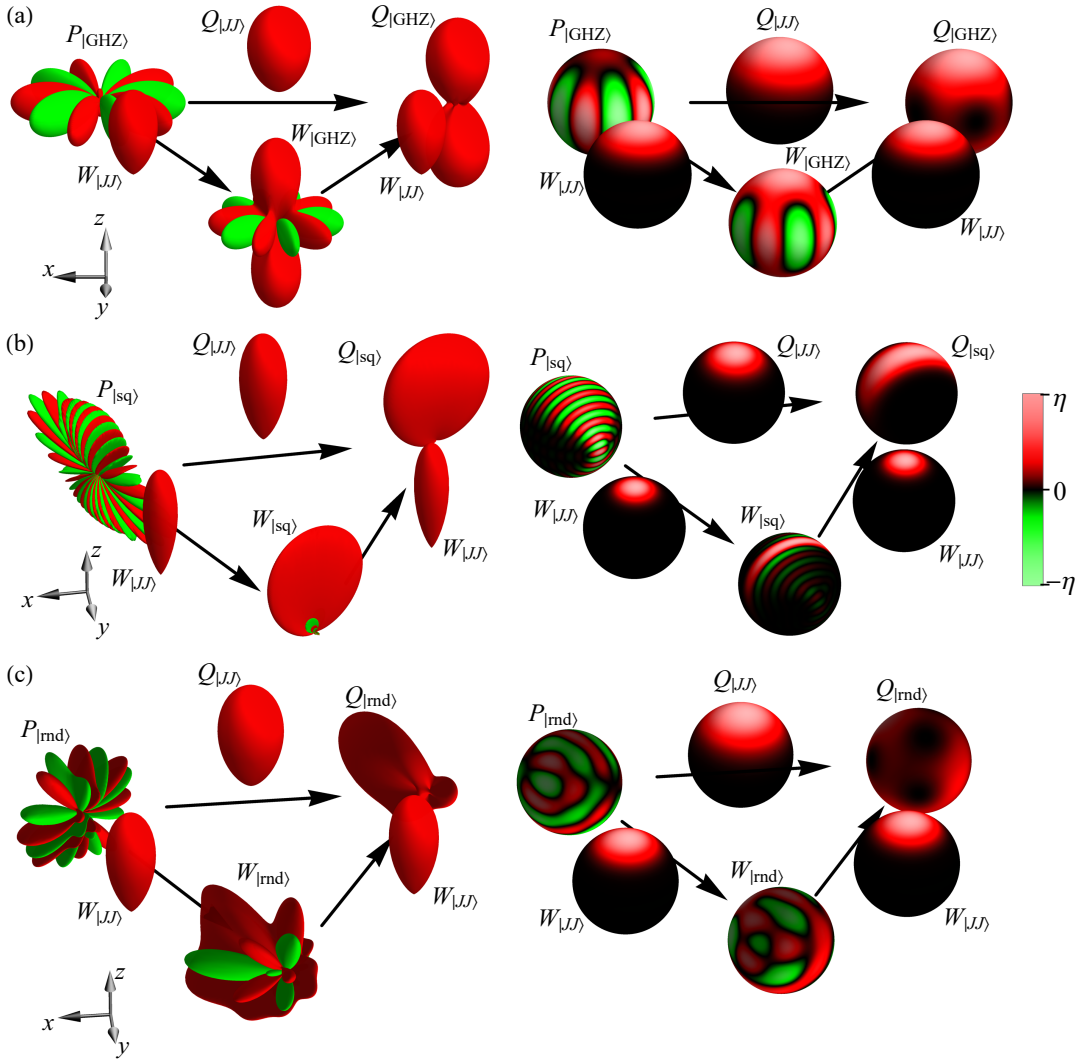

Figure 2.5: P, Wigner, and Q functions with their corresponding convolution kernels for (a) a quantum state of a spin $J = 5/2$ corresponding to the GHZ state $|\mathrm{GHZ}\rangle$ of $2J$ indistinguishable qubits, (b) a squeezed state $|\mathrm{sq}\rangle$ of a spin $J = 10$, and (c) a random state $|\mathrm{rnd}\rangle$ of a spin $J = 4$ (see Section 2.5.3). Red (dark gray) and green (light gray) represent positive and negative values, respectively. The absolute values of the spherical function relative to its global maximum η is given by the plotted surface (left) or the brightness (right), where each variant highlights different properties of the plotted functions.

the Q funtion can (e.g.) be determined by spherically convolving the Wigner function with the convolution kernel $W_{|JJ\rangle}$ (cf. Section 2.5.2), and the negative (green) lobes of $P_{|\mathrm{GHZ}\rangle}$ and $W_{|\mathrm{GHZ}\rangle}$ in Figure 2.5/(a) identify the direction of the Majorana vectors. The Q function largely resembles the classical superposition of a spin-up and a spin-down state, but has a five-fold symmetry.

Figure 2.5/(b) shows phase-space plots of the squeezed state $\exp[-i\theta\mathcal{I}_y^2/2]|JJ\rangle$ with squeezing angle $\theta := 0.3$ for a single spin with spin number $J = 10$, where the state is squeezed along the y axis [181]. A random pure state of a single spin with spin number $J = 4$ is depicted in Figure 2.5/(c), the state vector is approximately given by $(0.06+i0.02, -0.21-i0.19, 0.04+i0.27, 0.15-i0.11, 0.28-i0.28, -0.33-i0.25, 0.04-i0.44, -0.21-i0.24, -0.43+i0.00)^T$.

2.5.4 Tomography of phase-space functions

We now detail how phase-space representations are recovered from Stern-Gerlach experiments assuming that a chosen density operator ρ can be prepared identically and repeatedly. In a single Stern-Gerlach experiment, one detects the density matrix ρ in a projection eigenstate according to a reference frame rotated by Ω (i.e., by rotating the measurement device or inversely rotating ρ). For repeated Stern-Gerlach experiments, one measures frequencies which converge to the Stern-Gerlach probabilities $p_m(\Omega) = \langle Jm|\mathcal{R}^\dagger(\Omega)\rho\mathcal{R}(\Omega)|Jm\rangle$. The measured frequencies are identified in this work (in a simplified manner) with the Stern-Gerlach probabilities. This leads to the finite-dimensional equivalent of the 'direct measurement' technique [74, 180, 32, 21] in quantum optics:

Result 2.3. *The phase-space representations*

$$F_\rho(\Omega, s) = \sum_{m=-J}^{J} [M_s]_{mm}\, p_m(\Omega) \tag{2.25}$$

of a $(2J+1)$-dimensional quantum state ρ are directly determined by the probability distributions $p_m(\Omega)$ of Stern-Gerlach experiments. The weights $[M_s]_{mm}$ are given by the parity operator from Equation 2.19.

The phase-space functions in Figure 2.5 are reconstructed from Stern-Gerlach probabilities $p_m(\Omega)$ using Result 2.3, which has not been described in this generality before. In particular, the P functions $P_{|\mathrm{GHZ}\rangle}$, $P_{|\mathrm{sq}\rangle}$, and $P_{|\mathrm{rnd}\rangle}$ in Figure 2.5 show considerable detail, while mostly utilizing probabilities $p_m(\Omega)$ of small $|m|$ from Figure 2.3. The Wigner functions $W_{|\mathrm{GHZ}\rangle}$, $W_{|\mathrm{sq}\rangle}$, and $W_{|\mathrm{rnd}\rangle}$ in Figure 2.5 require all $2J+1$ Stern-Gerlach probabilities $p_m(\Omega)$ [228, 214, 188, 184, 221] and show fewer detail consistent with being smoothed versions of the corresponding P functions. Finally, the Q functions show little detail due to a second Gaussian smoothing (yet low-rank contributions would still be recognizable [178, 40, 122, 244, 228]) and are fixed by the probability $p_J(\Omega)$ of the spin-up state [8].

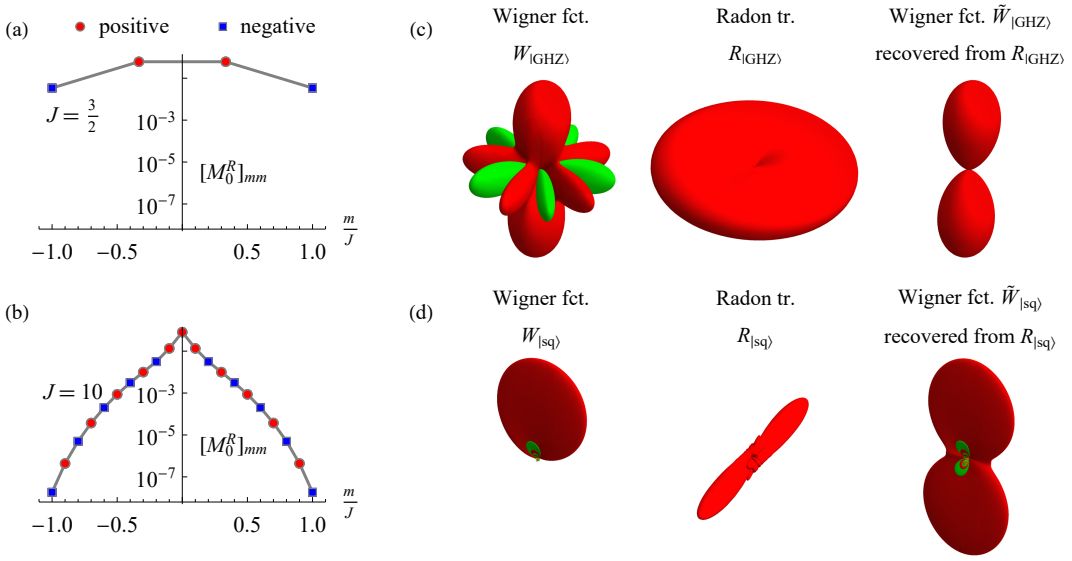

Figure 2.6: (a-b) Stern-Gerlach reconstruction weights $[M_0^R]_{mm}$ in Equation 2.26 for the Radon transform of a Wigner function applicable to a single spin J (cf. Figure 2.3); (c-d) Wigner function (cf. Figure 2.5), its Radon transform, and its point-symmetric part reconstructed by inverse Radon transformation: (c) quantum state of a single spin with $J = 5/2$ corresponding to the GHZ state of $2J$ qubits (cf. Figure 2.5/(a)), (d) squeezed state $|\mathrm{sq}\rangle$ of a single spin with $J = 10$ (cf. Figure 2.5/(b)) approximately localized on the upper hemisphere of its Wigner function $W_{|\mathrm{sq}\rangle}$, the corresponding Radon transform $R_{|\mathrm{sq}\rangle}$ is highly localized around the equator and can be reconstructed using few measurements. Red (dark gray) and green (light gray) represent positive and negative values, respectively.

2.5.5 Comparison to the spherical Radon approach

We also relate Result 2.3 to optical homodyne tomography [237, 171, 204] (cf. Eq. (6.12) in [47]) and especially to the finite-dimensional case as discussed in [228]. The planar Radon transformation of a Wigner function is replaced in finite dimensions with the spherical Radon transformation, which is the integral along the great circle orthogonal to the vector pointing to a phase-space point Ω [117]. Refer to Figure 2.6 for plots of the Radon transforms $R_{|\mathrm{GHZ}\rangle}$ and $R_{|\mathrm{sq}\rangle}$ of Wigner functions for a GHZ state and a squeezed state, respectively. The Radon transforms of Wigner functions can be directly obtained from the Stern-Gerlach probabilities $p_m(\Omega)$ by replacing the weights in Equation 2.25 with the relevant parity operators $[M_0^R]_{mm}$ [see Figure 2.6/(a-b)]. One has

$$M_s^R := \sum_{j=0}^{2J} \sqrt{\tfrac{2j+1}{4\pi}} P_j(0) (\gamma_j)^{-s} \, \mathrm{T}_{j,0} \tag{2.26}$$

for the general class of s-parametrized phase-space representations where the Legendre polynomial $P_j(0)$ [117] is used. The point symmetric parts $\tilde{W}_{|\mathrm{GHZ}\rangle}$ and $\tilde{W}_{|\mathrm{sq}\rangle}$ of the Wigner functions are recovered via an inverse spherical Radon transform (right of Figure 2.6/(c-d)). In general, one does *not* recover the complete Wigner function using this approach, compare, e.g., the left and right part of Figure 2.6/(c). But in typical experiments with large J, the Wigner function is localized around the north pole and measuring probabilities $p_m(\Omega)$

close to the equator still allows for its reconstruction from its Radon transform (middle of Figure 2.6/(d)) by assuming a point-symmetric Wigner function (right of Figure 2.6/(d)), which—in this particular case—still contains the full information of the quantum state, cf. Sec. 3 in [228]. The great-circle integrals for the spherical Radon transform converge to the usual line integrals of the planar Radon transformation.

2.6 Discussion

Let us compare our work to the 'filtered backprojection' technique in Sec. 2 of [228] which recovers a Wigner function from a finite number N of Stern-Gerlach measurements (each performed in a rotated reference frame Ω_n): The Wigner functions $W_{|m_n\rangle}$ of the projection eigenstates $|m_n\rangle$ are inversely rotated and summed up as $\sum_{n=1}^{N} c_n \mathcal{R}^{-1}(\Omega_n)[W_{|m_n\rangle}]$. A subsequent spherical convolution with a filter function reconstructs the Wigner function in [228], which is in the limit of infinite and evenly distributed measurements agrees with the general Result 2.3. In addition, Result 2.3 does not rely on a spherical convolution and enables diverse reconstruction strategies as the distribution function $F_\rho(\Omega, s)$ can be independently determined for each phase-space point Ω.

As for infinite-dimensional phase-space methods (cf. Eq. (6.8) in [50]), one can also reconstruct the density matrix (which, however, is not the subject of this work)

$$\rho = \int_{S^2} F_\rho(\Omega, s)\ \mathcal{R}(\Omega) M_{-s} \mathcal{R}^\dagger(\Omega)\, \mathrm{d}\Omega, \tag{2.27}$$

from its phase-space representation by inverting Result 2.1 with a spherical integration; the reconstruction from the Q function is more precarious as M_1 diverges for large J. A tomography formula $\rho = \sum_{m=-J}^{J} [M_s]_{mm} \int_{S^2} p_m(\Omega)\ \mathcal{R}(\Omega) M_{-s} \mathcal{R}^\dagger(\Omega)\, \mathrm{d}\Omega$ in terms of the Stern-Gerlach probabilities $p_m(\Omega)$ is obtained by combining Equation 2.25 and Equation 2.27, where the integrals can be numerically estimated from finitely many spherical samples via (e.g.) Gaussian quadratures [147]. This generalizes [15, 80, 184], and the 'filtered backprojection' technique for the density matrix (see Eq. (9) in [228]) agrees in the limit of infinitely many measurements with our result. A similar formula is also obtained by restricting [168] to a single spin, and results of [168] were recently also extended to the experimental tomography of propagators and quantum gates [167]. Certain features, e.g., weights in Equation 2.25 along with the results in Section 2.5, are invariant under slight variations of a sufficiently large spin number J, which might be useful in atomic ensembles [188, 122], Bose-Einstein condensates [214, 228, 17, 132, 240, 176], or trapped ions [166, 40, 193].

While a majority of earlier work focuses on reconstructing density matrices or infinite-dimensional phase-space functions from measured data (see, e.g., [233, 157, 86, 236, 239, 215, 245, 204]), we have presented in Equation 2.25 of Result 2.3 a general tomography formula for finite-dimensional phase-space representations. Such a tomography formula has not been reported before for the full class of all (finite-dimensional) s-parametrized phase-space representations. Result 2.3 provides the foundation for engineering statistical estimators [226] for the reconstruction of finite-dimensional phase-space representations in future

research, which minimize the necessary Stern-Gerlach measurements while guaranteeing robustness via precisely bounded confidence intervals and ensuring a physical estimate. For this purpose, a deeper understanding of the systematic and random errors involved would be beneficial. However, all the general statistical aspects are quite similar to the widely discussed cases of reconstructing density matrices or infinite-dimensional phase-space functions [233, 157, 86, 236, 239, 215, 245, 204]. Leaving statistical and robustness discussions to future work, we want to only remark that reconstructing a Wigner function directly using Result 2.3 is—under noise—preferable to convolving/deconvolving noisy P or Q functions via Result 2.2 as convolutions are well known to be sensitive to noise (cf. [8, 47]). Therefore, not all reconstruction strategies will be equally advisable under experimental noise. Concrete experiments will have to be designed explicitly depending on characteristics of the desired final (phase-space) representation.

2.7 Conclusion

We have developed a unified formalism for spherical phase-space representations of finite-dimensional quantum states based on rotated parity operators. This formalism applies to the full class of (finite-dimensional) s-parametrized phase-space representations. We have (a) systematically defined spherical phase spaces for spin systems which recover the planar phase spaces from quantum optics in the large spin limit; (b) different types of phase-space representations can be translated into each other by convolving with spin-up state representations; (c) tomographic approaches can be now formulated consistently for all (finite-dimensional) s-parametrized phase-space representations. Our results pave the way for innovative tomography schemes applicable to finite-dimensional quantum states.

CHAPTER 3

Time evolution of coupled spin systems in a generalized Wigner representation

3.1 Foreword to Chapter 3

This chapter is based on the manuscript [159] and discusses continuous phase-space representations for coupled spins and their time evolution. This work can therefore be viewed as an extension of the single spin approach form Chapter 2 to the far-reaching scenario of coupled spins. We first discuss related literature on phase-space representations of finite-dimensional quantum systems in detail and our motivation for considering the case of coupled, distinguishable spins. In particular, we construct continuous, spherical Wigner functions for an arbitrary system of N distinguishable spins J. These phase-space representations have the advantage that they allow for natural visualizations of abstract, quantum-mechanical operators of coupled spin systems. We describe a procedure to visualize the high-dimensional structure of coupled spin Wigner functions in the form of spherical plots. We then systematically develop a star product approach for an arbitrary number of coupled spins $1/2$, which then allows for determining their time evolution directly in phase space. We detail the special cases of one, two and three coupled spins in detail with explicit equations. Our approach of calculating time evolutions is illustrated on simple spin systems using multiple examples which are relevant in, e.g, quantum information processing or NMR spectroscopy. We finally discuss properties of these coupled spin Wigner functions.

3.1.1 Connection to rotated parity operators and to Chapter 2

Result 3.1, as described later in this chapter, states the spherical Wigner function of N coupled spin J as the expectation value of a kernel operator which depends on $2N$ spherical variables. Result 3.1 can therefore be considered as a generalization of the single-spin Wigner function from Result 2.1 that is obtained for the special case $s = 0$. We now relate these two results by defining general s-parametrized phase-space representations for N coupled spins J (with identical J, but its generalization to non-identical J is straightforward).

Theorem 3.1. *The s-parametrized phase-space representation of an arbitrary operator A of N coupled spins J is denoted by $F_A(s,\Omega)$ and depends on the spherical coordinates $\Omega := (\theta_1, \phi_1, \ldots, \theta_N, \phi_N)$. It is given by the expectation value of the rotated parity operator $\mathcal{M}_s := \bigotimes_{k=1}^{N} M_s$ from Result 2.1 via*

$$F_A(s,\Omega) := \mathrm{Tr}[A\,\mathcal{R}(\Omega)\mathcal{M}_s\mathcal{R}^\dagger(\Omega)], \tag{3.1}$$

where local rotations act on N spins $\mathcal{R}(\Omega) = \bigotimes_{k=1}^{N} \mathcal{R}(\theta_k, \phi_k)$.

This construction by definition satisfies the generalized Stratonovich postulates described in Appendix B.3.2 and is equivalent to Result 3.1 for the special case $s = 0$. Note that a similar form has been attained in Eq. (9) of [248] for Wigner functions ($s = 0$), which coincides with our results for the special case $s = 0$ and $J = 1/2$. However, for arbitrary spins J, results contained in [248] are in fact linearly shifted Q functions ($s = -1$) and, therefore, do not satisfy the Stratonovich postulates. Since convolutions from Result 2.2 are reversible, phase-space representation, such as Q functions can be easily translated to Wigner functions or to density operators, and an equivalent procedure is described in Sec. VII of [221] to overcome this difficulty. The follow-up [222] finally considers the single spin-J Wigner function from previous works, e.g., [253, 47, 78].

Note that the coupled spin-J phase-space representations in Theorem 3.1 naturally recover their infinite-dimensional analogues, as coupled harmonic oscillator phase-spaces, in the large-spin limit due to Result 2.1.

3.1.2 List of Symbols in Chapter 3

symbol	description
J	spin number: related to dimension $d = 2J + 1$
d	dimension of the quantum system (and of Hilbert space) with $d = 2, 3, \ldots$
N	number of coupled spins
ρ	quantum state as a density operator (positive semidefinite and unit trace)
$\mathcal{H}$	Hamilton operator
(θ, ϕ)	spherical coordinates
$\mathcal{W}(A)$	Wigner transformation of the operator A
$\mathcal{W}^{-1}[f(\theta,\phi)]$	inverse Wigner transformation of a spherical function
W_ρ	Wigner function of a quantum state ρ
$W_\mathcal{H}$	Wigner function of a Hamiltonian $\mathcal{H}$
$[W_\mathcal{H}, W_\rho]_\star$	star commutator of two Wigner functions
$W_A \star W_B$	star product of Wigner functions of operators A and B
$\{\cdot,\cdot\}$	Poisson bracket
$\{\cdot,\cdot\}^{\{i\}}$	Poisson bracket that acts on coordinates (θ_k, ϕ_k)
$\lvert\alpha\rangle$	spin-up state of a spin $1/2$: corresponds to the vector $(1,0)^T$
$\lvert\beta\rangle$	spin-down state of a spin $1/2$: corresponds to the vector $(0,1)^T$
${}^J I_\eta$	angular momentum operators with $\eta = x, y, z, +, -$ for a spin J
I_η	angular momentum operators with $\eta = x, y, z, +, -$ for a spin $1/2$
I_α	projection operator onto the spin-up state via $\lvert\alpha\rangle\langle\alpha\rvert$
I_β	projection operator onto the spin-down state via $\lvert\beta\rangle\langle\beta\rvert$
$I_{k\eta}$	spin-$1/2$ operator with $\eta = x, y, z, +, -, \alpha, \beta$ that acts on the kth spin
$\mathcal{L}$	angular momentum differential operator as $(\mathcal{L}_x, \mathcal{L}_y, \mathcal{L}_z)$
$\mathcal{L}^2$	square of the angular momentum differential operator: its eigenfunctions are spherical harmonics
${}^J\mathrm{T}_{jm}$	tensor operators with $0 \le j \le 2J$, $-j \le m \le j$ for a spin J
T_{jm}	tensor operators with $0 \le j \le 1$, $-j \le m \le j$ for a spin $1/2$
${}^J\mathrm{T}^{\{k\}}_{jm}$	tensor operator ${}^J\mathrm{T}_{jm}$ embedded in an n-spin system with $k \in \{1, \ldots, N\}$
N_J	prefactor in the equations $\mp N_J {}^J I_\pm = {}^J\mathrm{T}_{1,\pm1}$ and $N_J\sqrt{2}\,{}^J I_z = {}^J\mathrm{T}_{1,0}$
$C^{jm}_{j_1 m_1, j_2 m_2}$	Clebsch-Gordan coefficients of angular momentum
Y_{jm}	spherical harmonics with $-j \le m \le j$
R	parameter in the Poisson bracket and its value is $R = \sqrt{3/(8\pi)}$
$\mathcal{P}^{\{k\}}$	projection onto spherical harmonics $\mathrm{Y}_{jm}(\theta_k, \phi_k)$ of rank 0 and 1
$\mathcal{P}^{\{1\ldots N\}}$	projection in all subspaces via the product $\prod_{k=1}^N \mathcal{P}^{\{k\}}$
$W_A \star W_B$	prestar product, i.e., star product before truncation
$\Delta_J(\theta,\phi)$	kernel operator used for the Wigner transformation of a spin J
$\Delta_J^{\{1\ldots N\}}$	kernel operator for N coupled spins J
$\star^{\{k\}}$	prestar product that acts on coordinates (θ_k, ϕ_k)

3.2 Summary

Phase-space representations as given by Wigner functions are a powerful tool for representing the quantum state and characterizing its time evolution in the case of infinite-dimensional quantum systems and have been widely used in quantum optics and beyond. Continuous phase spaces have also been studied for finite-dimensional quantum systems such as spin systems. However, much less is known for finite-dimensional, *coupled* systems, and we present a complete theory of Wigner functions for this case. In particular, we provide a self-contained Wigner formalism for describing and predicting the time evolution of coupled spins which lends itself to visualizing the high-dimensional structure of multi-partite quantum states. We completely treat the case of an arbitrary number of coupled spins $1/2$, thereby establishing the equation of motion using Wigner functions. The explicit form of the time evolution is then calculated for up to three spins $1/2$. The underlying physical principles of our Wigner representations for coupled spin systems are illustrated with multiple examples which are easily translatable to other experimental scenarios.

3.3 Introduction

Prior to the emergence of quantum mechanics, geometric intuition played a particularly strong role in the formulation of classical physics. Breaking with this tradition, quantum mechanics is often formulated abstractly by Hilbert-space operators such as the density operator describing the quantum state or the Hamiltonian corresponding to the total energy of the system. The demand for an intuitive formulation of quantum mechanics has driven the development of the so-called Wigner-Weyl formalism [259, 260, 261, 262] which is equivalent to other formulations of quantum mechanics, but its phase-space approach mirrors the classical phase space. Moreover, the time evolution of these quantum systems can be entirely characterized on the level of Wigner functions [118, 195] and in a similar fashion as the evolution of a statistical ensemble of classical particles.

Similar as quantum systems with an infinite-dimensional Hilbert space as studied in quantum optics, the Wigner formalism for describing the time evolution on a continuous phase space has been extended to finite-dimensional quantum systems such as spins (see Sec. 3.3.2). However, much is less is known for finite-dimensional, *coupled* systems. We present a complete theory of Wigner functions applicable to arbitrary density matrices and operators of coupled spin systems. In particular, we specify Wigner functions for operators of arbitrary coupled spin systems, i.e., systems that consist of an arbitrary number of coupled spins J. Furthermore, we address the following questions for coupled quantum systems: How does the Wigner function of a quantum state evolve in this case? Given the Wigner function of a Hamiltonian, how can one predict the Wigner function of a quantum state at a later time without relying on explicit matrices?

In finite-dimensional quantum systems, so far only the Wigner formalism for systems consisting of uncoupled spins has been fully developed and only special results for systems consisting of two coupled spins have been reported in the literature. Here we solve the open

question of how to exactly compute the time evolution of arbitrary coupled spin systems using a consistent Wigner frame that allows for natural visualizations (refer also to Sections 3.3.4 and 3.3.6). Our characterization of the time evolution relies on explicit partial derivatives of Wigner functions. Moreover, our Wigner representation is also suited for graphically visualizing the high-dimensional structure of multi-partite quantum states or operators in a compact and instructive form. This allows for geometric reasoning beyond matrix mechanics and provides a novel didactic approach complementary to matrix treatments of the time evolution.

As our results might be of interest to a wider audience, we present our work on several levels. Most importantly, the underlying physical principles are *first* highlighted through a set of illustrative examples for coupled spin systems, which are easily translatable to experimental approaches for realizing qubits in trapped ions, quantum dots, or superconducting circuits. This demonstrates that our novel approach for calculating the time evolution nicely conforms with conventional Hilbert-space quantum mechanics. Building on the intuition from the examples, we *then* develop and discuss the mathematical formulation of our Wigner representation coupled quantum systems and its time evolution in sufficient detail for facilitating theoretical extensions in the future. These theoretical advances on computing the time evolution for coupled quantum systems in a consistent Wigner frame constitute our central results.

We continue this introduction by first reviewing basic properties of Wigner functions of infinite-dimensional quantum systems which will motivate and guide our approach. Then, we summarize results from the literature for both Wigner functions and visualization techniques of finite-dimensional quantum systems. Finally, before starting the main text, we provide a summary of our results, motivate them further, and outline the structure of this work.

3.3.1 Wigner functions of infinite-dimensional quantum systems

Even though we almost exclusively focus on Wigner functions of finite-dimensional quantum systems such as spin systems, we will shortly review how the time evolution is established for Wigner functions of infinite-dimensional quantum systems. This will also set the stage for related techniques in the finite-dimensional case. In general, quantum mechanics describes how the quantum state evolves under the action of a Hamiltonian and there are at least three independent approaches to this description: the Hilbert-space formalism relying on matrices and operators [61], the path-integral method [93], and the Wigner phase-space approach [53, 131, 149, 165, 97, 266, 232, 227, 62].

We consider here the latter approach which particularly eases the comparison with classical mechanics. Groenewold [118] and Moyal [195] formalized quantum mechanics as a statistical theory on a classical phase space by associating the density operator in the Hilbert space with a function on the phase space and interpreting this correspondence as the inverse of the Weyl transformation [259, 260, 261]. In particular, the density operator ρ can be represented by a Wigner function [262] $W_\rho(x,p)$ which constitutes a quasiprobability function in classical phase-space coordinates x and p. A general framework for this theory was given by Bayen *et al.* [25, 26].

More precisely, the Wigner formalism represents the density operator ρ of an infinite-dimensional quantum system as the Fourier transformation (cf. p. 68 in [227])

$$W_\rho(x,p) = \mathcal{W}(\rho) = 1/(2\pi h) \int_{-\infty}^{\infty} \tilde{\rho}(x,\xi) \exp(-ip\xi/h)\, \mathrm{d}\xi,$$

where $\tilde{\rho}(x,\xi)$ is given by $\langle x + \xi/2|\rho|x - \xi/2\rangle$, $\mathcal{W}(\rho)$ denotes the Wigner transformation of ρ, and h is the Planck constant. The Wigner function $W_\rho(x,p)$ is real, normalized (i.e., $\int W_\rho(x,p)\, \mathrm{d}x\, \mathrm{d}p = \mathrm{Tr}(\rho) = 1$), and bounded (i.e., $-2/h \leq W_\rho(x,p) \leq 2/h$). Integrating $W_\rho(x,p)$ over the variable p results in the quantum-mechanical probability densities $P(x)$ in the coordinate x, and *vice versa* if x and p are exchanged. More generally, an arbitrary operator A is associated with its Wigner function $W_A(x,p)$, and the quantum-mechanical expectation value $\langle A\rangle = \int W_\rho(x,p) W_A(x,p)\, \mathrm{d}x\, \mathrm{d}p$ is then computed as a classical, statistical average over phase-space distributions.

In the Hilbert-space formalism, a quantum state is described by the density operator ρ and its time evolution is governed by the von-Neumann equation

$$i\frac{\partial \rho}{\partial t} = [\mathcal{H}, \rho] := \mathcal{H}\rho - \rho\mathcal{H} \tag{3.2}$$

where $\mathcal{H}$ denotes the Hamiltonian of the quantum system. The time evolution of a Wigner function can be directly calculated in the phase-space representation by introducing a so-called star product [118, 25, 26], which mimics the Wigner function $\mathcal{W}(AB) = W_A(x,p) \star W_B(x,p)$ of the product AB of Hilbert space operators. The appropriate form of the star product $\star = \exp(i\hbar\{\cdot,\cdot\}/2)$ was given by Groenewold [118] where $\{\cdot,\cdot\} = \overleftarrow{\partial}_x \overrightarrow{\partial}_p - \overleftarrow{\partial}_p \overrightarrow{\partial}_x$ is the Poisson bracket known from classical physics (cf. Vol. 1, §42 in [163]). As an important consequence reflecting a classical equation of motion, the time evolution of a Wigner function is given by (see Eq. (10) in [266])

$$i\hbar\frac{\partial W_\rho}{\partial t} = [W_\mathcal{H}, W_\rho]_\star := W_\mathcal{H} \star W_\rho - W_\mathcal{H} \star W_\rho. \tag{3.3}$$

and can be determined as an expansion series in $\hbar$, whose first term is given by the Poisson bracket $\{W_\mathcal{H}, W_\rho\}$. The Wigner formalism and its star product for infinite-dimensional quantum systems are well established and widely used in quantum optics and beyond. Along with what is known for the star product of finite-dimensional quantum systems (see Sec. 3.3.2), it is our aim to develop an analogous theory leading to a version of a differential star product for *coupled* spin systems which is comparable to the one in Eq. (3.3).

3.3.2 Prior work on Wigner functions of finite-dimensional quantum systems

Fundamental postulates for phase-space representations of finite-dimensional quantum systems were proposed by Stratonovich [243] (see B.3.1), and these build the foundations for Wigner functions of finite-dimensional quantum systems. Reflecting the translational covariance of Wigner functions of infinite-dimensional quantum systems, one of these postulates

Table 3.1: Results from the literature for the Wigner formalism of N spins with spin number J. Explicit references are given for the Wigner transformation $\mathcal{W}(A)$, the star product $f \star g$, and the equation of motion $\partial W_\rho/\partial t$. Cases not considered in the literature are left blank.

N	Descr.	Arb. J (incl. $J = 1/2$)
$N = 1$	$\mathcal{W}(A)$	Eq. (2.14) in [253] + Eq. (3.29) in [47]
	$f \star g$	[151]
	$\partial W_\rho/\partial t$	[a] [b]
$N = 2$	$\mathcal{W}(A)$	Eq. (30) in [152]
	$f \star g$	
	$\partial W_\rho/\partial t$	[c]
Arb. N	$\mathcal{W}(A)$	[d]

[a] Equation (61) in [151] states the equation of motion for the limit of $J \to \infty$ using only the Poisson bracket.

[b] Equation (5.13) in [253] provides the equation of motion of a spin J for linear Hamiltonians using only the Poisson bracket.

[c] The semiclassical equation of motion (for $J \gg 1$) is computed for a particular Hamiltonian ($\chi I_{1z} I_{2z}$) in Eq. (34) of [152] and conforms with our results shown in Sec. 3.4.2.2.

[d] Phase-space representations are given in terms of the so-called displaced parity operator for a single spin J (see Eq. (8) in [248]) and for N coupled spins $1/2$ (see Eq. (9) in [248]). However, our Result 3.1 for coupled spins-J differs from the approach of [248]: we view their Wigner function as a linearly shifted Q function $aQ_\rho - b$ (for $J > 1/2$), which also relaxes the Stratonovich postulates (iiia) and (iiib) from B.3.

states that the Wigner function has to transform naturally under rotations. The rotational covariance constrains continuous Wigner representations of spins into a spherical coordinate systems. The resulting Wigner functions can then be given by linear combinations of spherical harmonics, which offers a convenient tool for visualizing spins (see Sec. 3.3.4).

The Wigner transformation of single-spin operators was developed by Várilly and Gracia-Bondía [253] and was then further extended by Brif and Mann [46, 47]. In particular, [253] provides an explicit formula for the Wigner transformation for a single spin J, which satisfies the Stratonovich postulates. This formula uses a rank-j-dependent kernel which is based on mapping transition operators $|Jm\rangle\langle Jm'|$ onto their corresponding Wigner functions $W_{|Jm\rangle\langle Jm'|}$; the connection between tensor operators ${}^J\mathrm{T}_{jm}$ and spherical harmonics Y_{jm} was also mentioned. A more general kernel for the continuous phase-space representation of a single spin was stated in [46, 47]. It defines Wigner functions of tensor operators ${}^J\mathrm{T}_{jm}$ of single spins as the corresponding spherical harmonics Y_{jm}. We build on these results in Sec. 3.5.2 while also unifying normalization factors.

Parallel to our work, a general approach for phase-space representations was proposed in [248] which is based on the so-called displaced parity operator [34]. The explicit form of the transformation kernel is computed for the special cases of a single spin J (see Eq. (8) in [248]) and for N coupled spins $1/2$ (see Eq. (9) in [248]). This also mostly conforms with our results on spin Wigner functions and fulfills the covariance property under local operations.

However, our results differ from the approach of [248] since we view their Wigner function as a linearly shifted Q function $aQ_\rho - b$ (for $J > 1/2$), which also relaxes the Stratonovich postulates (iiia) and (iiib) from B.3.

Complementing the star-product formalism in the infinite-dimensional case, Várilly and Gracia-Bondía [253] discuss both the integral and differential form of a (twisted) star product of Wigner representations in finite dimensions. Carrying out explicit calculations for particular Hamiltonians (containing only I_x, I_y, I_z [85]) they conclude that in this case a stronger version of the Ehrenfest theorem holds for the equation of motion. Namely the time evolution is exactly given by the Poisson bracket known from classical physics.

Klimov and Espinoza [151] determined an exact form of the differential star product for an arbitrary spin number J. This star product is a sum of a pointwise product of two functions and combinations of derivatives with respect to spherical coordinates. The method also requires a rank-j-dependent correction in the spherical-harmonics decomposition which defines the Wigner function, as well as the truncation of the maximal rank j. For the restriction of their expression to a spin number of $1/2$, the calculation of the star product is more complicated then in the current paper (details for generalizing our approach to an arbitrary spin number J are discussed in the follow-up [161]), however, the derived equation of motion results in the Poisson bracket [150], just as in [253] and in the current paper. Similarly, the results of [115] contain spherical functions in a particular limit in which the star commutator is given by the Poisson bracket. For the case of a global $\mathrm{SU}(2)$-dynamical symmetry, a Wigner representation and its corresponding star product was developed in [154] along the lines of [151], leading to a representation which is not unique in the general case of coupled spins (without global $\mathrm{SU}(2)$ symmetry). See Table 3.1 for a summary of results known in the literature. We contrast our work to other selected Wigner representations for finite-dimensional quantum systems in Sec. 3.3.6.

3.3.3 Discrete Wigner functions

Several approaches [263, 170, 101, 92] exist to construct a discrete analog of Wigner functions for finite-dimensional quantum systems (see Table 1 in [92]). For example, Wootters [263] proposed a discrete Wigner function by introducing a discrete phase space on a discrete square grid of $p \times p$ points for each Hilbert space of prime dimension p. For composite systems such as coupled spins, the Hilbert space is composed of subsystems of prime dimension and the corresponding discrete phase space contains a Cartesian product of discrete square grids of prime dimension. The Wigner function is finally defined over this grid and forms a flat, but discretized analogue of the continuous classical phase space. The negativity of discrete and general Wigner functions will be discussed in the conclusion (see Sec. 3.8).

As discrete Wigner functions are not discussed in the main text, we shortly contrast them with our approach of finite-dimensional (continuous) Wigner functions for coupled quantum systems. Building on the work of Stratonovich [243], we obtain a spherical phase space which features continuous spherical functions as Wigner functions. In contrast, discrete Wigner functions on a square grid exhibit a considerable different geometry. In particular,

the continuous degrees of freedom of our finite-dimensional Wigner representation allow us to describe the time evolution in terms of partial derivatives of Wigner functions leading to a differential form of the star product as an analog to the infinite-dimensional case in Eq. (3.3). This differential picture is not entirely natural for discrete Wigner functions, and therefore integral forms of the time evolution are usually considered in the discrete case (cf. [185]).

3.3.4 Visualization techniques for spins

There are numerous approaches for visualizing finite-dimensional quantum systems. Feynman *et al.* [94] represents operators in a two-level quantum system using three-dimensional (real) vectors which can be interpreted as a Bloch vector, field vector, or rotation vector. This representation is widely used in many fields, including magnetic resonance imaging [31, 85] and spectroscopy [85] or quantum optics [227].

As in the present work, spin operators (as tensor operators [209]) have often been represented and visualized by spherical harmonics [136]. In early work by Pines *et al.* [207], selected density operator terms of a spin-1 particle are illustrated using spherical harmonics, see also [124, 224]. Quantum states of a collection of indistinguishable two-level atoms are depicted by Wigner functions in Dowling *et al.* [78]. We also refer to similar illustrations in [138]. Single-spin systems are visualized in [206] using spherical harmonics while stressing applications in nuclear-magnetic resonance. The appendix of [206] also discusses whether their method could be extended to coupled spins. Certain restricted cases of two coupled spins were considered in [191]. Harland *et al.* [128] introduces a method for visualizing particular states in two- and three-spin systems.

A general method for representing and visualizing arbitrary operators of coupled spin systems was proposed in [98]: This so-called DROPS representation establishes a bijective mapping between operators and spherical functions by mapping tensor operators to spherical harmonics. Important features as symmetries under simultaneous rotations or certain permutations and the set of involved spins are preserved and highlighted in its pictorial presentation. We discuss relations to our visualization method in B.4.

The theoretical methods used in [248] (as discussed in Sec. 3.3.2) also yield a visualization technique for finite-dimensional coupled quantum systems, which is covariant under rotations as in this work. For single spins, their approach (see Fig. 1(a)-(c) in [248]) is comparable to [98] and this work. However for coupled spins, [248] depicts only slices of their high-dimensional Wigner functions (see Figure 1(d)-(f) and Figure 2 in [248]). In our representation, high-dimensional Wigner functions are visualized by decomposing them into sums of product operators.

3.3.5 Summary of results

We will now summarize and discuss our results for finite-dimensional coupled quantum systems, while emphasizing the mathematical and theoretical advances contained in Sec. 3.5. The current work systematically develops a generalized Wigner formalism for the case of finite-dimensional coupled quantum systems. Most importantly, we solve the open question

of how to exactly compute the time evolution of coupled quantum systems using a consistent Wigner frame frame that allows for natural visualizations. In particular, our results include (see also Table 3.2):

- the Wigner function $W(\theta_1, \phi_1, \ldots, \theta_N, \phi_N)$ in Result 3.1 which represents arbitrary operators of N coupled, distinguishable qudits ($d = 2J+1$) or spins J;
- the particular explicit form of the exact, differential star product in Result 3.2 for the Wigner function of a single qubit or spin $1/2$ (the general case of a single spin J is treated in the follow-up [161]);
- the explicit and exact differential star product in Result 3.3 for the Wigner function $W(\theta_1, \phi_1, \ldots, \theta_N, \phi_N)$ of N coupled, distinguishable qubits or spins $1/2$ (the general case of spins J is discussed in the follow-up [161]);
- the simplified forms of Result 3.3 for two ($N = 2$) qubits or spins $1/2$ in Corollary 3.1 and three ($N = 3$) qubits or spins $1/2$ in Corollary 3.3;
- the explicit and exact differential equation of motion in Result 3.4 for the Wigner function $W(\theta_1, \phi_1, \ldots, \theta_N, \phi_N)$ of N coupled, distinguishable qubits or spins $1/2$ (the general case of spins J is discussed in the follow-up [161]);
- the simplified forms of Result 3.4 for two ($N = 2$) qubits or spins $1/2$ in Corollary 3.2 and three ($N = 3$) qubits or spins $1/2$ in Corollary 3.4;
- the simplified form of Result 3.4 for N coupled, distinguishable qubits or spins $1/2$ and a system Hamiltonian that contains at most pairwise interactions in Corollary 3.5.

It is our goal to describe the time evolution of these coupled systems only using Wigner functions and not relying on operators or matrices. Wigner functions of coupled quantum systems can be uniquely characterized using multiple spherical coordinates θ_k and ϕ_k. This leads to intricate, high-dimensional functions which are difficult to visualize. We resolve this difficulty and present an approach that decomposes a high-dimensional Wigner function into a linear combination of products of spherical harmonics, which can be conveniently visualized while highlighting crucial properties of coupled quantum systems. We denote our approach by the abbreviation PROPS which is assembled from the letters of "product operators." We emphasize that a given high-dimensional Wigner function has usually multiple different but equivalent PROPS representations.

Even though the visualization in the PROPS representation might require in general exponentially many terms as the number N of spins grows, the Wigner function is still uniquely characterized by a single $2N$-variate function (see Result 3.1). This necessary exponential scaling might limit plotting to a moderate number of spins. However, visualizing the dynamics of even a moderate number of spins is useful for many active areas of research and education, such as quantum information processing [197] or magnetic resonance [85]. This visualization technique will allow us, for example, to explore the underlying mechanisms of efficient experimental control schemes [104]. We want to also stress that the potential

Table 3.2: Results presented in this work for the Wigner formalism of N coupled spins with spin number J. Explicit references are given for the Wigner transformation $\mathcal{W}(A)$, the star product $f \star g$, and the equation of motion $\partial W_\rho/\partial t$. Cases not considered here are left blank.

N	Descr.	$J = 1/2$	Arb. J
$N = 1$	$\mathcal{W}(A)$		Eq. (3.25)
	$f \star g$	Result 3.2	
	$\partial W_\rho/\partial t$	Eq. (3.54)	[a]
$N = 2$	$\mathcal{W}(A)$		Sec. 3.5.5.1
	$f \star g$	Corollary 3.1	
	$\partial W_\rho/\partial t$	Corollary 3.2	
$N = 3$	$\mathcal{W}(A)$		Sec. 3.5.5.2
	$f \star g$	Corollary 3.3	
	$\partial W_\rho/\partial t$	Corollary 3.4[b]	
Arb. N	$\mathcal{W}(A)$		Result 3.1
	$f \star g$	Result 3.3	
	$\partial W_\rho/\partial t$	Result 3.4[b]	

[a] The case of linear Hamiltonians is considered in Eq. (3.55).
[b] A simplified form for natural Hamiltonians with linear and bilinear terms is given in Corollary 3.5.

plotting inefficiencies do not affect our main theory as presented in Sec. 3.5 as it directly operates on the defining $2N$-variate function (see Result 3.1). For a single spin-$1/2$ system, our Wigner functions are similar to the Bloch vector (cf. Sec. 3.3.4). But even in this simple case, our Wigner approach is more expressive and allows for a natural representation and visualization of non-hermitian operators as given by coherence order operators (see Fig. 3.12 below) which cannot be represented using a single Bloch vector. For coupled spins, our Wigner representation can be compared to a collection of Bloch vectors for the special cases shown in Figs. 3.7 and 3.8 below. However, our Wigner representation goes well beyond a simple collection of Bloch vectors as the number of elements in the linear decomposition for the PROPS representation is in general not constant (see Figs. 3.5 and 3.10 below).

Our characterization of the time evolution leads to a self-contained theory of finite-dimensional quantum systems, while we focus in this work mainly on coupled spins $1/2$. The determination of the correct star product for coupled spins $1/2$ constitutes the cornerstone of our approach for providing a replacement of the von-Neumann equation applicable to Wigner functions. The explicit equation of motion is calculated for an arbitrary number of coupled spins $1/2$ in Result 3.4 and discussed separately for the particular case of natural coupling Hamiltonians in Corollary 3.5. Refer to Table 3.2 for an overview of the results presented in the current work. Further details for a single spin J and coupled spins are respectively summarized in following Sections 3.3.5.1 and 3.3.5.2.

3.3.5.1 Results for a single spin J

A single-spin operator A is mapped to a Wigner function $W_A(\theta, \phi)$ by decomposing A into a linear combination of tensor operators which can be directly mapped to spherical harmonics (see Sec. 3.5.2), and the corresponding Wigner transformation is stated in Eq. (3.25). For specifying the time evolution of Wigner functions, one needs to introduce the star product $W_A \star W_B$ of Wigner functions W_A and W_B which is defined by its relation to the Wigner function $W_{AB} = W_A \star W_B$ of a product of operators A and B (see Sec. 3.5.2.3). There are two approaches to compute the star product. The first approach is known as the integral star product and relies on an integral transformation of the functions W_A and W_B using a so-called trikernel [253], and we detail this form in B.6 for a single spin J.

The second approach features a differential form which is more convenient for computations. This differential star product relies on the partial derivatives of the corresponding Wigner functions W_A and W_B, which is comparable to the infinite-dimensional case discussed in Sec. 3.3.1. We calculate this new differential form of the exact star product for a single spin $1/2$ in Result 3.2: it is a sum of a pointwise product $W_A W_B$ and the Poisson bracket $\{W_A, W_B\}$ followed by a projection. This form was not reported previously in the literature, and provides a simplified approach as compared to the results of [151] while its structure is similar to the structure of the infinite-dimensional star product. We also derive an algebraic expansion formula for the star product of spherical harmonics in general (see Sec. 3.5.3.1), paving the way for a generalization to an arbitrary spin number J (refer to the follow-up [161]). The explicit form of the star product determines the equation of motion for a single spin $1/2$ and we obtain a particularly simple form given by the Poisson bracket [see Eq. (3.54)].

We also point out connections to similar characterizations. The Poisson bracket is directly related to the canonical angular momentum operator $\mathcal{L} = r \times p$ which generates infinitesimal rotations of the sphere and is known from infinite-dimensional quantum mechanics (see Sec. 3.7.1). Even though spins have no classical counterparts, a classical description emerges from the quantum one in the limit of $J \to \infty$ as detailed in Sec. 3.7.2. This leads to a localized distribution and arbitrary large values in the Wigner function. Relations to Wigner functions of infinite-dimensional quantum systems are investigated in Sec. 3.7.2: the flat phase-space coordinates (p, q) known from classical mechanics are replaced with spherical phase-space coordinates $(R\cos\theta, \phi)$ for spins (see Section 3.7.2.1), and the resulting equation of motion given in Sec. 3.7.2.2 is formally equivalent to the one obtained in the main text [see Eq. (3.54)]. The star product for a single spin $1/2$ given in the main text can also be interpreted as a quaternionic product (see Sec. 3.7.3).

3.3.5.2 Results for coupled spins

The Wigner representation is generalized in Result 3.1 to an arbitrary number of coupled spins J by extending the formula for the Wigner transformation of product operators. We consider Wigner functions for coupled spins of identical spin number J, but a generalization to systems that are composed of particles of different spin number J is straightforward. The

Wigner functions for N coupled spins are defined on a spherical phase space of N spheres and have $2N$ coordinates of the form $R\cos\theta_k$ and ϕ_k. This setup satisfies the Stratonovich postulates of B.3.2, which includes the covariance under arbitrary local rotations, and generalizes the covariance under simultaneous spin rotations in [98].

The Wigner formalism for coupled spins $1/2$ is obtained by extending the differential star product to multiple spins in Result 3.3, and this also establishes the equation of motion, which we computed in Result 3.4 for an arbitrary number of coupled spins $1/2$. This allows us to describe the quantum properties as corrections to the classical case which are given in a finite power-series expansion. Truncations to this expansion could be used to characterize a semi-classical approximation. The equation of motion is then applied in Sec. 3.5.5 in order to derive its simplified form for up to three spins $1/2$. In Corollary 3.5, the simplified equation of motion for an arbitrary number of spins is explicitly given for the case of natural Hamiltonians containing only linear and bilinear operators.

3.3.6 Motivation

Let us now further motivate our approach by highlighting its benefits as well as crucial differences to other work in the context of Wigner functions (and phase-space representations). This discussion aims to clarify the choices made in this work.

The previous parts of this introduction have already emphasized our focus on coupled spin systems. In principle, their Wigner functions could be defined by interpreting the coupled spin system as a single spin with a large enough spin number and applying the Wigner function techniques for single spins as in [78] (similarly as discussed in Sec. 3.3.2 and 3.3.5.1). This would, however, neglect important features of coupled spin systems we want to *stress* in our approach such as symmetries under spin-local rotations or permutations of spins as well as spin-local properties of the quantum system (cf. p. 3 in [98]). This distinguishability of spins is of crucial importance in, e.g., quantum information processing [197] where local control is often assumed. These locality features are a focal point of our work and they critically depend on describing the system in a suitably chosen basis which highlights the underlying tensor-product structure. In this regard, Result 3.4 (see Sec. 3.5.4) provides a novel perspective of expanding the time evolution into its parts according to their degree of nonlocality. Therefore, our results for the time evolution of Wigner functions go well beyond the established theory for Wigner functions of single spins (see Sec. 3.3.2) and enable contributions into a significant new direction. And this aim to highlight nonlocality properties is quite natural as one can infer, for example, from work on matrix product states in many-body physics (see, e.g., [230, 203]) or, more generally, entanglement in quantum information (see, e.g., [197, 133, 121, 83]).

We want to also emphasize that—in the context of Wigner functions—this focus on coupled spin systems (and their locality features) emerged only recently [206, 191, 128, 98, 248] (refer to Sec. 3.3.4). The Wigner function for coupled spin systems is defined as a unique $2N$-variate function (see Result 3.1). Due to its high dimensionality, the Wigner function cannot be directly plotted in three dimensions, and one would have to resort to plotting slices

as discussed at the end of Sec. 3.3.4. This has motivated us to depict a Wigner function of N coupled spins using three-dimensional figures (without loss of information) which are denoted as the PROPS representation (see Sec. 3.3.5 and 3.4) and show decompositions into tensor-product operators. For a moderate number of coupled spins, our results can therefore be used as an analytic tool for characterizing the time evolution in application areas such as quantum information processing [197], magnetic resonance [85], or quantum control [104]. We want to emphasize that our plotting choice of using the PROPS representation does not affect the theory in Sec. 3.5 as it directly operates on the $2N$-variate function defining the Wigner function. All relevant operators in Sec. 3.5, including the star product, act linearly on its arguments resulting in completely natural PROPS plots. In addition, the PROPS representation stresses—as intended—important nonlocality features of the depicted Wigner function.

We recall that bosonic quantum systems (and similarly fermionic ones) demonstrate different characteristics as compared to coupled spin systems with distinguishable spins. Foremost, the dimensionality of a bosonic quantum system is polynomial in the number of particles while the dimensionality of a coupled spin system is exponential in the number of spins. Also, due its permutation symmetry, a bosonic system does not exhibit any localized properties and can be therefore (for a fixed number of particles) *naturally* embedded into a single spin with a large enough spin number (see [75, 241, 250, 178, 160, 223, 234]). As discussed above, the same does not apply to general coupled spin systems and one needs to be cautious in extending intuition from bosonic quantum systems to coupled spin systems considered in this work.

We further stress differences to other phase-space approaches by discussing recent work [225, 5, 72, 264] which approximately simulate quantum dynamics of lattice spin systems while relying on phase-space techniques. References [225, 5] employ discrete Wigner functions which are not considered in this work (see Sec. 3.3.3). References [72, 264] utilize techniques for infinite-dimensional (continuous) phase-space functions [234, 223, 50] (refer also to Sec. 3.3.1) in order to describe finite-dimensional quantum states. In [72], a continuous Wigner function for simulating quantum dynamics of *indistinguishable* qudits or spins J was constructed by applying Schwinger's oscillator representation of the special unitary group [55] and by mapping the resulting harmonic oscillators to their infinite-dimensional (planar) Wigner functions [50]. This eliminated non-linearities in the time evolution and enables efficient approximations of quantum dynamics of lattice spin-1 systems [72]. But it also has the drawback of an increased phase-space dimension, the loss of natural symmetries, and intertwined phase-space variables. In particular, the infinite-dimensional (planar) Wigner functions in [72] have $(2J{+}1)^2 - 1$ harmonic-oscillator phase-space variables $\alpha_1, \ldots, \alpha_{(2J+1)^2-1}$. They are easily contrasted to the finite-dimensional (spherical) Wigner functions in this work where any single spin J is represented using two independent variables θ and ϕ, while observing inherent rotational symmetries and leading to natural visualizations. Also, our approach makes it possible to consider infinite-dimensional Wigner functions as a natural limit of finite-dimensional (spherical) Wigner functions [160, 161]. Building on the approach of [72], infinite-dimensional (planar) Wigner functions have been used in [264]

to represent the state of a cluster of N strongly interacting, *distinguishable* qubits or spins $1/2$. The resulting Wigner function has, after a reduction of dimensionality, still exponentially many (i.e. 2^N) harmonic-oscillator phase-space variables $\alpha_1, \ldots, \alpha_{2^N}$. In contrast, our general $2N$-variate Wigner function for N coupled spins J requires only $2N$ phase-space variables $\theta_1, \phi_1, \ldots, \theta_N, \phi_N$ which naturally transform under rotations (and related visualization methods have been summarized above). Consequently, this comparison should further illustrate our motivation and how it differs from the one for [72, 264].

Finally, we want to clarify that this work does *not* provide any progress on reducing the complexity of simulating the time evolution of coupled spin systems. Long-standing complexity hypotheses suggest that simulating the time evolution of a coupled spin system with a classical computer should (in general) have an exponential complexity in the number of spins [197]. We believe that this applies to both matrix methods and Wigner-function techniques.

3.3.7 Structure of this work

Our work is structured as follows: We start in Sec. 3.4 with a set of introductory examples which establish and illustrate the main ideas of our Wigner formalism for spins. The theoretical methods that form the central results of this work are detailed in Sec. 3.5 where the Wigner transformation of coupled spin operators and their star product are developed; later parts of this work can be read first as they do not explicitly depend on the detailed argument contained in Sec. 3.5. In Sec. 3.6, we apply our methods to advanced examples further exploring the Wigner formalism in the case of two and three coupled spins and also considering the creation of entanglement. We discuss connections to other important concepts in Sec. 3.7 which includes the quantum angular momentum, the infinite-dimensional Wigner formalism, quaternionic Wigner functions, and the evolution of non-hermitian states. We conclude in Sec. 3.8, and certain details are deferred to appendices.

3.4 Introductory examples

Our approach to directly determine the time evolution of a quantum system using Wigner functions is now illustrated with concrete examples, while the corresponding theory is detailed in Sec. 3.5 below. We start in Sec. 3.4.1 with the case of a single spin $1/2$ and juxtapose the well-known matrix method with our Wigner function approach. We also analyze the case of two coupled spins $1/2$ (see Sec. 3.4.2) and consider in particular the time evolution under a scalar coupling.

More advanced examples are deferred to Sec. 3.6 considering the evolution of two coupled spins $1/2$ under the CNOT gate (see Sec. 3.6.1), and the evolution of three coupled spins $1/2$ (see Sec. 3.6.2). Recall that in all these cases the von-Neumann equation (see Eq. 3.2) determines the time evolution of the density operator by specifying its time derivative.

3.4.1 Time evolution of a single spin

3.4.1.1 Evolution of the density operator

A simple example is presented which considers the precession of a single spin 1/2 in an external magnetic field. Here, explicit matrices are used, and these are decomposed into irreducible tensor operators. In Sec. 3.4.1.2, the time evolution is then computed directly in the Wigner representation. Recall the irreducible tensor operators [85]

$$\mathrm{T}_{00} := \tfrac{1}{\sqrt{2}}\mathrm{Id}_2 = \tfrac{1}{\sqrt{2}}\begin{pmatrix}1 & 0\\ 0 & 1\end{pmatrix}, \quad \mathrm{T}_{1,-1} := I_- = \begin{pmatrix}0 & 0\\ 1 & 0\end{pmatrix}, \tag{3.4a}$$

$$\mathrm{T}_{10} := \sqrt{2}I_z = \tfrac{1}{\sqrt{2}}\begin{pmatrix}1 & 0\\ 0 & -1\end{pmatrix}, \quad \mathrm{T}_{11} := -I_+ = \begin{pmatrix}0 & -1\\ 0 & 0\end{pmatrix} \tag{3.4b}$$

for the case of a single spin $1/2$. For arbitrary spin number J, the definition of tensor operators ${}^J\mathrm{T}_{jm}$ is based on their commutation relations

$$[{}^J I_z, {}^J\mathrm{T}_{jm}] = m\,{}^J\mathrm{T}_{jm} \;\text{ and }\; [{}^J I_\pm, {}^J\mathrm{T}_{jm}] = \sqrt{(j \mp m)\,(j \pm m + 1)}\,{}^J\mathrm{T}_{j,m\pm1}, \tag{3.5}$$

as described by Racah [209], where ${}^J I_z$ and ${}^J I_\pm = {}^J I_x \pm i\,{}^J I_y$ are representations of arbitrary spin-J operators;[1] the index J is dropped in the spin-$1/2$ case.

An arbitrary spin-1/2 density matrix can be written as $\rho = r_0\,\mathrm{Id}_2 + \sum_\alpha r_\alpha I_\alpha$, with $\alpha \in \{x, y, z\}$. Even though our Wigner representation is completely general and applicable to arbitrary density matrices and operators, we omit the identity part $r_0\,\mathrm{Id}_2$ in some of the following examples without affecting the time evolution and continue our discussion considering only the second term $\sum_\alpha r_\alpha I_\alpha$. This term is usually referred to as the deviation density matrix in quantum information processing (cf. Eq. 7.166 on p. 336 in [197] or Eq. 2.5.13 on p. 47 in [201]) or as partial density matrix in magnetic resonance (cf. Eq. 6 in [88], Eq. 2.125 on p. 55 in [54], or p. 243 in [3]). Although this simplification is also valid for individual quantum systems (consisting of one or more coupled spins), it is especially useful when considering thermal ensemble states for sufficiently large temperatures, i.e. for $r_0 \gg \sqrt{\sum_\alpha r_\alpha^2}$.

In our example, a rotation around the z axis with an angular frequency ω is generated by the Hamiltonian

$$\mathcal{H} = \omega I_z = \omega\tfrac{1}{\sqrt{2}}\mathrm{T}_{10}, \tag{3.6}$$

and the quantum state of a single spin at time $t = 0$ is chosen as the traceless deviation density matrix

$$\rho(0) = I_x = \tfrac{1}{2}\mathrm{T}_{1,-1} - \tfrac{1}{2}\mathrm{T}_{11}. \tag{3.7}$$

The time evolution is described by the von-Neumann equation, see Eq. (3.2), and the first time derivative $i\partial\rho(0)/\partial t$ is determined by the commutator

$$[\mathcal{H}, \rho(0)] = \tfrac{\omega}{2\sqrt{2}}[\mathrm{T}_{10}, \mathrm{T}_{1,-1}] - \tfrac{\omega}{2\sqrt{2}}[\mathrm{T}_{10}, \mathrm{T}_{11}] = -\tfrac{\omega}{2}\mathrm{T}_{1,-1} - \tfrac{\omega}{2}\mathrm{T}_{11} = i\omega I_y,$$

[1] As usual, the Cartesian spin operators are defined as $I_x = \sigma_x/2$, $I_y = \sigma_y/2$, and $I_z = \sigma_z/2$, where the Pauli matrices are $\sigma_x = \left(\begin{smallmatrix}0 & 1\\ 1 & 0\end{smallmatrix}\right)$, $\sigma_y = \left(\begin{smallmatrix}0 & -i\\ i & 0\end{smallmatrix}\right)$, and $\sigma_z = \left(\begin{smallmatrix}1 & 0\\ 0 & -1\end{smallmatrix}\right)$.

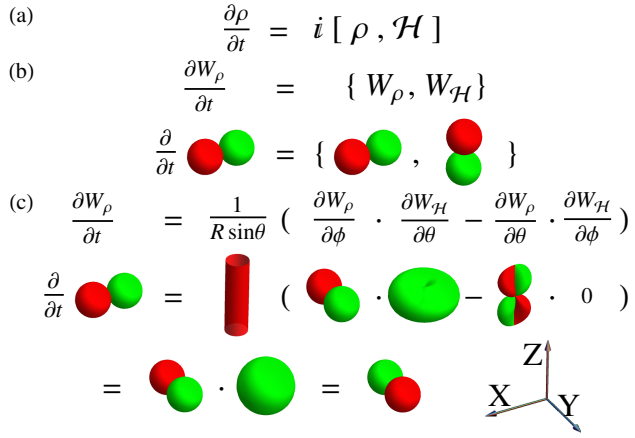

Figure 3.1: (Color online) (a) The equation of motion in the Hilbert space given by the von-Neumann equation. (b) The equation of motion of a single spin 1/2 in Winger space (upper row) and its graphical representation (lower row) in the particular case of $\mathcal{H} = \omega I_z$ with $\omega = 1$ and $\rho = I_x$. (c) Graphical representation of the Poisson bracket from (b). The spherical functions corresponding to the partial derivatives of the Wigner function $W_\rho = R\sin\theta\cos\phi$ and the Hamiltonian $W_\mathcal{H} = R\cos\theta$ are shown and $1/(R\sin\theta)$ is visualized as an infinitely long cylinder.[3]

whose form can also be inferred from the definitions in Eq. (3.5). The solution of this differential equation results in[2]

$$\rho(t) = \tfrac{1}{2}e^{i\omega t}\mathrm{T}_{1,-1} - \tfrac{1}{2}e^{-i\omega t}\mathrm{T}_{11} = \cos(\omega t)I_x + \sin(\omega t)I_y.$$

3.4.1.2 Evolution of the Wigner functions

Mirroring the preceding discussion in terms of matrices, the Hamiltonian $\mathcal{H}$ and the traceless deviation density matrix $\rho(0)$ from Eqs. (3.6)–(3.7) are mapped to their Wigner functions

$$W_\mathcal{H}(\theta,\phi) = \tfrac{\omega}{\sqrt{2}}\mathrm{Y}_{10} = \omega R\cos\theta \;\text{ and }\; W_\rho(\theta,\phi,t=0) = \tfrac{1}{2}(\mathrm{Y}_{1,-1} - \mathrm{Y}_{11}) = R\sin\theta\cos\phi \tag{3.8}$$

by replacing the tensor operators T_{jm} by the corresponding spherical harmonics $\mathrm{Y}_{jm} = \mathrm{Y}_{jm}(\theta,\phi)$ [136]. This basic example conforms with the general discussion in Sec. 3.5.2 [see Eq. (3.29)]; note that $R := \sqrt{3/(8\pi)}$.

Here, the Wigner function $W_A(\theta,\phi) = |W_A(\theta,\phi)|\exp[i\eta(\theta,\phi)]$ of a single spin is visualized in the following way: A surface is plotted whose surface element in the direction (θ,ϕ) is at a distance $|W_A(\theta,\phi)|$ from the origin. The complex phase factor $\exp[i\eta(\theta,\phi)]$ of the Wigner function is represented by the color of its surface element. This method visualizes spherical functions as three-dimensional shapes (see Figs. 3.1 and 3.2).

[2] Similarly as for $\rho(0)$, the time derivative of $\rho(t)$ decomposes into a linear combination of the tensor operators $\mathrm{T}_{1,-1}$ and T_{11}. It follows that the general solution can be parameterized as $\rho(t) = a(t)\,\mathrm{T}_{1,-1} - b(t)\,\mathrm{T}_{11}$ with $a(0) = b(0) = 1/2$. This formula is substituted back into the von-Neumann equation [see Eq. (3.2)] and yields $\partial[a(t)\mathrm{T}_{1,-1} - b(t)\mathrm{T}_{11}]/\partial t = i\omega[a(t)\mathrm{T}_{1,-1} + b(t)\mathrm{T}_{11}]$, which splits up into the equations $\partial a(t)/\partial t = i\omega a(t)$ and $\partial b(t)/\partial t = -i\omega b(t)$. Consequently, the solution is given by $a(t) = \exp(i\omega t)/2$ and $b(t) = \exp(-i\omega t)/2$.

[3] Hermitian operators result only in positive and negative values depicted as red (dark gray) and green (light gray).

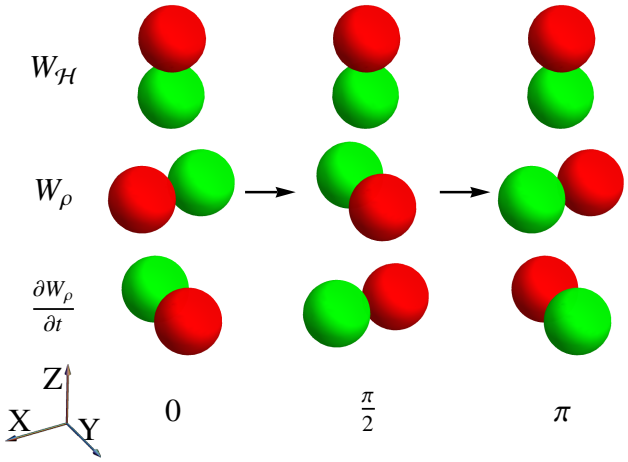

Figure 3.2: (Color online) Plots of the Wigner functions $W_{\mathcal{H}}$ of the Hamiltonian $\mathcal{H} = \omega I_z$ (upper row), W_ρ of the traceless deviation density matrix ρ (middle row), and the time derivative $\partial W_\rho(\theta,\phi,t)/\partial t$ (lower row) corresponding to $\partial\rho/\partial t$ at times $t = 0$, $\omega t = \pi/2$, and $\omega t = \pi$.[3]

The time evolution is governed by the shape of the appearing Wigner functions via its angular derivatives. The von-Neumann equation for a single spin $1/2$ translates in the Wigner representation to the equation (see Fig. 3.1)

$$\frac{\partial W_\rho(\theta,\phi,t)}{\partial t} = \{W_\rho(\theta,\phi,t)\ ,\ W_{\mathcal{H}}(\theta,\phi)\} = \frac{1}{R\sin\theta}\left(\frac{\partial W_\rho}{\partial\phi}\frac{\partial W_{\mathcal{H}}}{\partial\theta} - \frac{\partial W_\rho}{\partial\theta}\frac{\partial W_{\mathcal{H}}}{\partial\phi}\right). \tag{3.9}$$

The Poisson bracket $\{W_\rho(\theta,\phi,t), W_{\mathcal{H}}(\theta,\phi)\}$ is further detailed in Sec. 3.5.3. In our example, the time derivative at time $t = 0$ is given by

$$\frac{\partial W_\rho(\theta,\phi,0)}{\partial t} = \omega R^2\{\sin\theta\cos\phi, \cos\theta\} = \omega R\sin\theta\sin\phi. \tag{3.10}$$

Refer also to Figure 3.1 for a graphical representation of this particular example. The solution of the differential equation in Eq. (3.10) is given by[4]

$$W_\rho(\theta,\phi,t) = R\sin\theta[\cos(\omega t)\cos\phi + \sin(\omega t)\sin\phi]. \tag{3.11}$$

Figure 3.2 shows the Wigner function of the Hamiltonian and the density matrix evolving in time, including the time derivative of $W_\rho(\theta,\phi,t)$. All operators depicted in Figure 3.2 are hermitian and consequently only the colors red (dark gray) and green (light gray) appear, which correspond to positive and negative real values in their Wigner functions. Note how the shapes govern the rotation of $W_\rho(\theta,\phi,t)$ around the z axis. The state of a spin 1/2 can be characterized by the Bloch vector and the unitary time evolution translates to rotations of this three-dimensional vector. The Wigner function provides a description similar to the Bloch vector (refer to Section 3.7.3) and its time evolution, which is supported by the

[4] The Wigner function can be written as $W_\rho(\theta,\phi,t) = R\sin\theta[a(t)\cos\phi + b(t)\sin\phi]$ with $a(0) = 1$ and $b(0) = 0$. Substituting this parametrization back into Eq. (3.9), one derives the differential equation $\sin\theta[(\partial a(t)/\partial t)\cos\phi + (\partial b(t)/\partial t)\sin\phi] = \omega\sin\theta[a(t)\sin\phi - b(t)\cos\phi]$, which splits up into $\partial a(t)/\partial t = -\omega b(t)$ and $\partial b(t)/\partial t = \omega a(t)$.

Poisson bracket corresponds to the rotation of the Wigner function (refer to Section 3.7.1). Non-hermitian parts of the density operator are relevant for coherent spectroscopy [105] but cannot be represented by a single Bloch vector. The Wigner function, however, provides a natural way to represent, visualize, and predict the time evolution of these non-hermitian operators. An example describing the time evolution of non-hermitian spin states is detailed in Section 3.7.4.1.

3.4.2 Time evolution of two coupled spins

As discussed in Sec. 3.4.1, the Wigner function of single spin-$1/2$ states is similar to the Bloch-vector description, and the unitary time evolution translates to the rotation of these Wigner functions. For multiple, coupled spins the underlying quantum dynamics becomes significantly more involved, and the time evolution can in general not be fully characterized in terms of rotations of Bloch vectors (see Fig. 3.5 below). In contrast, the quantum state can still be represented uniquely by a single Wigner function which is visualized by its PROPS representation using a linear combination of products of spherical harmonics. The corresponding time evolution is governed by a generalization of the Poisson bracket. In the following example, we present one of the simplest examples where the Bloch vector picture breaks down. Even though the initial quantum state is representable by a Bloch vector, the time evolution creates a superposition of states (see Fig. 3.5 below).

3.4.2.1 Evolution of the density matrix

We consider now the time evolution for an example of two coupled spins $1/2$. Similarly as in Sec. 3.4.1, we first rely on explicit matrices, and our approach using Wigner functions is detailed in Sec. 3.4.2.2 below. In order to simplify and highlight the transformation to the Wigner space, we will subsequently differentiate between tensor operators acting on different spins: The linear operators $\mathrm{T}^{\{1\}}_{jm} = \mathrm{T}_{jm} \otimes \mathrm{T}_{00}$ and $\mathrm{T}^{\{2\}}_{jm} = \mathrm{T}_{00} \otimes \mathrm{T}_{jm}$ act respectively on the first and second spin, and they are constructed using a tensor product leading to four-by-four matrices. A bilinear operator $\mathrm{T}^{\{1\}}_{j_1 m_1} \mathrm{T}^{\{2\}}_{j_2 m_2}$ acts on both spins and consists of a matrix product of single-spin operators. Details on definitions and properties of product operators are deferred to Sec. 3.5.1 (see Table 3.4) and a short summary is given in B.1.

Let us now consider a system of two coupled spins which evolve under the bilinear Hamiltonian

$$\mathcal{H} = \pi\nu 2 I_{1z} I_{2z} = \pi\nu 2 \mathrm{T}^{\{1\}}_{10} \mathrm{T}^{\{2\}}_{10}, \tag{3.12}$$

which can arise from a heteronuclear scalar or dipolar coupling. Here, we have applied the notations $\mathrm{T}^{\{1\}}_{10} := \mathrm{T}_{10} \otimes \mathrm{T}_{00} = (\mathrm{T}_{10}/\sqrt{2}) \otimes (\sqrt{2}\mathrm{T}_{00}) = I_z \otimes \mathrm{Id}_2 = I_{1z}$ and $\mathrm{T}^{\{2\}}_{10} := \mathrm{T}_{00} \otimes \mathrm{T}_{10} = I_{2z}$ (see Sec. 3.5.1). In addition, we specify the traceless deviation density matrix at time $t = 0$ as

$$\rho(0) = I_{1x} = (\mathrm{T}^{\{1\}}_{1,-1} - \mathrm{T}^{\{1\}}_{11})/\sqrt{2}. \tag{3.13}$$

Table 3.3: Wigner representations of the identity as well as linear and bilinear Cartesian operators; $\lambda = R/\sqrt{2\pi}^{N-1}$ with $R = \sqrt{3/(8\pi)}$ and $a, b \in \{x, y, z\}$. The projection $I_{k\beta}$ onto the pure state $|\beta\rangle$ of a single spin is discussed in Sec. 3.6.1.1.

A	$\mathcal{W}(A)$	A	$\mathcal{W}(A)$
Id_{2^N}	$1/\sqrt{2\pi}^N$	$I_{k\beta}$	$1/(2\sqrt{2\pi}^N) - \lambda\cos\theta_k$
I_{kx}	$\lambda\sin\theta_k\cos\phi_k$	$I_{kx}I_{\ell x}$	$\sqrt{2\pi}^N\lambda^2\sin\theta_k\cos\phi_k\sin\theta_\ell\cos\phi_\ell$
I_{ky}	$\lambda\sin\theta_k\sin\phi_k$	$I_{kx}I_{\ell z}$	$\sqrt{2\pi}^N\lambda^2\sin\theta_k\cos\phi_k\cos\theta_\ell$
I_{kz}	$\lambda\cos\theta_k$	$I_{ka}I_{\ell b}$	$\sqrt{2\pi}^N\mathcal{W}(I_{ka})\mathcal{W}(I_{\ell b})$

Equation (3.2) determines the time differential $i\partial\rho(0)/\partial t$ as the commutator

$$[\mathcal{H}, \rho(0)] = -\sqrt{2}\pi\nu\,(\mathrm{T}^{\{1\}}_{1,-1}+\mathrm{T}^{\{1\}}_{11})\mathrm{T}^{\{2\}}_{10} = i\pi\nu 2I_{1y}I_{2z}.$$

One deduces that only the four tensor operators $\mathrm{T}^{\{1\}}_{11}$, $\mathrm{T}^{\{1\}}_{1,-1}$, $\mathrm{T}^{\{1\}}_{11}\mathrm{T}^{\{2\}}_{10}$, and $\mathrm{T}^{\{1\}}_{1,-1}\mathrm{T}^{\{2\}}_{10}$ can appear in the decomposition of $\rho(t)$, as $\partial^2\rho(0)/\partial t^2 \propto \rho(t)$.[5] Consequently, the time-dependent deviation density matrix can be written as

$$\rho(t) = a(t)A + b(t)B, \text{ where} \tag{3.14}$$
$$A = \tfrac{1}{\sqrt{2}}(\mathrm{T}^{\{1\}}_{1,-1}-\mathrm{T}^{\{1\}}_{11}) = I_{1x}, \quad B = \sqrt{2}(\mathrm{T}^{\{1\}}_{1,-1}+\mathrm{T}^{\{1\}}_{11})\mathrm{T}^{\{2\}}_{10} = 2I_{1y}I_{2z},$$

and $a(0) = 1$ and $b(0) = 0$. Substituting this back into Eq. (3.2), one obtains the solution[6]

$$\rho(t) = \cos(\pi\nu t)I_{1x} + \sin(\pi\nu t)2I_{1y}I_{2z}. \tag{3.15}$$

The detectable NMR signal is proportional to $\cos(\pi\nu t)$, and one obtains a doublet spectrum with equal intensities and lines separated by ν.

3.4.2.2 Evolution of Wigner functions

We switch now to the Wigner picture and explain shortly how product operators in a two-spin system are represented as Wigner functions, while details will be given in Sec. 3.5.2 below. Moreover, we translate the von-Neumann equation for two spins into the Wigner picture. This is then applied to the example of Sec. 3.4.2.1.

Wigner representations of operators acting on different spins are distinguished by different variables, thus an operator acting on the first spin is transformed to its Wigner function by mapping the basis states $\mathrm{T}^{\{1\}}_{jm}$ to their corresponding spherical harmonics $\mathrm{Y}^{\{1\}}_{jm}$ =

[5] Computing the second time derivative $-\partial^2\rho(0)/\partial t^2$ via the double commutator $[\mathcal{H}, [\mathcal{H}, \rho(0)]] = \pi^2\nu^2\rho(0)$ and applying the formulas $[\mathrm{T}^{\{1\}}_{10}\mathrm{T}^{\{2\}}_{10}, \mathrm{T}^{\{1\}}_{1,-1}\mathrm{T}^{\{2\}}_{10}] = -\mathrm{T}^{\{1\}}_{1,-1}/4$ and $[\mathrm{T}^{\{1\}}_{10}\mathrm{T}^{\{2\}}_{10}, \mathrm{T}^{\{1\}}_{11}\mathrm{T}^{\{2\}}_{10}] = \mathrm{T}^{\{1\}}_{1,1}/4$, the result follows.

[6] The differential equation $\partial[a(t)A + b(t)B]/\partial t = \pi\nu[a(t)B - b(t)A]$, decomposes into $\partial a(t)/\partial t = -\pi\nu b(t)$ and $\partial b(t)/\partial t = \pi\nu a(t)$. The solution follows from $a(0) = 1$, $b(0) = 0$, $a(t) = \cos(\pi\nu t)$, and $b(t) = \sin(\pi\nu t)$.

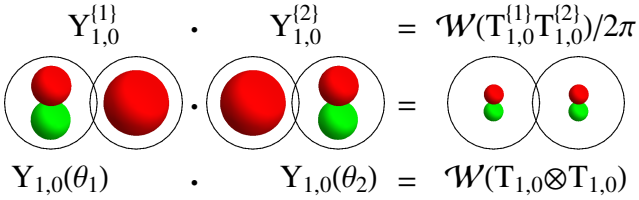

Figure 3.3: (Color online) The tensor product of the normalized 2×2 matrix T_{10} with itself results in a normalized 4×4 matrix $\mathrm{T}_{10} \otimes \mathrm{T}_{10}$ whose Wigner representation $\mathrm{Y}_{10}(\theta_1)\mathrm{Y}_{10}(\theta_2)$ with $\mathrm{Y}_{10}(\theta_j) = \sqrt{2}R\cos\theta_j$ is also normalized (lower row). While the 4×4 matrix $\mathrm{T}^{\{1\}}_{1,0}$ is normalized, the matrix product $\mathrm{T}^{\{1\}}_{10}\mathrm{T}^{\{2\}}_{10} = \mathrm{T}_{10} \otimes \mathrm{T}_{10}/2$ is not. Similarly, $\mathrm{Y}^{\{1\}}_{10} = 1/\sqrt{2\pi}R\cos\theta_1$ and $\mathrm{Y}^{\{2\}}_{10}$ are normalized but their pointwise product is not (middle and upper row). Note that both the middle and the upper row is by a factor of 4π larger than the lower row. In summary, the norm changes in general when spherical functions are multiplied.[3]

$\mathrm{Y}_{jm}(\theta_1,\phi_1)/\sqrt{4\pi}$. Similarly, the operator $\mathrm{T}^{\{2\}}_{jm}$ is mapped onto $\mathrm{Y}^{\{2\}}_{jm} = \mathrm{Y}_{jm}(\theta_2,\phi_2)/\sqrt{4\pi}$. Product operators are constructed as simple pointwise products of their Wigner functions and $\mathrm{T}^{\{1\}}_{j_1m_1}\mathrm{T}^{\{2\}}_{j_2m_2}$ is mapped to the product $2\pi\mathrm{Y}^{\{1\}}_{j_1m_1}\mathrm{Y}^{\{2\}}_{j_2m_2} = \mathrm{Y}_{j_1m_1}(\theta_1,\phi_1)\mathrm{Y}_{j_2,m_2}(\theta_2,\phi_2)/2$. Important examples are summarized in Table 3.3. Suitable prefactors are introduced to ensure consistent normalizations for matrix representations and Wigner functions (see Sec. 3.5.2), and the different normalization factors are also illustrated in Figure 3.3.

The time evolution of the density matrix via the von-Neumann equation translates for Wigner functions of two spins to the equation [see Sec. 3.5.5.1 and Corollary 3.2]

$$\partial W_\rho/\partial t = \sqrt{2\pi}\mathcal{P}^{\{1,2\}}(\{W_\rho, W_\mathcal{H}\}^{\{1\}} + \{W_\rho, W_\mathcal{H}\}^{\{2\}}). \tag{3.16}$$

Here, the Poisson brackets from Eq. (3.9) gain an additional index in order to identify their spin dependence, i.e., the Poisson bracket $\{f_a, f_b\}^{\{1\}}$ contains derivatives with respect to the variables θ_1 and ϕ_1, while $\{f_a, f_b\}^{\{2\}}$ is defined with reference to θ_2 and ϕ_2. As spherical harmonics with rank two or higher are not allowed for spins $1/2$, the projector $\mathcal{P}^{\{1,2\}}$ removes these superfluous contributions, but leaves spherical harmonics Y_{jm} with rank j equal to zero or one unchanged. The Poisson brackets in Eq. (3.16) can be simplified for product operators $W_\rho = W_{\rho_1}(\theta_1,\phi_1)W_{\rho_2}(\theta_2,\phi_2)$ and $W_\mathcal{H} = W_{\mathcal{H}_1}(\theta_1,\phi_1)W_{\mathcal{H}_2}(\theta_2,\phi_2)$ into the form

$$\partial W_\rho/\partial t = \sqrt{2\pi}\,\{W_{\rho_1}, W_{\mathcal{H}_1}\}^{\{1\}}\mathcal{P}^{\{2\}}(W_{\rho_2}W_{\mathcal{H}_2}) + \sqrt{2\pi}\,\{W_{\rho_2}, W_{\mathcal{H}_2}\}^{\{2\}}\mathcal{P}^{\{1\}}(W_{\rho_1}W_{\mathcal{H}_1}); \tag{3.17}$$

refer to Figure 3.4(a) for a visualization of this computation. In the PROPS representation, product operators are indicated as overlapping circles (refer also to B.2) and the overall Wigner function of a tensor product $W_{1,2} = W_1W_2$ is given as a product of its parts. The corresponding Wigner functions W_1 is drawn in the left circle and the Wigner functions W_2 in the right one.

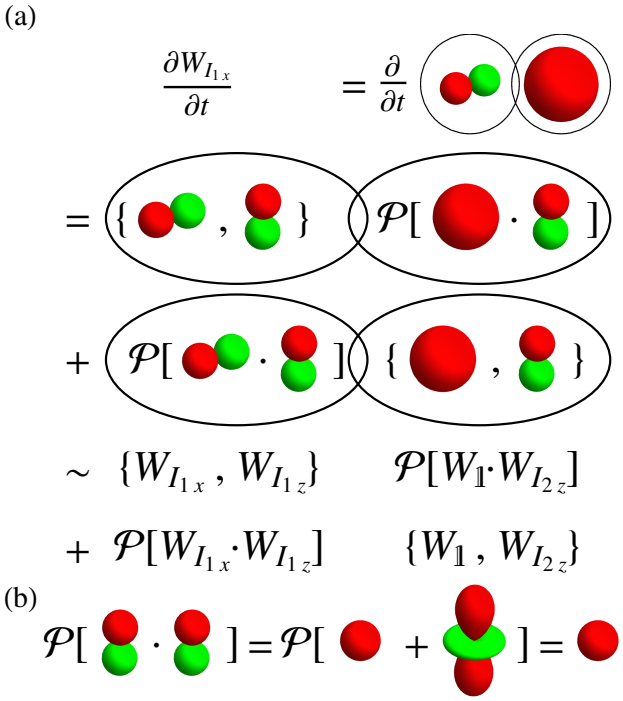

Figure 3.4: (Color online) (a) Graphical representation of the equation of motion for two spins 1/2 for the Hamiltonian $\mathcal{H} = \pi\nu 2 I_{1z} I_{2z}$ and the deviation density matrix $\rho = I_{1x}$, see Eqs. (3.16)-(3.17). (b) Graphical representation of the projection onto rank-one and rank-zero spherical harmonics for the example of $\mathcal{P}(\cos^2\theta_2) = 1/3$ as discussed around Eq. (3.21).[3]

Using aforementioned techniques, the Hamiltonian and the deviation density matrix from Eqs. (3.12)-(3.13) can be transformed into their respective Wigner function

$$W_{\mathcal{H}} = 4\pi^2 \nu \, \mathrm{Y}_{10}^{\{1\}} \mathrm{Y}_{10}^{\{2\}} = \pi\nu 2 R^2 \cos\theta_1 \cos\theta_2, \tag{3.18}$$

$$W_{\rho}(0) = (\mathrm{Y}_{1,-1}^{\{1\}} - \mathrm{Y}_{1,1}^{\{1\}})/\sqrt{2} = R \sin\theta_1 \cos\phi_1 / \sqrt{2\pi}. \tag{3.19}$$

The time derivative of the initial Wigner function $W_\rho(0)$ at $t = 0$ is now given by Eq. (3.16) and it depends only on the variables θ_1, ϕ_1, and consequently, the second Poisson bracket $\{W_\rho(0), W_{\mathcal{H}}\}^{\{2\}}$ is zero. One applies Eq. (3.9) and obtains up to projections

$$\begin{aligned} \partial W_\rho(0)/\partial t &= \sqrt{2\pi}\{W_\rho(0), W_{\mathcal{H}}\}^{\{1\}} = \pi\nu 2 R^3 \{\sin\theta_1 \cos\phi_1, \cos\theta_1\}^{\{1\}} \cos\theta_2 \\ &= \pi\nu 2 R^3 [\sin\theta_1 \frac{\partial \cos\phi_1}{\partial \phi_1} \frac{\partial \cos\theta_1}{\partial \theta_1}] \cos\theta_2 / (R \sin\theta_1) \\ &= \pi\nu 2 R^2 \cos\theta_2 \sin\theta_1 \sin\phi_1 = \pi\nu \mathcal{W}(2 I_{1y} I_{2z}). \end{aligned} \tag{3.20}$$

Here, $\mathcal{W}(2I_{1y}I_{2z})$ denotes the Wigner transformation of $2I_{1y}I_{2z}$, refer to Table 3.3. For the graphical representation of this computation refer to Figure 3.4(a). One deduces that the time derivative of $\mathcal{W}(2I_{1y}I_{2z})$ is up to projections proportional to

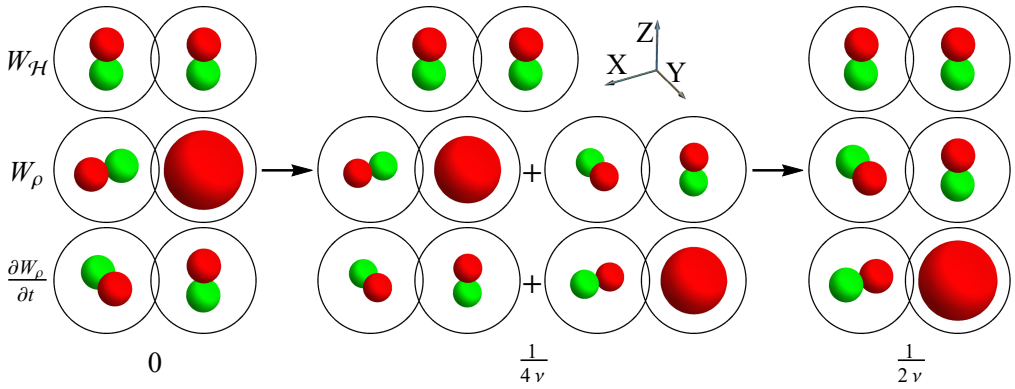

Figure 3.5: (Color online) Time evolution of the initial deviation density matrix I_{1x} under the bilinear coupling Hamiltonian $\mathcal{H} = \pi\nu 2I_{1z}I_{2z}$, computed with our Wigner formalism. PROPS representation of the Wigner functions of the Hamiltonian (upper row), the traceless deviation density matrix (middle row), and the time derivative of the deviation density matrix (lower row). Note that $\rho(0) = I_{1x}$, $\rho[1/(4\nu)] = (I_{1x} + 2I_{1y}I_{2z})/\sqrt{2}$, and $\rho[1/(2\nu)] = 2I_{1y}I_{2z}$.[3]

$$\partial^2 W_\rho(0)/\partial t^2 \propto \partial(\cos\theta_2 \sin\theta_1 \sin\phi_1)/\partial t$$
$$\propto \{\sin\theta_1 \sin\phi_1, \cos\theta_1\}^{\{1\}} \cos\theta_2 \cos\theta_2 + \cos\theta_1 \sin\theta_1 \sin\phi_1 \{\cos\theta_2, \cos\theta_2\}^{\{2\}}.$$

Using that the term vanishes $\{\cos\theta_2, \cos\theta_2\}^{\{2\}} = 0$ and the following term is calculated via $\{\sin\theta_1 \sin\phi_1, \cos\theta_1\}^{\{1\}} = -\sin\theta_1 \cos\phi_1 \sin\theta_1/(R\sin\theta_1)$, we obtain up to projections that

$$\partial\mathcal{W}(2I_{1y}I_{2z})/\partial t = -2\sqrt{3}R^2\pi\nu \sin\theta_1 \cos\phi_1 \cos^2\theta_2.$$

It is however important to understand that the term

$$\cos^2\theta_2 = [\sqrt{4\pi}\mathrm{Y}_{00}(\theta_2,\phi_2) + 4\sqrt{\pi/5}\,\mathrm{Y}_{20}(\theta_2,\phi_2)]/3 \tag{3.21}$$

linearly decomposes into spherical harmonics of rank zero and two, as also visualized in Figure 3.4(b). After applying the projector $\mathcal{P}^{\{2\}}$ from Eq. (3.17), only a term proportional to $\mathrm{Y}_{00} = 1/\sqrt{4\pi}$ remains;[7] and this leads to

$$\partial\mathcal{W}(2I_{1y}I_{2z})/\partial t = -\tfrac{2R^2\pi\nu}{\sqrt{3}} \sin\theta_1 \cos\phi_1 = \mathcal{W}(-\pi\nu I_{1x}).$$

It is now apparent, that the second time derivative of $W_\rho(0)$ is proportional to $W_\rho(0)$, i.e., $\partial^2 W_\rho(0)/\partial t^2 = -(\pi\nu)^2 W_\rho(0)$ and that the time evolution of W_ρ is parametrized by only two Wigner functions

$$W_A := \mathcal{W}(I_{1x}) = R\sin\theta_1 \cos\phi_1/\sqrt{2\pi}, \quad W_B := \mathcal{W}(2I_{1y}I_{2z}) = 2R^2 \sin\theta_1 \sin\phi_1 \cos\theta_2.$$

[7] The term $\cos^2\theta_2$ is proportional to $\mathcal{W}(I_{2z})\mathcal{W}(I_{2z})$. Note that in general $\mathcal{P}^{\{k\}}\mathcal{W}(I_{ka})\mathcal{W}(I_{kb}) = \delta_{ab}/[4(2\pi)^N]$ with $a, b \in \{x, y, z\}$ holds for the pointwise product of Wigner functions, where N denotes the number of spins 1/2.

Note the similarity with Eq. (3.14). The solution for the Wigner function is then given by[8]

$$W_\rho(t) = R\,c(t)\sin\theta_1\cos\phi_1/\sqrt{2\pi} + 2R^2 s(t)\sin\theta_1\sin\phi_1\cos\theta_2, \tag{3.22}$$

where $c(t) := \cos(\pi\nu t)$ and $s(t) := \sin(\pi\nu t)$. Figure 3.5 illustrates the time evolution of Wigner functions for the Hamiltonian $\mathcal{H} = \pi\nu 2I_{1z}I_{2z}$ (upper row), the traceless deviation density matrix $\rho(t) = c(t)I_{1x} + s(t)2I_{1y}I_{2z}$ (middle row), and the corresponding time derivative $\partial\rho/\partial t = -s(t)I_{1x} + c(t)2I_{1y}I_{2z}$ (lower row) at different times $t = 0$, $\pi\nu t = \pi/4$, and $\pi\nu t = \pi/2$. Arbitrary operators are visualized in the PROPS representation by decomposing them into sums of product operators (refer also to B.2). An alternative representation of the Wigner function in Eq. (3.22) based on a decomposition into non-hermitian operators is given in Sec. 3.7.4.2.

3.5 Theory: Wigner formalism for the time evolution of coupled spins

The central parts of the Wigner formalism for coupled spins are now systematically developed. Most of our theoretical concepts were already introduced in Sec. 3.4 using easily understandable examples. We present now the mathematical details for our Wigner formalism for coupled spins which form the main results of this work. Identifying the underlying physical principles, the description of the time evolution of coupled spin systems is consequently derived via our theoretical approach.

We want to emphasize that our theoretical approach, which relies on the irreducible tensor operators is applicable to arbitrary density matrices and operators of coupled spin systems, even though our technical tools (including Clebsch-Gordan coefficients and Wigner 6-j symbols [192]) might spuriously suggest some superficial similarity to the description of indistinguishable particles using reducible representations of the special unitary group of dimension two. In particular, the star product specifying the time evolution is not determined by a simple addition of angular momenta, not even for a single spin [cf. Eq. (3.53) below].

First, we recall basic properties of product operators and the tensor product of matrices (see Sec. 3.5.1); the main properties are summarized in Table 3.4. We detail the Wigner transformation of spin operators for single and coupled spin systems in Sec. 3.5.2. This then leads in Sec. 3.5.3 to a simplified approach to compute the star product of single-spin-1/2 operators and allows us to derive the corresponding equation of motion. In Sec. 3.5.4, the star product is then extended to coupled spin-$1/2$ operators and the corresponding equation of motion is determined. Finally, we provide an optimized form of our formalism for two and three coupled spins $1/2$ as well as natural Hamiltonians for multiple spins $1/2$ (see Sec. 3.5.5).

[8] The parametrized Wigner function $W_\rho(t) = a(t)W_A + b(t)W_B$ is substituted into Eq. (3.16), and one obtains $\partial[a(t)W_A + b(t)W_B]/\partial t = \pi\nu[a(t)W_B - b(t)W_A]$. This splits into $\partial a(t)/\partial t = -\pi\nu b(t)$ and $\partial b(t)/\partial t = \pi\nu a(t)$ and results in $W_\rho(t) = \cos(\pi\nu t)W_A + \sin(\pi\nu t)W_B$.

Table 3.4: Normalized product operators and tensor products for basis operators embedded into an N-spin system; see also B.1. The names in the first column refer to the case when all indices $j_k > 0$; but the prefactors are correct even if some j_k are zero.

Type	Product-operator notation	Tensor-product notation
Linear	${}^{J}\mathrm{T}^{\{k\}}_{jm}$	$\underbrace{{}^{J}\mathrm{T}_{00}}_{\#1} \otimes \cdots \otimes {}^{J}\mathrm{T}_{00} \otimes \underbrace{{}^{J}\mathrm{T}_{jm}}_{\#k} \otimes {}^{J}\mathrm{T}_{00} \otimes \cdots \otimes \underbrace{{}^{J}\mathrm{T}_{00}}_{\#N}$
Bilinear	$\sqrt{2J+1}^{N}\, {}^{J}\mathrm{T}^{\{k\}}_{j_k m_k}\, {}^{J}\mathrm{T}^{\{\ell\}}_{j_\ell m_\ell}$	$\underbrace{{}^{J}\mathrm{T}_{00}}_{\#1} \otimes \cdots \otimes \underbrace{{}^{J}\mathrm{T}_{j_k m_k}}_{\#k} \otimes \cdots \otimes \underbrace{{}^{J}\mathrm{T}_{j_\ell m_\ell}}_{\#\ell} \otimes \cdots \otimes \underbrace{{}^{J}\mathrm{T}_{00}}_{\#N}$
M-linear	$\sqrt{2J+1}^{N(M-1)}$ $\times \prod_{k\in K,\lvert K\rvert=M} {}^{J}\mathrm{T}^{\{k\}}_{j_k m_k}$	$\bigotimes_{k\in\{1,\ldots,N\}} A_k$, where $A_k := \begin{cases} {}^{J}\mathrm{T}_{j_k m_k} & \text{if } k \in K, \\ {}^{J}\mathrm{T}_{00} & \text{otherwise.} \end{cases}$
N-linear	$\sqrt{2J+1}^{N(N-1)}$ $\times {}^{J}\mathrm{T}^{\{1\}}_{j_1 m_1} \ldots {}^{J}\mathrm{T}^{\{N\}}_{j_N m_N}$	${}^{J}\mathrm{T}_{j_1 m_1} \otimes \cdots \otimes {}^{J}\mathrm{T}_{j_N m_N}$

3.5.1 Product-operator and tensor-product notation

We recapitulate elementary definitions and properties of tensor operators acting on a coupled N-spin system consisting of spin-J particles. For single spins, the tensor components ${}^{J}\mathrm{T}_{jm}$ are indexed with rank $j \in \{0, \ldots, 2J\}$ and order $m \in \{-j, \ldots, j\}$; the index J can be dropped if $J = 1/2$. Recall the defining relations of tensor operators in Eq. (3.5), and their matrix elements given in the standard basis $|Jm\rangle$ can be specified in terms of Clebsch-Gordan coefficients [192, 47, 33, 87]

$$[{}^{J}\mathrm{T}_{jm}]_{m_1 m_2} := \langle Jm_1 | {}^{J}\mathrm{T}_{jm} | Jm_2 \rangle = \sqrt{\tfrac{2j+1}{2J+1}}\, C^{Jm_1}_{Jm_2, jm} = (-1)^{J-m_2}\, C^{jm}_{Jm_1 J, -m_2}, \tag{3.23}$$

where $m_1, m_2 \in \{J, \ldots, -J\}$. The single-spin operator ${}^{J}\mathrm{T}_{jm}$ is normalized and can be embedded as the product operator

$${}^{J}\mathrm{T}^{\{k\}}_{jm} := {}^{J}\mathrm{T}_{00} \otimes \cdots \otimes {}^{J}\mathrm{T}_{00} \otimes {}^{J}\mathrm{T}_{jm} \otimes {}^{J}\mathrm{T}_{00} \otimes \cdots \otimes {}^{J}\mathrm{T}_{00} \tag{3.24}$$

acting on the kth spin of an N-spin system (recall that $\mathrm{Id}_{2J+1} = \sqrt{2J+1}\, {}^{J}\mathrm{T}_{00}$). More generally, the embedded form of a single-spin operator A acting on the kth spin is denoted by $A^{\{k\}} := {}^{J}\mathrm{T}_{00} \otimes \cdots \otimes {}^{J}\mathrm{T}_{00} \otimes A \otimes {}^{J}\mathrm{T}_{00} \otimes \cdots \otimes {}^{J}\mathrm{T}_{00}$. We consider products of single-spin tensor operators, and certain cases are summarized in Table 3.4 as normalized product operators A with $\mathrm{Tr}(A^\dagger A) = 1$, Table 3.4 also shows the complementary tensor-product notation, and we will switch between product operators and the tensor-product notation. Elementary properties of product operators can usually directly be inferred from properties of tensor products

of operators A_k and B_k with $k \in \{1,\dots,N\}$:

$$(A_1\cdots A_N)\otimes(B_1\cdots B_N) = (A_1\otimes B_1)\cdots(A_N\otimes B_N),\ (A_1\otimes\cdots\otimes A_N)^\dagger = A_1^\dagger\otimes\cdots\otimes A_N^\dagger,$$
$$\text{and}\ \ \mathrm{Tr}(A_1\otimes\cdots\otimes A_N) = \mathrm{Tr}(A_1)\cdots\mathrm{Tr}(A_N).$$

Moreover, we gather the following properties of embedded single-spin product operators:

Lemma 3.1. *Embedded single-spin product operators have the following properties:*

(a) $\mathrm{Tr}[({}^J\mathrm{T}^{\{k_1\}}_{j_1m_1})^\dagger {}^J\mathrm{T}^{\{k_2\}}_{j_2m_2}] = \delta_{k_1k_2}\delta_{j_1j_2}\delta_{m_1m_2}$,

(b) $[{}^J\mathrm{T}^{\{k_1\}}_{j_1m_1}, {}^J\mathrm{T}^{\{k_2\}}_{j_2m_2}] = \frac{\delta_{k_1k_2}}{\sqrt{2J+1}^{N-1}}([{}^J\mathrm{T}_{j_1m_1}, {}^J\mathrm{T}_{j_2m_2}])^{\{k_1\}}$,

(c) ${}^J\mathrm{T}^{\{k\}}_{j_1m_1}\,{}^J\mathrm{T}^{\{k\}}_{j_2m_2} = \frac{1}{\sqrt{2J+1}^{N-1}}({}^J\mathrm{T}_{j_1m_1}\,{}^J\mathrm{T}_{j_2m_2})^{\{k\}}$.

These properties imply that normalized products of single-spin tensor operators give rise to a basis of the full operator space of N spins (cf. Table 3.4):

Lemma 3.2. *The normalized product operators*

$$\sqrt{2J+1}^{N(N-1)}\,{}^J\mathrm{T}^{\{1\}}_{j_1m_1}\cdots{}^J\mathrm{T}^{\{N\}}_{j_Nm_N} = {}^J\mathrm{T}_{j_1m_1}\otimes\cdots\otimes{}^J\mathrm{T}_{j_Nm_N}$$

form an orthonormal basis of the full N-spin system, and an arbitrary spin operator A can be decomposed as

$$A = \sum_{j_1m_1\ldots j_Nm_N} a_{j_1m_1\ldots j_Nm_N}\sqrt{2J+1}^{N(N-1)}\,{}^J\mathrm{T}^{\{1\}}_{j_1m_1}\cdots{}^J\mathrm{T}^{\{N\}}_{j_Nm_N}.$$

Given an M-linear operator acting on $M \le N$ spins, all indices j_k in the decomposition of A given in Lemma 3.2 are greater equal to zero for $k \in \{1,\dots,N\}$. Yet, certain indices j_k have to be zero if $M < N$. B.1 provides a non-technical tutorial on elementary properties of product operators.

3.5.2 The Wigner formalism for spins

We describe the Wigner representation of spin operators which are mapped by the Wigner transformation to spherical functions. This bijective mapping between operators and phase-space functions fulfills the so-called Stratonovich postulates (and generalizations thereof) which are discussed in B.3 for single spins as well as multiple coupled spins.

3.5.2.1 Wigner representation of single spins

The continuous Wigner representation of an arbitrary operator A acting on a single spin J is defined as [253]

$$\mathcal{W}(A) := W_A(\theta,\phi) = \mathrm{Tr}[\Delta_J(\theta,\phi)A], \tag{3.25}$$

where $\mathcal{W}(A)$ denotes the Wigner transform of A. In Eq. (3.25), we have used the kernel $\Delta_J(\theta,\phi)$ for a single spin J which maps spin operators onto spherical functions, and it is given by[9]

$$\Delta_J(\theta,\phi) := \sum_{j=0}^{2J}\sum_{m=-j}^{j} \mathrm{Y}^*_{jm}(\theta,\phi)\ {}^J\mathrm{T}_{jm} = \Delta_J^\dagger(\theta,\phi). \tag{3.26}$$

The form of the kernel builds on the work of [243, 253, 47, 46], see, in particular, Eqs. (4.16)-(4.17) in [47], Eq. 2.14 in [253], and Eq. (9) in [151]. Here, the tensor operators ${}^J\mathrm{T}_{jm}$ for a given spin number J form an orthonormal set of basis operators for $(2J{+}1) \times (2J{+}1)$ matrices, i.e.,

$$\mathrm{Tr}({}^J\mathrm{T}^\dagger_{j_1m_1}\ {}^J\mathrm{T}_{j_2m_2}) = \delta_{j_1j_2}\delta_{m_1m_2}; \tag{3.27}$$

likewise the spherical harmonics $\mathrm{Y}_{jm}(\theta,\phi)$ [136] are orthonormal with respect to the scalar product

$$\int_{\theta=0}^{\pi}\int_{\phi=0}^{2\pi} \mathrm{Y}^*_{j_1m_1}(\theta,\phi)\mathrm{Y}_{j_2m_2}(\theta,\phi)\sin\theta\,\mathrm{d}\theta\,\mathrm{d}\phi = \delta_{j_1j_2}\delta_{m_1m_2}. \tag{3.28}$$

Equations (3.25) and (3.27) imply that the Wigner representation of a tensor operator ${}^J\mathrm{T}_{jm}$ is equal to the spherical harmonic $\mathrm{Y}_{jm}(\theta,\phi)$, i.e.,

$$\mathcal{W}({}^J\mathrm{T}_{jm}) = W_{J_{\mathrm{T}_{jm}}}(\theta,\phi) = \mathrm{Y}_{jm}(\theta,\phi). \tag{3.29}$$

Tensor operators can be reconstructed from their Wigner representation by applying the inverse Wigner transformation (usually referred to as the Weyl transformation) which is defined as

$$\mathcal{W}^{-1}[F(\theta,\phi)] := \int_{\theta=0}^{\pi}\int_{\phi=0}^{2\pi} \Delta_J(\theta,\phi)F(\theta,\phi)\ \sin\theta\,\mathrm{d}\theta\,\mathrm{d}\phi. \tag{3.30}$$

By substituting $F = W_A$ in Eq. (3.30), one obtains that $A = \mathcal{W}^{-1}[W_A(\theta,\phi)]$. The orthonormality relation of Eq. (3.28) implies that the inverse Wigner transformation of the spherical harmonics $\mathrm{Y}_{jm}(\theta,\phi)$ are given by the tensor operators ${}^J\mathrm{T}_{jm}$.

3.5.2.2 Wigner representation of coupled spins

We now generalize the definition of the kernel for a single spin [see Eq. (3.26)] to multiple spins J, but for simplicity with identical J for each spin, while a generalization to systems that are composed of particles of different spin number J is straightforward.

[9] We verify that $\Delta_J(\theta,\phi) = \sum_{j=0}^{2J}\sum_{m=-j}^{j} \mathrm{Y}^*_{j,-m}\ {}^J\mathrm{T}_{j,-m} = \Delta_J^\dagger(\theta,\phi)$ is hermitian by using the Condon-Shortley phase convention and $\Delta_J^\dagger(\theta,\phi) = \sum_{j=0}^{2J}\sum_{m=-j}^{j} \mathrm{Y}_{jm}\ {}^J\mathrm{T}^\dagger_{jm}$.

Result 3.1. *For N coupled spins, the kernel is defined as the N-fold tensor product*

$$\Delta_J^{\{1\ldots N\}} := \Delta_J^{\{1\ldots N\}}(\theta_1,\phi_1,\ldots,\theta_N,\phi_N) = \bigotimes_{k=1}^{N} \Delta_J(\theta_k,\phi_k)$$

of the individual kernels and involves a set of $2N$ spherical (phase-space) variables $(\theta_1,\phi_1,\ldots,\theta_N,\phi_N)$ describing points on N spheres.[a] *Using the definition of the kernel $\Delta_J(\theta,\phi)$ from Eq.* (3.26) *and applying the correspondence of Table 3.4, one obtains the explicit form*

$$\begin{aligned}\Delta_J^{\{1\ldots N\}} &= \sum_{\substack{j_1\ldots j_N\\ m_1\ldots m_N}} [{}^J\mathrm{T}_{j_1m_1}\otimes\cdots\otimes{}^J\mathrm{T}_{j_Nm_N}]\,\mathcal{Y}\\ &= \sum_{\substack{j_1\ldots j_N\\ m_1\ldots m_N}} [\sqrt{2J+1}^{N(N-1)}\,{}^J\mathrm{T}^{\{1\}}_{j_1m_1}\cdots{}^J\mathrm{T}^{\{N\}}_{j_Nm_N}]\,\mathcal{Y},\end{aligned} \tag{3.31}$$

where $\mathcal{Y} := \prod_{k=1}^{N}\mathrm{Y}^{*}_{j_km_k}(\theta_k,\phi_k)$. Consequently, this defines the Wigner transformation as

$$\mathcal{W}(A) := W_A(\theta_1,\phi_1,\ldots,\theta_N,\phi_N) = \mathrm{Tr}(\Delta_J^{\{1\ldots N\}}A), \tag{3.32}$$

and it satisfies the generalized Stratonovich postulates described in B.3.2.

[a] A similar result has been attained in Eq. (9) of [248].

We now apply orthonormality properties of tensor operators [see Lemma 3.1(a)] and verify that the Wigner representation for the linear embedded tensor operator ${}^J\mathrm{T}^{\{k\}}_{jm}$ is proportional to the spherical harmonic $\mathrm{Y}_{jm}(\theta_k,\phi_k)$, which depends on the angular variables θ_k and ϕ_k. More precisely, we obtain the relation

$$\mathcal{W}({}^J\mathrm{T}^{\{k\}}_{jm}) = \mathrm{Y}^{\{k\}}_{jm} := \underbrace{\mathrm{Y}_{00}}_{\#1}\cdots\underbrace{\mathrm{Y}_{00}}_{\#(k-1)}\underbrace{\mathrm{Y}_{jm}(\theta_k,\phi_k)}_{\#k}\underbrace{\mathrm{Y}_{00}}_{\#(k+1)}\cdots\underbrace{\mathrm{Y}_{00}}_{\#N} = \mathrm{Y}_{jm}(\theta_k,\phi_k)/\sqrt{4\pi}^{N-1}. \tag{3.33}$$

Similarly as for the Wigner transformation, the inverse Wigner transformation of a spherical function $F = F(\theta_1,\phi_1,\ldots,\theta_N,\phi_N)$ is generalized to multiple spins as

$$\mathcal{W}^{-1}(F) := \int_{\theta_k,\phi_k\geq 0}^{\theta_k\leq\pi,\phi_k\leq 2\pi}\cdots\int \Delta_J^{\{1\ldots N\}}F\prod_{k=1}^{N}\sin\theta_k\,\mathrm{d}\phi_k\,\mathrm{d}\theta_k. \tag{3.34}$$

Setting $F = W_A$ in Eq. (3.34) also verifies that $A = \mathcal{W}^{-1}[W_A(\theta_1,\phi_1\ldots\theta_N,\phi_N)]$ holds. In particular, the inverse Wigner transformation maps the spherical harmonic $\mathrm{Y}^{\{k\}}_{jm}$ with variables (θ_k,ϕ_k) to the linear tensor operators ${}^J\mathrm{T}^{\{k\}}_{jm}$ acting on the kth spin. Finally, our approach establishes that the Wigner representation of products of embedded tensor operators

can be written as products of the corresponding spherical harmonics involving different variables, i.e.,

$$\begin{aligned}\mathcal{W}(\sqrt{2J+1}^{N(N-1)}\,{}^{J}\mathrm{T}^{\{1\}}_{j_1m_1}\cdots{}^{J}\mathrm{T}^{\{N\}}_{j_Nm_N}) &= \mathcal{W}({}^{J}\mathrm{T}_{j_1m_1}\otimes\cdots\otimes{}^{J}\mathrm{T}_{j_Nm_N}) \\ &= \mathrm{Y}_{j_1m_1}(\theta_1,\phi_1)\cdots\mathrm{Y}_{j_Nm_N}(\theta_N,\phi_N).\end{aligned} \tag{3.35}$$

3.5.2.3 Star product, star commutator, and Moyal equation

In the following, we wish to compute the Wigner representation W_{AB} of the product AB of two operators A and B from their respective Wigner representations W_A and W_B. This is accomplished by recalling the defining relation

$$W_{AB} = W_A \star W_B \tag{3.36}$$

of the star product $\star$ of two Wigner functions. The star product mimics the matrix product of two operators. Note that the product AB is restricted to the subspace of tensor operators with rank at most $2J$, just as for the operators A and B.

The time evolution of the density operator ρ is governed by the von-Neumann equation $i\partial\rho/\partial t = [\mathcal{H},\rho] = \mathcal{H}\rho - \rho\mathcal{H}$, see Eq. (3.2). This can be mapped to the Wigner representation by applying Eq. (3.25) and exploiting that the symbols $W_{\rho\mathcal{H}}$ and $W_{\mathcal{H}\rho}$ can according to Eq. (3.36) be restated in terms of star products. Hence, the equation of motion in the Wigner representation is given as

$$i\frac{\partial W_\rho}{\partial t} = [W_\mathcal{H}, W_\rho]_\star := W_\mathcal{H}\star W_\rho - W_\rho\star W_\mathcal{H}. \tag{3.37}$$

This defines the star commutator $[\cdot,\cdot]_\star$, which constitutes an analogue of the matrix commutator.

3.5.3 Star product for a single spin $1/2$

Wigner representations and their defining star products are well studied in the case of infinite-dimensional quantum-mechanical operators [232, 227]. Similarly as in the case of infinite-dimensional systems, the star product from Eq. (3.36) can be computed using an integral or differential form (as discussed in Sections 3.3.2 and 3.3.5.1). The integral form is an integral transformation of the Wigner functions $W_A(\theta_1,\phi_1)$ and $W_B(\theta_2,\phi_2)$ which is weighted with a so-called trikernel. We provide an explicit expression for the integral form in Eq. (B.3) of B.6 (along the lines of [253]) by evaluating the exact star product and by applying expansion formulas from Sec. 3.5.3.1 below. This result provides a formal definition of the star product, but is less useful in applications.

In contrast, the differential star product is more convenient for explicit calculations since only partial derivatives and the pointwise product of W_A and W_B are required, which is afterwards followed by a projection.

For an arbitrary spin number J, Klimov and Espinoza [151] state the differential star product for two so-called Beresin P symbols P_A and P_B as a sum of the pointwise product of two functions combined with partial derivatives. The order and number of the partial derivatives grow rapidly with increasing J, and a truncation of the resulting P symbol is required. Klimov and Espinoza [151] also provide formulas to compute the star product of Wigner functions. Their method is virtually equivalent to transforming the Wigner functions into P symbols, then after computing the star product of P symbols, the P symbols are transformed back. In summary, the star product of two spin-1/2 Wigner functions W_A and W_B can be computed by first decomposing W_A and W_B into spherical harmonics and by reweighting the expansion coefficients one obtains $\tilde{W}_A$ and $\tilde{W}_B$, where $\tilde{W}_A$ and $\tilde{W}_B$ are proportional to the P symbols P_A and P_B. The differential star product of the P symbols is then applied to $\tilde{W}_A$ and $\tilde{W}_B$, and one obtains the four summands $a\,\tilde{W}_A\tilde{W}_B$, $b\,\{\tilde{W}_A, \tilde{W}_B\}$, $c\,(\partial\tilde{W}_A/\partial\theta)\,(\partial\tilde{W}_B/\partial\theta)$, and $d\,(\partial\tilde{W}_A/\partial\phi)\,(\partial\tilde{W}_B/\partial\phi)/\sin^2\theta$, where a, b, c, and d denote suitable prefactors. The resulting function $\tilde{W}_{AB}$ is transformed back by reweighting the terms in its decomposition into spherical harmonics. Finally, a result W_{AB} is obtained that satisfies the defining property $W_{AB} = W_A \star W_B$.

We consider only the case of $J = 1/2$ and provide a simplified approach, which nevertheless leads to the same star product and the same equation of motion that is given by the Poisson bracket (see [150] and [253]). The resulting differential star product $W_A \star W_B$ [see Result 3.2 below] is simply a sum of the pointwise product W_AW_B and the Poisson bracket $\{W_A, W_B\}$ of the two Wigner functions. In Sec. 3.5.3.1 we provide formulas necessary to evaluate the star product, and Sec. 3.5.3.2 contains the details on how the star product is calculated. This simplified approach allows us then to extend the star product to multiple, coupled spins as detailed in Sec. 3.5.4.

3.5.3.1 Matrix products, pointwise products, and Poisson brackets

We detail how to expand products of tensor operators (resp. spherical harmonics) into a linear combination of tensor operators (resp. spherical harmonics). A similar expansion is described for the Poisson bracket of spherical harmonics. The product of two irreducible tensor operators can be expanded as [151, 254]

$$ {}^{J}\mathrm{T}_{j_1m_1}\,{}^{J}\mathrm{T}_{j_2m_2} = \sum_{L=|j_1-j_2|}^{n} {}^{J}Q_{j_1j_2L}\,C^{LM}_{j_1m_1j_2m_2}\,{}^{J}\mathrm{T}_{LM}. \tag{3.38} $$

Here, the upper bound of the summation does not need to exceed $2J$ and is given by $n := \min(j_1{+}j_2, 2J)$ as ${}^{J}Q_{j_1j_2L} = 0$ for $L > 2J$; note $M = m_1{+}m_2$.[10] Also, $C^{LM}_{j_1m_1j_2m_2}$ are the Clebsch-Gordan coefficients [192], and the coefficients

$$ {}^{J}Q_{j_1j_2L} := (-1)^{2J+L}\sqrt{(2j_1{+}1)(2j_2{+}1)}\begin{Bmatrix} j_1 & j_2 & L \\ J & J & J \end{Bmatrix} \tag{3.39} $$

[10] The lower bound in the summation can be enlarged to $\max(|j_1{-}j_2|, m_1{+}m_2)$ without changing the result.

are proportional to Wigner 6-j symbols [192] and depend only on j_1, j_2, and L, but are independent of m_1, m_2, and M. This also conforms with the fact that only tensor operators of rank zero and one are allowed for the case of a spin $1/2$ in the product AB (see Sec. 3.5.2.3).

In order to determine the Poisson bracket of two spherical functions, we first recall its definition [refer also to Eq. (3.9)]

$$\{W_F, W_G\}^{\{i\}} := W_F \left(\frac{\overleftarrow{\partial}}{\partial\phi_i} \frac{1}{R\sin\theta_i} \frac{\overrightarrow{\partial}}{\partial\theta_i} - \frac{\overleftarrow{\partial}}{\partial\theta_i} \frac{1}{R\sin\theta_i} \frac{\overrightarrow{\partial}}{\partial\phi_i} \right) W_G, \tag{3.40}$$

where the arrows $\leftarrow$ and $\rightarrow$ indicate whether the derivatives act to the left or the right, respectively. Moreover, the normalization factor is set to $R = \sqrt{3/(8\pi)}$. Based on [95], the Poisson bracket of two spherical harmonics can be expanded as

$$\{\mathrm{Y}_{j_1 m_1}, \mathrm{Y}_{j_2 m_2}\} = \sum_{L=|j_1-j_2|}^{j_1+j_2} U_{j_1 j_2 L}\, C^{LM}_{j_1 m_1 j_2 m_2} \mathrm{Y}_{LM}. \tag{3.41}$$

The product of two spherical harmonics decomposes into a linear combination of spherical harmonics as (see Sec. 12.9 of [19])

$$\mathrm{Y}_{j_1 m_1} \mathrm{Y}_{j_2 m_2} = \sum_{L=|j_1-j_2|}^{j_1+j_2} Z_{j_1 j_2 L}\, C^{LM}_{j_1 m_1 j_2 m_2} \mathrm{Y}_{LM}. \tag{3.42}$$

Here, the coefficients $Z_{j_1 j_2 L}$ and $U_{j_1 j_2 L}$ depend only on j_1, j_2, and L and are given by

$$Z_{j_1 j_2 L} := \sqrt{\tfrac{(2j_1+1)(2j_2+1)}{4\pi(2L+1)}}\, C^{L0}_{j_1 0 j_2 0}, \tag{3.43}$$

$$U_{j_1 j_2 L} := -\tfrac{i}{2R}[1-(-1)^{L-j_1-j_2}] \sqrt{j_1(j_1+1)L(L+1)} \times \sqrt{\tfrac{(2j_1+1)(2j_2+1)}{4\pi(2L+1)}}\, C^{L1}_{j_1 1\, j_2 0}. \tag{3.44}$$

Although the Poisson bracket $\{\cdot,\cdot\}$ will not be completely analogous to the star commutator $[\cdot,\cdot]_\star$ for arbitrary J, there is a strong relation between these two operations. Recalling that the star commutator in the Wigner representation corresponds to the commutator of matrix representations (see Sec. 3.5.2.3), we can in analogy compare the Poisson bracket from Eq. (3.41) with the usual commutator of tensor operators. Using Eq. (3.38), the commutator of tensor operators can be brought into a similar form ($M = m_1 + m_2$)

$$[{}^J\mathrm{T}_{j_1 m_1}, {}^J\mathrm{T}_{j_2 m_2}] = \sum_{L=|j_1-j_2|}^{n} {}^J Q'_{j_1 j_2 L}\, C^{LM}_{j_1 m_1 j_2 m_2}\, {}^J\mathrm{T}_{LM} \tag{3.45}$$

by applying ${}^J Q'_{j_1 j_2 L} := [1-(-1)^{j_1+j_2-L}]\, {}^J Q_{j_1 j_2 L}$ and the symmetry properties $C^{LM}_{j_1 m_1 j_2 m_2} = (-1)^{j_1+j_2-L} C^{LM}_{j_2 m_2 j_1 m_1}$ of the Clebsch-Gordan coefficients. We compare Eq. (3.41) with Eq. (3.45) and note that the coefficients $Q'^{(J)}_{j_1 j_2 L}$ and $U_{j_1 j_2 L}$ will in general differ. However, their nonzero values within the range $j_1, j_2, L \leq 2J$ appear at coinciding values of j_1, j_2, and L, highlighting the close relation of the Poisson bracket and the star commutator. Finally, we

provide a particular case where this equivalence is strict up to a prefactor:

$$\{\mathrm{Y}_{10}, \mathrm{Y}_{jm}\} = i\sqrt{2}\, m\, \mathrm{Y}_{jm}, \quad \{\mathrm{Y}_{1,\pm1}, \mathrm{Y}_{jm}\} = \mp i\sqrt{(j \mp m)\,(j \pm m + 1)}\, \mathrm{Y}_{j,m\pm1}, \tag{3.46a}$$

$$[{}^{J}I_z, {}^{J}\mathrm{T}_{jm}] = m\, {}^{J}\mathrm{T}_{jm}, \qquad [{}^{J}I_\pm, {}^{J}\mathrm{T}_{jm}] = \sqrt{(j \mp m)\,(j \pm m + 1)}\, {}^{J}\mathrm{T}_{j,m\pm1}. \tag{3.46b}$$

The Equations (3.46b) show how the basic definition of spherical tensor operators relies on commutators, c.f. Eq. (3.5). By comparing them to the Equations (3.46a) it is clear that the defining relation is also satisfied by the Poisson bracket of spherical harmonics up to the prefactor i (and an additional prefactor implied by $\mp N_J \mathcal{W}({}^{J}I_\pm) = \mathrm{Y}_{1,\pm1}$ and $N_J\sqrt{2}\mathcal{W}({}^{J}I_z) = \mathrm{Y}_{1,0}$).[11] The particular cases of Eq. (3.46) are also considered in Equation (5.13) of [253].

3.5.3.2 Evaluation of the star product

In this section, we detail the explicit form of the differential star product for a single spin $1/2$ while ensuring that its form conforms with Sec. 3.5.2.3. We build on the work in [151, 253] and provide a simplified approach. The differential star product is given as the sum of the pointwise product and the Poisson bracket of two spherical functions, followed by the projection onto rank-one and rank-zero spherical harmonics, i.e., by truncating spherical harmonics with rank greater than one. Two distinct symbols are used: the exact star product $\star$ is obtained from the prestar product $\star$ after truncating certain spherical harmonics.

[11] The prefactor N_J is implied by the formula ${}^{J}\mathrm{T}_{1,\pm1} = \mp {}^{J}I_\pm N_J = \mp {}^{J}I_\pm / \sqrt{\mathrm{Tr}({}^{J}I_\pm\, {}^{J}I_\mp)}$ where ${}^{J}I_\pm = {}^{J}I_x \pm i\,{}^{J}I_y$. The trace is given by $\mathrm{Tr}({}^{J}I_\pm\, {}^{J}I_\mp) = \mathrm{Tr}[({}^{J}I_x \pm i\,{}^{J}I_y)({}^{J}I_x \mp i\,{}^{J}I_y)] = \mathrm{Tr}[{}^{J}(I^2)] - \mathrm{Tr}[({}^{J}I_z)^2]$, where ${}^{J}(I^2) = ({}^{J}I_x)^2 + ({}^{J}I_y)^2 + ({}^{J}I_z)^2$, $\mathrm{Tr}[{}^{J}(I^2)] = J(J{+}1)(2J{+}1)$, and $\mathrm{Tr}[({}^{J}I_z)^2] = \sum_{m=-J}^{J} m^2 = J(J{+}1)(2J{+}1)/3$. It follows that $N_J = 1/\sqrt{\mathrm{Tr}({}^{J}I_\pm {}^{J}I_\mp)} = 1/\sqrt{2J(J{+}1)(2J{+}1)/3}$.

Result 3.2. *Given the Wigner functions $W_F(\theta,\phi)$ and $W_G(\theta,\phi)$ of the operators F and G acting on a single spin $1/2$, the prestar product (i.e., the product that results in the star product after truncation) is defined as*

$$W_F(\theta,\phi) \star W_G(\theta,\phi) := \sqrt{2\pi} W_F W_G - \tfrac{i}{2}\{W_F, W_G\} \tag{3.47}$$

using the Poisson bracket $\{\cdot,\cdot\}$ from Eq. (3.40). Note that the factor $\sqrt{2\pi} = 1/W_{\mathrm{Id}}$ is the inverse of the identity Wigner function. The corresponding star product

$$W_F(\theta,\phi) \star W_G(\theta,\phi) := \mathcal{P}[W_F(\theta,\phi) \star W_G(\theta,\phi)] \tag{3.48}$$

is obtained by projecting onto spherical functions of rank zero or one, e.g., by applying the projection operator

$$\mathcal{P}\,\mathrm{Y}_{jm} := (1 + \mathcal{L}^2/12 - \mathcal{L}^4/24)\mathrm{Y}_{jm} = \begin{cases} \mathrm{Y}_{jm} & \text{for} \quad j < 2 \\ 0 & \text{for} \quad j = 2 \end{cases} \tag{3.49}$$

which uses the angular momentum operator $\mathcal{L}$ with eigenvalues $\mathcal{L}^2\,\mathrm{Y}_{jm} = j(j+1)\mathrm{Y}_{jm}$.[a]

[a] The projector $\mathcal{P}f(\theta,\phi) = \sum_{j=0}^{1}\sum_{m=-j}^{j} \mathrm{Y}_{jm}(\theta,\phi)\int_{\theta=0}^{\pi}\int_{\phi=0}^{2\pi} f(\theta,\phi)\mathrm{Y}^*_{jm}(\theta,\phi)\,\sin\theta\,\mathrm{d}\theta\,\mathrm{d}\phi$ can be applied to an arbitrary spherical function, but Equation (3.48) is fulfilled by the differential operator in Equation (3.49).

We will now verify that this definition satisfies the defining property of a star product, i.e., $W_{FG}(\theta,\phi) = W_F(\theta,\phi) \star W_G(\theta,\phi)$ [see Eq. (3.36)]. We start by expanding the operators $F = \sum_{j=0}^{1}\sum_{m=-j}^{j} f_{jm}\mathrm{T}_{jm}$ and $G = \sum_{j=0}^{1}\sum_{m=-j}^{j} g_{jm}\mathrm{T}_{jm}$ into tensor operators T_{jm}. One directly obtains that

$$FG = \sum_{j_1,j_2=0}^{1}\sum_{m_1=-j_1}^{j_1}\sum_{m_2=-j_2}^{j_2} f_{j_1m_1}g_{j_2m_2}\,\mathrm{T}_{j_1m_1}\mathrm{T}_{j_2m_2}. \tag{3.50}$$

This summation involves products $\mathrm{T}_{j_1m_1}\mathrm{T}_{j_2m_2}$ of tensor operators which can be rewritten following Eq. (3.38) as

$$\mathrm{T}_{j_1m_1}\mathrm{T}_{j_2m_2} = \sum_{L=|j_1-j_2|}^{n} Q^{(1/2)}_{j_1j_2L}\, C^{LM}_{j_1m_1j_2m_2}\mathrm{T}_{LM}, \tag{3.51}$$

where n can be limited to $n = \min(j_1{+}j_2, 2J)$ and $M = m_1{+}m_2$. In order to compare Eqs. (3.50) and (3.51) with their counterparts in the Wigner space, we also compute the star product $W_F(\theta,\phi) \star W_G(\theta,\phi)$. Recall from Eq. (3.29) that the Wigner representations of F and G are given by $W_F = \sum_{j=0}^{1}\sum_{m=-j}^{j} f_{jm}\mathrm{Y}_{jm}$ and $W_G = \sum_{j=0}^{1}\sum_{m=-j}^{j} g_{jm}\mathrm{Y}_{jm}$. The prestar product (i.e., the product that results in the star product after truncation) evaluates to

$$W_F(\theta,\phi) \star W_G(\theta,\phi) = \sum_{j_1,j_2=0}^{1}\sum_{m_1=-j_1}^{j_1}\sum_{m_2=-j_2}^{j_2} f_{j_1m_1}g_{j_2m_2}\,\mathrm{Y}_{j_1m_1} \star \mathrm{Y}_{j_2m_2}, \tag{3.52}$$

Table 3.5: Prestar product $\star$ (i.e., the product that results in the star product after truncation) of spherical harmonics for a single spin $1/2$. The corresponding star product $\star$ is obtained by discarding the underlined components Y_{jm} with $j > 1$.

$\downarrow \star \rightarrow$	Y_{00}	$\mathrm{Y}_{1,-1}$	Y_{10}	Y_{11}
Y_{00}	$\frac{1}{\sqrt{2}}\mathrm{Y}_{00}$	$\frac{1}{\sqrt{2}}\mathrm{Y}_{1,-1}$	$\frac{1}{\sqrt{2}}\mathrm{Y}_{10}$	$\frac{1}{\sqrt{2}}\mathrm{Y}_{11}$
$\mathrm{Y}_{1,-1}$	$\frac{1}{\sqrt{2}}\mathrm{Y}_{1,-1}$	$\underline{0+\sqrt{\frac{3}{5}}\mathrm{Y}_{2,-2}}$	$\frac{1}{\sqrt{2}}\mathrm{Y}_{1,-1}\underline{+\sqrt{\frac{3}{10}}\mathrm{Y}_{2,-1}}$	$-\frac{1}{\sqrt{2}}\mathrm{Y}_{00}+\frac{1}{\sqrt{2}}\mathrm{Y}_{10}\underline{+\frac{1}{\sqrt{10}}\mathrm{Y}_{20}}$
Y_{10}	$\frac{1}{\sqrt{2}}\mathrm{Y}_{10}$	$-\frac{1}{\sqrt{2}}\mathrm{Y}_{1,-1}\underline{+\sqrt{\frac{3}{10}}\mathrm{Y}_{2,-1}}$	$\frac{1}{\sqrt{2}}\mathrm{Y}_{00}\underline{+\sqrt{\frac{2}{5}}\mathrm{Y}_{20}}$	$\frac{1}{\sqrt{2}}\mathrm{Y}_{11}\underline{+\sqrt{\frac{3}{10}}\mathrm{Y}_{21}}$
Y_{11}	$\frac{1}{\sqrt{2}}\mathrm{Y}_{11}$	$-\frac{1}{\sqrt{2}}\mathrm{Y}_{00}-\frac{1}{\sqrt{2}}\mathrm{Y}_{10}\underline{+\frac{1}{\sqrt{10}}\mathrm{Y}_{20}}$	$-\frac{1}{\sqrt{2}}\mathrm{Y}_{11}\underline{+\sqrt{\frac{3}{10}}\mathrm{Y}_{21}}$	$\underline{0+\sqrt{\frac{3}{5}}\mathrm{Y}_{22}}$

where the explicit formula of Eq. (3.47) results in

$$\mathrm{Y}_{j_1m_1} \star \mathrm{Y}_{j_2m_2} = \sqrt{2\pi}\,\mathrm{Y}_{j_1m_1}\mathrm{Y}_{j_2m_2} - \tfrac{i}{2}\{\mathrm{Y}_{j_1m_1}, \mathrm{Y}_{j_2m_2}\} = \sum_{L=|j_1-j_2|}^{j_1+j_2} \Lambda_{j_1j_2L} C^{LM}_{j_1m_1j_2m_2} \mathrm{Y}_{LM}. \tag{3.53}$$

Here, we have applied the formulas in Eqs. (3.41) and (3.42) and use the notation $\Lambda_{j_1j_2L} \coloneqq \sqrt{2\pi}Z_{j_1j_2L} - (i/2)U_{j_1j_2L}$. The corresponding star product $\star$ is obtained if we substitute the upper summation bound in Eq. (3.53) with $n = \min(j_1+j_2, 2J)$, which is the same bound as in Eq. (3.51). We are now ready to compare the tensor operators in Eqs. (3.50) and (3.51) with their respective complements in the Wigner space in Eqs. (3.52) and (3.53). Consequently, we have to compare the explicit values of the coefficients $Q^{(1/2)}_{j_1j_2L}$ and $\Lambda_{j_1j_2L}$ and we obtain that

$$\begin{aligned} &Q^{(1/2)}_{000} = Q^{(1/2)}_{011} = Q^{(1/2)}_{101} = \Lambda_{000} = \Lambda_{011} = \Lambda_{101} = \tfrac{1}{\sqrt{2}}, \\ &Q^{(1/2)}_{110} = \Lambda_{110} = -\tfrac{\sqrt{3}}{\sqrt{2}},\ Q^{(1/2)}_{111} = \Lambda_{111} = -1, \end{aligned}$$

and all other values are zero. This verifies that $\mathrm{Y}_{j_1m_1} \star \mathrm{Y}_{j_2m_2} = \mathcal{P}(\mathrm{Y}_{j_1m_1} \star \mathrm{Y}_{j_2m_2}) = \mathcal{W}(\mathrm{T}_{j_1m_1}\mathrm{T}_{j_2m_2})$, and one respectively concludes that $W_{FG}(\theta,\phi) = W_F(\theta,\phi) \star W_G(\theta,\phi)$. The preceding discussion is summarized as

Theorem 3.2. *The explicit form of the star product $\star$ in Eq.* (3.48) *observes its defining property from Eq.* (3.36)*, i.e. $W_{FG}(\theta,\phi) = W_F(\theta,\phi) \star W_G(\theta,\phi)$.*

The explicit values for the prestar product $\star$ (i.e., the product that results in the star product after truncation) for Wigner functions forming a basis for a single spin $1/2$ are presented in Table 3.5. The corresponding star product $\star$ is obtained by truncating the underlined parts in Table 3.5.

3.5.3.3 Equation of motion based on the star product

We can now apply Result 3.2 to the differential equation given in Eq. (3.37) in order to provide its explicit form for a single spin $1/2$. This results in the time evolution [253, 150]

$$\partial W_A/\partial t = \{W_A, W_{\mathcal{H}}\} \tag{3.54}$$

in the Wigner space which is governed by the Poisson bracket. A detailed visualization of the whole structure of our formalism leading to Eq. (3.54) is given in Figure B.2 of B.5. It can be inferred from Table 3.5 (as Y_{jm} with $j > 1$ in the decomposition are symmetric with respect to the order of multiplication) that $\{W_A, W_B\} = i(W_A \star W_B - W_B \star W_A) = i(W_A \star\!\!\!\star W_B - W_B \star\!\!\!\star W_A)$ holds for a single spin $1/2$. This means that a truncation is not required to compute the time evolution in this particular case. In the case of Hamiltonians that contain only ${}^J I_x$, ${}^J I_y$ and ${}^J I_z$ in the form ${}^J\mathcal{H} = c_x\,{}^J I_x + c_y\,{}^J I_y + c_z\,{}^J I_z$ Eq. (3.54) holds for arbitrary spin J [up to a global prefactor N_J as implied by Eq. (3.46)],[11] and agrees with the results of [253, 150]. Consequently, the time differential for an arbitrary spin J evolving under a linear Hamiltonian is given as

$$\partial W_{{}^J A}/\partial t = N_J\{W_{{}^J A}, W_{{}^J\mathcal{H}}\}, \tag{3.55}$$

where N_J is a global prefactor[11] and ${}^J A$ denotes an arbitrary spin-J operator.

3.5.4 Star product for multiple coupled spins with spin number $J = 1/2$

We extend the star product from Result 3.2 to multiple coupled spins. To this end, we introduce a projection operator $\mathcal{P}^{\{1\ldots N\}} := \prod_{k=1}^{N} \mathcal{P}^{\{k\}}$ which restricts resulting spherical harmonics to rank zero and one[12] and which can be via Equation (3.49) written as

$$\mathcal{P}^{\{k\}} := (1 + (\mathcal{L}^{\{k\}})^2/12 - (\mathcal{L}^{\{k\}})^4/24). \tag{3.56}$$

The angular momentum operator $\mathcal{L}$ acts as $(\mathcal{L}^{\{k\}})^2\,\mathrm{Y}_{jm}(\theta_k, \phi_k)$ and has the eigenvalues $j(j{+}1)\mathrm{Y}_{jm}(\theta_k, \phi_k)$. This projection will be used to truncate superfluous terms in the following definition of the star product:

[12] In general, an arbitrary, multivariate spherical function $f = f(\theta_1, \phi_1, \ldots, \theta_N, \phi_N)$ is projected using $\mathcal{P}^{\{k\}} f = \sum_{j_k=0}^{1} \sum_{m_k=-j_k}^{j_k} \mathrm{Y}_{j_k m_k}(\theta_k, \phi_k) \int_{\theta_k=0}^{\pi} \int_{\phi_k=0}^{2\pi} f\, \mathrm{Y}^*_{j_k m_k}(\theta_k, \phi_k) \sin\theta_k \,\mathrm{d}\phi_k \,\mathrm{d}\theta_k$.

Result 3.3. *The prestar product (the product that results in the star product after truncation) of two Wigner functions W_A and W_B corresponding to operators A and B in a system of N coupled spins $1/2$ is defined as*

$$W_A \star W_B := W_A(\prod_{k=1}^{N} \star^{\{k\}})W_B,$$

where the individual prestar operators are given by $\star^{\{k\}} := \sqrt{2\pi} - i\{\cdot,\cdot\}^{\{k\}}/2$ (cf. Result 3.2, Eq. (3.47)) and $\{\cdot,\cdot\}^{\{k\}}$ denotes the Poisson bracket taken with respect to the variables θ_k and ϕ_k, see Eq. (3.40). The star product

$$W_A \star W_B := \mathcal{P}^{\{1\ldots N\}}(W_A \star W_B) = \mathcal{P}^{\{1\ldots N\}}(W_A[\prod_{k=1}^{N}(\sqrt{2\pi} - \tfrac{i}{2}\{\cdot,\cdot\}^{\{k\}})]W_B). \quad (3.57)$$

is obtained by applying the projection operator $\mathcal{P}^{\{1\ldots N\}}$.

The star product for coupled spins in Result 3.3 allows us to establish the form of the Wigner representation for multispin product operators $\mathrm{T}^{\{1\}}_{j_1m_1}\cdots\mathrm{T}^{\{N\}}_{j_Nm_N}$, which consists of matrix products of single-spin operators, cf. Table 3.4. In the Wigner representation, matrix products are substituted by star products:

Lemma 3.3. *The Wigner representation of product operators $\mathrm{T}^{\{1\}}_{j_1m_1}\cdots\mathrm{T}^{\{N\}}_{j_Nm_N}$ is given by the prestar products (i.e., the product that results in the star product after truncation) of the Wigner representations $\mathcal{W}(\mathrm{T}^{\{k\}}_{j_km_k})$ of the individual single-spin operators, i.e.,*

$$\mathcal{W}(\mathrm{T}^{\{1\}}_{j_1m_1}\cdots\mathrm{T}^{\{N\}}_{j_Nm_N}) = \mathcal{W}(\mathrm{T}^{\{1\}}_{j_1m_1}) \star \cdots \star \mathcal{W}(\mathrm{T}^{\{N\}}_{j_Nm_N}) = \mathcal{W}(\mathrm{T}^{\{1\}}_{j_1m_1}) \star \cdots \star \mathcal{W}(\mathrm{T}^{\{N\}}_{j_Nm_N}). \quad (3.58)$$

Proof. From Eq. (3.33), we know that $\mathcal{W}(\mathrm{T}^{\{k\}}_{j_km_k}) = \mathrm{Y}^{\{k\}}_{j_km_k}$. All the Poisson brackets in the star product vanish as their arguments operate on different spins. Therefore, the right hand side of Eq. (3.58) is equal to [c.f. Eq. (3.57)]

$$\begin{aligned}\mathrm{Y}^{\{1\}}_{j_1m_1} \star \cdots \star \mathrm{Y}^{\{N\}}_{j_Nm_N} &= \sqrt{2\pi}^{N(N-1)}\, \mathrm{Y}^{\{1\}}_{j_1m_1}\cdots\mathrm{Y}^{\{N\}}_{j_Nm_N} \\ &= \mathrm{Y}_{j_1m_1}(\theta_1,\phi_1)\cdots\mathrm{Y}_{j_Nm_N}(\theta_N,\phi_N)/\sqrt{2}^{N(N-1)}.\end{aligned}$$

Equation (3.58) is now a consequence of Eq. (3.35). □

As a consequence of Lemma 3.3 and the linearity of the star product, the Wigner representation of an arbitrary product operator $A_1A_2\cdots A_N$ can be simplified as

$$\mathcal{W}(A_1A_2\cdots A_N) = \sqrt{2\pi}^{N(N-1)}\, \mathcal{W}(A_1)\mathcal{W}(A_2)\cdots\mathcal{W}(A_N),$$

where each linear operator is a linear combination of tensor operators acting on spin k $A_k = \sum_{j_k,m_k} c_{j_k m_k} \mathrm{T}^{\{k\}}_{j_k m_k}$. For example, the Wigner representation of Cartesian product operators is obtained by substituting A_k with $I_{k\alpha_k}$ for $\alpha_k \in \{x, y, z\}$.

The product of single-spin operators is computed via Lemma 3.1(c) as $\mathrm{T}^{\{k\}}_{j_1 m_1} \mathrm{T}^{\{k\}}_{j_2 m_2} = (\mathrm{T}_{j_1 m_1} \mathrm{T}_{j_2 m_2})^{\{k\}} / \sqrt{2}^{N-1}$. Also, the star product of Wigner functions can be concisely stated by applying the notation for embedded Wigner functions $W^{\{k\}}_A := \mathrm{Y}_{00} \cdots \mathrm{Y}_{00} W_A(\theta_k, \phi_k)\, \mathrm{Y}_{00} \cdots \mathrm{Y}_{00} = W_A(\theta_k, \phi_k) / \sqrt{4\pi}^{N-1}$. This results in the following

Lemma 3.4. *The star product of the two Wigner functions $\mathcal{W}(\mathrm{T}^{\{k\}}_{j_1 m_1}) = \mathrm{Y}^{\{k\}}_{j_1 m_1}$ and $\mathcal{W}(\mathrm{T}^{\{k\}}_{j_2 m_2}) = \mathrm{Y}^{\{k\}}_{j_2 m_2}$ is given by*

$$\mathrm{Y}^{\{k\}}_{j_1 m_1} \star \mathrm{Y}^{\{k\}}_{j_2 m_2} = W_{(\mathrm{T}_{j_1 m_1} \mathrm{T}_{j_2 m_2})}(\theta_k, \phi_k) / \sqrt{8\pi}^{N-1} = W^{\{k\}}_{(\mathrm{T}_{j_1 m_1} \mathrm{T}_{j_2 m_2})} / \sqrt{2}^{N-1}. \quad (3.59)$$

Proof. We set $F := \mathrm{T}_{j_1 m_1}$ and $G := \mathrm{T}_{j_2 m_2}$, and Lemma 3.2 verifies that $W_{FG}(\theta, \phi) = W_F(\theta, \phi) \star W_G(\theta, \phi)$. Applying the definition of the multispin star product form Eq. (3.57) of Result 3.3 to $\mathrm{Y}^{\{k\}}_{j_1 m_1} \star \mathrm{Y}^{\{k\}}_{j_2 m_2}$ results in

$$\sqrt{2\pi}^{N-1} \mathcal{P}^{\{k\}} \big[\tfrac{\mathrm{Y}_{j_1 m_1}(\theta_k, \phi_k)}{\sqrt{4\pi}^{N-1}} \,\text{✯}^{\{k\}}\, \tfrac{\mathrm{Y}_{j_2 m_2}(\theta_k, \phi_k)}{\sqrt{4\pi}^{N-1}} \big].$$

The formula $\mathcal{P}^{\{k\}}[\mathrm{Y}_{j_1 m_1}(\theta_k, \phi_k) \,\text{✯}^{\{k\}}\, \mathrm{Y}_{j_2 m_2}(\theta_k, \phi_k)] = W_{FG}(\theta_k, \phi_k)$ from Thm. 3.2 or Eq. (3.48) concludes the proof. □

After these preparations, we can prove that the star product given in Result 3.3 actually satisfies its defining property from Eq. (3.36):

Theorem 3.3. *In a system of N interacting spins $1/2$, the Wigner representations W_A and W_B of two operators A and B satisfy the equation $\mathcal{W}(AB) = W_A \star W_B$.*

Proof. We introduce the abbreviations for the multiple indexes $\vec{j} := (j_1, \ldots, j_N)$, $\vec{m} := (m_1, \ldots, m_N)$, $\vec{j}' := (j'_1, \ldots, j'_N)$, as well as $\vec{m}' := (m'_1, \ldots, m'_N)$. The product AB can be expanded as

$$\sum_{\vec{j},\vec{m},\vec{j}',\vec{m}'} a_{\vec{j},\vec{m}} b_{\vec{j}',\vec{m}'} 2^{N(N-1)}\, \mathrm{T}^{\{1\}}_{j_1 m_1} \mathrm{T}^{\{1\}}_{j'_1 m'_1} \cdots \mathrm{T}^{\{N\}}_{j_N m_N} \mathrm{T}^{\{N\}}_{j'_N m'_N},$$

and the matrix product can be independently evaluated on each individual spin. And each product $\mathrm{T}^{\{k\}}_{j_k m_k} \mathrm{T}^{\{k\}}_{j'_k m'_k}$ can be written as $(\mathrm{T}_{j_k m_k} \mathrm{T}_{j'_k m'_k})^{\{k\}} / \sqrt{2}^{N-1}$, cf. Lemma 3.1(c), and its Wigner transformation is given by $W^{\{k\}}_{(\mathrm{T}_{j'_k m'_k} \mathrm{T}_{j'_k m'_k})} / \sqrt{2}^{N-1}$. On the other hand, we get from

Lemma 3.3 that

$$W_A = \sum_{\vec{j},\vec{m}} a_{\vec{j},\vec{m}} \sqrt{2}^{N(N-1)} \mathrm{Y}^{\{1\}}_{j_1 m_1} \star \cdots \star \mathrm{Y}^{\{N\}}_{j_N m_N},$$
$$W_B = \sum_{\vec{j}',\vec{m}'} b_{\vec{j}',\vec{m}'} \sqrt{2}^{N(N-1)} \mathrm{Y}^{\{1\}}_{j_1 m_1} \star \cdots \star \mathrm{Y}^{\{N\}}_{j_N m_N},$$

and the star product is given by $W_A \star W_B = \sum_{\vec{j},\vec{m},\vec{j}',\vec{m}'} a_{\vec{j},\vec{m}} b_{\vec{j}',\vec{m}'} 2^{N(N-1)} C$, where

$$\begin{aligned} C &= \mathcal{P}^{\{1\ldots N\}}(\mathrm{Y}^{\{1\}}_{j_1 m_1} \star \cdots \star \mathrm{Y}^{\{N\}}_{j_N m_N} \star \mathrm{Y}^{\{1\}}_{j'_1 m'_1} \star \cdots \star \mathrm{Y}^{\{N\}}_{j'_N m'_N}) \\ &= [\mathcal{P}^{\{1\}}(\mathrm{Y}^{\{1\}}_{j_1 m_1} \star \mathrm{Y}^{\{1\}}_{j'_1 m'_1})] \star \cdots \star [\mathcal{P}^{\{N\}}(\mathrm{Y}^{\{N\}}_{j_N m_N} \star \mathrm{Y}^{\{N\}}_{j'_N m'_N})] \\ &= W^{\{1\}}_{(\mathrm{T}_{j_1 m_1} \mathrm{T}_{j'_1 m'_1})}/\sqrt{2}^{N-1} \star \cdots \star W^{\{N\}}_{(\mathrm{T}_{j_N m_N} \mathrm{T}_{j'_N m'_N})}/\sqrt{2}^{N-1}. \end{aligned}$$

Note that the second equality holds since two spherical harmonics $\mathrm{Y}^{\{k\}}_{j_k m_k}$ and $\mathrm{Y}^{\{\ell\}}_{j_\ell m_\ell}$ do star-commute under the assumption that $k \neq \ell$, i.e. $[\mathrm{Y}^{\{k\}}_{j_k m_k}, \mathrm{Y}^{\{\ell\}}_{j_\ell m_\ell}]_\star = 0$. The third equality follows from Lemma 3.4 which shows that $\mathrm{Y}^{\{k\}}_{j_k m_k} \star \mathrm{Y}^{\{k\}}_{j'_k m'_k} = W^{\{k\}}_{(\mathrm{T}_{j_k m_k} \mathrm{T}_{j'_k m'_k})}/\sqrt{2}^{N-1}$. The proof is now a consequence of Lemma 3.3 which verifies that $W^{\{1\}}_{(\mathrm{T}_{j_1 m_1} \mathrm{T}_{j'_1 m'_1})} \star \cdots \star W^{\{N\}}_{(\mathrm{T}_{j_N m_N} \mathrm{T}_{j'_N m'_N})} = \mathcal{W}[(\mathrm{T}_{j_1 m_1} \mathrm{T}_{j'_1 m'_1})^{\{1\}} \cdots (\mathrm{T}_{j_N m_N} \mathrm{T}_{j'_N m'_N})^{\{N\}}]$. □

After verifying the correctness of the star product from Result 3.3, we highlight how the star product governs the time evolution of an arbitrary number N of coupled spins $1/2$. We introduce the notations $a := \sqrt{2\pi}$ and $b_k := -\frac{i}{2}\{\cdot,\cdot\}^{\{k\}}$ and start by rewriting the star product [see Eq. (3.57) in Result 3.3] into a more convenient form

$$\star = \prod_{k=1}^{N} (a + b_k) = \sum_{\ell=0}^{N} a^{N-\ell} \Big[\sum_{\substack{k_1,k_2,\ldots,k_\ell \\ k_\mu \neq k_\nu \text{ if } \mu \neq \nu}} b_{k_1} b_{k_2} \cdots b_{k_\ell} \Big], \tag{3.60}$$

where $k_\mu \in \{1,\ldots,N\}$. The first four terms in the sum of Eq. (3.60) are given by

$$\begin{aligned} \star =& a^N + a^{N-1}(b_1 + b_2 + \cdots + b_N) + a^{N-2}(b_1 b_2 + \cdots + b_{N-1} b_N) \\ &+ a^{N-3}(b_1 b_2 b_3 + \cdots + b_{N-2} b_{N-1} b_N) + \cdots, \end{aligned}$$

and there are in total $\sum_{\ell=0}^{N} \binom{N}{\ell} = 2^N$ terms. The star product is then obtained by applying the projector $\mathcal{P}^{\{1\ldots N\}}$ from Eq. (3.56). Result 3.3 now determines the equation of motion via the star commutator from Eq. (3.37) while the terms with even indices ℓ in Eq. (3.60) cancel each other out.

Result 3.4. *The equation of motion in a system of N coupled spins $1/2$ is given by*

$$i\frac{\partial W_\rho}{\partial t} = 2(W_{\mathrm{Id}})^{-1}\,\mathcal{P}^{\{1\ldots N\}}[W_{\mathcal{H}} \sum_{\substack{\ell=1\\ \ell\ odd}}^{N} c^\ell \sum_{\substack{k_1,k_2,\ldots,k_\ell\\ k_\mu\neq k_\nu\ if\ \mu\neq\nu}} p_{k_1}p_{k_2}\cdots p_{k_\ell}\,W_\rho], \tag{3.61}$$

where $c := -i/\sqrt{8\pi}$, $W_{\mathrm{Id}} = 1/\sqrt{2\pi}^N$ is the Wigner transform of the identity operator (see Table 3.3), $\mathcal{P}^{\{1\ldots N\}}$ denotes the projection from Eq. (3.56)*, and $p_{k_\mu} := \{\cdot,\cdot\}^{\{k_\mu\}}$ is the Poisson bracket from Eq.* (3.40)*. The first two terms in the expansion are*

$$\begin{aligned} i\frac{\partial W_\rho}{\partial t} = 2(W_{\mathrm{Id}})^{-1}\,\mathcal{P}^{\{1\ldots N\}}[&c\,W_{\mathcal{H}}(p_1+p_2+\cdots+p_N)W_\rho \\ &+ c^3\,W_{\mathcal{H}}(p_1p_2p_3+\cdots+p_{N-2}p_{N-1}p_N)W_\rho+\cdots]. \end{aligned}$$

The first term in this expansion is given as a sum $W_{\mathcal{H}}(p_1 + p_2 + \cdots + p_N)W_\rho$ of Poisson brackets, which corresponds to a classical evolution of a phase-space probability distribution W_ρ. This truncated version of the expansion could be used to study the evolution of spin-$1/2$ systems in a semi-classical approximation. And the first-order approximation $-(W_{\mathrm{Id}})^{-1}/\sqrt{2\pi}\,\mathcal{P}^{\{1\ldots N\}}[\,W_{\mathcal{H}}(p_1 + p_2 + \cdots + p_N)W_\rho]$ to the time derivative corresponds to the classical equation of motion, and the number of terms (i.e. the number of Poisson brackets p_k) scales linearly with the number N of degrees of freedom. The complete, exact equation of motion of a spin-$1/2$ system is then established by introducing quantum corrections as a power series of odd powers in c, similar as in the infinite-dimensional case. The number of these quantum corrections grows exponentially for increasing number of coupled spins. Consequently, the equation of motion is a sum of those terms that contain odd number of products of Poisson brackets. The contribution of each term $p_{k_1}p_{k_2}\cdots p_{k_\ell}$ shrinks exponentially for increasing N as the number of Poisson brackets grows.

3.5.5 Results for multiple coupled spins $1/2$

The Wigner formalism for an arbitrary number of coupled spins $1/2$ is completely determined by the previous sections: the star product and the equation of motion are given in Results 3.3 and 3.4, respectively. In the following, these results are summarized and simplified for the special cases of two and three coupled spins $1/2$, as these cases are important for applications.

3.5.5.1 Two coupled spins

The star product from Result 3.3 is now detailed in a convenient formula for the case of two coupled spins $1/2$:

Corollary 3.1. *In case of two coupled spins* $1/2$*, we obtain the prestar product as*

$$\begin{aligned} \star &= (\sqrt{2\pi}-\tfrac{i}{2}\{\cdot,\cdot\}^{\{1\}})(\sqrt{2\pi}-\tfrac{i}{2}\{\cdot,\cdot\}^{\{2\}}) \\ &= 2\pi - i\sqrt{\tfrac{\pi}{2}}(\{\cdot,\cdot\}^{\{1\}}+\{\cdot,\cdot\}^{\{2\}}) - \{\cdot,\cdot\}^{\{1\}}\{\cdot,\cdot\}^{\{2\}}/4. \end{aligned} \tag{3.62}$$

The star product $W_A(\theta_1,\phi_1,\theta_2,\phi_2) \star W_B(\theta_1,\phi_1,\theta_2,\phi_2)$ *of two Wigner functions can be consequently computed as* $\mathcal{P}^{\{1,2\}}[W_A(\theta_1,\phi_1,\theta_2,\phi_2) \star W_B(\theta_1,\phi_1,\theta_2,\phi_2)]$*, where the corresponding projections* $\mathcal{P}^{\{1,2\}} = \mathcal{P}^{\{2\}}\mathcal{P}^{\{1\}}$ *act on two spheres by projecting onto rank-one and rank-zero spherical harmonics; refer to the definition of* $\mathcal{P}^{\{k\}}$ *in Eq.* (3.56)*.*

Table 3.4 implies that tensor operators acting on single spins are expressed as $\mathrm{T}^{\{1\}}_{j_1m_1} = \mathrm{T}_{j_1m_1} \otimes \mathrm{T}_{0,0}$ and $\mathrm{T}^{\{2\}}_{j_2m_2} = \mathrm{T}_{0,0} \otimes \mathrm{T}_{j_2m_2}$, and their Wigner transformations from Result 3.1 are $\mathcal{W}(\mathrm{T}^{\{1\}}_{jm}) = \mathrm{Y}^{\{1\}}_{jm} = \mathrm{Y}_{jm}(\theta_1,\phi_1)/\sqrt{4\pi}$ and $\mathcal{W}(\mathrm{T}^{\{2\}}_{jm}) = \mathrm{Y}^{\{2\}}_{jm} = \mathrm{Y}_{jm}(\theta_2,\phi_2)/\sqrt{4\pi}$. Similarly, one obtains the form $\mathcal{W}(2\mathrm{T}^{\{1\}}_{j_1m_1}\mathrm{T}^{\{2\}}_{j_2m_2}) = \mathrm{Y}_{j_1m_1}(\theta_1,\phi_1)\mathrm{Y}_{j_2m_2}(\theta_2,\phi_2)$ of the Wigner representation for bilinear operators, cf. Result 3.1. The star commutator

$$[W_A,W_B]_\star = W_A \star W_B - W_B \star W_A = -i\sqrt{2\pi}\mathcal{P}^{\{1,2\}}(\{W_A,W_B\}^{\{1\}} + \{W_A,W_B\}^{\{2\}})$$

is given by the antisymmetric part of the star product from Result 3.3, which in the case of two spins $1/2$ results in the truncated Poisson bracket over both spheres. The time evolution of the density matrix ρ under the Hamiltonian $\mathcal{H}$ is proportional to the star commutator (see Result 3.4):

Corollary 3.2. *The equation of motion for two coupled spins* $1/2$ *is given by*

$$\tfrac{\partial W_\rho}{\partial t} = \sqrt{2\pi}\mathcal{P}^{\{1,2\}}(\{W_\rho,W_\mathcal{H}\}^{\{1\}}+\{W_\rho,W_\mathcal{H}\}^{\{2\}}). \tag{3.63}$$

3.5.5.2 Three coupled spins

For three coupled spins, we also obtain the star product by applying Result 3.3:

Corollary 3.3. *The prestar product for three coupled spins* $1/2$ *simplifies to*

$$\star = (\sqrt{2\pi}-\tfrac{i}{2}\{\cdot,\cdot\}^{\{1\}})(\sqrt{2\pi}-\tfrac{i}{2}\{\cdot,\cdot\}^{\{2\}})(\sqrt{2\pi}-\tfrac{i}{2}\{\cdot,\cdot\}^{\{3\}}), \tag{3.64}$$

and the star product $W_A \star W_B = \mathcal{P}^{\{1,2,3\}}(W_A \star W_B)$ *is obtained by applying the projection* $\mathcal{P}^{\{1,2,3\}} = \mathcal{P}^{\{3\}}\mathcal{P}^{\{2\}}\mathcal{P}^{\{1\}}$*; refer to the definition of* $\mathcal{P}^{\{k\}}$ *in Eq.* (3.56)*.*

Normalized linear tensor operators are given as $\mathrm{T}^{\{1\}}_{j_1m_1} = \mathrm{T}_{j_1m_1} \otimes \mathrm{T}_{00} \otimes \mathrm{T}_{00}$, $\mathrm{T}^{\{2\}}_{j_2m_2} = \mathrm{T}_{00} \otimes \mathrm{T}_{j_2m_2} \otimes \mathrm{T}_{00}$ and $\mathrm{T}^{\{3\}}_{j_3m_3} = \mathrm{T}_{00} \otimes \mathrm{T}_{00} \otimes \mathrm{T}_{j_3m_3}$. Their Wigner representation from Result 3.1 is $\mathcal{W}(\mathrm{T}^{\{1\}}_{jm}) = \mathrm{Y}^{\{1\}}_{jm} = \mathrm{Y}_{jm}(\theta_1, \phi_1)/4\pi$. In the bilinear case, the Wigner functions have the form

$$\begin{aligned}
\mathcal{W}(\sqrt{2}^3 \mathrm{T}^{\{1\}}_{j_1m_1} \mathrm{T}^{\{2\}}_{j_2m_2}) &= \mathrm{Y}_{j_1m_1}(\theta_1, \phi_1)\mathrm{Y}_{j_2m_2}(\theta_2, \phi_2)/\sqrt{4\pi}, \\
\mathcal{W}(\sqrt{2}^3 \mathrm{T}^{\{2\}}_{j_2m_2} \mathrm{T}^{\{3\}}_{j_3m_3}) &= \mathrm{Y}_{j_2m_2}(\theta_2, \phi_2)\mathrm{Y}_{j_3m_3}(\theta_3, \phi_3)/\sqrt{4\pi}, \\
\mathcal{W}(\sqrt{2}^3 \mathrm{T}^{\{1\}}_{j_1m_1} \mathrm{T}^{\{3\}}_{j_3m_3}) &= \mathrm{Y}_{j_1m_1}(\theta_1, \phi_1)\mathrm{Y}_{j_3m_3}(\theta_3, \phi_3)/\sqrt{4\pi}.
\end{aligned}$$

The correctly normalized trilinear operator $\sqrt{2}^6 \mathrm{T}^{\{1\}}_{j_1m_1} \mathrm{T}^{\{2\}}_{j_2m_2} \mathrm{T}^{\{3\}}_{j_3m_3}$ results in the Wigner function $\mathrm{Y}_{j_1m_1}(\theta_1, \phi_1)\mathrm{Y}_{j_2m_2}(\theta_2, \phi_2)\mathrm{Y}_{j_3m_3}(\theta_3, \phi_3)$. The time evolution is determined by the star commutator

$$[W_A, W_B]_\star = -2\pi i \mathcal{P}^{\{1,2,3\}} \sum_{k=1}^{3} \{W_A, W_B\}^{\{k\}} + \tfrac{i}{4} \mathcal{P}^{\{1,2,3\}} W_A(\{.,.\}^{\{1\}}\{.,.\}^{\{2\}}\{.,.\}^{\{3\}}) W_B, \tag{3.65}$$

i.e., the antisymmetric part of the star product from Result 3.3. Using Result 3.4, we obtain the equation of motion:

Corollary 3.4. *The equation of motion for three coupled spins $1/2$ is determined as*

$$\tfrac{\partial W_\rho}{\partial t} = 2\pi \mathcal{P}^{\{1,2,3\}} \sum_{k=1}^{3} \{W_\rho, W_\mathcal{H}\}^{\{k\}} - \tfrac{1}{4} \mathcal{P}^{\{1,2,3\}} W_\rho(\{.,.\}^{\{1\}}\{.,.\}^{\{2\}}\{.,.\}^{\{3\}}) W_\mathcal{H}.$$

Here, the triple Poisson bracket $p_1p_2p_3$ in Result 3.4 is the first quantum correction (which vanishes except when acting on trilinear Wigner functions) and leads to the explicit form

$$\begin{aligned}
\{\cdot,\cdot\}^{\{1\}}\{\cdot,\cdot\}^{\{2\}}\{\cdot,\cdot\}^{\{3\}} = &\tfrac{1}{R^3 \sin\theta_1 \sin\theta_2 \sin\theta_3} \\
&\times \big(+ \overleftarrow{\partial}^3_{\phi_1,\phi_2,\phi_3} \overrightarrow{\partial}^3_{\theta_1,\theta_2,\theta_3} - \overleftarrow{\partial}^3_{\phi_2,\phi_3,\theta_1} \overrightarrow{\partial}^3_{\phi_1,\theta_2,\theta_3} \\
&\quad - \overleftarrow{\partial}^3_{\phi_1,\phi_3,\theta_2} \overrightarrow{\partial}^3_{\phi_2,\theta_1,\theta_3} - \overleftarrow{\partial}^3_{\phi_1,\phi_2,\theta_3} \overrightarrow{\partial}^3_{\phi_3,\theta_1,\theta_2} \\
&\quad + \overleftarrow{\partial}^3_{\phi_1,\theta_2,\theta_3} \overrightarrow{\partial}^3_{\phi_2,\phi_3,\theta_1} + \overleftarrow{\partial}^3_{\phi_2,\theta_1,\theta_3} \overrightarrow{\partial}^3_{\phi_1,\phi_3,\theta_2} \\
&\quad + \overleftarrow{\partial}^3_{\phi_3,\theta_1,\theta_2} \overrightarrow{\partial}^3_{\phi_1,\phi_2,\theta_3} - \overleftarrow{\partial}^3_{\theta_1,\theta_2,\theta_3} \overrightarrow{\partial}^3_{\phi_1,\phi_2,\phi_3} \big),
\end{aligned}$$

where the notation $\partial^3_{\theta_1,\theta_2,\theta_3} = \partial^3/(\partial\theta_1\partial\theta_2\partial\theta_3)$ is used and the direction of an arrow signifies whether the derivative is taken with respect to the function on the left or right side of the expression.

3.5.5.3 Geometrical interpretation of the scalar product of vector operators in the Wigner representation

Let us consider the following two vector operators in a system of two coupled spins $1/2$ as $\mathrm{I}_k = (I_{kx}, I_{ky}, I_{kz})$ for $k \in \{1, 2\}$. The scalar product of these two operators yields

$$\mathrm{I}_1 \cdot \mathrm{I}_2 = I_{1x}I_{2x} + I_{1y}I_{2y} + I_{1z}I_{2z} = \sum_{m=-1}^{1} \mathrm{T}_{1m} \otimes \mathrm{T}_{1m}^{\dagger}/2, \tag{3.66}$$

where the second equality is given by a decomposition into tensor operators. Equation (3.66) can be generalized to arbitrary J.[11] Many important coupling Hamiltonians of two angular momenta can be described in this form including the scalar coupling and the spin-orbit coupling. The Wigner representation directly follows as

$$\mathcal{W}(\mathrm{I}_1 \cdot \mathrm{I}_2) = \sum_{m=-1}^{1} \mathrm{Y}_{1m}(\theta_1, \phi_1)\mathrm{Y}_{1m}^{*}(\theta_2, \phi_2)/2. \tag{3.67}$$

Given the unit vectors $\vec{r}_k$ in $\mathbb{R}^3$ which are parametrized in spherical coordinates as

$$\vec{r}_k := (x_k, y_k, z_k)^T = (\sin\theta_k \cos\phi_k, \sin\theta_k \sin\phi_k, \cos\theta_k)^T,$$

their scalar product is given by $\vec{r}_1 \cdot \vec{r}_2 = \cos\gamma$, where γ denotes the angle between the two unit vectors $\vec{r}_1$ and $\vec{r}_2$. Consequently the addition theorem of spherical harmonics [19] results in

$$P_j(\cos\gamma) = \frac{4\pi}{2j+1} \sum_{m=-j}^{j} \mathrm{Y}_{jm}(\theta_1, \phi_1)\mathrm{Y}_{jm}^{*}(\theta_2, \phi_2), \tag{3.68}$$

where $P_j(\alpha)$ is the Legendre polynomial of degree j. Thus, one can rewrite the Wigner function in Eq. (3.67) in terms of the angle γ as $\mathcal{W}(\mathrm{I}_1 \cdot \mathrm{I}_2) = R^2 \cos\gamma$, with $R := \sqrt{3/(8\pi)}$.

The arguments of the Wigner function of two coupled spins $W = W(\theta_1, \phi_1, \theta_2, \phi_2)$ can also be given in terms of the unit vectors $\vec{r}_1$ and $\vec{r}_2$ as $W = W(\vec{r}_1, \vec{r}_2)$, consequently Eq. (3.67) becomes $\mathcal{W}(\mathrm{I}_1 \cdot \mathrm{I}_2) = R^2\, \vec{r}_1 \cdot \vec{r}_2$ by applying Eq. (3.68). Expanding this expression results in

$$\mathcal{W}(\mathrm{I}_1 \cdot \mathrm{I}_2) = R^2\,(x_1x_2 + y_1y_2 + z_1z_2) = R^2[\cos\theta_1 \cos\theta_2 + \sin\theta_1 \sin\theta_2 \cos(\phi_1 - \phi_2)].$$

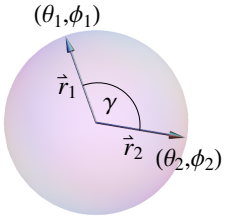

Figure 3.6: (Color online) The Wigner function $W(\theta_1, \phi_1, \theta_2, \phi_2)$ of two spins is determined by their arguments which define two points on the surface of the unit sphere. These points correspond to the unit vectors $\vec{r}_1$ and $\vec{r}_2$.

In general, the Wigner function of two spins is a complex number $W(\theta_1, \phi_1, \theta_2, \phi_2)$ which depends on the arguments θ_1, ϕ_1, θ_2, and ϕ_2. These arguments define two points on a sphere, see Fig. 3.6. The Wigner function $\tilde{W}(\vec{r}_1, \vec{r}_2) \coloneqq \mathcal{W}(\mathrm{I}_1 \cdot \mathrm{I}_2)$ is now completely determined by the angle γ between the two vectors $\vec{r}_1$ and $\vec{r}_2$. The value of the Wigner function is given by $\tilde{W}(\vec{r}_1', \vec{r}_2') = 0$ for the particular choices of $\vec{r}_1' = (0,0,1)$ and $\vec{r}_2' = (1,0,0)$. And similarly for $\vec{r}_1'' = (1/\sqrt{2}, 1/\sqrt{2}, 0)$ and $\vec{r}_2'' = (0, 1/\sqrt{2}, 1/\sqrt{2})$, one obtains $\tilde{W}(\vec{r}_1'', \vec{r}_2'') = R^2/2$.

3.5.5.4 Spins evolving under a natural Hamiltonian

Let us finally consider the case where an arbitrary number N of coupled spins $1/2$ evolve under a Hamiltonian

$$\mathcal{H} = \sum_{k=1}^{N} \sum_{j,m} a_{j,m,k} \mathrm{T}_{jm}^{\{k\}} + \sum_{k_1 \neq k_2}^{N} \sum_{\substack{j_1, j_2 \\ m_1, m_2}} b_{j_1,m_1,k_1}^{j_2,m_2,k_2} \mathrm{T}_{j_1 m_1}^{\{k_1\}} \mathrm{T}_{j_2 m_2}^{\{k_2\}}$$

which contains only linear and bilinear interactions, i.e., natural interactions of physical systems. Refer also to Eq. (3.66) in Sec. 3.5.5.3 for the form of the coupling Hamiltonian.

Corollary 3.5. *For natural Hamiltonians consisting only of linear and bilinear terms, the time evolution of a system of N interacting spins $1/2$ is given by*

$$\partial W_\rho / \partial t = \sqrt{2\pi}^{N-1} \mathcal{P}^{\{1\ldots N\}} \sum_{k=1}^{N} \{W_\rho, W_{\mathcal{H}}\}^{\{k\}}, \tag{3.69}$$

where W_ρ denotes the Wigner function of an arbitrary N-spin density matrix ρ and $\mathcal{P}^{\{1\ldots N\}}$ is the projection from Eq. (3.56).

Exact time evolution of spin-$1/2$ Wigner functions under natural Hamiltonians is therefore given by the sum of Poisson brackets, i.e., the classical equation of motion for phase-space probability distributions. The only non-classical term is the projection $\mathcal{P}^{\{1\ldots N\}}$ from Eq. (3.56).

3.6 Advanced examples

In this section, we consider two advanced examples to convey our approach of using sums of product operators and directly determining the time evolution of quantum systems in Wigner space. We analyze the case of two coupled spins evolving under the CNOT gate (see Sec. 3.6.1). Finally, we present an example for the time evolution of three coupled spins $1/2$ (see Sec. 3.6.2).

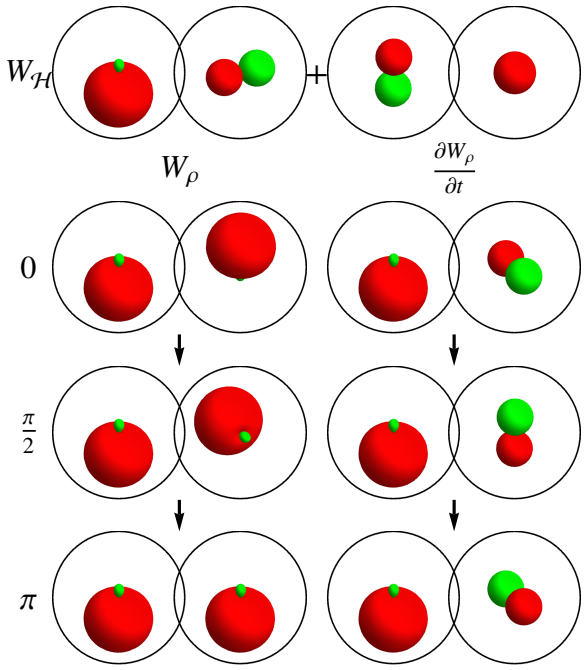

Figure 3.7: (Color online) Evolution of the density matrix of a pure quantum state $|\psi(0)\rangle = |\beta\alpha\rangle$ under the CNOT gate, implemented by the Hamiltonian $\mathcal{H} = \omega[I_{1\beta}I_{2x} + I_{1z}/2]$. PROPS representations of the Wigner functions W_ρ and $\partial W_\rho/\partial t$ are shown for the times $t = 0$, $\omega t = \pi/2$, and $\omega t = \pi$. The control spin is set to $|\beta\rangle$, and the second spin flips, i.e., $|\psi(\pi/\omega)\rangle = |\beta\beta\rangle$.[3]

3.6.1 CNOT gate

We continue our discussion of Wigner functions for two coupled spins 1/2 from Sec. 3.4.2 and consider the evolution of pure states under the controlled NOT (CNOT) gate [197]. Section 3.6.1.1 starts with the computation of the time evolution in the Wigner frame. In Sec. 3.6.1.2, we analyze the creation of entanglement using Wigner functions and their pictorial representations.

3.6.1.1 Evolution under the CNOT gate

In the following, we consider the time evolution of pure spin-1/2 states. Let us first introduce the notation $|\alpha\rangle := (1,0)^T$ and $|\beta\rangle := (0,1)^T$ (cf. p. 308 in [45], p. 126 in [210], or p. 3 in [52]), which is very similar to the notation $|0\rangle$ and $|1\rangle$ often used in quantum mechanics and quantum information theory [197], but avoids confusion with different conventions in the literature relating $|0\rangle$ to either the excited or ground state. A pure initial state $|\psi(0)\rangle := |\beta\rangle \otimes |\alpha\rangle \equiv |\beta\alpha\rangle$ is evolving under the effective Hamiltonian

$$\mathcal{H} = \omega(I_{1\beta}I_{2x} + I_{1z}/2) = \omega[(\mathrm{Id}_4/2 - I_{1z})I_{2x} + I_{1z}/2], \tag{3.70}$$

where $I_{1\beta} := I_\beta \otimes \mathrm{Id}_2$ and $I_\beta := \mathrm{Id}_2/2 - I_z = |\beta\rangle\langle\beta|$ projects onto the pure state $|\beta\rangle$; likewise $I_\alpha := \mathrm{Id}_2/2 + I_z = |\alpha\rangle\langle\alpha|$. Exponentiation of $-it\mathcal{H}$ leads to the unitary

$$U_t = \exp(-i\mathcal{H}t) = \xi(t)\begin{pmatrix} 1 & 0 & 0 & 0 \\ 0 & 1 & 0 & 0 \\ 0 & 0 & \frac{1+e^{i\omega t}}{2} & \frac{1-e^{i\omega t}}{2} \\ 0 & 0 & \frac{1-e^{i\omega t}}{2} & \frac{1+e^{i\omega t}}{2} \end{pmatrix} \tag{3.71}$$

of determinant one with $\xi(t) = \exp(-i\omega t/4)$, and U_T with $T = \pi/\omega$ is the CNOT gate. The initial state $|\psi(0)\rangle$ evolves into

$$|\psi(t)\rangle = U_t|\psi(0)\rangle = \tfrac{\xi(t)}{2}[(1+e^{i\omega t})|\beta\alpha\rangle + (1-e^{i\omega t})|\beta\beta\rangle], \tag{3.72}$$

where $|\psi(T)\rangle \propto |\beta\beta\rangle$. In preparation to switch to Wigner functions, Eq. (3.72) is rewritten in its density-matrix form

$$\rho(t) = |\psi(t)\rangle\langle\psi(t)| = \rho_A\,\rho_B(t) \text{ where} \tag{3.73}$$

$$\rho_A := I_{1\beta} \text{ and } \rho_B(t) := \mathrm{Id}_4/2 + \cos(\omega t) I_{2z} - \sin(\omega t) I_{2y}. \tag{3.74}$$

Recalling the respective Wigner functions from Table 3.3, one obtains for ρ_A, $\rho_B(t)$, and $\mathcal{H}$ the Wigner functions

$$W_{\rho_A} = \tfrac{1}{4\pi} - \lambda\cos\theta_1 = \mathcal{W}(I_{1\beta}), \tag{3.75a}$$

$$W_{\rho_B}(t) = \tfrac{1}{4\pi} + \cos(\omega t)\,\lambda\cos\theta_2 - \sin(\omega t)\,\lambda\sin\theta_2\sin\phi_2, \tag{3.75b}$$

$$W_{\mathcal{H}} = \omega[2\pi(\tfrac{1}{4\pi} - \lambda\cos\theta_1)\lambda\sin\theta_2\cos\phi_2 + \lambda\cos\theta_1/2], \tag{3.75c}$$

where $\lambda = \sqrt{3}/(4\pi) = R/\sqrt{2\pi}$. The product of W_{ρ_A} and $W_{\rho_B}(t)$ yields the overall Wigner function $W_\rho(t) = 2\pi W_{\rho_A} W_{\rho_B}(t)$. Its time evolution is shown in Fig. 3.7 where only one of the two spherical functions varies in time, reflecting the product form of $W_\rho(t)$.

The explicit form of the time evolution can also be derived from Eq. (3.16), hence $\partial W_\rho/\partial t = \sqrt{2\pi}\mathcal{P}^{\{1,2\}}(P_1 + P_2)$, where the Poisson brackets can be computed as $P_1 = 2\pi W_{\rho_B}(t)\{W_{\rho_A}, W_{\mathcal{H}}\}^{\{1\}}$ and $P_2 = 2\pi W_{\rho_A}\{W_{\rho_B}(t), W_{\mathcal{H}}\}^{\{2\}}$. As the Wigner function W_{ρ_A} depends only on the variable θ_1 and $W_{\mathcal{H}}$ does not depend on the variable ϕ_1, it is straightforward to deduce that $P_1 = 0$. This implies that W_{ρ_A} is time independent. The other Poisson bracket P_2 can be written as

$$\begin{aligned} P_2 = \omega[\sqrt{2\pi}R\mathcal{W}(I_{1\beta})]^2[&\cos(\omega t)\,\{\cos\theta_2, \sin\theta_2\cos\phi_2\}^{\{2\}} \\ &- \sin(\omega t)\,\{\sin\theta_2\sin\phi_2, \sin\theta_2\cos\phi_2\}^{\{2\}}]. \end{aligned} \tag{3.76}$$

Applying the definition of Eq. (3.9), the Poisson brackets in Eq. (3.76) are computed as

$$\{\cos\theta_2, \sin\theta_2\cos\phi_2\}^{\{2\}} = -\sin\theta_2\sin\phi_2/R, \quad \{\sin\theta_2\sin\phi_2, \sin\theta_2\cos\phi_2\}^{\{2\}} = \cos\theta_2/R.$$

The idempotency $(I_{k\beta})^2 = I_{k\beta}$ implies $2\pi\mathcal{P}^{\{1\}}\mathcal{W}(I_{1\beta})^2 = \mathcal{W}(I_{1\beta})$ where $\mathcal{P}^{\{1\}}$ projects

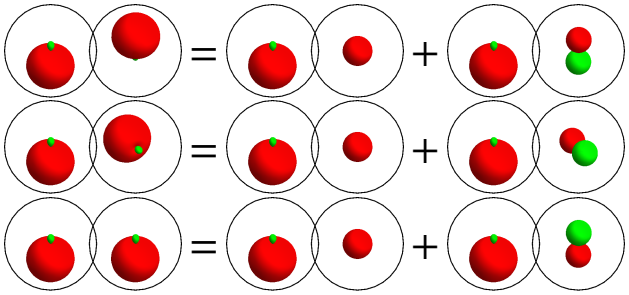

Figure 3.8: (Color online) The Wigner functions $W_\rho(t)$ from Fig. 3.7 are decomposed for $\omega t \in \{0, \pi/2, \pi\}$ into $1/(4\pi)$ and $\cos(\omega t)\,(\lambda\cos\theta_2) - \sin(\omega t)\,(\lambda\sin\theta_2\sin\phi_2)$ via Eqs. (3.74)-(3.75).[3]

onto rank-one and rank-zero spherical harmonics, i.e., the term from Eq. (3.76) results in $[\sqrt{2\pi}R\mathcal{W}(I_{1\beta})]^2 = R^2\mathcal{W}(I_{1\beta})$. Finally, the equation of motion based on Eq. (3.16) is

$$\partial W_\rho/\partial t = 2\pi\omega\lambda\mathcal{W}(I_{1\beta})[-\cos(\omega t)\sin\theta_2\sin\phi_2 - \sin(\omega t)\cos\theta_2],$$

which conforms with the explicitly known Wigner function from Eq. (3.75) as $\partial W_\rho/\partial t = 2\pi W_{\rho_A}\partial W_{\rho_B}(t)/\partial t$.

Similarly, one could start with $\tilde{\rho}_A = I_{1\alpha}$ and one would obtain for $t = 0$ that $\tilde{P}_2 \propto \mathcal{W}(I_{1\beta})\mathcal{W}(I_{1\alpha}) \propto (1-\sqrt{3}\cos\theta_1)(1+\sqrt{3}\cos\theta_1)$ and the result $1-3\cos^2\theta_1$ is proportional to Y_{20}, which is projected by $\mathcal{P}^{\{1\}}$ to zero. Consequently, the quantum state $\tilde{\rho}(t)$ would be constant, reflecting the nature of the CNOT gate.

Figure 3.7 visualizes the time evolution: starting from $|\psi(0)\rangle = |\beta\alpha\rangle$ one has the control state $|\beta\rangle$, and the state of the second spin flips from $|\alpha\rangle$ to $|\beta\rangle$, resulting in $|\psi(T)\rangle \propto |\beta\beta\rangle$. The Wigner function of the density matrix $I_{1\beta}$ of the pure state $|\beta\rangle$ is proportional to $1 - \sqrt{3}\cos\theta$ and is depicted in Fig. 3.7 as a big positive lobe in red (i.e. dark gray) lying below a small negative lobe in green (i.e. light gray), refer to the spherical function in the left circle of W_ρ. The spherical function in the right circle of W_ρ, starts with a big positive lobe lying over a small negative lobe, and this object is rotated. At time $T/2$, one observes for the second spin an equal superposition of $|\alpha\rangle$ and $|\beta\rangle$. The form of the Wigner function $W_\rho(t)$ during the time evolution is further highlighted in Fig. 3.8 by decomposing it into a time-independent part $1/(4\pi)$ and a time-dependent part $\cos(\omega t)\,(\lambda\cos\theta_2) - \sin(\omega t)\,(\lambda\sin\theta_2\sin\phi_2)$. The time-dependent part is simply a rotation of I_{2z} around the x axis.

3.6.1.2 Entanglement creation with the CNOT gate

In order to highlight the generation of entanglement, the time evolution under the Hamiltonian of Eq. (3.70) from Sec. 3.6.1.1 is applied to the initial state $|\gamma(0)\rangle = (|\alpha\alpha\rangle + |\beta\alpha\rangle)/\sqrt{2}$. The notation $|\alpha\rangle$ and $|\beta\rangle$ for spin-1/2 eigenstates was introduced in Sec. 3.6.1.1. This results in the time-dependent state $|\gamma(t)\rangle = U_t|\gamma(0)\rangle = (\xi(t)|\alpha\alpha\rangle + |\psi(t)\rangle)/\sqrt{2}$, cf. Eqs. (3.71)-(3.72). In particular for $t = T$ with $T = \pi/\omega$, one obtains (up to a phase) a maximally entangled Bell state $|\phi^+\rangle = (|\alpha\alpha\rangle + |\beta\beta\rangle)/\sqrt{2}$.

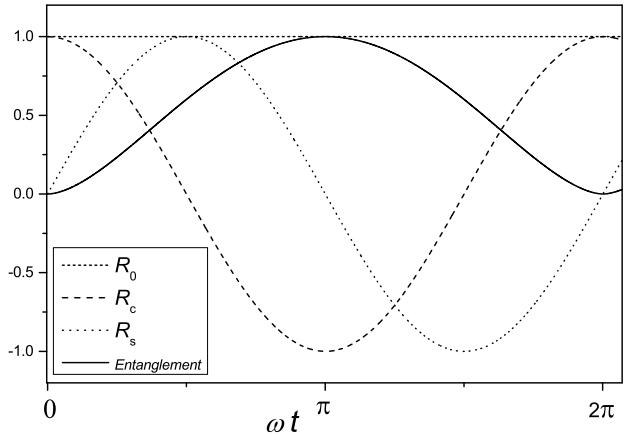

Figure 3.9: Entanglement and contributions of the density operator $\sigma(t) = |\gamma(t)\rangle\langle\gamma(t)| = R_0 + \cos(\omega t)R_c + \sin(\omega t)R_s$ [see Eq. (3.77)] during the evolution under the Hamiltonian of Eq. (3.70). The von-Neumann entropy of the partial trace is used as entanglement measure [197].

Equivalently, the time evolution can be described on the density operator with the expression $\sigma(t) = |\gamma(t)\rangle\langle\gamma(t)| = I_{1\alpha}I_{2\alpha} + \rho(t) + A(t) + A^\dagger(t)$, where $\rho(t)$ is given in Eq. (3.73) and $A(t) = \bar{\xi}(t)|\psi(t)\rangle\langle\alpha\alpha|$. The density operator can also be rewritten as $\sigma(t) = R_0 + \cos(\omega t)R_c + \sin(\omega t)R_s$[13], where

$$\begin{aligned} R_0 &= [+I_{1x}I_{2x} - I_{1y}I_{2y} + I_{1x}I_{2\alpha} + I_{1\alpha}I_{2\alpha} + \tfrac{1}{2}I_{1\beta}]/2, \\ R_c &= [-I_{1x}I_{2x} + I_{1y}I_{2y} + I_{1x}I_{2\alpha} + I_{1\beta}I_{2z}]/2, \\ R_s &= [I_{1y}(I_{2\alpha} - I_{2x}) - (I_{1x} + I_{1\beta})I_{2y}]/2. \end{aligned} \tag{3.77}$$

The evolution of these parts is shown in Fig. 3.9 together with the entanglement of the density operator as functions of time. Also, we obtain the decomposition

$$\begin{aligned} \sigma(0) &= R_0 + R_c = (\tfrac{1}{2}\mathrm{Id}_4 + I_{1x})I_{2\alpha}, \\ \sigma(T) &= R_0 - R_c = \tfrac{1}{4}\mathrm{Id}_4 + I_{1x}I_{2x} - I_{1y}I_{2y} + I_{1z}I_{2z}. \end{aligned} \tag{3.78}$$

We switch now to the Wigner functions

$$\begin{aligned} W_\sigma(0) &= 2\pi(\tfrac{1}{4\pi} + W_{1x})W_{2\alpha}, \\ W_\sigma(T) &= 2\pi(\tfrac{1}{8\pi} + W_{1x}W_{2x} - W_{1y}W_{2y} + W_{1z}W_{2z}), \\ W_{\mathcal{H}} &= 2\pi W_{1\beta}W_{2x} + \tfrac{1}{2}W_{1z}, \end{aligned} \tag{3.79}$$

for the density operators of Eq. (3.78) and the Hamiltonian $\mathcal{H}$ of Eq. (3.70) by applying Table 3.3, where W_{ka} denotes the Wigner function of I_{ka}. Figure 3.10 depicts the Wigner functions $W_\sigma(0)$, $W_\sigma(T)$, and W_{R_s} in their PROPS representations. The Wigner function

[13] One can establish that $\sigma(t)$ satisfies the von-Neumann equation (3.2) by verifying the commutators $[\mathcal{H}, R_0] = 0$, $[\mathcal{H}, R_c]/i = R_s$, and $[\mathcal{H}, R_s]/i = -R_c$ with the Hamiltonian $\mathcal{H}$ from Eq. (3.70).

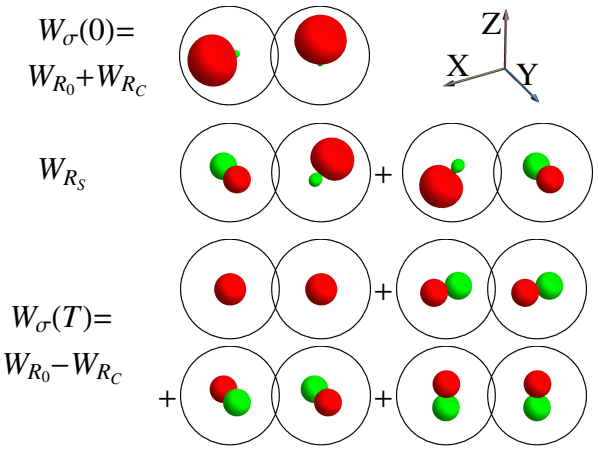

Figure 3.10: (Color online) Illustration of the Wigner functions $W_\sigma(0)$, W_{R_s}, and $W_\sigma(T)$ with $T = \pi/\omega$ using the PROPS representation. The generation of the maximally entangled Bell state $|\phi^+\rangle = (|\alpha\alpha\rangle + |\beta\beta\rangle)/\sqrt{2}$ at time T is reflected by the higher number of terms for $W_\sigma(T)$.[3]

$W_\sigma(t) = W_{R_0} + \cos(\omega t)W_{R_c} + \sin(\omega t)W_{R_s}$ satisfies the equation of motion in Eq. (3.16).[14]

As for $|\phi^+\rangle$, the maximal entangled pure states

$$|\phi^\pm\rangle = (|\alpha\alpha\rangle \pm |\beta\beta\rangle)/\sqrt{2} \text{ and } |\psi^\pm\rangle = (|\alpha\beta\rangle \pm |\beta\alpha\rangle)/\sqrt{2}$$

of a system of two spins $1/2$ have the density matrices

$$|\phi^+\rangle\langle\phi^+| = \tfrac{1}{4}\mathrm{Id}_4 + I_{1x}I_{2x} - I_{1y}I_{2y} + I_{1z}I_{2z}, \quad |\phi^-\rangle\langle\phi^-| = \tfrac{1}{4}\mathrm{Id}_4 - I_{1x}I_{2x} + I_{1y}I_{2y} + I_{1z}I_{2z},$$
$$|\psi^+\rangle\langle\psi^+| = \tfrac{1}{4}\mathrm{Id}_4 + I_{1x}I_{2x} + I_{1y}I_{2y} - I_{1z}I_{2z}, \quad |\psi^-\rangle\langle\psi^-| = \tfrac{1}{4}\mathrm{Id}_4 - I_{1x}I_{2x} - I_{1y}I_{2y} - I_{1z}I_{2z},$$

whose Wigner functions can be computed as in Eq. (3.79).

As detailed in Sec. 3.5.5.3 above, the Wigner transform of an operator of the form $I_{1x}I_{2x} + I_{1y}I_{2y} + I_{1z}I_{2z}$ results in the scalar product of two vectors $W(\vec{r}_1, \vec{r}_2) = R^2\,\vec{r}_1 \cdot \vec{r}_2$, providing a geometrical interpretation. Here, the argument of the Wigner function is given by the unit vectors $\vec{r}_1$ and $\vec{r}_2$ in $\mathbb{R}^3$, corresponding to the angles θ_1, ϕ_1 and θ_2, ϕ_2. As a result of the addition theorem of spherical harmonics, the Wigner function is given by the scalar product $\vec{r}_1 \cdot \vec{r}_2$ of the two vectors. The Wigner function of the maximally entangled state $|\psi^-\rangle\langle\psi^-|$ is consequently given as

$$\mathcal{W}(|\psi^-\rangle\langle\psi^-|) = 1/(8\pi) - R^2\,\vec{r}_1 \cdot \vec{r}_2,$$

it is thus entirely described by the angle between the two argument vectors. Similarly, the maximally entangled state $|\phi^+\rangle\langle\phi^+|$ has the Wigner function $1/(8\pi) + R^2\,\vec{r}_1' \cdot \vec{r}_2$, where the y entry of $\vec{r}_1'$ is negated, i.e., $\vec{r}_1'$ has the entries $[\vec{r}_1]_x$, $-[\vec{r}_1]_y$, and $[\vec{r}_1]_z$. Therefore, all Wigner

[14] This can be demonstrated for $\omega W_{R_s} = \partial W_\sigma(0)/\partial t$ [and likewise for $W_\sigma(t)$] by calculating the Poisson brackets $\{W_\sigma(0), W_\mathcal{H}\}^{\{1\}} = \omega[-(2\pi)^2\{W_{1x}, W_{1\beta}\}^{\{1\}}W_{2\alpha}W_{2x} + \pi\{W_{1x}, W_{1z}\}^{\{1\}}W_{2\alpha}]$ and also $\{W_\sigma(0), W_\mathcal{H}\}^{\{2\}} = \omega[(2\pi)^2\{W_{2\alpha}, W_{2x}\}^{\{2\}}[W_{1x} + (4\pi)^{-1}]W_{1\beta}]$. Afterwards, they are substituted back into the equation of motion; note the projection formulas $\mathcal{P}^{\{2\}}W_{2\alpha}W_{2x} = W_{2x}/(4\pi)$ and $\mathcal{P}^{\{1\}}W_{1x}W_{1\beta} = W_{1x}/(4\pi)$ as well as $\{W_{1x}, W_{1\beta}\}^{\{1\}} = -W_{1y}/\sqrt{2\pi}$ and $\{W_{2\alpha}, W_{2x}\}^{\{2\}} = -W_{2y}/\sqrt{2\pi}$.

functions of maximally entangled pure states for two spins $1/2$ can be described using the scalar product of their argument vectors after negating certain entries.

3.6.2 Evolution of three coupled spins

Let us now also discuss an example for the case of three coupled spins. The system starts from the traceless deviation density matrix $\rho(0) = I_{2x}$ and evolves under the Hamiltonian $\mathcal{H} = \pi\nu(2I_{1z}I_{2z}+2I_{2z}I_{3z})$ which couples both the first and second spin as well as the second and third spin with the same coupling strength ν. This results in anti-phase and double anti-phase operators [144]. The corresponding solution of the von-Neumann equation is given by

$$\rho(t) = \sin(2\pi\nu t)[2I_{1z}I_{2y}+2I_{2y}I_{3z}]/2+[\cos(2\pi\nu t)-1]4I_{1z}I_{2x}I_{3z}/2+[\cos(2\pi\nu t)+1]I_{2x}/2.$$

The detectable NMR signal corresponding to I_{2x} is proportional to $[\cos(2\pi\nu t) + 1]$, and the corresponding spectrum has the well-known form of a triplet (see, e.g., Figure 18.9 in [173]) whose lines are separated by ν and whose relative intensities are given by $1 : 2 : 1$.

The relevant Wigner functions are given by $W_{\mathcal{H}} = \pi\nu 2R^2(\cos\theta_1 + \cos\theta_3)\cos\theta_2/\sqrt{2\pi}$ and $W_\rho(t) = W_0 + \sin(2\pi\nu t)W_s + \cos(2\pi\nu t)W_c$, where

$$W_0 = \tfrac{2R^3}{3}(1-3\cos\theta_1\cos\theta_3)\sin\theta_2\cos\phi_2,\ W_s = \tfrac{R^2}{\sqrt{2\pi}}(\cos\theta_1+\cos\theta_3)\sin\theta_2\sin\phi_2,$$
$$\text{and } W_c = \tfrac{2R^3}{3}(1+3\cos\theta_1\cos\theta_3)\sin\theta_2\cos\phi_2.$$

Their form can be inferred from Table 3.3 and also the product structure of the Wigner functions $\mathcal{W}(I_{1a}I_{2b}I_{3c}) = (2\pi)^N\mathcal{W}(I_{1a})\mathcal{W}(I_{2b})\mathcal{W}(I_{3c})$ for $a, b, c \in \{x, y, z\}$. The evolution of these parts is shown in Figure 3.11. For this particular case, the equation of motion is given by (see Corollary 3.5)

$$\partial W_\rho/\partial t = 2\pi\mathcal{P}^{\{1,2,3\}}\sum_{k=1}^{3}\{W_\rho, W_{\mathcal{H}}\}^{\{k\}}.$$

We verify that $W_\rho(t)$ satisfies the equation of motion by checking that the following conditions $\partial W_0/\partial t = 0$, $\partial W_c/\partial t \propto W_s$, and $\partial W_s/\partial t \propto W_c$ hold. In the first case, the Poisson brackets $\{W_0, W_{\mathcal{H}}\}^{\{1\}}$ and $\{W_0, W_{\mathcal{H}}\}^{\{3\}}$ vanish as they are respectively proportional to $\{\cos\theta_1, \cos\theta_1\}^{\{1\}}$ and $\{\cos\theta_3, \cos\theta_1\}^{\{3\}}$. The Poisson bracket $\{W_0, W_{\mathcal{H}}\}^{\{2\}}$ is nonzero, however its projection by $\mathcal{P}^{\{1,2,3\}}$ is zero. Similarly, one can calculate all Poisson brackets and projections to complete the verification of the equation of motion for this example.

3.7 Discussion and connections

In this section, we complement the description of the Wigner formalism for coupled spins from Sec. 3.5 and discuss connections to alternative or related characterizations. This will

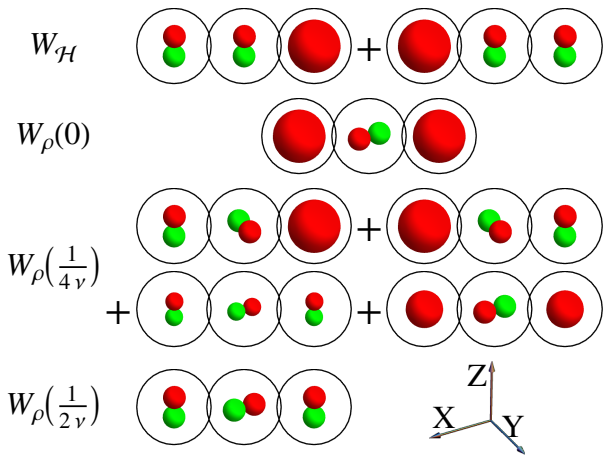

Figure 3.11: (Color online) Visualization of the Wigner functions for the time evolution of three coupled spins: the Hamiltonian $\mathcal{H} = \pi\nu(2I_{1z}I_{2z} + 2I_{2z}I_{3z})$ acts on the starting deviation density matrix $\rho(0) = I_{2x}$; $\rho[1/(4\nu)] = I_{1z}I_{2y} + I_{2y}I_{3z} - 2I_{1z}I_{2x}I_{3z} + I_{2x}/2$ and $\rho[1/(2\nu)] = -4I_{1z}I_{2x}I_{3z}$.[3]

allow for simpler interpretations of our formalism and will link to notions which might provide further avenues to our work. First, we draw important connections between the Poisson bracket and the canonical angular momentum (see Sec. 3.7.1). We continue in Sec. 3.7.2 by relating the Wigner formalism of finite- and infinite-dimensional quantum systems. Certain Wigner functions are interpreted in terms of quaternions (see Sec. 3.7.3). Finally, the evolution of non-hermitian states is considered in Sec. 3.7.4.

3.7.1 Poisson bracket and the canonical angular momentum

We detail how the Wigner formalism for coupled spins relates to the angular momentum of infinite-dimensional quantum systems described by the canonical angular momentum operator $\mathcal{L} = r \times p$. The eigenfunctions of the canonical angular momentum operator $\mathcal{L}$ are spherical harmonics. The corresponding pure eigenstates are represented by spherical functions $\psi(\theta, \phi)$ and evolve according to the time-dependent Schrödinger equation

$$\partial\psi(\theta,\phi)/\partial t = -i\mathcal{H}\psi(\theta,\phi). \tag{3.80}$$

Each component $\mathcal{L}_\alpha$ of the vector operator corresponding to the Hamiltonian of the form $\mathcal{H} = \sum_{\alpha\in\{x,y,z\}} \omega_\alpha I_\alpha$ generates a rotation $\mathcal{L}_\alpha\psi(\theta,\phi)$ of the spherical functions around the axis α for $\alpha \in \{x, y, z\}$. Providing a direct correspondence, spin operators $\mathrm{I} = (I_x, I_y, I_z)$ generalize the angular momentum $\mathcal{L} = (\mathcal{L}_x, \mathcal{L}_y, \mathcal{L}_z)$. The Wigner representation for spins describes in general a mixed quantum state using a linear combination of spherical harmonics. We show that the time evolution of the Wigner representation of a spin $1/2$ is closely related to the time evolution of an infinite-dimensional quantum system by rewriting the equation of motion into a form which is analogous to the Schrödinger equation in Eq. (3.80).

The equation of motion of a single spin $1/2$ is given by Eq. (3.54) combining the Hamiltonian $\mathcal{H}$ and an operator A, while applying the Poisson bracket from Eq. (3.40). It can be reformulated by defining a differential operator $\mathcal{D}$ as a function of the Hamiltonian, acting

on the Wigner function W_A of A:

$$\partial W_A/\partial t = -i\mathcal{D}(W_A) = -i\left(f^{\theta}_{(\mathcal{H})}\frac{\partial}{\partial\phi} - f^{\phi}_{(\mathcal{H})}\frac{\partial}{\partial\theta}\right)W_A. \tag{3.81}$$

Here, the definitions $f^{\theta}_{(\mathcal{H})} = (\partial W_{\mathcal{H}}/\partial\theta)(i/R\sin\theta)$ and $f^{\phi}_{(\mathcal{H})} = (\partial W_{\mathcal{H}}/\partial\phi)(i/R\sin\theta)$ have been applied. Integrating the differential equation, one obtains the propagator

$$W_A(t) = \exp(-i\mathcal{D}t)W_A(0), \tag{3.82}$$

where the differential operator $\mathcal{D}$ depends on $\mathcal{H}$. We consider the Hamiltonians $\mathcal{H} = \omega_z I_z$, $\mathcal{H} = \omega_x I_x$, and $\mathcal{H} = \omega_y I_y$: Assuming $\mathcal{H} = \omega_z I_z$, it follows that $W_{\mathcal{H}} = \omega_z \mathrm{Y}_{1,0}/\sqrt{2} = R\omega_z\cos\theta$. One obtains the differential operator $\mathcal{D} = -\omega_z i(\partial/\partial\phi) - 0 = \omega_z\mathcal{L}_z$, where $\mathcal{L}_z$ is the canonical angular momentum operator $\mathcal{L}_z = (r\times p)_z$ in spherical coordinates (see pp. 662 in [61]). The corresponding propagator is then given by $\exp(-i\omega_z\mathcal{L}_z t)$, which by its definition rotates the Wigner function by an angle $\omega_z t$ around the z axis. In the case of $\mathcal{H} = \omega_x I_x$, the Wigner representation has the form $W_{\mathcal{H}} = \omega_x R\sin\theta\cos\phi$ and the differential operator is given by the expected canonical angular momentum component $\mathcal{D} = i\omega_x[\sin\phi(\partial/\partial\theta) + \cot\theta\cos\phi(\partial/\partial\phi)] = \omega_x\mathcal{L}_x$. Finally, $\mathcal{H} = \omega_y I_y$ leads to the differential operator $\mathcal{D} = \omega_y\mathcal{L}_y$.

As a conclusion for a single spin $1/2$, Wigner functions together with a star commutator correspond to canonical angular momentum operators with a cross product. This means that a Hamiltonian $\mathcal{H} = \sum_{\alpha\in\{x,y,z\}}\omega_\alpha I_\alpha$ is mapped to the differential operator $\mathcal{D} = f(\mathcal{L}) = \sum_\alpha \omega_\alpha(r\times p)_\alpha$, and the time evolution is given by

$$i\partial W_\rho/\partial t = [W_{\mathcal{H}}, W_\rho]_\star = f(\mathcal{L})W_\rho. \tag{3.83}$$

The corresponding propagator can be written as

$$\exp(-i\mathcal{D}t) = \exp[-itf(\mathcal{L})]. \tag{3.84}$$

Generalizations to the case of linear Hamiltonians ${}^J\mathcal{H} = \omega_x\,{}^J I_x + \omega_y\,{}^J I_y + \omega_z\,{}^J I_z$ with arbitrary J are also possible, cf. Eq. (3.55).

Comparing Eq. (3.83) with Eq. (3.80), one concludes that the time evolution of Wigner functions for spins is formally equivalent to the time evolution of the angular part of infinite-dimensional quantum states. The time evolution of spin-$1/2$ Wigner functions described in Section 3.5.2.3 is based on the equation of motion given by the star commutator [refer to Eq. (3.54)], however, Eq. (3.83) provides an alternative formulation for a spin $1/2$ based on the Schrödinger equation by mapping the spin operator I_α onto $(r\times p)_\alpha$.

3.7.2 Finite- and infinite-dimensional degrees of freedom

We discuss now important relations between Wigner representations for finite- and infinite-dimensional degrees of freedom. In the finite-dimensional case (i.e. for spins), Wigner representations have been developed in Sec. 3.5 for coupled systems extending approaches based

on the Stratonovich postulates (see Sec. 3.5.2). Methods for Wigner representations applicable to infinite-dimensional quantum systems with a flat phase space have been more widely discussed in the literature, see Sec. 3.3.1 and [53, 131, 149, 165, 97, 266, 232, 227, 62]. We explore how spin operators can be uniquely mapped onto functions over a phase space that are restricted to the surface of a sphere. This provides a rotational covariance for operators and their corresponding Wigner representations. Expectation values of operators are calculated as quasi-probability weighted integrals of phase-space functions.

We discuss basic properties of the (classical) Wigner functions for infinite-dimensional spaces (see Sec. 3.3.1) which have the quality of a flat phase space, in contrast to the case for spins. Flat phase-space coordinates translate in the case of spins to curvilinear spherical coordinates which form a Heisenberg pair as their star commutator (as described in Eq. (3.55) of Sec. 3.5.2.3) results in the canonical commutation relation $[q,p]_\star = i\hbar$. We also compute an upper bound for the absolute value of Wigner functions and we show by investigating its limit for $J \to \infty$ that arbitrary large values corresponding to localized probability distributions are possible.

3.7.2.1 Phase-space coordinates

Flat phase-space coordinates (p,q) are replaced by curvilinear coordinates $(R\cos\theta,\phi)$ in the Wigner formalism for spins, where R denotes a proportionality factor. This implies that p and q describe coordinates on the surface of a three-dimensional sphere. In analogy to infinite-dimensional quantum mechanics, where the momentum operator p generates the translation $(p,q+\mathrm{d}q)$ in the (p,q) phase-space, the spin-1/2 Wigner function $R\cos\theta = \mathcal{W}(I_z)$ generates a rotation $(R\cos\theta,\phi+\mathrm{d}\phi)$ by the infinitesimal angle $\mathrm{d}\phi$ in the spherical phase-space coordinates $(R\cos\theta,\phi)$. In general, the operator ${}^{J}I_z$ generates a rotation of a spin J around the z axis, and ${}^{J}I_z$ is mapped to the function $R\cos\theta/N_J$.[11]

3.7.2.2 Commutators

In the case of the infinite-dimensional Wigner representation, the star commutator $[f,g]_\star$ is given by $f\star g - g\star f = i\hbar\{f,g\}$ up to $\mathcal{O}(\hbar^3)$ [266, 232, 227] where $\{f,g\} = \partial_q f\partial_p g - \partial_p f\partial_q g$ denotes here the Poisson bracket from classical physics (see, e.g., Vol. 1, §42 of [163]). Switching from flat phase-space coordinates (p,q) to the curvilinear coordinates $(R\cos\theta,\phi)$ of the spin-1/2 Wigner representation and setting $\hbar \to 1$, one obtains the same star commutator as in 3.5.3, see Eq. (3.54).

The canonical commutation relation $[q,p] = i\hbar$, which translates to $[q,p]_\star = i\hbar$ in the Wigner representation, states that the infinite-dimensional coordinate and momentum operators are not simultaneously determined. The coordinates $(R\cos\theta,\phi)$ also form a Heisenberg pair, as conjugate variables via the star commutator $[\phi,R\cos\theta]_\star = i$. In general, the formula $[\phi,\mathcal{W}({}^{J}I_z)]_\star = i$ is implied by Eqs. (3.46) and (3.55), and ${}^{J}I_z$ is mapped to the function $R\cos\theta/N_J$.[11]

The canonical commutation relation implies that the infinite-dimensional operators p and q have only infinite-dimensional matrix representations. The same holds in case of spins for

the coordinate ϕ describing the phase angle in the x-y plane: it has no finite-dimensional matrix representation as $\mathcal{W}[\mathcal{W}^{-1}(\phi)] = \phi$ is valid only in the case of $J \to \infty$. This can be verified by defining the inverse Wigner transform of ϕ as $\mathcal{W}^{-1}(\phi)$ [see Eq. (3.30)], and this results in

$$\begin{aligned} &\int_{\theta=0}^{\pi} \int_{\phi=0}^{2\pi} \phi\, \Delta_J(\theta,\phi)\, \sin\theta \,\mathrm{d}\theta \,\mathrm{d}\phi \\ &\propto \sum_{j=0}^{2J} \sum_{m=-j}^{j} {}^{J}\mathrm{T}_{jm} \int_{\theta=0}^{\pi} P_{j|m|}(\cos\theta) \sin\theta \,\mathrm{d}\theta \int_{\phi=0}^{2\pi} \phi\, \exp(-im\phi)\,\mathrm{d}\phi. \end{aligned} \tag{3.85}$$

Here, the last integral is the Fourier series expansion of ϕ and it specifies an infinite series in m. This implies that a unique matrix representation for ϕ exists only in case of $J \to \infty$. The canonical commutation relation $[q,p] = i\hbar$ is only valid for infinite-dimensional representations. Likewise, the kernel defining the Wigner transformation of spin operators [see Eq. (3.26)] becomes in the limit of $J \to \infty$ identical to the kernel of an infinite-dimensional quantum system [16].

3.7.2.3 Normalization and upper bound

In general, normalized operators $\mathrm{Tr}(AA^\dagger) = 1$ are mapped to functions $W_A(\theta,\phi)$ on the unit sphere, where the square $|W_A(\theta,\phi)|^2$ of the complex absolute value provides a normalized surface integral. This can be checked by expanding the operator $A = \sum_{j,m} c_{jm}\, {}^{J}\mathrm{T}_{jm}$ into tensor operators, then its Wigner transformation is given by $W_A = \sum_{j,m} c_{jm} \mathrm{Y}_{jm}$. The condition $\mathrm{Tr}(AA^\dagger) = 1$ is mapped to the condition $\sum_{j,m} c_{jm} c_{jm}^* = 1$; the normalized surface integral $|W_A(\theta,\phi)|^2 = |\sum_{j,m} c_{jm}\mathrm{Y}_{jm}|^2$ for a linear combination of spherical harmonics follows from the orthonormality of spherical harmonics in Eq. (3.28). Also, the norm of a matrix is conserved in the Wigner representation.

We compute now an upper bound for the absolute value of the Wigner function W_A of a normalized operator A with $\mathrm{Tr}(AA^\dagger) = 1$. The Cauchy-Schwarz inequality, implies the inequality

$$\mathrm{Tr}(\Delta_J \Delta_J)\mathrm{Tr}(AA^\dagger) \geq |\mathrm{Tr}(A\,\Delta_J)|^2. \tag{3.86}$$

The right-hand side is equal to $|W_A(\theta,\phi)|^2$ where we have applied the definition of the Wigner function $W_A(\theta,\phi)$ from Eq. (3.25). Assuming a normalized operator A, the left-hand side of Eq. (3.86) is equivalent to the trace of the square of the kernel defined in Eq. (3.26), i.e., the left-hand side is equal to

$$\mathrm{Tr}(\Delta_J \Delta_J) = \sum_{j=0}^{2J} \sum_{m=-j}^{j} \mathrm{Y}_{jm} \mathrm{Y}_{jm}^* = \sum_{j=0}^{2J} \frac{2j{+}1}{4\pi} = \frac{(2J{+}1)^2}{4\pi}.$$

The aforementioned statements imply the upper bound $|W_A(\theta,\phi)| \leq (2J{+}1)/\sqrt{4\pi}$ for normalized operators A. For $J \to \infty$, the upper bound goes to infinity, allowing localized but normalized quasiprobability distributions $W_A(\theta,\phi) = \delta_{\theta-\theta'}\delta_{\phi-\phi'}/\sin\theta$ w.r.t. both θ and ϕ, which correspond to classical vectors pointing to the surface of a sphere of unit radius. Even

though spins have no classical counterparts, a classical description emerges from the quantum one in the limit of $J \to \infty$. This follows as the growing number $2J{+}1$ of states allow for larger values in the Wigner function, while negative regions shrink.

3.7.2.4 Implications

The Stratonovich postulates provide an abstract formulation for the phase-space representation of spins. Here, we showed the most important links between Wigner functions of finite- and infinite-dimensional quantum systems and how to interpret basic properties of phase-space representations. Phase-space coordinates $(R\cos\theta/N_J, \phi)$ of spins span the surface of a sphere. These two coordinates form a Heisenberg pair with $[\phi, R\cos\theta/N_J]_\star = i$ and consequently $R\cos\theta/N_J$ generates the translation of the coordinate ϕ corresponding to the rotation of the sphere around the z axis. The coordinate ϕ has no unique matrix representation for a finite spin J. We also showed that an upper bound for the absolute value of a normalized Wigner functions is proportional to the number $(2J{+}1)$ of degrees of freedom.

3.7.3 Wigner functions and quaternions

In this section, we introduce a variant of Wigner functions based on quaternions. Quaternions can be represented by 2×2 matrices and the quaternionic product by matrix multiplication. In Sec. 3.7.3.1, we show that the Wigner transformation of these matrices combined with the star product derived in Sec. 3.5.3 also provides a valid representation of quaternions. Quaternions can also be represented as a three-dimensional vector equipped with a scalar part, offering a geometrical interpretation of the quaternionic product. In Sec. 3.7.3.2, we show how a three-dimensional vector, corresponding to the Pauli vector can be mapped onto Wigner functions. We provide an explicit form for the quaternionic product in this case.

Based on these results we show in Sec. 3.7.3.3 that the star product of spin-$1/2$ operators is formally analogous to the quaternionic product, when applied to quaternionic Wigner representations. This offers a geometrical interpretation for the star product derived in Sec. 3.5.3.

3.7.3.1 Matrix representation of quaternions

The set $\mathbb{H}$ of quaternions can be identified with a four-dimensional vector space over real numbers $\mathbb{R}^4$. Every element $q \in \mathbb{H}$ is given as a linear combination of the basis elements 1, i, j, and k, where $\mathrm{i}^2 = \mathrm{j}^2 = \mathrm{k}^2 = \mathrm{ijk} = -1$. Quaternions can be identified with 2×2 matrices spanned by the basis elements $1 \cong \mathrm{Id}_2$, $\mathrm{i} \cong -i\sigma_x$, $\mathrm{j} \cong -i\sigma_y$, $\mathrm{k} \cong -i\sigma_z$, where matrix multiplication replaces the quaternionic product. A quaternionic Wigner representation is obtained by mapping the Pauli matrices to their respective Wigner functions (see Sec. 3.5.2 for the Wigner transformation), i.e., $W_1 := 1/\sqrt{2\pi}$, $W_\mathrm{i} := -iW_x = -i\mathcal{W}(\sigma_x)$, $W_\mathrm{j} := -iW_y = -i\mathcal{W}(\sigma_y)$, $W_\mathrm{k} := -iW_z = -i\mathcal{W}(\sigma_z)$ where the Wigner representations have the form

$$W_x = 2R\sin\theta\cos\phi,\ W_y = 2R\sin\theta\sin\phi,\ W_z = 2R\cos\theta. \tag{3.87}$$

The corresponding quaternionic multiplication is given by the star product described in Sec. 3.5.3, namely $W_{\mathrm{i}} \star W_{\mathrm{i}} = W_{\mathrm{j}} \star W_{\mathrm{j}} = W_{\mathrm{k}} \star W_{\mathrm{k}} = W_{\mathrm{i}} \star W_{\mathrm{j}} \star W_{\mathrm{k}} = -W_1$.

3.7.3.2 Vectorial representation of quaternions

There are other ways to represent quaternions and the quaternionic product. Let us identify an arbitrary quaternion $q \in \mathbb{H}$ with a four-dimensional real vector $h = h(q) = (r, \vec{v})$ where $r \in \mathbb{R}$ is a real number and $\vec{v} \in \mathbb{R}^3$ defines a three-dimensional real vector. The product of two quaternions $(r_1, \vec{v}_1)$ and $(r_2, \vec{v}_2)$ is now given by [14]

$$(r_1, \vec{v}_1)(r_2, \vec{v}_2) = (r_1 r_2 - \vec{v}_1 \cdot \vec{v}_2, r_1 \vec{v}_2 + r_2 \vec{v}_1 + \vec{v}_1 \times \vec{v}_2), \tag{3.88}$$

where $\vec{v}_1 \cdot \vec{v}_2$ denotes the scalar product and $\vec{v}_1 \times \vec{v}_2$ is the cross product.

We can directly translate this into the Wigner representation. The vectorial part $\vec{v}$ of the quaternion is replaced by the Wigner function $\mathrm{W}_{\vec{v}}$[15], while the scalar part is replaced by the identity element $W_1 := 1/\sqrt{2\pi}$. The Wigner function W_h of a quaternion $h = (r, \vec{v})$ is then given by $\mathrm{W}_h = rW_1 + v_x W_x + v_y W_y + v_z W_z$ where the basis operators are defined as Wigner representations of the Pauli matrices, see Eq. (3.87). The scalar product for the Wigner functions corresponding to quaternions is given in terms of spherical functions by

$$\langle f|g\rangle = \tfrac{1}{2} \int_{\theta=0}^{\pi} \int_{\phi=0}^{2\pi} f(\theta,\phi) g(\theta,\phi) \sin\theta \, \mathrm{d}\theta \, \mathrm{d}\phi. \tag{3.89}$$

One can write the real coefficients (r, v_x, v_y, v_z) as projections onto the basis functions $r = \langle W_1 | \mathrm{W}_h \rangle$ and $v_\alpha = \langle W_\alpha | \mathrm{W}_h \rangle$ with $\alpha \in \{x, y, z\}$. Note that the factor $1/2$ before the integral in Eq. (3.89) is included to obtain normalized basis elements such that $\langle W_1 | W_1 \rangle = \langle W_\alpha | W_\alpha \rangle = 1$.

This construction represents quaternions in the Wigner space as real valued functions. The correspondence between $h = (r, \vec{v})$ and $\mathrm{W}_h = rW_1 + \mathrm{W}_{\vec{v}}$ is also implied by the rotational covariance of a three-dimensional vector $\vec{v}$ and its Wigner representation $\mathrm{W}_{\vec{v}}$. The respective quaternionic product in this case is detailed in the following

Lemma 3.5. *Given two quaternions $h_1 = (r_1, \vec{v}_1)$ and $h_2 = (r_2, \vec{v}_2)$, their product $h_3 = h_1 h_2$ is defined in Eq.* (3.88)*. The corresponding Wigner representations $\mathrm{W}_{h_1} = r_1 W_1 + \mathrm{W}_{\vec{v}_1}$, $\mathrm{W}_{h_2} = r_2 W_1 + \mathrm{W}_{\vec{v}_2}$, and $\mathrm{W}_{h_3} = r_3 W_1 + \mathrm{W}_{\vec{v}_3}$ satisfy $r_3 = (r_1 r_2 - \langle \mathrm{W}_{\vec{v}_1} | \mathrm{W}_{\vec{v}_2} \rangle)$ and $\mathrm{W}_{\vec{v}_3} = r_1 \mathrm{W}_{\vec{v}_2} + r_2 \mathrm{W}_{\vec{v}_1} - \frac{1}{2}\{\mathrm{W}_{\vec{v}_1}, \mathrm{W}_{\vec{v}_2}\}$, where the scalar product $\langle \mathrm{W}_{\vec{v}_1} | \mathrm{W}_{\vec{v}_2} \rangle$ is defined in Eq.* (3.89) *and $\{\mathrm{W}_{\vec{v}_1}, \mathrm{W}_{\vec{v}_2}\}$ is the Poisson bracket as defined in Eq.* (3.40)*.*

Proof. The equation $\langle \mathrm{W}_{\vec{v}_1} | \mathrm{W}_{\vec{v}_2} \rangle = \vec{v}_1 \cdot \vec{v}_2 = v_x v_x + v_y v_y + v_z v_z$ is implied by the orthonormality of basis elements, i.e., $\langle W_a | W_b \rangle = \delta_{ab}$ holds for $a, b \in \{1, x, y, z\}$. Finally, the Wigner representation $\mathrm{W}_{\vec{v}_1 \times \vec{v}_2}$ of the cross product is equal to $-\{\mathrm{W}_{\vec{v}_1}, \mathrm{W}_{\vec{v}_2}\}/2$, which can be verified by computing Poisson brackets $-\{W_\alpha, W_\beta\}/2 = \sum_\gamma \epsilon_{\alpha\beta\gamma} W_\gamma$ of basis elements. Here, $\epsilon_{\alpha\beta\gamma}$ denotes the fully antisymmetric Levi-Civita symbol. □

[15] The Wigner representation of $\vec{v} \cdot \vec{\sigma} = v_x \sigma_x + v_y \sigma_y + v_z \sigma_z$ is exactly $\mathrm{W}_{\vec{v}}$.

3.7.3.3 Relation to the star product

We will now explain how the star product defined in Result 3.2 can be decomposed into a sum of different terms which all relate to a simple multiplication, scalar product, or cross product originating from the quaternionic product in Eq. (3.88).

Consider the matrix representation $s_1 = r_1\mathrm{Id}_2 - i\vec{v}_1\cdot\vec{\sigma}$, and $s_2 = r_2\mathrm{Id}_2 - i\vec{v}_2\cdot\vec{\sigma}$ of two quaternions with $\vec{\sigma} := (\sigma_x, \sigma_y, \sigma_z)$ (see Sec. 3.7.3.1). The Wigner functions can be written as $\mathsf{W}_{s_1} = r_1 W_1 - i\mathrm{W}_{\vec{v}_1}$ and $\mathsf{W}_{s_2} = r_2 W_1 - i\mathrm{W}_{\vec{v}_2}$. The Wigner representation of three-dimensional vectors was discussed in Sec. 3.7.3.2 and it was shown in Sec. 3.7.3.1 that the quaternionic product corresponds to the star product [see Eq. (3.48)]

$$\mathsf{W}_{s_1} \star \mathsf{W}_{s_2} = \sqrt{2\pi}\mathcal{P}\mathsf{W}_{s_1}\mathsf{W}_{s_2} - \tfrac{i}{2}\mathcal{P}\{\mathsf{W}_{s_1}, \mathsf{W}_{s_2}\}, \tag{3.90}$$

which consists of a sum of two terms. The second term in Eq. (3.90) is proportional to a Poisson bracket and equals

$$-\tfrac{i}{2}\mathcal{P}\{\mathsf{W}_{s_1}, \mathsf{W}_{s_2}\} = \tfrac{i}{2}\{\mathrm{W}_{\vec{v}_1}, \mathrm{W}_{\vec{v}_2}\} = -i\mathrm{W}_{\vec{v}_1\times\vec{v}_2};$$

this illustrates the connection to the cross product $\vec{v}_1 \times \vec{v}_2$ corresponding to the vectorial parts of two quaternions.

The first term in Eq. (3.90) is a projected pointwise product of Wigner functions and can be computed as

$$\mathcal{P}\sqrt{2\pi}(\mathsf{W}_{s_1}\mathsf{W}_{s_2}) = r_1 r_2 W_1 + r_1(-i\mathrm{W}_{\vec{v}_2}) + r_2(-i\mathrm{W}_{\vec{v}_1}) - \sqrt{2\pi}\mathcal{P}(\mathrm{W}_{\vec{v}_1}\mathrm{W}_{\vec{v}_2}) \tag{3.91}$$

by applying the definitions of W_{s_1} and W_{s_2}. The last term in Eq. (3.91) is the projection of $\sqrt{2\pi}\mathcal{P}(\mathrm{W}_{\vec{v}_1}\mathrm{W}_{\vec{v}_2})$ onto the set of rank-zero spherical harmonics (as there are no rank-one contributions). Hence, we obtain

$$\begin{aligned}\sqrt{2\pi}\mathcal{P}(\mathrm{W}_{\vec{v}_1}\mathrm{W}_{\vec{v}_2}) &= \sqrt{2\pi}\mathrm{Y}_{00}\int_{\theta=0}^{\pi}\int_{\phi=0}^{2\pi}\mathrm{Y}_{00}^{*}\mathrm{W}_{\vec{v}_1}\mathrm{W}_{\vec{v}_2}\\ &\times\sin\theta\,\mathrm{d}\theta\,\mathrm{d}\phi = \langle\mathrm{W}_{\vec{v}_1}|\mathrm{W}_{\vec{v}_2}\rangle W_1 = (\vec{v}_1\cdot\vec{v}_2)W_1.\end{aligned} \tag{3.92}$$

Finally, substituting all results back into Eq. (3.90), the star product can be written as

$$\mathsf{W}_{s_1}\star\mathsf{W}_{s_2} = (r_1 r_2 - \vec{v}_1\cdot\vec{v}_2)\,W_1 - i[r_1\mathrm{W}_{\vec{v}_2} + r_2\mathrm{W}_{\vec{v}_1} + \mathrm{W}_{\vec{v}_1\times\vec{v}_2}].$$

Consequently, the star product of Wigner functions corresponding to a single spin $1/2$ (as given in Sec. 3.5.3) can be nicely described in geometrical terms related to quaternionic products.

3.7.3.4 Implications

The density operator of a spin-$1/2$ state can be represented in a geometrical fashion by mapping the Pauli vector $\vec{\sigma}$ onto $\vec{v} \in \mathbb{R}^3$ and Id_2 onto $r \in \mathbb{R}$, refer to Sec. 3.7.3.3. The Wigner

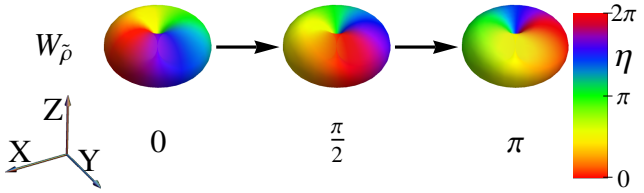

Figure 3.12: (Color online) Evolution of the non-hermitian state $\tilde{\rho} = I_-$ under the Hamiltonian $\mathcal{H} = \omega I_z$. The Wigner function $W_{\tilde{\rho}}(t) = \exp(i\omega t)\mathrm{Y}_{1,-1}$ is plotted at times $t = 0$, $\omega t = \pi/2$, and $\omega t = \pi$. The rainbow colors represent the complex phase factor $\exp(i\eta)$ of the Wigner function. The color changes clockwise from red (dark gray) at the phase value of zero via yellow to green (light gray) at the phase value of $\eta = \pi$ and continues via blue back to red at the phase value of $\eta = 2\pi$, refer to the color bar.

transformation of this geometrized density operator is then given by $W_\rho = r_\rho W_1 + \mathrm{W}_{\vec{v}_\rho}$, and also $W_\mathcal{H} = r_\mathcal{H} W_1 + \mathrm{W}_{\vec{v}_\mathcal{H}}$, refer to Sec. 3.7.3.2. The star product of two such Wigner functions was determined in Sec. 3.5.3 and can be decomposed into a sum of different terms, where each term from Eq. (3.47) can be given a geometrical interpretation. The Poisson bracket $\frac{i}{2}\{\mathrm{W}_{\vec{v}_\rho}, \mathrm{W}_{\vec{v}_\mathcal{H}}\}$ in Eq. (3.47) is the analogue of the cross product of two vectors and results in $-i\mathrm{W}_{\vec{v}_\rho \times \vec{v}_\mathcal{H}}$. The projection of the product $\sqrt{2\pi}\mathcal{P}(\mathrm{W}_{\vec{v}_\rho}\mathrm{W}_{\vec{v}_\mathcal{H}})$ in Eq. (3.47) results in the scalar product of two vectors $(\vec{v}_\rho \cdot \vec{v}_\mathcal{H})W_1$. Consequently, the time evolution from Eq. (3.54) translates to $\partial \mathrm{W}_{\vec{v}_\rho}/\partial t = 2\mathrm{W}_{\vec{v}_\rho \times \vec{v}_\mathcal{H}}$. For a single spin $1/2$ in an external magnetic field $\vec{B}$ the Hamiltonian has the form $\vec{v}_\mathcal{H} = \gamma\vec{B}/2$ with γ being the gyromagnetic ratio. The time evolution is therefore given by $\partial \mathrm{W}_{\vec{v}_\rho}/\partial t = \gamma \mathrm{W}_{\vec{v}_\rho \times \vec{B}}$, and is formally identical to the classical equation of motion, refer also to Theorem 5 in [253]. But we emphasize that non-hermitian states cannot be represented using a single quaternion, which can be very well achieved using a single Wigner function, see Figure 3.12. Non-hermitian spin operators are discussed further in Section 3.7.4.

3.7.4 Evolution of non-hermitian states

We consider the time evolution of non-hermitian states to highlight that Wigner functions offer a natural way to represent also non-hermitian spin operators. In Section 3.7.4.1, we discuss the time evolution of the coherence state I_- of a single spin, while Section 3.7.4.2 provides an alternative representation for a two-spin example from Section 3.4.2.2 utilizing a decomposition of the Wigner function of a hermitian operator into non-hermitian parts.

3.7.4.1 Evolution of a single spin

We consider the evolution of non-hermitian single-spin states. Starting from the traceless deviation matrix $\tilde{\rho} = I_- = \mathrm{T}_{1,-1}$, the corresponding Wigner function is $W_{\tilde{\rho}}(\theta, \phi) = \mathrm{Y}_{1,-1}(\theta, \phi)$. The time evolution is then determined by Eq. (3.9) via the following Poisson bracket as $\partial W_{\tilde{\rho}}(\theta, \phi, 0)/\partial t = \omega\{\mathrm{Y}_{1,-1}, \mathrm{Y}_{10}\}/\sqrt{2} = i\omega \mathrm{Y}_{1,-1}$ [see, e.g., Eq. (3.46)]. The complex Wigner function $W_{\tilde{\rho}}(t) = \exp(i\omega t)\mathrm{Y}_{1,-1}$ picks up only a phase factor during the evolution. Figure 3.12 shows $W_{\tilde{\rho}}(t)$ at different times. The Wigner functions capture the rotational

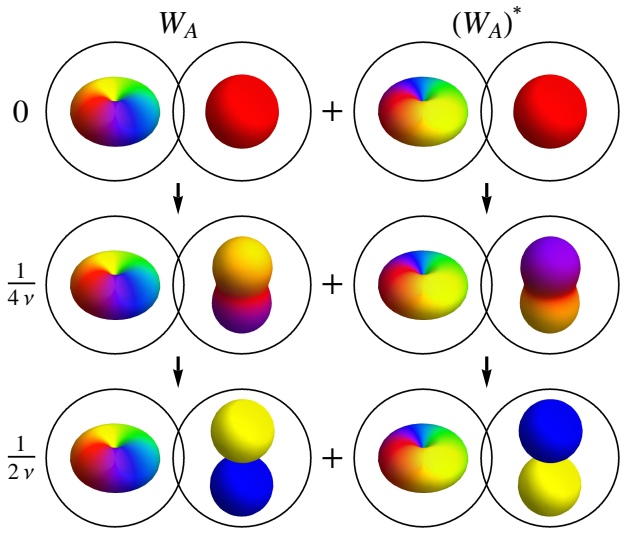

Figure 3.13: (Color online) Alternative representation of the deviation density matrix $\rho(t) = \cos(\pi\nu t)I_{1x} + \sin(\pi\nu t)2I_{1y}I_{2z}$ by the Wigner function in the form $W_\rho(t) = W_A(t) + W_A^*(t)$ as shown in Eq. (3.93). The Wigner function $W_A^*(t)$ can be obtained by rotating the Wigner function $W_A(t)$ by π around the x axis. Only the spherical function of the second spin is time dependent. The second component of $W_A(t)$ corresponds to $\cos(\pi\nu t)\mathrm{Y}_{00} + i\sin(\pi\nu t)Y_{10}(\theta_2,\phi_2)$, and the first one to $\mathrm{Y}_{1,-1}(\theta_1,\phi_1)$.

covariance of the coherence state I_-. The colors yellow and blue correspond to the phase factors i and $-i$, respectively.

3.7.4.2 Two coupled spins

The solution of the Wigner function in Eq. (3.22) can be rewritten in terms of spherical harmonics as

$$\begin{aligned} W_\rho(t) = {} & \tfrac{1}{\sqrt{2}}c(t)[\mathrm{Y}_{1,-1}(\theta_1,\phi_1) - \mathrm{Y}_{11}(\theta_1,\phi_1)]\mathrm{Y}_{00}(\theta_2,\phi_2) \\ & + \tfrac{i}{\sqrt{2}}s(t)[\mathrm{Y}_{1,-1}(\theta_1,\phi_1) + \mathrm{Y}_{11}(\theta_1,\phi_1)]\mathrm{Y}_{10}(\theta_2,\phi_2). \end{aligned}$$

Rearranging the terms as $W_\rho(t) = W_A(t) + W_A^*(t)$ with

$$W_A(t) = \tfrac{1}{\sqrt{2}}\mathrm{Y}_{1,-1}(\theta_1,\phi_1)[c(t)\mathrm{Y}_{00}(\theta_2,\phi_2) + is(t)Y_{10}(\theta_2,\phi_2)], \tag{3.93}$$

the time dependence can entirely be brought into the second spin, see Fig. 3.13. The overall Wigner function is still hermitian, even though it is represented as a sum of two not necessarily hermitian operators.

3.8 Conclusion

We presented a general approach for representing arbitrary coupled spin operators in the form of spherical functions, which we propose as an extension and unification of Wigner function formalisms for single spins. In particular, we solved the open question of how to exactly

compute the time evolution of coupled spins in a consistent Wigner frame. Our approach gives also rise to the possibility of visualizing spin operators in terms of a linear combination of spherical harmonics.

A Wigner function is formally a quasi-probability distribution as negative values appear for certain operators. The negativity of the Wigner function might be interpreted as a signature of quantumness [90]. However, the significance of the negativity of Wigner functions as an indicator of quantumness is still debated in the literature, even in the infinite-dimensional case [139, 23, 22, 146, 213, 64, 238, 183, 140, 256, 186]. In the finite-dimensional case of a spherical phase space, oscillating fringes and interference patterns have been interpreted as quantum signatures [78, 128, 7, 27, 9]; we refer to [90, 91, 92] for a more systematic approach. Recently, the negativity question has also been examined in the context of discrete Wigner functions [134]. Potential implications from the discussion of the negativity of Wigner functions do not impact our approach to describe the time evolution of coupled spins systems using Wigner functions and go well beyond the scope and intent of the current work.

We were especially interested in how the time evolution of a coupled spin system can be predicted if only the Wigner representations of both the Hamiltonian and the density operator are available. We introduced a general method for computing the time evolution of arbitrary coupled spin-$1/2$ systems while operating directly on their Wigner functions. This method is based on a generalization of the Poisson bracket, which consists of partial derivatives for both the Hamiltonian and the density operator. Hence, we provide an interpretation for how the time evolution in the Wigner space is governed. We focused in this work on the non-trivial case of coupled spins $1/2$, while the generalization to arbitrary spin numbers J is considered in the follow-up [161].

In order to describe the time evolution of coupled spins $1/2$, the star product of two spherical functions was discussed and developed in detail, and its properties were studied. Simplified formulas for the time evolution have been given for up to three coupled spins $1/2$. Multiple examples were analyzed and visualized to convey important features of our approach and to stress the operator decomposition into sums of product operators. We also discussed how the Wigner representation of spins is related to the canonical angular momentum and quaternions. Moreover, its relation to the classical, infinite-dimensional Wigner representation was investigated.

There are different possibilities for mapping spin operators onto visualizable objects like vectors or spherical functions. We focused on the Wigner-function technique generalizing spherical functions and applied these to coupled spins. This phase-space representation transforms naturally under arbitrary rotations of the individual spins. Similar visualization approaches such as the DROPS representation of [98] might have advantages for certain applications, and we hope to extend our method for modeling the time evolution in the Wigner representation to these approaches in the future. And interest in these Wigner methods in applications can also appreciated from recent related work [248, 49].

More broadly, we have made theoretical concepts usually established in the context of Wigner functions more palpable by visualizing their effects using three-dimensional illustrations. This provides a convenient tool for analyzing the time evolutions of finite-dimensional

coupled quantum systems using Wigner functions on a continuous phase space and facilitates the adoption of the Wigner formalism for coupled spin systems.

CHAPTER 4

Continuous phase spaces and the time evolution of spins: star products and spin-weighted spherical harmonics

4.1 Foreword to Chapter 4

This chapter is based on the manuscript [161] and the star product for continuous phase-space representations of spins with arbitrary spin number J is constructed. This work can therefore be viewed as an extension of the star-product approach for spins $1/2$ from Chapter 3 to the most general scenario of coupled spins J. We adapt the formalism of spin-weighted spherical harmonics which was introduced by Newman and Penrose in the context of general relativity. We employ these spin-weighted spherical harmonics to obtain a convenient and elegant description of spin-J star products which, nonetheless, naturally recover their infinite-dimensional counterparts from quantum optics in the large spin limit. In particular, we show that spin weight raising and lowering operators of Newman and Penrose recover partial derivatives in classical phase space in the large spin limit. Based on a related small-angle series expansion, we obtain $\mathcal{O}(J^{-1})$ approximations of spin-J star products. We detail examples for applying approximations to the time evolution in phase space and for calculating approximate phase-space functions of quantum states. Our approach is practically relevant for spins with large J, as in Chapter 2. We finally extend the single-spin approach to coupled

spins using results from Chapter 3. In particular, we obtain star products and the equation of motion for a systems of N coupled qudits or spins J. These results can also be viewed as a generalization of the coupled qubit or spin-$1/2$ approach from Chapter 3 to arbitrary qudits or spins J. Moreover, we consider the full class of s-parametrized distribution functions and develop their star-product formalism.

4.1.1 List of Symbols in Chapter 4

symbol	description
J	spin number: related to dimension $d = 2J + 1$
d	dimension of the quantum system (and of Hilbert space) with $d = 2, 3, \ldots$
ρ	quantum state as a density operator (positive semidefinite and unit trace)
$F_\rho(\Omega, s)$	s-parametrized phase-space distribution function of a quantum state ρ
Ω	abstract phase-space coordinate: can be α, (x, p), (θ, ϕ) etc.
s	parameter, which interpolates between Glauber P ($s = 1$) Wigner ($s = 0$) and Husimi Q ($s = -1$) functions
$\star^{(s)}$	star product of s-parametrized phase-space distribution functions
P_ρ	Glauber P function: abbreviated notation for $F_\rho(\Omega, 1)$
$\star^{(1)}$	star product of Glauber P functions
W_ρ	Wigner function: abbreviated notation for $F_\rho(\Omega, 0)$
$\star^{(0)}$	star product of Wigner functions
Q_ρ	Husimi Q function: abbreviated notation for $F_\rho(\Omega, -1)$
$\star^{(-1)}$	star product of Husimi Q functions
$\square(s)$	differential operator that translates between different s-parametrized phase-space functions
$\mathcal{D}(\Omega)$	displacement operator its parametrization Ω spans a planar phase space
α	phase-space coordinate of the complex plane parametrization
$\lvert 0\rangle$	vacuum state of the quantum-harmonic oscillator
$\lvert\alpha\rangle$	coherent states of the quantum-harmonic oscillator (also denoted by $\lvert\Omega\rangle$)
Π_s	s-parametrized parity operator for infinite-dimensional systems
θ	polar rotation angle
ϕ	azimuthal rotation angle
$\mathcal{R}(\Omega)$	rotation operator: its parametrization Ω spans a spherical phase space via $\mathcal{R}(\theta, \phi) = e^{i\phi\mathcal{J}_z} e^{i\theta\mathcal{J}_y}$
$\mathcal{J}_z$	z component of the angular momentum operator of a spin J
$\mathcal{J}_y$	y component of the angular momentum operator of a spin J
R	radius of the spherical phase-space $R := \sqrt{J/(2\pi)}$
α	arc length parametrization of the sphere relative to the north pole mapped to the complex plane via $\alpha = \sqrt{J/2}\,\theta\, e^{-i\phi}$
M_s	s-parametrized parity operator for finite-dimensional systems
T_{jm}	tensor operators of rank j and order m
γ_j	rotation invariant coefficients: real numbers, which depend only on the rank j
$C^{jm}_{j_1 m_1, j_2 m_2}$	Clebsch-Gordan coefficients of angular momentum
$\lvert JJ\rangle$	spin-up state as $\mathcal{J}_z\lvert JJ\rangle = J\lvert JJ\rangle$
Y_{jm}	spherical harmonics of rank j and order m
Y^{η}_{jm}	spin weighted spherical harmonics of rank j, order m and spin weight η
$D^j_{m\eta}$	Wigner D matrix
$\eth, \overline{\eth}$	spin weight raising and lowering operators
$\partial_{\alpha^*}, \partial_\alpha$	derivatives with respect to the complex variable α and its conjugate α^*
$\{.,.\}$	Poisson bracket
$\{.,.\}_S$	spherical Poisson bracket
$\mathcal{P}$	projection onto spherical harmonics $\mathrm{Y}_{jm}(\theta_k, \phi_k)$ of rank 0 and 1

4.2 Summary

We study continuous phase spaces of single spins and develop a complete description of their time evolution. The time evolution is completely specified by so-called star products. We explicitly determine these star products for general spin numbers using a simplified approach which applies spin-weighted spherical harmonics. This approach naturally relates phase spaces of increasing spin number to their quantum-optical limit and allows for efficient approximations of the time evolution for large spin numbers. We also approximate phase-space representations of certain quantum states that are challenging to calculate for large spin numbers. All of these applications are explored in concrete examples and we outline extensions to coupled spin systems.

4.3 Introduction

Phase-space techniques provide a complete description of quantum mechanics complementary to Hilbert-space [61] and path-integral [93] methods. These techniques are widely used in order to describe, visualize, and analyze quantum states [171, 53, 131, 149, 165, 97, 266, 232, 227, 62]. Particular cases include Wigner [262], Husimi Q [135], and Glauber P [50] functions. In this work, we are particularly interested in phase-space methods that are applicable to (finite-dimensional) spin systems [243, 7, 78, 253, 46, 47, 130, 151, 150, 152, 154, 153] and how these methods are related to infinite-dimensional phase spaces [160]. Building on earlier results in [47, 7, 78, 130, 153, 248], we have developed in [160] a unified description for the general class of s-parametrized phase spaces with $-1 \leq s \leq 1$ which is applicable to single spins with integer or half-integer spin number J and which naturally recovers the infinite-dimensional case in the large-J limit. The s-parametrized phase-space function corresponding to a Hilbert-space operator A is denoted by $F_A(\Omega, s)$.

A new focus emerged recently with the objective to faithfully describe *coupled* spin systems with the help of phase-space representations [206, 191, 128, 98, 248, 159, 221, 168, 167, 222] while also emphasizing their spin-local properties. In this context, we have completely characterized the time evolution of Wigner functions for coupled spins $1/2$ in [159] using explicit star products [253, 151, 159]. Star products are an important concept in the phase-space description of the time evolution and they determine the phase-space function

$$F_{AB}(\Omega, s) = F_A(\Omega, s) \star^{(s)} F_B(\Omega, s), \tag{4.1}$$

of a product of two Hilbert-space operators AB in terms of the individual phase-space functions $F_A(\Omega, s)$ and $F_B(\Omega, s)$ [159]. This results in the so-called Moyal equation

$$\frac{\partial F_\rho(\Omega, s)}{\partial t} = -i\, F_{\mathcal{H}}(\Omega, s) \star^{(s)} F_\rho(\Omega, s) + i\, F_\rho(\Omega, s) \star^{(s)} F_{\mathcal{H}}(\Omega, s) \tag{4.2}$$

which describes time evolution of a quantum state $F_\rho(\Omega, s)$ under a Hamiltonian $F_{\mathcal{H}}(\Omega, s)$ directly in phase-space (cf. [159]).

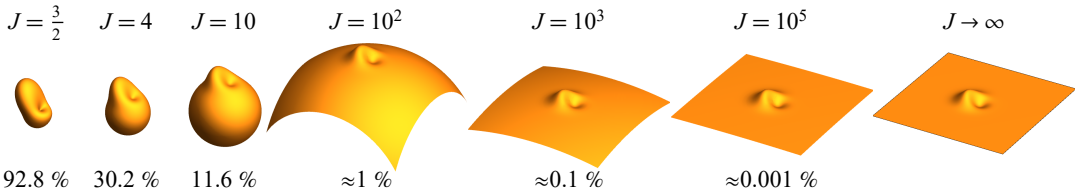

Figure 4.1: Example of how methods developed in this work can be applied (see Section 4.12): Efficiently computed approximations of spherical Wigner functions of the excited spin coherent state $|\Omega_0^+\rangle$ (see Equation 4.69) are shown together with their L^2 errors. They concentrate at the north pole for increasing spin number J and approach the photon-added coherent state $|\alpha_0^+\rangle$ (see Equation 4.64), as the spherical phase space converges to the planar one. The spherical Wigner functions are plotted on a sphere of radius $R := \sqrt{J/(2\pi)}$.

In this work, we extend our earlier results in [159] on Wigner functions of coupled spins $1/2$ and present the explicit form of the star product for the general class of s-parametrized phase spaces which is applicable to single and coupled spins of arbitrary spin number J. We also rely on phase-space techniques for single spins J that have been developed in [160]. We introduce spin-weighted spherical harmonics [196] as an important new technical tool to the theory of phase spaces, even though they have not been considered in this context before. This allows us to significantly simplify the theory of phase spaces and their star products. In particular, we can now efficiently approximate the time evolution of phase-space representations for single spins that have a large spin number J. Many quantum states have quite complicated phase-space representations which are challenging to calculate for large values of J. Approximation methods for the time evolution also lead to efficient computational techniques for approximating phase-space representations of spins with large J and Figure 4.1 illustrates this limit for Wigner functions of excited spin coherent states. Relying on results from [159], we outline in the main text how our results can be also extended to coupled spin systems.

Let us compare our work with earlier results. The star product of Husimi Q functions of single spins has been derived in [143] using angular-momentum operators. This approach has been independently rediscovered in [151, 150] and was used to calculate the star product and time evolution of Glauber P functions, and this has also been translated to the general case of s-parametrized phase-space representations. A semiclassical equation of motion was derived in [151] by neglecting quantum terms of the star product, which has then been applied to the semiclassical simulation of quantum dynamics [152] and the classical limit of spin Bopp operators [271]. In contrast to this approach relying on angular momentum operators, our techniques based on spin-weighted spherical harmonics and spin-weight raising and lowering operators facilitate a simplified and more systematic approach and also lead to additional formulas for the star product. The derivation of the exact star product is now completely transparent and all of its quantum contributions are accounted for. One particular strength of our approach is that the large-spin limit is naturally incorporated as spin-weight raising and lowering operators converge for large J to derivatives in the tangent plane (which are widely studied in infinite dimensions [12]).

This work has the following structure: We start in Section 4.4 by recapitulating elementary properties of infinite-dimensional phase spaces and their star products. In Section 4.5, we recall the structure of phase-space representations for single spins J following the approach of [160]. We introduce spin-weighted spherical harmonics and summarize their main features in Section 4.6. Important approximation formulas for spin-weight raising and lowering operators are derived in Section 4.7. The sections 4.8-4.10 constitute the main part of our work and various formulas for exact and approximate star products are obtained. Our methods are illustrated with concrete examples in sections 4.11-4.12. Before we conclude, extension to coupled spin systems are outlined in Section 4.13. Certain details and proofs are deferred to appendices.

4.4 Phase spaces and star products in infinite dimensions

An important class of infinite-dimensional phase-space representations of a density operator ρ contains s-parametrized phase-space distribution functions (where $-1 \leq s \leq 1$) which can be defined via [160, 50, 194, 171, 113]

$$F_\rho(\Omega, s) = \mathrm{Tr}\,[\,\rho\,\mathcal{D}(\Omega)\Pi_s\mathcal{D}^\dagger(\Omega)\,]. \tag{4.3}$$

The distribution function $F_\rho(\Omega, s)$ is determined by the expectation value of the parity operator Π_s which is transformed by the displacement operator $\mathcal{D}(\Omega)$. The parity operator inverts phase-space coordinates via $\Pi_0|\Omega\rangle = |-\Omega\rangle$ [113] and the displacement operator $\mathcal{D}(\Omega)$ is defined by the property that it translates the vacuum state $|0\rangle$ to coherent states $\mathcal{D}(\Omega)|0\rangle = |\Omega\rangle$. Here, Ω parametrizes a phase space with either the variables p and q or the complex eigenvalues α of the annihilation operator [171]. And the parameter s interpolates between the Glauber P function for $s = 1$ and the Husimi Q function for $s = -1$. The particular case of $s = 0$ corresponds to the Wigner function. All s-parametrized phase-space distribution functions are related to each other via Gaussian smoothing [160, 50], and the convolution of the vacuum-state representation $F_{|0\rangle}(\Omega, s')$ with the distribution function $F_\rho(\Omega, s)$ results in a distribution function

$$F_\rho(\Omega, s{+}s'{-}1) = F_{|0\rangle}(\Omega, s') * F_\rho(\Omega, s) = \exp[\,\tfrac{1-s'}{2}\partial_{\alpha^*}\partial_\alpha\,]\,F_\rho(\Omega, s) \tag{4.4}$$

of type $s{+}s'{-}1$. The r.h.s. of Equation 4.4 establishes the corresponding differential form, see, e.g., Eq. (5.29) in [11].

We adapt notations from [47] for the infinite-dimensional tensor operators $\mathrm{T}_\nu := \mathcal{D}(\nu)$ which define the displacement operators using a continuous, complex index ν. The phase-space representations $F_{\mathrm{T}_\nu}(\alpha, s) = \gamma_\nu^{-s}\,\mathrm{Y}_\nu(\alpha)$ are up to the weight factor $\gamma_\nu := \exp(-|\nu|^2/2)$ proportional to the harmonic functions $\mathrm{Y}_\nu(\alpha) := \exp(\nu\alpha^* - \alpha\nu^*)$ [47], where the power $-s$ of γ_ν is determined by the type s of the representation. Up to a complex prefactor, multiplying

two displacement operators results in a single displacement operator [50]:

$$\mathrm{T}_\mu \mathrm{T}_\nu = \exp[(\mu\nu^* - \nu\mu^*)/2]\, \mathrm{T}_{\mu+\nu}. \tag{4.5}$$

Applying the product in Equation 4.5 and the star product from Equation 4.1, one obtains the formula

$$[\gamma_\mu^{-s} \mathrm{Y}_\mu(\alpha)] \star^{(s)} [\gamma_\nu^{-s} \mathrm{Y}_\nu(\alpha)] = \exp[(\mu\nu^* - \nu\mu^*)/2]\, \gamma_{\mu+\nu}^{-s} \mathrm{Y}_{\mu+\nu}(\alpha). \tag{4.6}$$

The star product satisfies Equation 4.6 and it can be explicitly defined as a power series

$$\star^{(s)} := \exp[\tfrac{(1-s)}{2} \overleftarrow{\partial}_\alpha \overrightarrow{\partial}_{\alpha^*} - \tfrac{(1+s)}{2} \overleftarrow{\partial}_{\alpha^*} \overrightarrow{\partial}_\alpha] \tag{4.7}$$

of partial derivatives as in Eq. (3.5) of [12]. Setting $\alpha = (\lambda q + i\lambda^{-1} p)/\sqrt{2}$ for arbitrary real λ [50], the derivatives observe (see also Eq. (3.4') in [12])

$$\tfrac{(1-s)}{2} \overleftarrow{\partial}_\alpha \overrightarrow{\partial}_{\alpha^*} - \tfrac{(1+s)}{2} \overleftarrow{\partial}_{\alpha^*} \overrightarrow{\partial}_\alpha = i[\overleftarrow{\partial}_q \overrightarrow{\partial}_p - \overleftarrow{\partial}_p \overrightarrow{\partial}_q - s\lambda^2 \overleftarrow{\partial}_p \overrightarrow{\partial}_p - s\lambda^{-2} \overleftarrow{\partial}_q \overrightarrow{\partial}_q]/2.$$

The arrows represent whether derivatives are to be taken to the left or right. For $s = 0$, we obtain $\star^{(0)} = \exp(i\{\cdot,\cdot\}/2)$ as stated by Groenewold [118] and $\{\cdot,\cdot\} = \overleftarrow{\partial}_q \overrightarrow{\partial}_p - \overleftarrow{\partial}_p \overrightarrow{\partial}_q$ denotes the Poisson bracket.

4.5 Finite-dimensional phase spaces

We briefly review s-parametrized phase-space representations for a single spin J following the approach of [160], which recovers the previously discussed infinite-dimensional case in the large-spin limit. The continuous phase space for the finite-dimensional spin J is fully parametrized using the two Euler angles $\Omega := (\theta, \phi)$ of the rotation operator $\mathcal{R}(\Omega) = \mathcal{R}(\theta, \phi) := e^{i\phi\mathcal{J}_z} e^{i\theta\mathcal{J}_y}$. Here, $\mathcal{J}_z$ and $\mathcal{J}_y$ are components of the angular momentum operator that are defined by their commutation relations, i.e., $[\mathcal{J}_j, \mathcal{J}_k] = i \sum_\ell \epsilon_{jk\ell} \mathcal{J}_\ell$ where $j, k, \ell \in \{x, y, z\}$ and $\epsilon_{jk\ell}$ is the Levi-Civita symbol [192]. This leads to a spherical phase space with radius $R := \sqrt{J/(2\pi)}$. The displacement operator $\mathcal{D}(\Omega)$ from the infinite-dimensional case is replaced by the rotation operator $\mathcal{R}(\Omega)$ which maps the spin-up state $|JJ\rangle$ to spin coherent states $|\Omega\rangle = \mathcal{R}(\Omega)|JJ\rangle$ [205, 18, 78]. The s-parametrized phase-space representation

$$F_\rho(\Omega, s) := \mathrm{Tr}\,[\,\rho\, \mathcal{R}(\Omega) M_s \mathcal{R}^\dagger(\Omega)] \tag{4.8}$$

of a density operator ρ of a single spin J is then obtained as the expectation value of the rotated (generalized) parity operator (refer to [160])

$$M_s := \tfrac{1}{R} \sum_{j=0}^{2J} \sqrt{\tfrac{2j+1}{4\pi}} (\gamma_j)^{-s}\, \mathrm{T}_{j0}, \tag{4.9}$$

where M_s is specified in terms of a weighted sum of tensor operators T_{jm} of order zero (i.e., $m = 0$). The tensor components T_{jm} depend on the rank $j \in \{0, \ldots, 2J\}$, the order $m \in \{-j, \ldots, j\}$, and the spin number J. The explicit matrix elements are specified in terms of Clebsch-Gordan coefficients [192, 47, 33, 87] as

$$[\mathrm{T}_{jm}]_{m_1 m_2} \coloneqq \sqrt{\tfrac{2j+1}{2J+1}}\, C^{Jm_1}_{Jm_2,jm} = (-1)^{J-m_2}\, C^{jm}_{Jm_1 J,-m_2}, \tag{4.10}$$

where $m_1, m_2 \in \{J, \ldots, -J\}$. The weight factor has the explicit form

$$\gamma_j \coloneqq R\sqrt{4\pi}(2J)!\,[(2J+j+1)!\,(2J-j)!\,]^{-1/2}, \tag{4.11}$$

and the power $-s$ of γ_j determines the type s of the phase-space representation [160].

Tensor operators T_{jm} form an orthonormal basis of $(2J+1) \times (2J+1)$ matrices with respect to the Hilbert-Schmidt scalar product $\mathrm{Tr}\,[\,\mathrm{T}_{jm}\mathrm{T}^{\dagger}_{j'm'}\,] = \delta_{jj'}\delta_{mm'}$ where $0 \leq j \leq 2J$ and $m, m' \in \{-j, \ldots, j\}$. Similarly as in Equation 4.5, the product of two tensor operators can be decomposed into a sum (applying the notation of [159])

$$\mathrm{T}_{jm}\mathrm{T}_{j'm'} = \sum_{\ell=0}^{2J} K^{\ell}_{jm,j'm'}\mathrm{T}_{\ell,m+m'} \tag{4.12}$$

of tensor operators using the decomposition coefficients $K^{\ell}_{jm,j'm'}$ as detailed in C.1. The phase-space representations $F_{\mathrm{T}_{jm}}(\Omega, s) = \gamma_j^{-s}\,\mathrm{Y}_{jm}(\Omega)/R$ of tensor operators are proportional to spherical harmonics of rank j and order m and they are orthonormal with respect to a spherical integration

$$\int_{S^2} \mathrm{Y}_{jm}(\Omega)\mathrm{Y}^{*}_{j'm'}(\Omega)/R^2\,\mathrm{d}\Omega = \delta_{jj'}\delta_{mm'} \tag{4.13}$$

according to $\mathrm{d}\Omega = R^2 \sin\theta \mathrm{d}\theta\,\mathrm{d}\phi$. Similarly as in Equation 4.6, the defining property of the star product for phase-space representations of spins can be transferred to spherical harmonics since these distribution functions are always given as a finite linear combination of spherical harmonics:

Definition 4.1. As in Equation 4.1, the star product $\star^{(s)}$ of two phase-space representations of type s satisfies for a single spin J the condition

$$[\gamma_j^{-s}\,\mathrm{Y}_{jm}(\Omega)]\,\star^{(s)}\,[\gamma_{j'}^{-s}\,\mathrm{Y}_{j'm'}(\Omega)] = R\sum_{\ell=0}^{2J} K^{\ell}_{jm,j'm'}\,\gamma_{\ell}^{-s}\,\mathrm{Y}_{\ell,m+m'}(\Omega) \tag{4.14}$$

for all suitable indices with $j, j' \leq 2J$. The coefficients $K^{\ell}_{jm,j'm'}$ are determined by Equation 4.12.

One objective of this work is to apply this decomposition in order to define a star product $\star^{(s)}$ in terms of *spin-weighted* spherical harmonics and their spin-weight raising and lowering differential operators $\eth$ and $\overline{\eth}$.

4.6 Spin-weighted spherical harmonics

Spin-weighted spherical harmonics Y^{η}_{jm} with spin weight η have been introduced by Newman and Penrose [196] using spin-weight raising and lowering operators $\eth$ and $\overline{\eth}$ in order to describe the asymptotic behavior of the gravitational field. Since then, spin-weighted spherical harmonics have been widely used to analyze, in particular, gravitational waves [247, 235] or the cosmic microwave background [267, 200]. Moreover, efficient computational tools for spin-weighted spherical harmonics are available [212] and these can also be used in the fast calculation of spherical convolutions [145, 257].

Spin-weighted spherical harmonics Y^{η}_{jm} with $-j \le \eta \le j$ are defined as functions on the three-dimensional sphere as shown in Figure 4.2. Similarly as for ordinary spherical harmonics $\mathrm{Y}_{jm}(\theta,\phi)$, the spin-weight raising and lowering operators $\eth$ and $\overline{\eth}$ are used in their definition (see, e.g., [196] and Chapter 2.3 in [73])

$$\mathrm{Y}^{\eta}_{jm} := \begin{cases} \sqrt{(j-\eta)!/(j+\eta)!}\;\eth^{\eta}\,\mathrm{Y}_{jm} & \text{for } \eta \ge 0 \\ (-1)^{\eta}\sqrt{(j-|\eta|)!/(j+|\eta|)!}\;\overline{\eth}^{|\eta|}\,\mathrm{Y}_{jm} & \text{for } \eta < 0, \end{cases} \tag{4.15}$$

and the particular case of $\eta = 0$ corresponds to ordinary spherical harmonics. Note that spin-weighted spherical harmonics are related to Wigner D-matrices via the direct expression $D^{j}_{m\eta}(\phi,\theta,\psi) = (-1)^{m}\sqrt{(4\pi)/(2j+1)}\mathrm{Y}^{\eta}_{j,-m}(\theta,\phi)e^{-i\eta\psi}$, refer to Eq. (2.52) in [73]. The operators $\eth$ and $\overline{\eth}$ raise and lower the spin weight η with $-j \le \eta \le j$ in (see Eq. (3.20) in [196])

$$\eth\mathrm{Y}^{\eta}_{jm} = \sqrt{(j-\eta)(j+\eta+1)}\;\mathrm{Y}^{\eta+1}_{jm} \quad\text{and}\quad \overline{\eth}\mathrm{Y}^{\eta}_{jm} = -\sqrt{(j+\eta)(j-\eta+1)}\;\mathrm{Y}^{\eta-1}_{jm}. \tag{4.16}$$

Their explicit form can be specified in terms of the differential operators

$$\eth\mathrm{Y}^{\eta}_{jm} = -(\sin\theta)^{\eta}(\partial_\theta + i/\sin\theta\;\partial_\phi)[\,(\sin\theta)^{-\eta}\;\mathrm{Y}^{\eta}_{jm}] \quad\text{and} \tag{4.17}$$

$$\overline{\eth}\mathrm{Y}^{\eta}_{jm} = -(\sin\theta)^{-\eta}(\partial_\theta - i/\sin\theta\;\partial_\phi)[\,(\sin\theta)^{\eta}\;\mathrm{Y}^{\eta}_{jm}], \tag{4.18}$$

see Eq. (3.8) in [196]. Spin-weighted spherical harmonics are up to a constant factor invariant under the application of $\eth\overline{\eth}$ and $\overline{\eth}\eth$ (see Eq. (2.22) in [73]):

$$\overline{\eth}\eth\mathrm{Y}^{\eta}_{jm} = [\eta(\eta+1)-j(j+1)]\;\mathrm{Y}^{\eta}_{jm} \quad\text{and}\quad \eth\overline{\eth}\mathrm{Y}^{\eta}_{jm} = [\eta(\eta-1)-j(j+1)]\;\mathrm{Y}^{\eta}_{jm}. \tag{4.19}$$

Therefore, $\eth\overline{\eth}$ acts up to a minus sign as the total angular momentum operator when applied to spherical harmonics, i.e., $\eth\overline{\eth}\mathrm{Y}_{jm} = -j(j+1)\mathrm{Y}_{jm}$, refer to Eq. (2.25) in [73]. The commutator $[\overline{\eth},\eth] = 2\eta$ immediately follows from Equation 4.19. Products $\mathrm{Y}^{\eta}_{jm}\mathrm{Y}^{-\eta}_{j'm'} \propto$

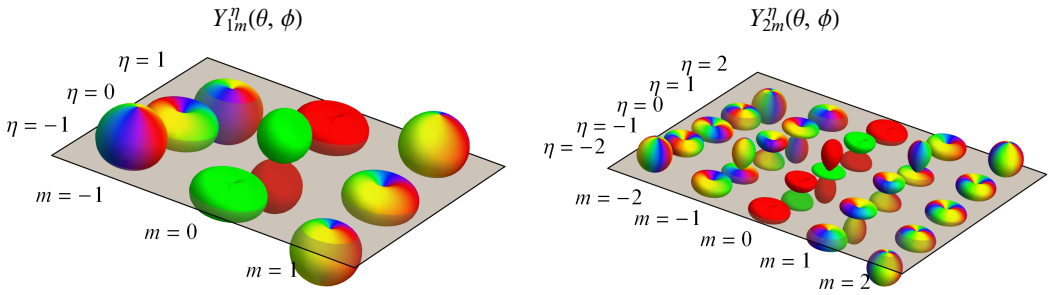

Figure 4.2: Spin-weighted spherical harmonics ${}_{\eta}Y_{jm}$ of rank one (left) and two (right). Colors represent the complex phase; red (dark gray) and green (light gray) depict positive and negative values, while blue and yellow represent i and $-i$.

$(\eth^{\eta} {}_{\eta}Y_{jm})(\overline{\eth}^{\eta} {}_{\eta}Y_{jm})$ of spin-weighted spherical harmonics decompose into the sums [73]

$$(\eth^{\eta} {}_{\eta}Y_{jm})(\overline{\eth}^{\eta} {}_{\eta}Y_{j'm'}) = \sum_{\ell=0}^{j+j'} {}^{\eta}\kappa^{\ell}_{jm,j'm'} \, {}_{\eta}Y_{\ell,m+m'}(\Omega) \quad \text{and} \tag{4.20}$$

$$(\overline{\eth}^{\eta} {}_{\eta}Y_{jm})(\eth^{\eta} {}_{\eta}Y_{j'm'}) = \sum_{\ell=0}^{j+j'} {}^{-\eta}\kappa^{\ell}_{jm,j'm'} \, {}_{\eta}Y_{\ell,m+m'}(\Omega) \tag{4.21}$$

of spherical harmonics. The decomposition coefficients ${}^{\eta}\kappa^{\ell}_{jm,j'm'}$ are explicitly specified in Equation C.6 and they are similar to the ones used in Definition 4.1. In sections 4.8-4.10, we utilize the products of spin-weighted spherical harmonics from Equation 4.20 and Equation 4.21 to explicitly determine the star product such that it satisfies its defining property from Equation 4.1.

4.7 Approximating spin-weight raising and lowering operators

As mentioned in Section 4.5, the spherical phase space converges for an increasing spin number J to the (infinite-dimensional) planar phase space [160]. The arc length θR becomes a measure of distance from the north pole, which is equivalent to its infinite-dimensional counterpart $|\alpha|$. The two phase spaces can be related using the formula $\alpha = \sqrt{J/2}\,\theta\, e^{-i\phi}$. In this parametrization, spin-weighted spherical harmonics can, up to an additive error that scales inversely with R, be expanded as derivatives

$${}_{\eta}Y_{jm}(\alpha) = (-1)^{\eta} e^{-i\eta\phi} (\partial_{\alpha^*})^{\eta} \, {}_{\eta}Y_{jm}(\alpha) + \mathcal{O}(|\alpha|/\sqrt{J}) \quad \text{and} \tag{4.22}$$

$${}_{-\eta}Y_{jm}(\alpha) = e^{i\eta\phi} (\partial_{\alpha})^{\eta} \, {}_{\eta}Y_{jm}(\alpha) + \mathcal{O}(|\alpha|/\sqrt{J}) \tag{4.23}$$

of ordinary spherical harmonics with respect to the coordinates α and α^* while assuming a fixed arc length $|\alpha|$. This is essentially an approximation of Equation 4.15 for small angles θ. Figure 4.3(a)-(b) plots the absolute value of the difference between the spin-weighted spherical harmonics ${}_{\eta}Y_{jm}(\alpha)$ and their approximations which rely on the derivatives from

Equation 4.22-Equation 4.23. The approximation error vanishes in the limit of large J assuming that the coordinates α are located at the north pole or that the values $|\alpha|/\sqrt{J}$ are small (e.g., $|\alpha|$ is bounded). Extending this to the spin-weight raising and lowering operators from Equation 4.17 and Equation 4.18, these operators $\eth$ and $\overline{\eth}$ can be shown to transform for large J into the derivatives ∂_{α^*} and ∂_α over the complex plane.

Proposition 4.1. *Assume that the phase-space function $f = F_\rho(\Omega, s)$ of a spin J is parametrized using the arc length $\alpha = \sqrt{J/2}\,\theta\, e^{-i\phi}$ and that its spherical-harmonics expansion coefficients might depend on J. The action of spin-weight raising and lowering operators $\eth$ and $\overline{\eth}$ at fixed α are given by*

$$[(\eth/\sqrt{2J})^\eta f](\alpha) = (-1)^\eta e^{-i\eta\phi}(\partial_{\alpha^*})^\eta f(\alpha) + \mathcal{O}(|\alpha|J^{-1}), \tag{4.24}$$

$$[(\overline{\eth}/\sqrt{2J})^\eta f](\alpha) = (-1)^\eta e^{i\eta\phi}(\partial_{\alpha})^\eta f(\alpha) + \mathcal{O}(|\alpha|J^{-1}), \tag{4.25}$$

$$[(\,\eth\overline{\eth}/(2J)\,)f](\alpha) = \partial_{\alpha^*}\partial_\alpha f(\alpha) + \mathcal{O}(|\alpha|J^{-1}), \text{ and} \tag{4.26}$$

$$[(\,\overline{\eth}\eth/(2J)\,)f](\alpha) = \partial_{\alpha}\partial_{\alpha^*} f(\alpha) + \mathcal{O}(|\alpha|J^{-1}), \tag{4.27}$$

and this action is up to an error term $\mathcal{O}(J^{-1})$ equivalent to applying the complex derivatives ∂_{α^*} and ∂_α for any powers of η. The error term $\mathcal{O}(J^{-1})$ vanishes in the limit of large J if the differentials $[\eth/\sqrt{2J}]^\eta f$ remain non-singular in the limit. This implies convergence in the L^2 norm if f and its differentials are also square integrable in the limit. Refer to C.5 for the proof.

Note that phase-space representations $F_\rho(\Omega, s)$ and all their derivatives are non-singular and square integrable if ρ is finite-dimensional, i.e., if $F_\rho(\Omega, s)$ is a finite linear combination of spherical harmonics. In general, singularities can however appear for $s > 0$ in the limit of large J, as the corresponding parity operators Π_s from Equation 4.3 are unbounded [50, 160] for $s > 0$. This can be illustrated using the example of the spin-up state $F_{|JJ\rangle}(\Omega, s)$: it is determined by a sum of $2J+1$ spherical harmonics and its expansion coefficients are proportional to γ_j^{1-s} and depend implicitly on J [160]. These rapidly decreasing expansion coefficients can be approximated for increasing j by $e^{-j^2(1-s)/(4J)}$ if $s < 1$ and $F_{|JJ\rangle}(\Omega, s)$ is bounded and square integrable in the large-J limit. But for $s = 1$ this expansion defines in the limit a delta distribution which is clearly singular and not square integrable. For example, the differentials $[\overline{\eth}/\sqrt{2J}]^\eta F_{|JJ\rangle}(\Omega, s)$ are sums of spin-weighted spherical harmonics with expansion coefficients which are proportional to $[(2J)(j-\eta)!/(j+\eta)!]^{-\eta/2}\,\gamma_j^{1-s}$ and which can be approximated by $[j^2/(2J)]^{\eta/2} e^{-j^2(1-s)/(4J)}$. The coefficients vanish for increasing j and define bounded, square integrable functions in the limit of large J for $s < 1$. Figure 4.3(c) shows the L^2 norm of the difference between the Wigner function's differential $[\overline{\eth}/\sqrt{2J}]^\eta\, W_{|JJ\rangle}(\Omega)$ and its approximation via Proposition 4.1. This difference vanishes for large J. Refer to C.5 for further details.

One example of an unbounded operator is the Wigner function $W_{\mathcal{I}^+/\sqrt{2J}}(\Omega)$ of the raising operator $\mathcal{I}^+/\sqrt{2J}$ which reproduces the annihilation operator a in the large-spin limit

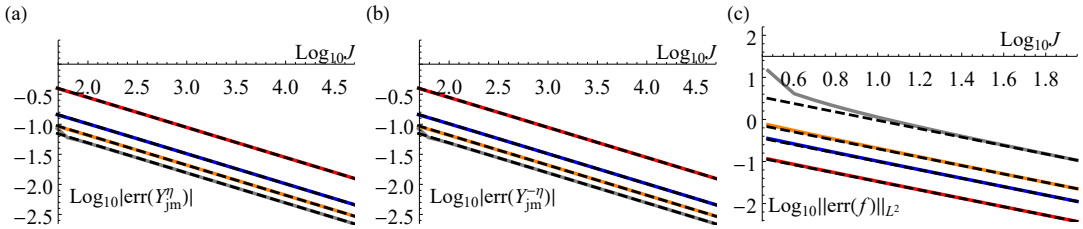

Figure 4.3: The absolute value of the difference between exact spin-weighted spherical harmonics (a) ${}_{\eta}Y_{jm}(\alpha)$ and (b) ${}_{-\eta}Y_{jm}(\alpha)$ and their approximations from Equation 4.22 and Equation 4.23 for fixed $\eta = 4$, $m = 4$, and $\alpha = 1.2e^{i2.1}$ and variable $j \in \{4, 8, 12, 16\}$ (red, blue, orange, gray). (c) L^2-norm of the difference between the exact derivative of the spin-up state Wigner function $f := [\overline{\eth}/\sqrt{2J}]^n W_{|JJ\rangle}(\Omega)$ and its approximation using Proposition 4.1 for $n \in \{2, 3, 4, 8\}$ (red, blue, orange, gray). Dashed lines show the expected scaling $\mathcal{O}(J^{-1/2})$ for (a) and (b) as well as $\mathcal{O}(J^{-1})$ for (c) with suitable prefactors.

[18]. One obtains

$$W_{\mathcal{I}^+/\sqrt{2J}}(\Omega) \propto \sqrt{J/2}\,{}_{1}Y_{1,1}(\theta,\phi) \propto \sqrt{J/2}\,\sin\theta e^{i\phi} \quad \text{and} \tag{4.28}$$

$$\overline{\eth}/\sqrt{2J}\, W_{\mathcal{I}^+/\sqrt{2J}}(\Omega) \propto \tfrac{1}{2}\,{}_{1}Y^{-1}_{1,1}(\theta,\phi) \propto \tfrac{1}{2}(1+\cos\theta)e^{i\phi}. \tag{4.29}$$

The corresponding L^2 norms (as defined with respect to Equation 4.13) diverge with increasing J and the Wigner functions are no longer square integrable. However, for any bounded $\alpha = \sqrt{J/2}\,\theta\, e^{-i\phi}$, the functions have the proper limits

$$\lim_{J\to\infty}\left[\sqrt{J/2}\,\sin(|\alpha|/\sqrt{J/2})e^{i\phi}\right] = \alpha \quad \text{and} \quad \lim_{J\to\infty}\left[\tfrac{1}{2}(1+\cos(|\alpha|/\sqrt{J/2}))\right] = 1,$$

where 1 is the derivative of α. Refer to C.5 for details.

Proposition 4.1 essentially approximates the differentials $\eth^{\eta} F_{\rho}(\Omega, s)$ of spherical functions with the derivatives $\partial_{\alpha^*} F_{\rho}(\Omega, s)$. This duality then becomes exact in the large-spin limit if the differentials $\eth^{\eta} F_{\rho}(\Omega, s)$ remain non-singular. In particular, we use the spin-weight raising and lowering operators to construct the star product by applying Equation 4.14, which then naturally recovers the infinite-dimensional star product from Equation 4.7:

Proposition 4.2. *Consider the arc-length parametrization $\alpha = \sqrt{J/2}\,\theta\, e^{-i\phi}$ and two spin-J phase-space functions $f = F_{\rho}(\Omega, s)$ and $g = F_{\rho'}(\Omega, s)$. Note that their spherical-harmonics expansion coefficients might depend on J. Following Proposition 4.1, one obtains the approximations*

$$f[\,(\overleftarrow{\eth}^{\eta})(\overrightarrow{\overline{\eth}}^{\eta})/(2J)^{\eta}\,]g = f[\,(\overleftarrow{\partial}_{\alpha^*})^{\eta}(\overrightarrow{\partial}_{\alpha})^{\eta}\,]g + \mathcal{O}(J^{-1}), \tag{4.30}$$

$$f[\,(\overleftarrow{\overline{\eth}}^{\eta})(\overrightarrow{\eth}^{\eta})/(2J)^{\eta}\,]g = f[\,(\overleftarrow{\partial}_{\alpha})^{\eta}(\overrightarrow{\partial}_{\alpha^*})^{\eta}\,]g + \mathcal{O}(J^{-1}). \tag{4.31}$$

The error vanishes in the limit of large J if the differentials $[\eth^{\eta} f]\,[\overline{\eth}^{\eta} g]/(2J)^{\eta}$ remain non-singular in the limit.

4.8 Star products of spin Glauber P and Husimi Q functions

4.8.1 The exact star product

We start by determining the exact star product of Q functions ($s=-1$) and P functions ($s=1$) which are given uniquely in terms of spin-weight raising and lowering operators:

Result 4.1. *The (finite-dimensional) exact star product of two Q functions Q_A and Q_B and two P functions P_A and P_B is determined for the spin number J by*

$$Q_A \star^{(-1)} Q_B = Q_A \sum_{\eta=0}^{2J} \lambda_\eta^{(-1)} (\overleftarrow{\eth}^\eta)(\overrightarrow{\eth}^\eta) Q_B \quad \text{and} \quad P_A \star^{(1)} P_B = P_A \sum_{\eta=0}^{2J} \lambda_\eta^{(1)} (\overleftarrow{\eth}^\eta)(\overrightarrow{\eth}^\eta) P_B, \tag{4.32}$$

where the coefficients (see C.2)

$$\lambda_\eta^{(-1)} = \frac{(2J-\eta)!}{\eta!(2J)!} \quad \text{and} \quad \lambda_\eta^{(1)} = \frac{R^2 4\pi\,(-1)^\eta\,(2J)!}{\eta!(2J+\eta+1)!} \tag{4.33}$$

depend on J. Terms in Equation 4.32 related to spherical harmonics Y_{jm} with rank $j > 2J$ are not relevant and can be projected out as detailed in C.4 and [159].

The proof of Result 4.1 is given in C.2. The upper bounds in the sums in Equation 4.32 can be lowered to $\min(j_A, j_B)$ where j_A and j_B are the maximal ranks in the tensor-operator decompositions of A and B. Similar results have been attained for Q functions in Eq. (86) of [143] using angular momentum operators, refer also to Eq. (45) in [151]. We improve and simplify these results for star products of phase-space representations of spins with the help of spin-weighted spherical harmonics. In particular, this approach enables us to efficiently approximate phase-space representations for large spin numbers J as discussed below.

4.8.2 Approximations of the star product

The coefficients in Equation 4.33 of Result 4.1 can be expanded as (see C.3)

$$\lambda_\eta^{(-1)} = [\eta!(2J)^\eta]^{-1} \text{ for } \eta = 0 \text{ or } \eta = 1, \tag{4.34}$$

$$\lambda_\eta^{(-1)} = [\eta!(2J)^\eta]^{-1} + \mathcal{O}(J^{-\eta-1}) \text{ for } \eta \geq 2, \text{ and} \tag{4.35}$$

$$\lambda_\eta^{(1)} = (-1)^\eta [\eta!(2J)^\eta]^{-1} + \mathcal{O}(J^{-\eta-1}) \text{ for } \eta \geq 0. \tag{4.36}$$

Also, the finite sums in Equation 4.32 are unchanged if higher-order differentials (with respect to η) are added since all the higher-order differentials vanish, i.e., $\eth^\eta \mathrm{Y}_{jm} = 0$ for $\eta > j$. The scaling $\mathcal{O}(J^{-\eta-1})$ of the approximations in Equation 4.35 and Equation 4.36 is highlighted in Figure 4.4(a)-(b) for different values of η.

Result 4.2. *The exact star product in Result 4.1 can be approximated as*

$$Q_A \star^{(-1)} Q_B = Q_A \exp[(\overleftarrow{\eth})(\overrightarrow{\eth})/(2J)]\, Q_B + \mathcal{O}(J^{-3}) \tag{4.37}$$

$$P_A \star^{(1)} P_B = P_A \exp[-(\overleftarrow{\eth})(\overrightarrow{\eth})/(2J)]\, P_B + \mathcal{O}(J^{-1}). \tag{4.38}$$

One obtains from Proposition 4.1 a more convenient approximation

$$Q_A \star^{(-1)} Q_B = Q_A \exp[\,\overleftarrow{\partial}_\alpha \overrightarrow{\partial}_{\alpha^*}]\, Q_B + \mathcal{O}(J^{-1}) \tag{4.39}$$

$$P_A \star^{(1)} P_B = P_A \exp[-\overleftarrow{\partial}_{\alpha^*} \overrightarrow{\partial}_\alpha]\, P_B + \mathcal{O}(J^{-1}), \tag{4.40}$$

which recovers the infinite-dimensional case in the large-spin limit if the functions Q_A, Q_B, P_A, and P_B and their differentials remain non-singular in the limit.

4.9 Transforming between phase-space representations

4.9.1 Exact transformations

As detailed in [160], the convolution of the finite-dimensional distribution function $F_\rho(\Omega, s')$ with the spin-up state representation $F_{|JJ\rangle}(\Omega, s)$ transforms between different representations and results in a type-$(s{+}s'{-}1)$ distribution function (refer also to Equation 4.4)

$$F_\rho(\Omega, s{+}s'{-}1) = F_{|JJ\rangle}(\theta, s) \star F_\rho(\Omega, s') =: \square(s)\, F_\rho(\Omega, s'). \tag{4.41}$$

We rely on Equation 4.41 to define the differential operator $\square(s)$ which will be often used in the following as a convenient notational shortcut for the convolution. This differential operator satisfies the eigenvalue equation $\square(s)\, \mathrm{Y}_{jm} = \gamma_j^{1-s}\, \mathrm{Y}_{jm}$ when applied to spherical

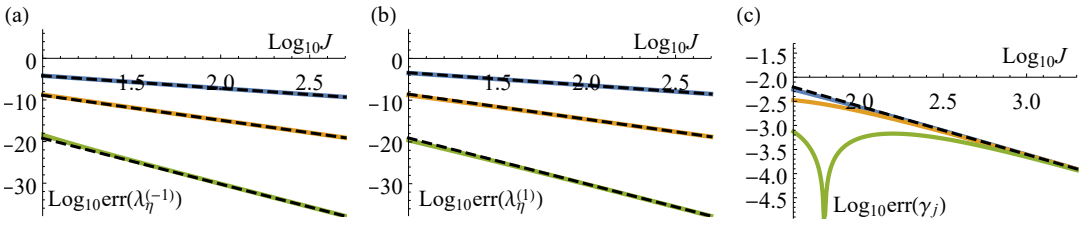

Figure 4.4: (a)-(b) Difference between the exact factors $\lambda_\eta^{(-1)}$ and $\lambda_\eta^{(1)}$ from Result 4.1 Equation 4.33 and their approximations from Equation 4.35 and Equation 4.36 for $\eta \in \{2, 5, 10\}$ (blue, orange, green). (c) Difference between the exact factor γ_j and its approximation from Result 4.4 for $j \in \{2, 5, 12\}$ (blue, orange, green). Dashed lines show the expected scaling $\mathcal{O}(J^{-\eta-1})$ for (a) and (b) as well as $\mathcal{O}(J^{-1})$ for (c) with suitable prefactors.

harmonics [160]. C.4 details how these eigenvalues γ_j^{1-s} can be written as a $2J$-order polynomial in $j(j+1)$ which enables us to specify $\square(s)$ as a polynomial in the differentials $\eth\overline{\eth}$ using Equation 4.19:

Result 4.3. *The operator $\square(s)$ from Equation 4.41 can be specified as a $2J$-order polynomial*

$$\square(s)F_\rho(\Omega,s') = \sum_{n=0}^{2J} c_n(s)\ (\eth\overline{\eth})^n F_\rho(\Omega,s') \tag{4.42}$$

in terms of the differentials $\eth\overline{\eth}$ (or equivalently $\overline{\eth}\eth$), where the coefficients $c_n(s)$ are uniquely determined and can be computed analytically (refer to C.4 for details).

The upper summation bound in Equation 4.42 can be enlarged to $4J$ if one performs a truncation of the higher-order spherical-harmonics terms in the resulting phase-space distribution function, refer to C.4.

4.9.2 Approximate transformations

The eigenvalue equation for the transformation operator $\square(s)$ from Section 4.9.1 is expanded into

$$\square(s)\,\mathrm{Y}_{jm} = \sum_{n=0}^{\infty}[-\tfrac{1-s}{4J}\,j(j+1)]^n/n!\,\mathrm{Y}_{jm} + \mathcal{O}(J^{-1}) \tag{4.43}$$

by applying results of C.3. This enables the following approximations which are also discussed in Figure 4.4(c):

Result 4.4. *Using the asymptotic expansion from Equation 4.43, $\square(s)$ can be approximated by*

$$\square(s)F_\rho(\Omega,s') = \exp[\,\tfrac{1-s}{4J}\,\eth\overline{\eth}]F_\rho(\Omega,s') + \mathcal{O}(J^{-1}). \tag{4.44}$$

Proposition 4.1 facilitates the approximation

$$\square(s)F_\rho(\Omega,s') = \exp[\,\tfrac{1-s}{2}\partial_{\alpha^*}\partial_\alpha\,]F_\rho(\Omega,s') + \mathcal{O}(J^{-1}) \tag{4.45}$$

in terms of the derivatives ∂_{α^*} and ∂_α. This recovers the infinite-dimensional case from Equation 4.4 in the large-spin limit if $F_\rho(\Omega,s')$ and its differentials remain non-singular.

4.10 Star products of s-parametrized phase spaces

4.10.1 The exact star product

Generalizing P and Q functions in Section 4.8, the star product of general s-parametrized phase spaces is now determined. The differential operator $\square(s)$ can be used to translate the star product of P or Q functions to the star product of arbitrary s-parametrized distribution

functions. In particular, we apply Result 4.1 to $Q_{AB} = Q_A \star^{(-1)} Q_B$ and $P_{AB} = P_A \star^{(1)} P_B$ and use the substitutions

$$\Box\,(s{+}2)Q_{AB} = F_{AB}(\Omega,s),\ Q_A = \Box(-s)F_A(\Omega,s),\ Q_B = \Box(-s)F_B(\Omega,s),$$
$$\Box\,(s)P_{AB} = F_{AB}(\Omega,s),\ P_A = \Box(2{-}s)F_A(\Omega,s),\ P_B = \Box(2{-}s)F_B(\Omega,s)$$

from Result 4.2 in order to compute the star product:

Result 4.5. *The star product of two s-parametrized phase-space distribution functions $F_A(\Omega,s)$ and $F_B(\Omega,s)$ is given by either of the two equations*

$$F_A(\Omega,s) \star^{(s)} F_B(\Omega,s) = \Box(s{+}2)\{F_A(\Omega,s)\,[\overleftarrow{\Box}(-s) \star^{(-1)} \overrightarrow{\Box}(-s)]\,F_B(\Omega,s)\} \tag{4.46}$$

$$F_A(\Omega,s) \star^{(s)} F_B(\Omega,s) = \Box(s)\{F_A(\Omega,s)\,[\overleftarrow{\Box}(2{-}s) \star^{(1)} \overrightarrow{\Box}(2{-}s)]\,F_B(\Omega,s)\}. \tag{4.47}$$

An explicit expansion can be calculated by expanding $\Box(s)$ using Equation 4.42 and $\star^{(\pm1)}$ using Equation 4.32 and by applying the Leibniz identity $\eth(fg) = (\eth f)g + f(\eth g)$. This results in an alternative form of the exact star product in Equation 4.46 and Equation 4.47:

$$f \star^{(s)} g = \sum_{\underline{a},\underline{b},\underline{c},\underline{d}} \lambda^{(s)}_{\underline{a},\underline{b},\underline{c},\underline{d}} [\ldots(\overline{\eth})^{a_2}(\eth)^{b_1}(\overline{\eth})^{a_1} f][\ldots(\overline{\eth})^{d_2}(\eth)^{c_1}(\overline{\eth})^{d_1} g]. \tag{4.48}$$

The suitably chosen coefficients $\lambda^{(s)}_{\underline{a},\underline{b},\underline{c},\underline{d}}$ are nonzero only if all of the indices a_i, b_i, c_i, d_i are smaller than $2J{+}1$. Different values for these coefficients are possible as the product of spin-weight raising and lowering operators can be reordered using their commutators from Section 4.6. But all possible values of the coefficients lead to the same unique result.

Although the choice of the coefficients in the finite sum in Equation 4.48 is in general not unique due to the non-commutativity of $\eth$ and $\overline{\eth}$, convenient formulas can be obtained for explicit values of J by reordering products of $\eth$ and $\overline{\eth}$. The particular case of $J = 1/2$ is discussed in Section 4.10.2. For large J, the star product can be approximated using the commutative derivatives $\partial_{\alpha^\star}$ and ∂_α from the infinite-dimensional case as discussed in Section 4.10.3. Also, Equation 4.46 can always be used to calculate the exact star product, but this approach consists of three consecutive steps, as demonstrated in Section 4.11.

4.10.2 The case of a single spin $1/2$

In the particular case of $J = 1/2$, the *exact* star product in Equation 4.46 can be simplified into a more convenient form by applying Equation 4.48. Let A and B denote spin-1/2 operators and their phase-space representations are given by $f = F_A(\Omega,s)$ and $g = F_B(\Omega,s)$. The star

product is then determined by

$$f \star^{(s)} g = N_s \mathcal{P}(f\,[1 + a_s(\overleftarrow{\eth})(\overrightarrow{\eth}) - b_s(\overleftarrow{\eth})(\overrightarrow{\eth})]\,g), \tag{4.49}$$

where the s-dependent coefficients are $N_s = 2^{-\frac{s}{2}-\frac{1}{2}}$,

$$a_s = \frac{1}{4}3^{-s-\frac{1}{2}}[2\,3^{s/2} - 3^{s+\frac{1}{2}} + \sqrt{3}], \text{ and } b_s = \frac{1}{4}3^{-s-\frac{1}{2}}[2\,3^{s/2} + 3^{s+\frac{1}{2}} - \sqrt{3}].$$

The projection $\mathcal{P} := 1 - \eth\bar{\eth}/12 - \eth\bar{\eth}\eth\bar{\eth}/24$ removes superfluous terms in the spherical-harmonics decomposition, i.e., contributions Y_{jm} with $j > 1$ that do not correspond to spin-$1/2$ distribution functions (refer to Result 2 in [159]). Note that for Wigner functions (i.e. $s = 0$) the explicit form of the star product can be calculated as (see, e.g., [159])

$$W_A \star^{(0)} W_B = \mathcal{P}R\,[\sqrt{2\pi}\,W_A W_B - \tfrac{i}{2}\sqrt{\tfrac{8\pi}{3}}\,\{W_A, W_B\}_S] \tag{4.50}$$

where $a_0 = b_0 = 1/(2\sqrt{3})$ and $N_0 = 1/\sqrt{2}$. For $J = 1/2$, we have the radius $R = (4\pi)^{-1/2}$ and the spherical Poisson bracket has the form $i\{.,.\}_S = \overleftarrow{\partial}_\phi(\sin\theta)^{-1}\overrightarrow{\partial}_\theta - \overleftarrow{\partial}_\theta(\sin\theta)^{-1}\overrightarrow{\partial}_\phi$, which should also be compared to Equation 4.53.

4.10.3 Approximations of the star product

Applying Result 4.2 and Result 4.4, the exact star product in Result 4.5 can be efficiently approximated as detailed in the following:

Result 4.6. *Let $f = F_A(\Omega, s)$ and $g = F_B(\Omega, s)$ denote the phase-space functions of the spin-J operators A and B. The star product in Equation 4.46 can be expanded in terms of spin-weight raising and lowering operators as (refer to C.6 for a proof)*

$$f \star^{(s)} g = \sum_{n=0}^{4J}\sum_{m=0}^{n} \frac{c_{nm}(s)}{(2J)^n}[\bar{\eth}^m \eth^{n-m} f][\eth^m \bar{\eth}^{n-m} g] + \mathcal{O}(J^{-1}), \tag{4.51}$$

where the coefficients $c_{nm}(s)$ are defined in C.6. Similarly, the star product can be specified in terms of the derivatives

$$f \star^{(s)} g = f \exp[\tfrac{(1-s)}{2}\overleftarrow{\partial}_\alpha\overrightarrow{\partial}_{\alpha^*} - \tfrac{(1+s)}{2}\overleftarrow{\partial}_{\alpha^*}\overrightarrow{\partial}_\alpha]\,g + \mathcal{O}(J^{-1}). \tag{4.52}$$

The infinite-dimensional case from Equation 4.7 is recovered in the large-spin limit by applying Proposition 4.1 if f and g and their differentials remain non-singular.

Note that the first-order term (i.e. $n = 1$) of the star product $\star^{(0)}$ in Equation 4.51 is for the case of a Wigner function (i.e. $s = 0$) proportional to the spherical Poisson bracket [159]

$$\{.,.\}_S := i[(\overleftarrow{\eth})(\overrightarrow{\eth}) - (\overleftarrow{\eth})(\overrightarrow{\eth})]/(2J) = \overleftarrow{\partial}_\phi(2J\sin\theta)^{-1}\overrightarrow{\partial}_\theta - \overleftarrow{\partial}_\theta(2J\sin\theta)^{-1}\overrightarrow{\partial}_\phi, \tag{4.53}$$

which corresponds to the classical part of the time evolution [159]. The approximate star product can be also used to derive efficient approximations of finite-dimensional phase-space representations for large J as illustrated in Section 4.12.

4.11 Time evolution of quantum states for a spin J

4.11.1 Description of the time evolution using the star product

The time evolution of a quantum state ρ for a single spin J can be described in a phase space via the Moyal equation from Equation 4.2. We discuss now the general structure of the time evolution of phase-space functions along the lines of [159] and present an explicit example in Section 4.11.2. We refer to [159] for further background and additional examples. Substituting the s-parametrized star product in Equation 4.2 with one of its forms from Result 4.5 yields the *exact* equation of motion for an arbitrary quantum state $F_\rho(\Omega, s)$ under a Hamiltonian $F_\mathcal{H}(\Omega, s)$ as (refer, e.g., Equation 4.47)

$$\begin{aligned}\frac{\partial F_\rho(\Omega,s)}{\partial t} = \; & -i \,\square\, (s)\{F_\mathcal{H}(\Omega,s)\,[\,\overleftarrow{\square}(2-s) \star^{(1)} \overrightarrow{\square}(2-s)]\,F_\rho(\Omega,s)\} \\ & +i \,\square\, (s)\{F_\rho(\Omega,s)\,[\,\overleftarrow{\square}(2-s) \star^{(1)} \overrightarrow{\square}(2-s)]\,F_\mathcal{H}(\Omega,s)\}. \end{aligned} \tag{4.54}$$

The use of this equation is illustrated in Section 4.11.2 with the particular case of a Wigner function ($s = 0$). One can approximate this time evolution by substituting the s-parametrized star product in Equation 4.2 with one of its approximations from Result 4.6. This yields for $f := F_\mathcal{H}(\Omega, s)$ and $g := F_\rho(\Omega, s)$ an approximate equation of motion up to an error of order $\mathcal{O}(J^{-1})$ as (e.g.)

$$\frac{\partial F_\rho(\Omega,s)}{\partial t} \approx \sum_{n=1}^{4J} \sum_{m=0}^{n} \frac{c_{nm}(s)}{(2J)^n} \{-i[\overline{\eth}^m \eth^{n-m} f][\eth^m \overline{\eth}^{n-m} g] + i[\overline{\eth}^m \eth^{n-m} g][\eth^m \overline{\eth}^{n-m} f]\}. \tag{4.55}$$

Note that the first term of the summation ($n = 1$) coincides with the spherical Possion bracket from Equation 4.53 for the special case of Wigner functions ($s = 0$) and corresponds to a semiclassical time evolution [159]. These semiclassical approximations have been widely used, refer to, e.g., [151, 152, 271]. Higher order contributions $n \geq 2$ are used to approximate quantum contributions in the time evolution.

4.11.2 Example of an explicit and exact time evolution for a single spin J

We discuss in this section an example for a single spin with arbitrary spin number J which illustrates the application of the exact star product from Equation 4.46. Let us consider an experimental system with a single spin J that is controlled as, e.g., in solid state nuclear magnetic resonance [96]. The density operator of a single spin J is in the thermal equilibrium given by $\rho_0 \propto \mathrm{Id} + \beta \mathcal{I}_z$ where β depends on the temperature. (We use the

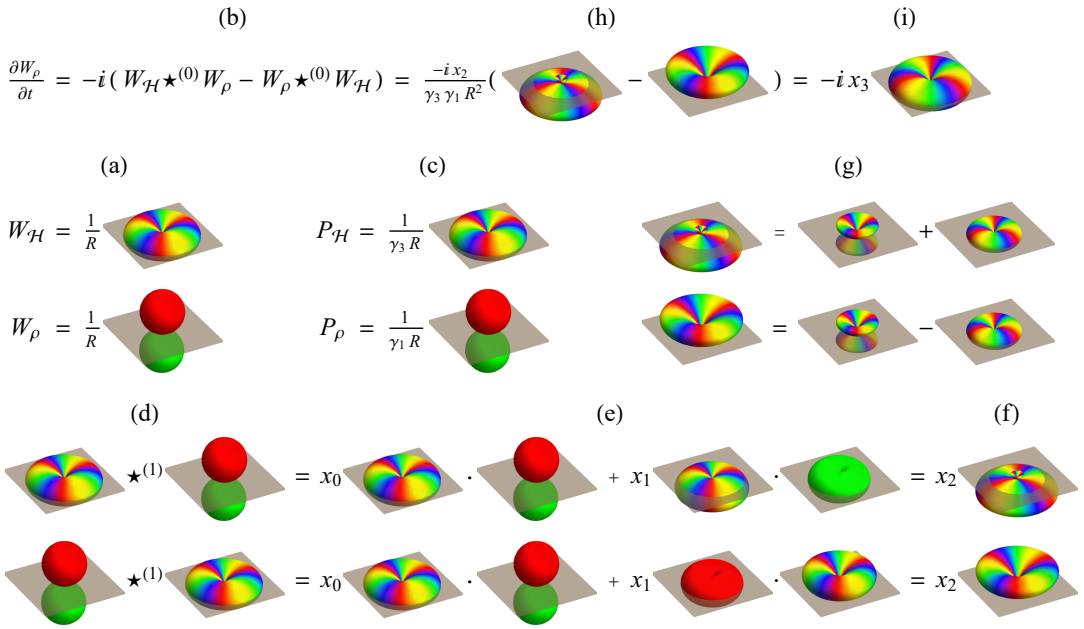

Figure 4.5: Visualizing the calculation of the exact time evolution using the star product of Wigner functions for a single spin with an arbitrary spin number J: (a) $W_{\mathcal{H}} := \frac{1}{R}\mathrm{Y}_{33}(\theta,\phi)$ and $W_\rho := \frac{1}{R}\mathrm{Y}_{10}(\theta,\phi)$ and (c) their corresponding P functions, (b) time evolution in the phase space via the Moyal equation Equation 4.56, (d)-(f) star products $P_{\mathcal{H}} \star^{(1)} P_\rho$ and $P_\rho \star^{(1)} P_{\mathcal{H}}$ using Equation 4.58-Equation 4.59, (g) the resulting star products decompose into two spherical harmonics as in Equation 4.60; (h) substituting (f) back into the Moyal equation (b) leads to (i) where the symmetric contribution from (g) is canceled out. The prefactors x_0, x_1, x_2, x_3 are used to rescale some of the plots.

notations $\mathcal{I}_z = \mathrm{T}_{10}/(\sqrt{2}N_J)$ and $\mathcal{I}_+ = \mathrm{T}_{11}/N_J$ with $N_J = 1/\sqrt{2J(J+1)(2J+1)/3}$.) We assume an effective Hamiltonian of the form $\mathcal{H}_{eff} := \omega(\mathcal{I}_+)^3 + \mathcal{H}_{res}$. The first-order time evolution under this effective Hamiltonian is given by the von-Neumann equation $\frac{\partial \rho_0}{\partial t} = -i\omega[(\mathcal{I}_+)^3, \mathcal{I}_z] - i[\mathcal{H}_{res}, \rho_0]$, and the commutator $[(\mathcal{I}_+)^3, \mathcal{I}_z]$ is proportional to $(\mathcal{I}_+)^3$. The term $(\mathcal{I}_+)^3$ is responsible for creating multiple quantum coherences which are often desirable. One can design experimental controls that maximize this contribution in the effective Hamiltonian [96].

Equivalently, the time evolution of the density operator $\rho := \mathrm{T}_{10}$ under the Hamiltonian $\mathcal{H} := \mathrm{T}_{33}$ can be calculated for a single spin with arbitrary spin number J directly in a phase-space representation. The corresponding spin Wigner functions $W_{\mathcal{H}} := \frac{1}{R}\mathrm{Y}_{33}(\theta,\phi)$ and $W_\rho := \frac{1}{R}\mathrm{Y}_{10}(\theta,\phi)$ are specified in terms of spherical harmonics, see Figure 4.5(a). The time evolution of the Wigner function W_ρ is described in the phase space by the Moyal equation (cf. [159])

$$\frac{\partial W_\rho}{\partial t} = -i\, W_{\mathcal{H}} \star^{(0)} W_\rho + i\, W_\rho \star^{(0)} W_{\mathcal{H}} \tag{4.56}$$

by relying on the star commutator which is determined in terms of star products, see Figure 4.5(b). The star product $W_{\mathcal{H}} \star^{(0)} W_\rho$ is evaluated via Result 4.5. Using Equation 4.47, we get

$$W_{\mathcal{H}} \star^{(0)} W_\rho = \square(0)\big(W_{\mathcal{H}}\,[\overleftarrow{\square}(2) \star^{(1)} \overrightarrow{\square}(2)]\, W_\rho\big), \tag{4.57}$$

where $\square(2)$ is determined by Result 4.3 (refer to Equation 4.41) and transforms the Wigner

functions to the corresponding P functions $P_{\mathcal{H}} = W_{\mathcal{H}} \overleftarrow{\Box}(2) = \frac{1}{R\gamma_3}\mathrm{Y}_{33}(\theta,\phi)$ and $P_\rho = \overrightarrow{\Box}(2)W_\rho = \frac{1}{R\gamma_1}\mathrm{Y}_{10}(\theta,\phi)$, see Figure 4.5(c). Note that spherical harmonics Y_{jm} are eigenfunctions of $\Box(2)$ with eigenvalues γ_j^{-1}. The right hand side of Equation 4.57 is then equal to $\Box(0)(\, P_{\mathcal{H}} \star^{(1)} P_\rho\,)$, for which the star product of P functions is computed using Equation 4.32 in Result 4.1. This yields (see Figure 4.5(d-f))

$$P_{\mathcal{H}} \star^{(1)} P_\rho = \frac{\mathrm{Y}_{33}\star^{(1)}\mathrm{Y}_{10}}{R^2\gamma_1\gamma_3} = \frac{1}{R^2\gamma_1\gamma_3}[\lambda_0^{(1)}\mathrm{Y}_{33}\mathrm{Y}_{10} + \lambda_1^{(1)}(\eth\mathrm{Y}_{33})(\overline{\eth}\mathrm{Y}_{10})], \tag{4.58}$$

$$P_{\mathcal{H}} \star^{(1)} P_\rho = \frac{1}{R^2\gamma_1\gamma_3}[\lambda_0^{(1)}\mathrm{Y}_{33}\mathrm{Y}_{10} - \lambda_1^{(1)}2\sqrt{6}\,\mathrm{Y}_{33}^{1}\mathrm{Y}_{10}^{-1}]. \tag{4.59}$$

The coefficients $\lambda_0^{(1)}$ and $\lambda_1^{(1)}$ are defined in Equation 4.33 and the operators $\eth$ and $\overline{\eth}$ from Equation 4.16 are responsible for raising and lowering the spin weight of the spherical harmonics.

Products of spin-weighted spherical harmonics can be decomposed into sums $\mathrm{Y}_{33}\mathrm{Y}_{10} = \frac{1}{2\sqrt{3\pi}}\mathrm{Y}_{43}$ and $\mathrm{Y}_{33}^{1}\mathrm{Y}_{10}^{-1} = -\frac{3}{4\sqrt{2\pi}}\mathrm{Y}_{33} + \frac{1}{4\sqrt{2\pi}}\mathrm{Y}_{43}$ of spherical harmonics. The corresponding star product of Wigner functions is obtained by rescaling spherical harmonics Y_{jm} by γ_j, which results in (refer to Figure 4.5(g-h))

$$W_{\mathcal{H}} \star^{(0)} W_\rho = \frac{1}{R^2\gamma_1\gamma_3}[+\frac{\lambda_1^{(1)}3\sqrt{3}}{2\sqrt{\pi}}\,\gamma_3\mathrm{Y}_{33} + (\frac{\lambda_0^{(1)}}{2\sqrt{3\pi}} - \frac{\lambda_1^{(1)}\sqrt{3}}{2\sqrt{\pi}})\,\gamma_4\mathrm{Y}_{43}] \tag{4.60}$$

$$W_\rho \star^{(0)} W_{\mathcal{H}} = \frac{1}{R^2\gamma_1\gamma_3}[-\frac{\lambda_1^{(1)}3\sqrt{3}}{2\sqrt{\pi}}\,\gamma_3\mathrm{Y}_{33} + (\frac{\lambda_0^{(1)}}{2\sqrt{3\pi}} - \frac{\lambda_1^{(1)}\sqrt{3}}{2\sqrt{\pi}})\,\gamma_4\mathrm{Y}_{43}]. \tag{4.61}$$

Note that $\gamma_4 = 0$ for $J < 2$ which is responsible for truncating the spherical-harmonics decomposition [159], refer to C.4. The final result determining the time evolution is obtained via the star commutator from Equation 4.56, and we obtain (for arbitrary J)

$$\frac{\partial W_\rho}{\partial t} = -i\,\frac{3\sqrt{3}}{\sqrt{\pi}}\,\frac{\lambda_1^{(1)}}{R^2\gamma_1}\mathrm{Y}_{33}. \tag{4.62}$$

4.11.3 Extending the example to an arbitrary quantum state

Applying the same Hamiltonian $W_{\mathcal{H}} = \frac{1}{R}\mathrm{Y}_{33}$ to an arbitrary quantum state $g := W_\rho$, we could apply Equation 4.54 to determine the time evolution exactly. But we will consider here only the approximate time evolution (see Equation 4.55)

$$\frac{\partial W_\rho}{\partial t} \approx \frac{1}{R}\sum_{n=1}^{4J}\sum_{m=0}^{n}\frac{c_{nm}(0)}{(2J)^n}\{-i[\overline{\eth}^m\eth^{n-m}\mathrm{Y}_{33}][\eth^m\overline{\eth}^{n-m}g] + i[\overline{\eth}^m\eth^{n-m}g][\eth^m\overline{\eth}^{n-m}\mathrm{Y}_{33}]\},$$

where one can apply Equation 4.15 to simplify differentials. For example, one obtains (up to a factor) the spin-weighted spherical harmonics

$$\overline{\eth}^m\eth^{n-m}\mathrm{Y}_{33} \propto \begin{cases}\mathrm{Y}_{33}^{n-2m} & \text{for } |n-m|\le 3 \text{ and } |n-2m|\le 3,\\ 0 & \text{otherwise.}\end{cases} \tag{4.63}$$

This highlights that most of the terms in the sum vanish for a general spin number J. But this example makes it also apparent that a semiclassical approximation [151, 152, 271] that

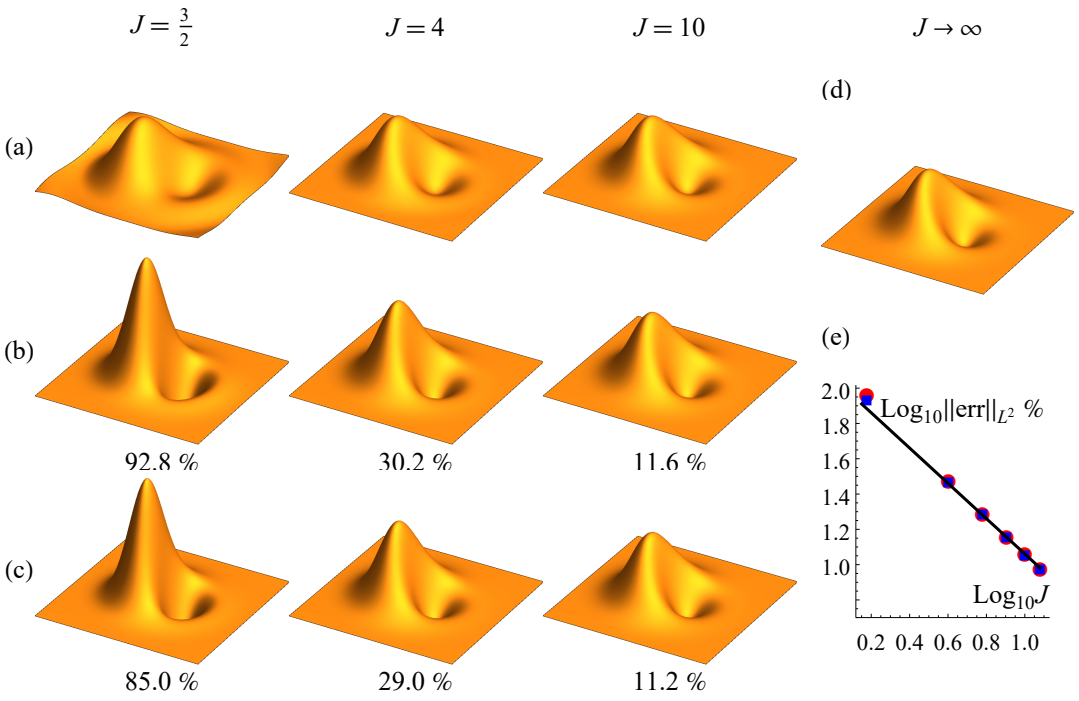

Figure 4.6: (a) Plots of the exact phase-space representations $F_{|\Omega_0^+\rangle}(\Omega,0)$ of $|\Omega_0^+\rangle$ for increasing spin numbers J using Equation 4.69. (b)-(c) Approximations of $F_{|\Omega_0^+\rangle}(\Omega,0)$ using Equation 4.71 and the Gaussian function $F_{|0\rangle\langle 0|}(\Omega,0)$, also applying the *approximate* star product in Equation 4.51 for (b) and Equation 4.52 for (c). Both (b) and (c) converge to (a) in order $\mathcal{O}(J^{-1})$ as they approach their infinite-dimensional counterpart (d) from Equation 4.64. The approximation errors in the L^2 norm shown below the plots are graphed in (e) for $J \in \{3/2, 4, 6, 8, 10, 12\}$, where red dots and blue squares refer, respectively, to (b) and (c) and the black line shows the expected scaling $\mathcal{O}(J^{-1})$ with a suitable prefactor. The distance from the origin in these planar plots represent the arc distance from the north pole in the spherical phase space. The rotation parameter in Equation 4.69 has been chosen as $\Omega_0 = (\theta_0, \phi_0) = (1.2/\sqrt{J/2}, 0)$ and the translation parameter in Equation 4.64 is given by $\alpha_0 = 1.2$. Plot limits are ± 2. Refer also to Figure 4.1 and Figure 4.7.

restricts the summation to $n = 1$ will neglect relevant quantum contributions.

4.12 One example of photon-added coherent states

Creation and annihilation operators are widely used and account for numerous non-classical effects including, for example, photon-added coherent states which were demonstrated experimentally [269, 270, 268, 24, 162, 6]. Photon-added coherent states are obtained from coherent states $|\alpha_0\rangle := \mathcal{D}(\alpha_0)|0\rangle$ as $a^\dagger|\alpha_0\rangle$ by applying the creation operator $a^\dagger$. The inversely translated version of these quantum states is created from the vacuum state by applying the operator $Q(\alpha_0)$ and one has

$$|\alpha_0^+\rangle = Q(\alpha_0)|0\rangle \quad \text{with} \quad Q(\alpha_0) := \frac{1}{\sqrt{1+|\alpha_0|^2}}\mathcal{D}(\alpha_0)^{-1}a^\dagger\mathcal{D}(\alpha_0). \tag{4.64}$$

Phase-space representations of these photon-added coherent states can be obtained using the star products of the individual phase-space representations

$$F_{|\alpha_0^+\rangle}(\alpha,s) = F_{Q(\alpha_0)} \star^{(s)} F_{|0\rangle}(\alpha,s) \star^{(s)} (F_{Q(\alpha_0)})^*, \tag{4.65}$$

where the Gaussian function $F_{|0\rangle}(\alpha,s) = 2\exp[-2\alpha\alpha^*/(1-s)]/(1-s)$ represents the vacuum state [50] and $F_{Q(\alpha_0)} := (\alpha^*+\alpha_0^*)/\sqrt{1+|\alpha_0|^2}$ corresponds to the creation operator. Applying the star product from Equation 4.7 yields

$$F_{|\alpha_0^+\rangle}(\alpha,s) = [\alpha+\alpha_0-\tfrac{1+s}{2}\partial_{\alpha^*}][\alpha^*+\alpha_0^*-\tfrac{1+s}{2}\partial_\alpha]F_{|0\rangle}(\alpha,s) =: \overline{\mathcal{Q}}(\alpha_0)\mathcal{Q}(\alpha_0)F_{|0\rangle}(\alpha,s), \tag{4.66}$$

where the second equality describes the photon creation in the shifted phase space in terms of the differential operators $\mathcal{Q}(\alpha_0)\overline{\mathcal{Q}}(\alpha_0) = \overline{\mathcal{Q}}(\alpha_0)\mathcal{Q}(\alpha_0)$. Setting $\alpha_0 = 0$ yields the phase-space equivalent of the creation operator, i.e., essentially Bopp operators [42]

$$\mathcal{Q} := \mathcal{Q}(0) = [\alpha^* - \tfrac{1+s}{2}\partial_\alpha], \text{ and } \overline{\mathcal{Q}} := \overline{\mathcal{Q}}(0) = [\alpha - \tfrac{1+s}{2}\partial_{\alpha^*}]. \tag{4.67}$$

For the number state $|n\rangle$, one can calculate the phase-space functions

$$F_{|n\rangle}(\alpha,s) = \tfrac{1}{n!}[\overline{\mathcal{Q}}\mathcal{Q}]^n F_{|0\rangle}(\alpha,s), \text{ and } F_{|n_1\rangle\langle n_2|}(\alpha,s) = \tfrac{1}{\sqrt{n_1!}\sqrt{n_2!}}(\overline{\mathcal{Q}})^{n_2}(\mathcal{Q})^{n_1}F_{|0\rangle}(\alpha,s) \tag{4.68}$$

corresponds to tilted projectors $|n_1\rangle\langle n_2|$ which span a complete, orthonormal basis [50].

We define finite-dimensional analogues of photon-added coherent states in the form

$$|\Omega_0^+\rangle := K(\Omega_0)|JJ\rangle \text{ with } K(\Omega_0) := \tfrac{N}{\sqrt{2J}}\mathcal{R}^{-1}(\Omega_0)\mathcal{J}_-\mathcal{R}(\Omega_0), \tag{4.69}$$

where $|JJ\rangle$ is the spin-up state and $\mathcal{J}_-/\sqrt{2J}$ is the finite-dimensional analogue of the creation operator which approaches $a^\dagger$ in the large-spin limit. Refer to Table 1 in [18] and C.7 for details. Following the infinite-dimensional characterization, the phase-space representation $F_{|\Omega_0^+\rangle}$ can be written in terms of the exact star product of the individual phase-space representations as (see Result 4.5)

$$F_{|\Omega_0^+\rangle}(\Omega,s) = F_{K(\Omega_0)} \star^{(s)} F_{|0\rangle\langle 0|}(\Omega,s) \star^{(s)} (F_{K(\Omega_0)})^*, \tag{4.70}$$

where the Gaussian-like function $F_{|0\rangle\langle 0|}(\Omega,s)$ represents the spin-up state and $F_{K(\Omega_0)}$ is the phase-space representation of the rotated lowering operator $K(\Omega_0)$. Refer to Figure 4.6(a) for plots of the (unapproximated) $F_{|\Omega_0^+\rangle}(\Omega,s)$ for $s = 0$. Using, e.g., the exact star product in Equation 4.46, the phase-space representation

$$F_{|\Omega_0^+\rangle}(\Omega,s) = \mathcal{K}(\Omega_0)\overline{\mathcal{K}}(\Omega_0)\, F_{|0\rangle\langle 0|}(\Omega,s) = \overline{\mathcal{K}}(\Omega_0)\mathcal{K}(\Omega_0)\, F_{|0\rangle\langle 0|}(\Omega,s) \tag{4.71}$$

of the excited coherent state $F_{|\Omega_0^+\rangle}(\Omega, s)$ is obtained by applying the differential operators $\mathcal{K}(\Omega_0)$ and $\overline{\mathcal{K}}(\Omega_0)$ which are defined via their action on phase space functions f, i.e.,

$$\mathcal{K}(\Omega_0) f \coloneqq F_{K(\Omega_0)} \star^{(s)} f \text{ and } \overline{\mathcal{K}}(\Omega_0) f \coloneqq f \star^{(s)} (F_{K(\Omega_0)})^*. \tag{4.72}$$

Approximations of these operators can be used to approximate $F_{|\Omega_0^+\rangle}(\Omega, s)$ by applying them to a Gaussian approximation of $F_{|0\rangle\langle 0|}(\Omega, s)$ as given in [160]. Approximations of $\mathcal{K}(\Omega_0)$ and $\overline{\mathcal{K}}(\Omega_0)$ are calculated in terms of spin-weighted spherical harmonics and their raising and lowering operators in C.7 using the *approximate* star products in Equation 4.52 and Equation 4.51. These approximations converge in Figure 4.6 to the exact phase-space functions, and the infinite-dimensional case from Equation 4.64 is recovered in the large-spin limit.

Comparable to the infinite-dimensional case, the unrotated ladder operator $\mathcal{K} \coloneqq \mathcal{K}(0)$ is specified in C.7 in terms of spin-weighted spherical harmonics and their raising and lowering operators. One can calculate representations

$$F_{|Jm\rangle}(\Omega, s) \propto [\mathcal{K}\overline{\mathcal{K}}]^{J-m} F_{|0\rangle\langle 0|}(\Omega, s) \tag{4.73}$$

of the Dicke state $|Jm\rangle$ using the operators $\mathcal{K}$ and $\overline{\mathcal{K}}$, and similar representations

$$F_{|Jm_1\rangle\langle Jm_2|}(\Omega, s) \propto (\overline{\mathcal{K}})^{J-m_2} (\mathcal{K})^{J-m_1} F_{|0\rangle\langle 0|}(\Omega, s) \tag{4.74}$$

are obtained for the tilted projectors $|Jm_1\rangle\langle Jm_2|$. All of these states have typically quite complicated spherical-harmonics expansions which are challenging to calculate for large values of J. Approximations based on the star product in Equation 4.52 facilitate efficient calculations of these and similar phase-space representations for large J.

We want to close this section by remarking that the general (infinite-dimensional) class of s-parametrized phase spaces naturally appear in experimental homodyne measurements [171, 269, 270, 268, 24, 162] of the discussed photon-added coherent states. As is explained in [172], the relevant experiment yields s-parametrized phase-space functions with $s = -(1-\xi)/\xi$ for a detector efficiency of ξ. This provides an example for the occurrence of s-parametrized phase spaces beyond the particular cases of $s \in \{-1, 0, 1\}$.

4.13 Generalization to coupled spins

The explicit form of the star product for Wigner functions of coupled spin-$1/2$ systems was detailed in Result 3 of [159]. Building on results in [159], we outline how to generalize these results to s-parameterized phase spaces of coupled spins J. We consider two operators A and B in a system of N coupled spins J. Their phase-space representations are determined similarly as in Result 1 of [159] and can be calculated as

$$F_A(s, \theta_1, \phi_1, \ldots, \theta_N, \phi_N) \coloneqq \mathrm{Tr}[A \bigotimes_{k=1}^{N} \mathcal{R}(\theta_k, \phi_k) M_s \mathcal{R}^\dagger(\theta_k, \phi_k)], \tag{4.75}$$

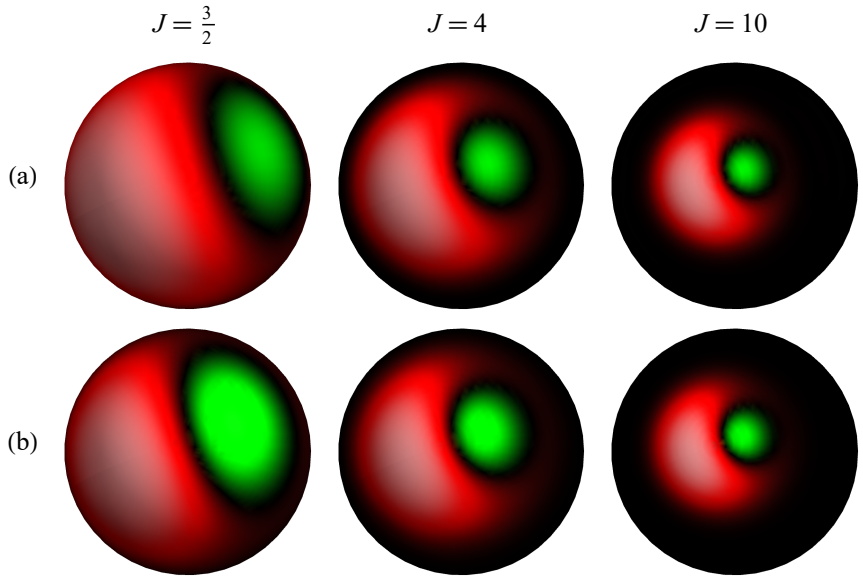

Figure 4.7: Alternative representation of Figure 4.6(a)-(b). (a) Plots of the exact phase-space representations $F_{|\Omega_0^+\rangle}(\Omega, 0)$ of $|\Omega_0^+\rangle$ for increasing J using Equation 4.69. (b) Approximations of $F_{|\Omega_0^+\rangle}(\Omega, 0)$ via Equation 4.71 and Equation 4.51 assuming a Gaussian $F_{|0\rangle\langle 0|}(\Omega, 0)$. (b) converges to (a) in order $\mathcal{O}(J^{-1})$. Spherical functions $f(\theta, \phi)$ are plotted on the sphere where the brightness represents the absolute value and the colors red (dark gray) and green (light gray) depict positive and negative values, respectively.

where the transformation kernel in Result 1 of [159] is expressed here in terms of rotated parity operators from Equation 4.8. We generalize the star product described in Result 4.5 to the star product

$$F_A \star F_B := F_A \Big(\prod_{k=1}^{N} [\star^{(s)}]^{\{k\}}\Big) F_B \tag{4.76}$$

of phase-space representations for coupled spins by applying Result 3 of [159], where $\star^{(s)}$ is the star product from Result 4.5 and $[\star^{(s)}]^{\{k\}}$ describes that the star product acts only on the variables θ_k and ϕ_k. Equation 4.76 completely specifies the exact star product for a system of N interacting spins J, and the corresponding approximations via Result 4.6 can be conveniently expressed using the commutativity of partial derivatives. For example, the approximate star product in terms of the derivatives ∂_α and $\partial_{\alpha^\star}$ from Equation 4.52 is generalized for coupled spins to

$$F_A \star^{(s)} F_B = F_A \exp\Big[\sum_{k=1}^{N} \Big(\tfrac{(1-s)}{2} \overleftarrow{\partial}_{\alpha_k} \overrightarrow{\partial}_{\alpha_k^*} - \tfrac{(1+s)}{2} \overleftarrow{\partial}_{\alpha_k^*} \overrightarrow{\partial}_{\alpha_k}\Big)\Big] F_B + \mathcal{O}(J^{-1}). \tag{4.77}$$

The equation of motion for Wigner functions, i.e., the Moyal equation from Equation 4.56, can be consequently established for a system of coupled spins J using Equation 4.77 as

$$i\frac{\partial W_\rho}{\partial t} = W_{\mathcal{H}} \star^{(0)} W_\rho - W_\rho \star^{(0)} W_{\mathcal{H}} = W_{\mathcal{H}}[e^{i\{.,.\}/2} - e^{-i\{.,.\}/2}]W_\rho + \mathcal{O}(J^{-1}),$$

where $\{.,.\} := \sum_{k=1}^{N} g_k$ and $g_k := -i \overleftarrow{\partial}_{\alpha_k} \overrightarrow{\partial}_{\alpha_k^*} + i \overleftarrow{\partial}_{\alpha_k^*} \overrightarrow{\partial}_{\alpha_k}$ specify a Poisson bracket acting on the variables α_k and α_k^*. This results in the expansion

$$i\frac{\partial W_\rho}{\partial t} = W_{\mathcal{H}}[2 \sum_{\substack{n=0,\\ n \text{ odd}}} (-i\{.,.\}/2)^n/n!]W_\rho + \mathcal{O}(J^{-1}) \tag{4.78}$$

$$= W_{\mathcal{H}}[-i \sum_{k=1}^{N} g_k + \tfrac{i}{24} \sum_{k_1,k_2,k_3=1}^{N} g_{k_1} g_{k_2} g_{k_3} + \cdots]W_\rho + \mathcal{O}(J^{-1}). \tag{4.79}$$

Using Proposition 4.1, the differential operators $-g_k$ can be replaced by the spherical Poisson brackets $p_k := \{.,.\}_S^{\{k\}}$ from Equation 4.53, which results in the time evolution

$$i\frac{\partial W_\rho}{\partial t} = W_{\mathcal{H}}[\, i \sum_{k=1}^{N} p_k - \tfrac{i}{24} \sum_{\substack{k_1,k_2,k_3=1 \\ k_\mu \neq k_\nu \text{ for } \mu \neq \nu}}^{N} p_{k_1} p_{k_2} p_{k_3} + \cdots + \tfrac{i}{24} \sum_{k=1}^{N} g_k^3 + \cdots]W_\rho + \mathcal{O}(J^{-1}). \tag{4.80}$$

The first two terms (before the first dots) can be directly compared to the ones appearing in the star product of coupled spins $1/2$ in Result 4 of [159]. The leading term corresponds to the classical equation of motion, and the following terms in the expansion are ordered according to their degree of non-locality as proposed in Result 4 of [159].

4.14 Conclusion

We have derived the exact star product for continuous s-parametrized phase-space representations of single spins J in terms of spin-weighted spherical harmonics and their raising and lowering operators. Our construction naturally recovers the well-known case of infinite-dimensional quantum systems in the limit of large spin numbers J. Based on approximations of spin-weighted spherical harmonics, we have derived convenient formulas for approximating star products which, beyond time evolution, can be useful for efficiently calculating phase-space representations for large spin numbers. We have illustrated our methods and their application in concrete examples. We have finally outlined how the presented formalism can be extended to coupled spin systems. In summary, we have established a complete phase-space description for finite-dimensional quantum systems and their time evolution.

CHAPTER 5

Phase Spaces, Parity Operators, and the Born-Jordan Distribution

5.1 Foreword to Chapter 5

This chapter is based on the manuscript [158] and considers phase-space representations of a non-relativistic, spinless quantum particle or a bosonic quantum field, such as in quantum optics. Phase-space descriptions of these quantum systems and associated quantizations have been well studied since the pioneering work of Wigner [262]. Generalizations of the Wigner function, e.g., P and Q functions or the Born-Jordan distribution have been proposed in the 1960's in works of Cohen [59], Cahill and Galuber [51]. These distribution functions have been mostly described in terms of integral transformations and in the current work we develop a general parity operator approach which has conceptual and computational advantages. In particular, we show that generalized phase-space representations are quantum-mechanical expectation values of a parity operator. After discussing well-known distribution functions and their parity operators, we obtain significant, new results for the case of Born-Jordan distributions, which has not been considered previously in the context of bosonic quantum systems. We calculate explicit actions and eigenvalue decompositions of these parity operators. We finally obtain a matrix representation of the Born-Jordan parity operator, which can be calculated efficiently and can be used for approximating Born-Jordan distributions of harmonic-oscillator quantum states, such as in quantum optics.

5.1.1 List of Symbols in Chapter 5

symbol	description
x, p	classical coordinate and momentum
$\hat{x}$, $\hat{p}$	coordinate and momentum operators
$\hat{a}$, $\hat{a}^\dagger$	bosonic creation and annihilation operators
$\mathcal{S}(\mathbb{R}^n)$	space of functions that decay rapidly at infinity, i.e., Schwartz space
$\mathcal{S}'(\mathbb{R}^n)$	topological dual space of Schwartz functions, i.e., tempered distributions
$\langle \phi, \psi \rangle$	distributional pairing between $\psi \in \mathcal{S}(\mathbb{R}^n)$ and $\phi \in \mathcal{S}'(\mathbb{R}^n)$
$[F_\sigma a(\cdot)](x,p)$	symplectic Fourier transform of a function $a \in \mathcal{S}'(\mathbb{R}^2)$ or distribution
$\mathcal{H}$	abstract Hilbert space, i.e., state space
$\langle \cdot \vert \cdot \rangle$	scalar product between elements of a Hilbert space
$\vert\psi\rangle$	abstract state vector $\vert\psi\rangle \in \mathcal{H}$, describes a pure quantum state
$\vert\psi\rangle\langle\psi\vert$	projection operator onto the pure state $\vert\psi\rangle$
$\vert x\rangle$	abstract coordinate eigenstate
$\vert n\rangle$	abstract number state, i.e., eigenstate of the quantum-harmonic oscillator
$\psi_n^{\mathrm{Fock}}(x)$	coordinate representation of number states via the scalar product $\langle x \vert n \rangle$
$L^2(\mathbb{R})$	Hilbert space of square-integrable functions
$\Vert\psi(x)\Vert_{L^2}$	Hilbert-space norm calculated via the integral $\int_{\mathbb{R}} \vert\psi(x)\vert^2 \, \mathrm{d}x$
$\ell^2(\mathbb{C})$	Hilbert space of square-summable sequences
$\Vert\,\vert\psi\rangle\Vert_{\ell^2}$	Hilbert-space norm calculated via the convergent sum $\sum_{n=0}^{\infty} \vert\psi_n\vert^2$
$\mathcal{B}^1(\mathcal{H})$	set of trace-class operators on the Hilbert space $\mathcal{H}$
$\mathrm{Tr}(A)$	trace of a trace-class operator a
ρ	density operator, i.e., positive, trace-class operator with $\mathrm{Tr}(\rho) = 1$
$\Vert O \Vert_{\mathrm{sup}}$	'supremum' operator norm of a bounded operator O
$\vert\Omega\rangle$	coherent states which span a phase space via their parametrization Ω
Ω	abstract phase-space coordinate with $\Omega \simeq \alpha \simeq (x,p)$
$\mathcal{D}(\Omega)$	displacement operator: creates coherent states via $\vert\Omega\rangle = \mathcal{D}(\Omega)\vert 0\rangle$
$[\mathcal{D}(\alpha)]_{mn}$	number-state representation of displacements via $\langle m \vert \mathcal{D}(\alpha) \vert n \rangle$
Π	parity operator: inverts phase-space coordinates $\Pi\vert\Omega\rangle = \vert -\Omega\rangle$
$W_\rho(\Omega)$	Wigner function of a mixed quantum state ρ
$F_\rho(\Omega,\theta)$	generalized phase-space distribution function indexed by θ
$F_\rho(\Omega,\mathrm{BJ})$	Born-Jordan distribution of a density operator ρ
$a * \psi$	convolution of a function $\psi \in \mathcal{S}(\mathbb{R}^2)$ and a distribution $a \in \mathcal{S}'(\mathbb{R}^2)$
Π_θ	parity operator indexed by θ
$\Pi_{\tau s}$	τ and s-parametrized parity operator with $\Pi_s := \Pi_{1/2,s}$, $\Pi_\tau(\Omega) := \Pi_{\tau 0}(\Omega)$
Π_{BJ}	Born-Jordan parity operator
$K_\theta(\Omega)$	filter function, i.e., a mapping $\mathbb{R}^2 \mapsto \mathbb{C}$
$K_{\tau s}(\Omega)$	τ and s-parametrized filter function: special cases of s and τ correspond to well-known distribution functions
$K_{\mathrm{BJ}}(\Omega)$	Born-Jordan filter function
$\theta(\Omega)$	Cohen kernel as a function or distribution $\theta(\Omega) \in \mathcal{S}'(\mathbb{R}^2)$
$\mathrm{Op}_{\mathrm{Weyl}}[a(x,p)]$	Weyl quantization of a phase-space function $a \in \mathcal{S}'(\mathbb{R}^2)$ or distribution
$\mathrm{Op}_\theta[a(x,p)]$	quantization via the Cohen kernel $\theta(\Omega) \in \mathcal{S}'(\mathbb{R}^2)$
$S(\xi)$	squeezing operator with a real squeezing parameter $\xi \in \mathbb{R}$
$\vert\psi_\pm^E\rangle$	generalized eigenvectors of the Born-Jordan parity operator with $E \in \mathbb{R}$

5.2 Summary

Phase spaces as given by the Wigner distribution function provide a natural description of infinite-dimensional quantum systems. They are an important tool in quantum optics and have been widely applied in the context of time-frequency analysis and pseudo-differential operators. Phase-space distribution functions are usually specified via integral transformations or convolutions which can be averted and subsumed by (displaced) parity operators proposed in this work. Building on earlier work for Wigner distribution functions [119], parity operators give rise to a general class of distribution functions in the form of quantum-mechanical expectation values. We relate these distribution functions to the so-called Cohen class [59] and recover various quantization schemes and distribution functions from the literature. The parity-operator approach is also applied to the Born-Jordan distribution which originates from the Born-Jordan quantization [43]. The corresponding parity operator is written as a weighted average of both displacements and squeezing operators and we determine its generalized spectral decomposition. This leads to an efficient computation of the Born-Jordan parity operator in the number-state basis and example quantum states reveal unique features of the Born-Jordan distribution.

5.3 Introduction

There exist at least three logically independent descriptions of quantum mechanics: the Hilbert-space formalism [61], the path-integral method [93], and the phase-space approach such as given by the Wigner function [53, 131, 149, 165, 97, 266, 232, 227, 62]. The phase-space formulation of quantum mechanics was initiated by Wigner in his ground-breaking work [262] from 1932, in which the Wigner function of a spinless non-relativistic quantum particle was introduced as a probability quasi-distribution. The Wigner function can be used to express quantum-mechanical expectation values as classical phase-space averages. More than a decade later, Groenewold [118] and Moyal [195] formulated quantum mechanics as a statistical theory on a classical phase by mapping a quantum state to its Wigner function and they interpreted this correspondence as the inverse of the Weyl quantization [259, 260, 261].

Coherent states have become a natural way to extend phase spaces to more general physical systems [25, 26, 28, 29, 47, 205, 99, 13, 30]. And in this regard, a new focus on phase-space representations for coupled, finite-dimensional quantum systems (as spin systems) [98, 159, 160, 161, 153, 248, 222, 169] and their tomographic reconstructions [221, 168, 167, 160] has emerged recently. A spherical phase-space representation of a single, finite-dimensional quantum system has been used to naturally recover the infinite-dimensional phase space in the large-spin limit [160, 161]. But in the current work, we exclusively focus on the (usual) infinite-dimensional case which has Heisenberg-Weyl symmetries [47, 205, 99, 174]. This case has been playing a crucial role in characterizing the quantum theory of light [107] via coherent states and displacement operators [51, 50, 11, 10] and has also been widely used in the context of time-frequency analysis and pseudo-differential operators [59, 60, 38, 37, 39, 111, 113, 116]. Many particular phase spaces have been unified

under the concept of the so-called Cohen class [59, 60, 113] (see Definition 5.2 below), i.e. all functions which are related to the Wigner function via a convolution with a function or distribution (which is also known as the Cohen kernel).

Phase-space distribution functions are mostly described by one of the following three forms: (a) convolved derivatives of the Wigner function [111, 113], (b) integral transformations of a pure state (i.e. a rapidly decaying, complex-valued function) [262, 59, 60, 38, 37, 39, 111, 113], or (c) as integral transformations of quantum-mechanical expectation values [51, 50, 11, 10]. Also, Wigner functions (and the corresponding Weyl quantization) are usually described by integral transformations. But the seminal work of Grossmann [119, 113] allowed for a direct interpretation of the Wigner function as a quantum-mechanical expectation value of a displaced parity operator (refer also to [217]). In particular, Grossmann [119] showed that the Weyl quantization of the delta distribution determines the parity operator. This approach has been widely adopted [63, 67, 175, 34, 97, 218, 219, 56].

However, a parity-operator similar to the one by Grossmann and Royer [119, 217, 113] (which does not rely on integral transformations or convolutions) has still been lacking for general phase-space distribution functions. (Note that such a form appeared implicitly for s-parametrized distribution functions in [194, 50].) In the current work, we propose parity operators which give rise to distribution functions in the form of quantum-mechanical expectation values and thereby avert the use of Fourier transforms or convolutions. Therefore, the current work can also be regarded as a continuation of [160] where the parity-operator approach has been emphasized, but mostly for finite-dimensional quantum systems. Moreover, we connect results from quantum optics [50, 51, 107, 171], quantum-harmonic analysis [258, 113, 111, 69, 68, 70, 71, 148], and group-theoretical approaches [47, 205, 99, 174]. And it is also our aim to narrow the gap between different communities where phase-space methods have been successfully applied.

Motivated by the previously discussed parity operator [119, 217, 113] for Wigner functions (which reflects coordinates $\Pi\psi(x) = \psi(-x)$ of a quantum mechanical state ψ), we introduce in Definition 5.3 a family of parity operators Π_θ that are related to a function or distribution θ. Quantum-mechanical expectation values of these parity operators in (5.16) give rise to a rich family of phase-space distribution functions that represent arbitrary quantum states which are usually described by their density operators. This family of phase-space representations contains all elements from the (above mentioned) Cohen class and naturally includes Glauber P and Husimi Q functions as well as the Born-Jordan distribution function.

Similarly as the parity operator Π (which is the Weyl quantization of the delta distribution), we show that its generalizations Π_θ are Weyl quantizations of the corresponding Cohen kernel θ. We discuss how these general results reduce to well-known special cases and discuss properties of phase-space distributions in relation to their parity operators Π_θ. In particular, we consider the class of s-parametrized distribution functions [107, 50, 51, 194], which include the Wigner, Glauber P, and Husimi Q functions, as well as the τ-parametrized family, which has been proposed in the context of time-frequency analysis and pseudo-differential operators [111, 38, 37, 39]. We derive spectral decompositions of parity operators for all of these phase-space families, including the Born-Jordan distribution. Relations of the form

$\Pi_\theta = A_\theta \circ \Pi$ motivate the name "parity operators" as these are indeed compositions of the usual parity operator Π followed by some operator A_θ that usually corresponds to a geometric or physical operation (which commutes with Π). In particular, A_θ is a squeezing operator for the τ-parametrized family and corresponds to photon loss for the s-parametrized family. This structure of the parity operators Π_θ connects phase spaces to elementary geometric and physical operations (such as reflection, squeezing operators, photon loss) and these concepts are central to applications: the squeezing operator models a non-linear optical process which generates non-classical states of light in quantum optics [182, 108, 171]. These squeezed states of light have been widely used in precision interferometry [229, 114, 265, 189], or for enhancing the performance of imaging [179, 251] and the gravitational-wave detector GEO600 has been operating with squeezed light since 2010 [2, 120].

The Born-Jordan distribution and its parity operator constitute a most peculiar instance among the phase-space approaches. This distribution function has convenient properties, e.g., it satisfies the marginal conditions and therefore allows for a probabilistic interpretation [111]. The Born-Jordan distribution is however difficult to compute. But most importantly, the Born-Jordan distribution and its corresponding quantization scheme have a fundamental importance in quantum mechanics. In particular, there have been several attempts in the literature to find the "right" quantization rule for observables using either algebraic or analytical techniques. In a recent paper [110], one of us has analyzed the Heisenberg and Schrödinger pictures of quantum mechanics, and it is shown that the equivalence of both theories requires that one must use the Born–Jordan quantization rule (as proposed by Born and Jordan [43])

$$\text{(BJ)} \quad x^m p^\ell \mapsto \frac{1}{m+1} \sum_{k=0}^{m} \hat{x}^k \hat{p}^\ell \hat{x}^{m-k},$$

instead of the Weyl rule

$$\text{(Weyl)} \quad x^m p^\ell \mapsto \frac{1}{2^m} \sum_{k=0}^{m} \binom{m}{k} \hat{x}^k \hat{p}^\ell \hat{x}^{m-k}$$

for monomial observables. The Born–Jordan and Weyl rules yield the same result only if $m < 2$ or $\ell < 2$; for instance in both cases the quantization of the product xp is $\frac{1}{2}(\hat{x}\hat{p} + \hat{p}\hat{x})$. It is however easy to find physical examples which give different results. Consider for instance the square of the z component of the angular momentum: it is given by

$$\ell_z^2 = x^2 p_y^2 + y^2 p_x^2 - 2x p_x y p_y$$

and its Weyl quantization is easily seen to be

$$\mathrm{Op}_{\mathrm{Weyl}}(\ell_z^2) = \hat{x}_x^2 \hat{p}_y^2 + \hat{x}_y^2 \hat{p}_x^2 - \tfrac{1}{2}(\hat{x}_x \hat{p}_x + \hat{p}_x \hat{x}_x)(\hat{x}_y \hat{p}_y + \hat{p}_y \hat{x}_y) \tag{5.1}$$

while its Born–Jordan quantization is the different expression

$$\mathrm{Op}_{\mathrm{BJ}}(\ell_z^2) = \hat{x}_x^2 \hat{p}_y^2 + \hat{x}_y^2 \hat{p}_x^2 - \tfrac{1}{2}(\hat{x}_x \hat{p}_x + \hat{p}_x \hat{x}_x)(\hat{x}_y \hat{p}_y + \hat{p}_y \hat{x}_y) - \tfrac{1}{6}\hbar^2. \tag{5.2}$$

(Recall that $\hbar = h/(2\pi)$ is defined as the Planck constant h divided by 2π and that the operators $\hat{x}_\eta$ and $\hat{p}_\kappa$ satisfy the canonical commutation relations $[\hat{x}_\eta, \hat{p}_\kappa] = i\hbar\delta_{\eta\kappa}$ using the spatial coordinates $\eta, \kappa \in \{x, y, z\}$ and the Kronecker delta $\delta_{\eta\kappa}$.) One of us has shown in [112] that the use of (5.2) instead of (5.1) solves the so-called "angular momentum dilemma" [66, 65]. To a general observable $a(x, p)$, the Weyl rule associates the operator

$$\mathrm{Op}_{\mathrm{Weyl}}(a) = (2\pi\hbar)^{-1} \int F_\sigma a(x,p)\mathcal{D}(x,p)\,\mathrm{d}x\,\mathrm{d}p$$

where $F_\sigma a$ is the symplectic Fourier transform of a and $\mathcal{D}(x, p)$ the displacement operator (see Sec. 5.5.1); in the Born–Jordan case this expression is replaced with

$$\mathrm{Op}_{\mathrm{BJ}}(a) = (2\pi\hbar)^{-1} \int F_\sigma a(x,p) K_{\mathrm{BJ}}(x,p)\mathcal{D}(x,p)\,\mathrm{d}x\,\mathrm{d}p$$

where the filter function $K_{\mathrm{BJ}}(x, p)$ (also known as the Cohen kernel) is given by

$$K_{\mathrm{BJ}}(x,p) = \mathrm{sinc}(\tfrac{px}{2\hbar}) = \frac{\sin(\frac{px}{2\hbar})}{px/(2\hbar)}.$$

We obtain significant, new results for the case of Born-Jordan distributions and therefore substantially advance on previous characterizations. In particular, we derive its parity operator Π_{BJ} in the form of a weighted average of geometric transformations

$$\Pi_{\mathrm{BJ}} = \tfrac{1}{4\pi\hbar} \int \mathrm{sinc}(\tfrac{px}{2\hbar})\,\mathcal{D}(x,p)\,\mathrm{d}x\,\mathrm{d}p = [\,\tfrac{1}{4}\int_{-\infty}^{\infty} \mathrm{sech}(\tfrac{\xi}{2}) S(\xi)\mathrm{d}\,\xi\,]\;\Pi,$$

where $\mathcal{D}(x, p)$ is the displacement operator and $S(\xi)$ is the squeezing operator (see Eq. (5.34) below) with a real squeezing parameter ξ. We have used the *sinus cardinalis* $\mathrm{sinc}(x) := \sin(x)/x$ and the *hyperbolic secant* $\mathrm{sech}(x) := 1/\cosh(x)$ functions. We prove in Proposition 5.2 that Π_{BJ} is a bounded operator on the Hilbert space L^2 and therefore gives rise to well-defined phase-space distribution functions of arbitrary quantum states. We derive a generalized spectral decomposition of this parity operator based on a continuous family of generalized eigenvectors that satisfy the following generalized eigenvalue equation for every real E (see Theorem 5.5):

$$\Pi_{\mathrm{BJ}}\,|\psi_\pm^E\rangle = \pm\pi/2\,\mathrm{sech}(\pi E)\,|\psi_\pm^E\rangle.$$

Facilitating a more efficient computation of the Born-Jordan distribution, we finally derive explicit matrix representations in the so-called Fock or number-state basis, which constitutes a natural representation for bosonic quantum systems such as in quantum optics [182, 108, 171]. Curiously, the parity operator Π_{BJ} of the Born-Jordan distribution is not diagonal in the Fock basis as compared to the diagonal parity operators of s-parametrized phase spaces (cf. [160]) that enable the experimental reconstruction of distribution functions from photon-count statistics [74, 180, 32, 21] in quantum optics. We calculate the matrix elements $[\Pi_{\mathrm{BJ}}]_{mn}$ in the Fock or number-state basis and provide a convenient formula for a direct recursion, for which we conjecture that the matrix elements are completely determined

by eight rational initial values. We finally illustrate our results for simple quantum states by calculating their Born-Jordan distributions and comparing them to other phase-space representations. Let us summarize the main results of the current work:

- quantum-mechanical expectation values of the parity operators Π_θ from Definition 5.3 define distribution functions as the Cohen class (Theorem 5.1);
- the parity operators Π_θ are Weyl quantizations of the corresponding Cohen convolution kernels θ (Sec. 5.6.2);
- parity operators for important distribution functions are summarized in Sec. 5.6.3 along with their operator norms (Theorem 5.2) and spectral decompositions in Sec 5.7.2;
- the Born-Jordan parity operator is a weighted average of displacements (Theorem 5.3) or equivalently a weighted average of squeezing operators (Theorem 5.4), and it is bounded (Proposition 5.2);
- the Born-Jordan parity operator admits a generalized spectral decomposition (Theorem 5.5);
- its matrix representation is calculated in the number-state basis in Theorem 5.6; and an efficient, recursion-based computation scheme is proposed in Conjecture 5.1.

We start by recalling precise definitions of distribution functions and quantum states for infinite-dimensional Hilbert spaces in Sec. 5.4. In Sec. 5.5, we discuss phase-space translations of quantum states using coherent states, state one known formulation of translated parity operators, and relate a general class of phase spaces to Wigner distribution functions and their properties. This will guide our study of phase-space representations of quantum states as expectation values of displaced parity operators in Section 5.6. We present and discuss our results for the case of the Born-Jordan distribution and its parity operator in Section 5.7. Formulas for the matrix elements of the Born-Jordan parity operator are derived in Section 5.8. Explicit examples for simple quantum systems are discussed and visualized in Section 5.9, before we conclude. A larger part of the proofs have been relegated to Appendices.

5.4 Distributions and quantum states

All of our discussion and results in this work will strongly rely on precise notions of distributions and related descriptions of quantum states in infinite-dimensional Hilbert spaces. Although most (or all) of this material is quite standard and well-known [211, 142, 113, 123], we find it prudent to shortly summarize this background material in order to fix our notation and keep our presentation self-contained. This will also help to clarify differences and connections between divergent concepts and notations used in literature. We hope this will also contribute to narrowing the gap between different physics communities that are interested in this topic.

5.4.1 Schwartz space and Fourier transforms

We will now summarize function spaces that are central to this work, refer also to [113, Ch. 1.1.3]. The set of all smooth, complex-valued functions on $\mathbb{R}^n$ that decrease faster (together with all of their partial derivatives) than the reciprocal of any polynomial is called the Schwartz space and is usually denoted by $\mathcal{S}(\mathbb{R}^n)$, refer to [211, Ch. V.3] or [142, Ch. 6]. In particular, the function $\psi(x)$ is fast decreasing if the absolute values $|x^\beta \partial_x^\alpha \psi(x)|$ are bounded for each multi-index of natural numbers $\alpha := (\alpha_1, \ldots, \alpha_n)$ and $\beta := (\beta_1, \ldots, \beta_n)$, where by definition $x^\beta := x_1^{\beta_1} \cdots x_n^{\beta_n}$ and $\partial_x^\alpha := \partial_{x_1}^{\alpha_1} \cdots \partial_{x_n}^{\alpha_n}$, refer to [113, Ch. 1.1.3].

The topological dual space $\mathcal{S}'(\mathbb{R}^n)$ of $\mathcal{S}(\mathbb{R}^n)$ is often referred to as the space of tempered distributions, and we will denote the distributional pairing for $\phi \in \mathcal{S}'(\mathbb{R}^n)$ and $\psi \in \mathcal{S}(\mathbb{R}^n)$ as $\langle \phi, \psi \rangle := \phi(\psi) \in \mathbb{C}$. In Sec. 5.4, we will consistently use the symbol ϕ to denote distributions and ψ, ψ' to denote Schwartz or square-integrable functions. Also note that $\mathcal{S}(\mathbb{R}^n)$ is dense in $L^2(\mathbb{R}^n)$ and tempered distributions naturally include the usual function spaces $\mathcal{S}(\mathbb{R}^n) \subset L^2(\mathbb{R}^n) \subset \mathcal{S}'(\mathbb{R}^n)$ via distributional pairings in the form of an integral $\langle \phi, \psi \rangle = \int_{\mathbb{R}^n} \phi^*(x)\psi(x)\, dx$, where $\phi^*(x)$ is the complex conjugate of $\phi(x) \in L^2(\mathbb{R}^n)$ or $\phi(x) \in S(\mathbb{R}^n)$. This inclusion is usually referred to as a rigged Hilbert space [100, 57] or the Gelfand triple.

For this integral pairing, one can consider functions $\phi(x)$ that (together with all of their partial derivatives) grow slower than certain polynomials. More precisely, a map $\phi : \mathbb{R}^n \to \mathbb{C}$ is said to be slowly increasing if there exist for every $\alpha = (\alpha_1, \ldots, \alpha_n)$ constants C, m, and A such that $|[\partial^{\alpha_1+\cdots+\alpha_n}/\partial_x^\alpha]\, \phi(x)| \leq C\|x\|^m$ for all $\|x\| > A$, where $\|x\|$ is the Euclidean norm in $\mathbb{R}^n$, refer to [142, Ch. 6.2]. A classical example of such functions are polynomials. In particular, every slowly increasing function $\phi(x)$ generates a tempered distribution $\langle \phi, \psi \rangle = \int_{\mathbb{R}^n} \phi^*(x)\psi(x)\, dx$ for all $\psi \in \mathcal{S}(\mathbb{R}^n)$, and, therefore, such functions are usually denoted as $\phi(x) \in \mathcal{S}'(\mathbb{R}^n)$ (refer to [142, Ch. 6.2]). This also motivates the delta distribution $\langle \delta_b, \psi \rangle := \psi(b)$ which is in its integral representation commonly written as $\int_{\mathbb{R}^n} \delta(x-b)\psi(x)\, dx = \psi(b)$. We emphasize that the notation $\delta(x)$ is however only formal, cf. [211, Eq. (V.3)].

Recall that the symplectic Fourier transform $[F_\sigma a(\cdot)](x,p)$ (see App. B in [113]) of a phase-space distribution function $a(x,p)$ is related to the usual Fourier transform

$$[Fa(\cdot)](x,p) := (2\pi\hbar)^{-1} \int e^{-\frac{i}{\hbar}(x'p+xp')} a(x',p')\, \mathrm{d}x'\, \mathrm{d}p',$$

up to a coordinate reflection $[F_\sigma a(\cdot)](x,p) = [Fa(\cdot)](x,-p)$ where

$$[F_\sigma a(\cdot)](x,p) := (2\pi\hbar)^{-1} \int e^{\frac{i}{\hbar}(x'p-xp')} a(x',p')\, \mathrm{d}x'\, \mathrm{d}p'. \tag{5.3}$$

The square $[F_\sigma F_\sigma a](x,p) = a(x,p)$ is equal to the identity. Note that the Fourier transform of every function in $\mathcal{S}(\mathbb{R}^n)$ is also in $\mathcal{S}(\mathbb{R}^n)$, cf. [211, Ch. 6.3]. This allows us to define Fourier transforms of tempered distributions via the distributional pairing of the form $\langle F_\sigma \phi, \psi \rangle = \langle \phi, F_\sigma \psi \rangle$. The delta distribution can therefore be identified formally via the brackets $\langle \delta_0, F_\sigma \psi \rangle = [F_\sigma \psi](0) = \langle 1, \psi \rangle$ as the Fourier transform $\delta(x) = (2\pi\hbar)^{-1} F_\sigma[1]$ of the constant function, refer to [142, Ch. 6.4].

5.4.2 Quantum states and expectation values

Let us denote the abstract state vector of a quantum system by $|\psi\rangle$ which is an element of an abstract, infinite-dimensional, separable complex Hilbert space (here and henceforth denoted by) $\mathcal{H}$. The Hilbert space $\mathcal{H}$ is known as the state space and it is equipped with a scalar product $\langle\,\cdot\,|\,\cdot\,\rangle$ [123]. Considering projectors $\mathcal{P}_\psi := |\psi\rangle\langle\psi|$ defined via the open scalar products $\mathcal{P}_\psi = \langle\psi|\,\cdot\,\rangle\,|\psi\rangle$, an orthonormal basis of $\mathcal{H}$ is given by $\{|\phi_n\rangle, n \in \mathbb{N}\}$ if $\langle\phi_n|\phi_m\rangle = \delta_{nm}$ for all $m, n \in \mathbb{N}$ and $\sum_{n=0}^{\infty} \mathcal{P}_{\phi_n} = \mathrm{Id}$ in the strong operator topology. For a broader introduction to this topic we refer to [123].

Depending on the given quantum system, explicit representations of the state space can be obtained by specifying its Hilbert space [102]. In the case of bosonic systems, the Fock (or number-state) representation is widely used. A quantum state $|\psi\rangle$ is an element of the Hilbert space $\ell^2(\mathbb{C})$ of square-summable sequences [123], characterized by its expansion $|\psi\rangle = \sum_{n=0}^{\infty} \psi_n |n\rangle$ into the orthonormal Fock basis $\{|n\rangle, n = 0, 1, \dots\}$ of number states using the expansion coefficients $\psi_n = \langle n|\psi\rangle \in \mathbb{C}$, refer to, e.g., [51] and [123, Ch. 11]. The scalar product $\langle\psi|\psi'\rangle$ then corresponds to the usual scalar product of vectors, i.e. to the convergent sum $\sum_{n=0}^{\infty} (\psi_n)^* \psi'_n =: \langle\psi|\psi'\rangle_{\ell^2}$. The corresponding norm of vectors is then given by $||\psi||_{\ell^2} = ||(|\psi\rangle)||_{\ell^2} = [\langle\psi|\psi\rangle_{\ell^2}]^{1/2}$.

For a quantum state $|\psi\rangle$, the coordinate representation $\psi(x) \in \mathcal{S}(\mathbb{R})$ and its Fourier transform (or momentum representation) $\psi(p) \in \mathcal{S}(\mathbb{R})$ are given by complex, square-integrable, and smooth functions that are also fast decreasing. The quantum state $|\psi\rangle = \int_{\mathbb{R}} \psi(x)|x\rangle\,\mathrm{d}x$ of $\psi(x) = \langle x|\psi\rangle$ is then defined via coordinate eigenstates[1] $|x\rangle$. The coordinate representation of a coordinate eigenstate is given by the distribution $\delta(x'-x) \in \mathcal{S}'(\mathbb{R})$, refer to [123, 102]. The scalar product $\langle\psi|\psi'\rangle$ is then fixed by the usual L^2 scalar product, i.e. by the convergent integral $\int_{\mathbb{R}} \psi^*(x)\psi'(x)\,\mathrm{d}x =: \langle\psi|\psi'\rangle_{L^2}$. This integral induces the norm of square-integrable functions via $||\psi(x)||_{L^2} = [\langle\psi|\psi\rangle_{L^2}]^{1/2}$.

The above two examples are particular representations of the state space, which are convenient for particular physical systems, however these representations are equivalent via

$$\mathcal{H} \simeq \ell^2(\mathbb{C}) \simeq L^2(\mathbb{R}, \mathrm{d}x) \simeq L^2(\mathbb{R}, \mathrm{d}p), \tag{5.4}$$

refer to Theorem 2 in [102]. In particular, any coordinate representation $\psi(x) \in \mathcal{S}(\mathbb{R})$ of a quantum state $|\psi\rangle$ can be expanded in the number-state basis into $\psi(x) = \sum_{n=1}^{\infty} \psi_n\, \psi_n^{\mathrm{Fock}}(x)$ via $\psi_n = \int_{\mathbb{R}} [\psi_n^{\mathrm{Fock}}(x)]^*(x)\psi(x)\,\mathrm{d}x$ where $\psi_n^{\mathrm{Fock}}(x) \in \mathcal{S}(\mathbb{R})$ are eigenfunctions of the quantum-harmonic oscillator. For any $\psi(x), \psi'(x) \in \mathcal{S}(\mathbb{R})$, the L^2 scalar product is equivalent to the ℓ^2 scalar product

$$\int_{\mathbb{R}} \psi^*(x)\psi'(x)\,\mathrm{d}x = \sum_{n,m=1}^{\infty} \psi_n^* \psi'_m \int_{\mathbb{R}} [\psi_n^{\mathrm{Fock}}(x)]^* \psi_m^{\mathrm{Fock}}(x)\,\mathrm{d}x = \sum_{n=1}^{\infty} \psi_n^* \psi'_n, \tag{5.5}$$

[1] For the position operator $\hat{x} : \mathcal{S}(\mathbb{R}) \to \mathcal{S}(\mathbb{R}), \psi(x) \mapsto x\psi(x)$ one can consider the dual $\hat{x}' : \mathcal{S}'(\mathbb{R}) \to \mathcal{S}'(\mathbb{R}), \phi \mapsto \phi \circ \hat{x}$. This map satisfies the generalized eigenvalue equation $\hat{x}'|x_0\rangle = x_0|x_0\rangle$ for all $x_0 \in \mathbb{R}$ where its generalized eigenvector $|x_0\rangle \in \mathcal{S}'(\mathbb{R})$ is the delta distribution, which allows for the resolution of the position operator $\hat{x} = \int_{\mathbb{R}} x|x\rangle\langle x|\,\mathrm{d}x$. For more on this topic we refer to [100] or [102, p.1906].

and it is invariant with respect to the choice of orthonormal basis, i.e. any two orthonormal bases are related via a unitary transformation. The equivalence $L^2(\mathbb{R}, \mathrm{d}x) \simeq L^2(\mathbb{R}, \mathrm{d}p)$ follows from the Plancherel formula $\int_{\mathbb{R}} \psi^*(x)\psi'(x)\,\mathrm{d}x = \int_{\mathbb{R}} \psi^*(p)\psi'(p)\,\mathrm{d}p$.

In the following, we will consistently use the notation $\langle \cdot | \cdot \rangle$ for scalar products in Hilbert space, without specifying the type of representation. This is motivated by the invariance of the scalar product under the choice of representation. However, in order to avoid confusion with different types of operator or Euclidean norms, in the following we will use the explicit norms $\|\psi(x)\|_{L^2}$ and $\||\psi\rangle\|_{\ell^2}$, despite their equivalence.

We will now shortly define the trace of operators on infinite-dimensional Hilbert spaces, refer to [211, Ch.VI.6] for a comprehensive introduction. Recall that the trace of a positive semi-definite operator[2] $A \in \mathcal{B}(\mathcal{H})$ is defined via $\mathrm{Tr}(A) = \sum_{n=1}^{\infty} \langle \psi_n | A | \psi_n \rangle$, where the sum of non-negative numbers on the right-hand side is independent of the chosen orthonormal basis $\{|\psi_n\rangle\,,\, n \in \mathbb{N}\}$ of $\mathcal{H}$, but it does not necessarily converge. Recall that the set of trace-class operators is given by

$$\mathcal{B}^1(\mathcal{H}) := \{A \in \mathcal{B}(\mathcal{H}) \,|\, \mathrm{Tr}(\sqrt{A^\dagger A}) < \infty\} \subseteq \mathcal{K}(\mathcal{H}),$$

where $\mathcal{K}(\mathcal{H})$ denotes the set of compact operators on $\mathcal{H}$ and $A^\dagger$ is the adjoint of A (which is in finite dimensions given by the complex conjugated and transposed matrix). Every $A \in \mathcal{B}^1(\mathcal{H})$ has a finite trace via the absolutely convergent sum (of not necessarily positive numbers) $\mathrm{Tr}(A) := \sum_{n=1}^{\infty} \langle \psi_n | A | \psi_n \rangle$. For $A \in \mathcal{B}^1(\mathcal{H})$, the mapping $A \mapsto \mathrm{Tr}(A)$ is linear, continuous with respect to the trace norm and independent of the chosen orthonormal basis of $\mathcal{H}$. Trace-class operators $A \in \mathcal{B}^1(\mathcal{H})$ have the important property that their products with bounded operators $B \in \mathcal{B}(\mathcal{H})$ are also in the trace class, i.e. $AB, BA \in \mathcal{B}^1(\mathcal{H})$. Using this definition, one can calculate the trace independently from the choice of the orthonormal basis or representation that is used for evaluating scalar products.

A density operator or state $\rho \in \mathcal{B}^1(\mathcal{H})$ is defined to be positive semi-definite with $\mathrm{Tr}(\rho) = 1$. It therefore admits a spectral decomposition [190, Prop. 16.2], i.e. there exists an orthonormal system $\{|\psi_n\rangle, n \in \mathbb{N}\}$ in $\mathcal{H}$ such that

$$\rho := \sum_{n=1}^{\infty} p_n |\psi_n\rangle\langle\psi_n| \,. \tag{5.6}$$

The probabilities $\{p_n, n \in \mathbb{N}\}$ satisfy $p_1 \geq p_2 \geq \ldots \geq 0$ and $\sum_{n=1}^{\infty} p_n = 1$. Expectation values of observables are computed via the trace $\langle O \rangle_\rho = \mathrm{Tr}(\rho O) = \sum_{n=1}^{\infty} p_n \langle \psi_n | O | \psi_n \rangle$ where $O \in \mathcal{B}(\mathcal{H})$ is hermitian. The following is a simple consequence of, e.g., [190, Lemma 16.23].

[2] Here, $\mathcal{B}(\mathcal{H})$ denotes the set of bounded linear operators on $\mathcal{H}$, and one has $|\langle x|A|y\rangle| < \infty$ for every $A \in \mathcal{B}(\mathcal{H})$ and $x, y \in \mathcal{H}$. An operator $A \in \mathcal{B}(\mathcal{H})$ is said to be positive semi-definite if A is self-adjoint and $\langle x, Ax \rangle \geq 0$ for all $x \in \mathcal{H}$.

Lemma 5.1. *The expectation value of an observable O in a mixed quantum state is upper bounded by the operator norm $|\mathrm{Tr}(\rho O)| \leq ||O||_{\sup}$ for arbitrary density operators ρ, where we have used the definition $||O||_{\sup} := \sup_{||(|\psi\rangle)||_{\ell^2}=1} ||O|\psi\rangle||_{\ell^2}$ for the Hilbert space ℓ^2. Equivalently, one can use the definition $||O||_{\sup} := \sup_{||\psi(x)||_{L^2}=1} ||O\psi(x)||_{L^2}$ for square-integrable functions $\psi(x)$.*

5.5 Coherent states, phase spaces, and parity operators

We continue to fix our notation by discussing an abstract definition of phase spaces that relies on displaced parity operators. This usually appears concretely in terms of coherent states [47, 205, 99, 174], for which we consider two equivalent but equally important parametrizations of the phase space using the coordinates α or (x, p) (see below). This definition of phase spaces can be also related to convolutions of Wigner functions which is usually known as the Cohen class [113, 59, 60]. We also recall important postulates for Wigner functions as given by Stratanovich [243, 47] and these will be later considered in the context of general phase spaces.

5.5.1 Phase-space translations of quantum states

We will now recall a definition of the phase space for quantum-mechanical systems via coherent states, refer to [47, 205, 99, 174]. We consider a quantum system which has a specific dynamical symmetry group given by a Lie group G. The Lie group G acts on the Hilbert space $\mathcal{H}$ using an irreducible unitary representation $\mathcal{D}$ of G. By choosing a fixed reference state as an element $|0\rangle \in \mathcal{H}$ of the Hilbert space, one can define a set of coherent states as $|g\rangle := \mathcal{D}(g)|0\rangle$ where $g \in G$. Considering the subgroup $H \subseteq G$ of elements $h \in H$ that act on the reference state only by multiplication $\mathcal{D}(h)|0\rangle := e^{i\phi}|0\rangle$ with a phase factor $e^{i\phi}$, any element $g \in G$ can be decomposed into $g = \Omega h$ with $\Omega \in G/H$. The phase space is then identified with the set of coherent states $|\Omega\rangle := \mathcal{D}(\Omega)|0\rangle$. In the following, we will consider the Heisenberg-Weyl group H_3, for which the phase space $\Omega \in H_3/U(1)$ is a plane. We introduce the corresponding displacement operators that generate translations of the plane.

In particular, for harmonic oscillator systems, the phase space $\Omega \equiv \alpha \in \mathbb{C}$ is usually parametrized by the complex eigenvalues α of the annihilation operator a and Glauber coherent states can be represented explicitly [51] in the so-called Fock (or number-state) basis as

$$|\alpha\rangle = e^{-|\alpha|^2/2} \sum_{n=0}^{\infty} \frac{\alpha^n}{\sqrt{n!}} |n\rangle = e^{\alpha\hat{a}^\dagger - \alpha^*\hat{a}}|0\rangle =: \mathcal{D}(\alpha)|0\rangle. \tag{5.7}$$

Here, the second equality specifies the displacement operator $\mathcal{D}(\alpha)$ as a power series of the usual bosonic annihilation $\hat{a}$ and creation $\hat{a}^\dagger$ operators, which satisfy the commutation relation $[\hat{a}, \hat{a}^\dagger] = 1$, refer to Eq. (2.11) in [51]. In particular, the number state representation

of displacements is given by [51]

$$[\mathcal{D}(\alpha)]_{mn} := \langle m|\mathcal{D}(\alpha)|n\rangle = (\tfrac{n!}{m!})^{1/2}\alpha^{m-n}e^{-|\alpha|^2/2}L_n^{(m-n)}(|\alpha|^2), \tag{5.8}$$

where $L_n^{(m-n)}(x)$ are generalized Laguerre polynomials. This is the usual formulation for bosonic systems (e.g., in quantum optics) [171], where the optical phase space is the complex plane and the phase-space integration measure is given by $\mathrm{d}\Omega = 2\hbar\,\mathrm{d}^2\alpha = 2\hbar\,\mathrm{d}\Re(\alpha)\mathrm{d}\Im(\alpha)$ (where one often sets $h = 2\pi\hbar = 1$, cf., [51, 50, 47]). The annihilation operator admits a simple decomposition

$$\hat{a} = 2\hbar\int_{-\infty}^{\infty}\int_{-\infty}^{\infty}\alpha\,|\alpha\rangle\langle\alpha|\,\mathrm{d}\Re(\alpha)\mathrm{d}\Im(\alpha)$$

with respect to its eigenvectors, see, e.g., [51, Eqs. (2.21)-(2.27)].

Let us now consider the coordinate representation $\psi(x) \in \mathcal{S}(\mathbb{R})$ of a quantum state. The phase space is parametrized by $\Omega \equiv (x,p) \equiv z \in \mathbb{R}^2$ and the integration measure is $\mathrm{d}\Omega = \mathrm{d}z = \mathrm{d}x\,\mathrm{d}p$. The action of the displacement operator is given by

$$\mathcal{D}(x_0,p_0)\psi(x) := e^{\frac{i}{\hbar}(p_0x-\frac{1}{2}p_0x_0)}\psi(x-x_0) = e^{-\frac{i}{\hbar}(x_0\hat{p}-p_0\hat{x})}\psi(x), \tag{5.9}$$

where $x, x_0, p_0 \in \mathbb{R}$. The right hand side of Eq. (5.9) specifies the displacement operator as a power series of the usual $\hat{x}$ and $\hat{p}$ operators, which satisfy the commutation relation $[\hat{x},\hat{p}] = i\hbar$, refer to [113, Def. 2]. The most common representations of these two unbounded operators are $\hat{x}\psi(x) = x\psi(x)$ and $\hat{p}\psi(x) = -i\hbar\partial\psi(x)/\partial x$. Displacements of tempered distributions $\phi(x) \in \mathcal{S}'(\mathbb{R})$ are understood via the distribution pairings $\langle\phi|\mathcal{D}(\Omega)\psi\rangle = \langle\mathcal{D}^\dagger(\Omega)\phi|\psi\rangle$ as integrals from Section 5.4.1 (cf. Eq. (1.11) in [113]).

The two (above mentioned) physically motivated examples are particular representations of the displacement operator for the Heisenberg-Weyl group in different Hilbert spaces while relying on different parametrizations of the phase space. Let us now highlight the equivalence of these two representations. In particular, we obtain the formulas $\hat{a}_\lambda = (\lambda\hat{x} + i\lambda^{-1}\hat{p})/\sqrt{2\hbar}$ and $\hat{a}_\lambda^\dagger = (\lambda\hat{x} - i\lambda^{-1}\hat{p})/\sqrt{2\hbar}$ for any non-zero real λ, refer to Eqs. (2.1-2.2) in [51]. In the context of quantum optics, the operators $\hat{x}$ and $\hat{p}$ are the so-called optical quadratures [171]. The operators $\hat{a}_\lambda$ and $\hat{a}_\lambda^\dagger$ are now defined on the Hilbert space L^2, whereas $\hat{a}$ and $\hat{a}^\dagger$ act on elements of the Hilbert space ℓ^2. For any $\lambda \neq 0$ they reproduce the commutator $[\hat{a}_\lambda,\hat{a}_\lambda^\dagger] = \mathrm{id}_{L^2}$, i.e. $[\hat{a}_\lambda,\hat{a}_\lambda^\dagger]\,\psi(x) = \psi(x)$ for all $\psi(x) \in L^2(\mathbb{R})$, and they correspond to raising and lowering operators of the quantum harmonic-oscilator[3] eigenfunctions $\psi_n^{\mathrm{Fock}}(x)$, refer to [123]. Substituting now $\hat{x} = \sqrt{\hbar/2}\lambda^{-1}(\hat{a}_\lambda+\hat{a}_\lambda^\dagger)$ and $\hat{p} = -i\sqrt{\hbar/2}\lambda(\hat{a}_\lambda-\hat{a}_\lambda^\dagger)$ into the exponent on the right-hand side of (5.9) yields

$$-\tfrac{i}{\hbar}(x_0\hat{p} - p_0\hat{x}) = \hat{a}_\lambda^\dagger(x_0\lambda + i\lambda^{-1}p_0)/\sqrt{2\hbar} - \hat{a}_\lambda(x_0\lambda - i\lambda^{-1}p_0)/\sqrt{2\hbar}.$$

[3] For example, the choice $\lambda = \sqrt{m\omega}$ corresponds to the quantum-harmonic oscillator of mass m and angular frequency ω. And $\lambda = \sqrt{\epsilon\omega}$ is related to a normal mode of the electromagnetic field in a dielectric.

This then confirms the equivalence

$$\mathcal{D}(x_0,p_0)\psi(x) = e^{-\frac{i}{\hbar}(x_0\hat{p}-p_0\hat{x})}\psi(x) = e^{\hat{a}_\lambda^\dagger\alpha-\hat{a}_\lambda\alpha^*}\psi(x) = \mathcal{D}(\alpha)\psi(x), \tag{5.10}$$

where the phase-space coordinate α is defined by $\alpha := (x_0\lambda + i\lambda^{-1}p_0)/\sqrt{2\hbar}$. Note that the corresponding phase-space element is then $\mathrm{d}\Omega = 2\hbar\,\mathrm{d}\Re(\alpha)\mathrm{d}\Im(\alpha) = \mathrm{d}x\,\mathrm{d}p$ which is independent of the choice of λ.

In the following, we will use both of the phase-space coordinates α and (x,p) interchangeably. The displacement operator is obtained in both parametrizations, and they are equivalent via (5.10). Motivated by the group definition, we will also use the parametrization Ω for the phase space via $\mathcal{D}(\Omega)$, where Ω corresponds to any representation of the group, including the ones given by the coordinates α and (x,p).

5.5.2 Phase-space reflections and the Grossmann-Royer operator

Recall that the parity operator Π reflects wave functions via $\Pi\psi(x) := \psi(-x)$ and $\Pi\psi(p) := \psi(-p)$ for coordinate-momentum representations [119, 217, 113, 34, 175] and $\Pi|\Omega\rangle := |-\Omega\rangle$ for phase-space coordinates of coherent states [50, 217, 34, 175]. This parity operator is obtained as a phase-space average

$$\Pi := (4\pi\hbar)^{-1}\int \mathcal{D}(\Omega)\,\mathrm{d}\Omega = \tfrac{1}{2}\left\{F_\sigma[\mathcal{D}(\cdot)](\Omega)\right\}|_{\Omega=0} \tag{5.11}$$

of displacements, where the second equality follows from the symplectic Fourier transform of the displacement operator from (5.9) at the phase-space point $\Omega = 0$.

The symplectic Fourier transform of the displacement operator from Eq. (5.9) is the so-called Grossmann-Royer operator

$$\tfrac{1}{2}F_\sigma[\mathcal{D}(\cdot)](-\Omega) = \mathcal{D}(\Omega)\Pi\mathcal{D}^\dagger(\Omega), \tag{5.12}$$

which is the parity operator transformed by the displacement operator [119, 217, 113, 175, 34]. Here, we use in both (5.11) and (5.12) an abbreviated notation for formal integral transformations of the displacement operator. These integral transformations and the symplectic Fourier transform are more precisely given as in (5.9) via their action

$$\Pi\phi(x) := (4\pi\hbar)^{-1}\int \mathcal{D}(\Omega)\phi(x)\,\mathrm{d}\Omega = \tfrac{1}{2}\left\{F_\sigma[\mathcal{D}(\cdot)\phi(x)](\Omega)\right\}|_{\Omega=0}$$

on any element $\phi(x) \in \mathcal{S}'(\mathbb{R})$. This also matches the notation in [113, Prop. 8]. In the following, we will consistently use this abbreviated notation for formal integral transformations of the displacement operator, i.e. by dropping $\phi(x)$.

5.5.3 Wigner function and the Cohen class

The Wigner function $W_\psi(x,p)$ of a pure quantum state $|\psi\rangle$ was originally defined by Wigner in 1932 [262] and it is (in modern terms) the integral transformation of a pure state $\psi(x) \in$

$\mathcal{S}(\mathbb{R})$, i.e.

$$W_\psi(x,p) = (2\pi\hbar)^{-1}\int e^{-\frac{i}{\hbar}py}\psi^*(x-\tfrac{1}{2}y)\psi(x+\tfrac{1}{2}y)\,\mathrm{d}y$$
$$= (\pi\hbar)^{-1}\langle\psi|\,\mathcal{D}(x,p)\Pi\mathcal{D}^\dagger(x,p)|\psi\rangle = (\pi\hbar)^{-1}\,\mathrm{Tr}\left[\,(|\psi\rangle\langle\psi|)\,\mathcal{D}(\Omega)\Pi\mathcal{D}^\dagger(\Omega)\right].$$

The second and third equalities specify the Wigner function using the Grossmann-Royer operator [119, 113] from (5.12), refer to [113, Def. 12]. We use this latter form to extend the definition of the Wigner function to mixed quantum states as in [50, 11, 217, 34].

Definition 5.1. The Wigner function $W_\rho(\Omega) \in L^2(\mathbb{R}^2)$ of an infinite-dimensional density operator (or quantum state) $\rho = \sum_n p_n|\psi_n\rangle\langle\psi_n| \in \mathcal{B}^1(\mathcal{H})$ is proportional to the quantum-mechanical expectation value

$$W_\rho(\Omega) := (\pi\hbar)^{-1}\,\mathrm{Tr}\left[\,\rho\,\mathcal{D}(\Omega)\Pi\mathcal{D}^\dagger(\Omega)\right] = \sum_n p_n W_{\psi_n}(\Omega) \tag{5.13}$$

of the Grossmann-Royer operator from (5.12), which is the parity operator Π transformed by the displacement operator $\mathcal{D}(\Omega)$, refer also to [50, 11, 217, 34, 175, 113].

The square integrable cross-Wigner transform $W(\psi,\psi')(\Omega) \in L^2(\mathbb{R}^2)$ of two functions $\psi,\psi' \in L^2(\mathbb{R})$ used in time-frequency analysis [113, 111] is obtained via the trace-class operator $A = |\psi\rangle\langle\psi'|$ in the form $W(\psi,\psi')(\Omega) := W_A(\Omega)$. The Wigner representation is in general a bijective, linear mapping between the set of density operators (or, more generally, the trace-class operators) and the phase-space distribution functions W_ρ that satisfy the so-called Stratonovich postulates [243, 47]:

Postulate (i): $\rho \mapsto W_\rho$ is one-to-one (linearity),
Postulate (ii): $W_{\rho^\dagger} = W_\rho^*$ (reality),
Postulate (iiia): $\mathrm{Tr}(\rho) = \int W_\rho\,\mathrm{d}\Omega$ (normalization),
Postulate (iiib): $\mathrm{Tr}(A^\dagger\rho) = \int a^*\,W_\rho\,\mathrm{d}\Omega$ (traciality),
Postulate (iv): $W_{\mathcal{D}(\Omega')\rho}(\Omega) = W_\rho(\Omega-\Omega')$ (covariance).

The not necessarily bounded[4] operator A is the Weyl quantization of the phase-space function (or distribution) $a(\Omega) \in \mathcal{S}'(\mathbb{R}^2)$, refer to Sec. 5.6.2. Based on these postulates, the Wigner function was defined for phase-spaces of quantum systems with different dynamical symmetry groups via coherent states [205, 99, 47, 248, 159, 160]. Let us finally recall the definition of the Cohen class for density operators following [113, Def. 93] or [60]. We define the convolution

$$a * \psi = 2\pi\hbar F_\sigma[(F_\sigma a)\,(F_\sigma\psi)] \tag{5.14}$$

[4] For unbounded operators one has to at least ensure that A is defined on the range of $\rho = \sum_n p_n|\phi_n\rangle\langle\phi_n|$, i.e. $\mathrm{range}(\rho) \subseteq D(A)$ where $D(A)$ denotes the domain of A. Then formally $\mathrm{Tr}(A^\dagger\rho) := \mathrm{Tr}(\rho A)^* := (\sum_n p_n\langle\phi_n|A|\phi_n\rangle)^*$, but this sum does in general not converge. However, by relying on so-called Schwartz operators and their dual space from [148] one can address these technical difficulties.

of a fast decreasing phase-space function $\psi \in \mathcal{S}(\mathbb{R}^2)$ and a distribution $a \in \mathcal{S}'(\mathbb{R}^2)$.

Definition 5.2. The Cohen class is the set of all linear mappings from density operators to phase-space distributions that are related to the Wigner function via a convolution $\rho \mapsto \theta(\Omega) * W_\rho(\Omega)$ from (5.14). The convolution kernel is a function (or tempered distribution) $\theta(\Omega) \in \mathcal{S}'(\mathbb{R}^2)$ and so are the elements $\theta(\Omega) * W_\rho(\Omega) \in \mathcal{S}'(\mathbb{R}^2)$ of the Cohen class.

5.6 Parity operators and their relation to quantization

5.6.1 Phase-space distribution functions via parity operators

We propose a definition for phase-space distributions and the Cohen class based on parity operators, the explicit form of which will be calculated below. A similar form has already appeared in the context of quantum optics for the so-called s-parametrized distribution functions, see, e.g., [50, 194]. In particular, an explicit form of a parity operator that requires no integral-transformation appeared in (6.22) of [51], including its eigenvalue decomposition which was later rederived in the context of measurement probabilities in [194], refer also to [217, 175]. Apart from those results, mappings between density operators and their phase-space distribution functions have been established only in terms of integral transformations of expectation values, as in [50, 10, 11].

Definition 5.3. We define a general class of phase-space distribution functions, denoted as $F_\rho(\Omega, \theta)$ and indexed by θ, as a linear mapping from the density operator $\rho \in \mathcal{B}^1(\mathcal{H})$ to $F_\rho(\Omega, \theta)$ in the form of the quantum-mechanical expectation value

$$F_\rho(\Omega, \theta) := (\pi\hbar)^{-1} \operatorname{Tr}\left[\, \rho\, \mathcal{D}(\Omega) \Pi_\theta \mathcal{D}^\dagger(\Omega)\right] \tag{5.15}$$

of a displaced parity operator Π_θ that is defined by the relation

$$\Pi_\theta := (4\pi\hbar)^{-1} \int K_\theta(\Omega) \mathcal{D}(\Omega)\, \mathrm{d}\Omega \tag{5.16}$$

using the filter function $K_\theta(\Omega)$.

Properties of $K_\theta(\Omega)$ will be discussed below. Note that the distribution function $F_\rho(\Omega, \theta)$ might have singularities depending on the integrability of its filter function $K_\theta(\Omega)$, where one well-known case is given by the Glauber P function. First, let us relate these distribution functions to the Cohen class [113, Ch. 8] by considering filter functions $K_\theta(\Omega)$ as Fourier transforms of some function or tempered distribution θ.

Theorem 5.1. *If there exists a function or tempered distribution $\theta(\Omega) \in \mathcal{S}'(\mathbb{R}^2)$, such that its symplectic Fourier transform is $K_\theta(\Omega) = 2\pi\hbar[F_\sigma\theta(\cdot)](-\Omega)$, then the corresponding phase-space distribution function $F_\rho(\Omega,\theta) \in \mathcal{S}'(\mathbb{R}^2)$ is an element of the Cohen class. In particular, $F_\rho(\Omega,\theta)$ is related to the Wigner function $W_\rho(\Omega)$ via the convolution*

$$F_\rho(\Omega,\theta) = \theta(\Omega) * W_\rho(\Omega), \tag{5.17}$$

and the convolution kernel $\theta(\Omega) \in \mathcal{S}'(\mathbb{R}^2)$ is the symplectic Fourier transform of the filter function $\theta(\Omega) = (2\pi\hbar)^{-1}[F_\sigma K(\cdot)](-\Omega)$ from Eq. (5.16)*. In analogy to* (5.12)*, one has the equivalence*

$$\mathcal{D}(\Omega)\Pi_\theta\mathcal{D}^\dagger(\Omega) = \tfrac{1}{2}F_\sigma[K_\theta(\cdot)\mathcal{D}(\cdot)](-\Omega). \tag{5.18}$$

Proof. The Wigner function from Eq. (5.13) is transformed into the form $\theta(\Omega) * W_\rho(\Omega) = (\pi\hbar)^{-1}\,\mathrm{Tr}\,[\,\rho\,\theta(\Omega) * [\mathcal{D}(\Omega)\Pi\mathcal{D}^\dagger(\Omega)]]$, where the Grossmann-Royer operator is convolved with the kernel function. Applying (5.12) yields

$$\theta(\Omega) * [\mathcal{D}(\Omega)\Pi\mathcal{D}^\dagger(\Omega)] = \theta(\Omega) * [\tfrac{1}{2}F_\sigma\mathcal{D}(\cdot)](-\Omega) = \pi\hbar F_\sigma[[F_\sigma\theta(\cdot)](\cdot)\mathcal{D}^\vee(\cdot)](\Omega), \tag{5.19}$$

where the second equality uses the convolution property $a * b = 2\pi\hbar F_\sigma[(F_\sigma a)\,(F_\sigma b)]$ of Fourier transforms from (5.14), $\mathcal{D}^\vee(\Omega) = \mathcal{D}(-\Omega)$, and the fact that the square of symplectic Fourier transforms is given the identity $F_\sigma F_\sigma K_\theta(-\Omega) = K_\theta(-\Omega)$. The left-hand side of (5.19) is related formally to (5.15) via

$$(\pi\hbar)^{-1}\mathrm{Tr}\,[\,\rho\,\theta(\Omega) * [\mathcal{D}(\Omega)\Pi\mathcal{D}^\dagger(\Omega)]] = F_\rho(\Omega,\theta) = (\pi\hbar)^{-1}\,\mathrm{Tr}\,[\,\rho\,\mathcal{D}(\Omega)\Pi_\theta\mathcal{D}^\dagger(\Omega)],$$

which results in the formal equality $\theta(\Omega) * [\mathcal{D}(\Omega)\Pi\mathcal{D}^\dagger(\Omega)] = \mathcal{D}(\Omega)\Pi_\theta\mathcal{D}^\dagger(\Omega)$. After substituting the formula $F_\sigma\theta(\Omega) = (2\pi\hbar)^{-1}F_\sigma F_\sigma K_\theta(-\Omega) = (2\pi\hbar)^{-1}K_\theta(-\Omega)$ to the right-hand side of (5.19), which uses $\theta(\Omega) = (2\pi\hbar)^{-1}[F_\sigma K(\cdot)](-\Omega)$ and the fact that the square of symplectic Fourier transforms is equal to $F_\sigma F_\sigma K_\theta(-\Omega) = K_\theta(-\Omega)$, one obtains

$$\theta(\Omega) * [\mathcal{D}(\Omega)\Pi\mathcal{D}^\dagger(\Omega)] = \mathcal{D}(\Omega)\Pi_\theta\mathcal{D}^\dagger(\Omega) = \tfrac{1}{2}F_\sigma[K_\theta^\vee(\cdot)\mathcal{D}^\vee(\cdot)](\Omega) \tag{5.20}$$

$$= \tfrac{1}{2}F_\sigma[K_\theta(\cdot)\mathcal{D}(\cdot)](-\Omega), \tag{5.21}$$

where $K_\theta^\vee(\Omega) = K_\theta(-\Omega)$ and $\mathcal{D}^\vee(\Omega) = \mathcal{D}(-\Omega)$. The symplectic Fourier transform from (5.3) at the phase-space point $\Omega = 0$ reduces to

$$\Pi_\theta = [\mathcal{D}(\Omega)\Pi_\theta\mathcal{D}^\dagger(\Omega)]|_{\Omega=0} = \tfrac{1}{2}F_\sigma[K_\theta(\cdot)\mathcal{D}(\cdot)]|_{\Omega=0} = (4\pi\hbar)^{-1}\int K_\theta(\Omega)\mathcal{D}(\Omega)\,\mathrm{d}\Omega$$

the integral after the third equality and reproduces (5.16) which concludes the proof. □

The construction of a particular case of phase-space distribution functions was detailed in [11], where the term "filter function" also appeared in the context of mapping operators.

Property	Description	Requirement
Cohen class	Definition 5.2	K_θ is a function or tempered distribution
Boundedness	$\lvert F_\rho(\Omega,\theta)\rvert$ is bounded	Π_θ is bounded in $\lVert\Pi_\theta\rVert_{\sup}$
Square integrability	$F_\rho(\Omega,\theta) \in L^2(\mathbb{R}^2)$	$\lvert K_\theta(\Omega)\rvert$ is bounded
Linearity	$\rho \mapsto F_\rho(\Omega,\theta)$ is linear	by definition
Covariance	$\mathcal{D}(\Omega')\rho\mathcal{D}^\dagger(\Omega') \mapsto F_\rho(\Omega-\Omega',\theta)$	by definition
Rotations	covariance under rotations	K_θ is invariant under rotations
Reality	$\rho^\dagger \mapsto F_\rho^*(\Omega,\theta)$	Symmetry $K_\theta^*(-\Omega) = K_\theta(\Omega)$
Traciality	$\mathrm{Tr}\,[\rho] \mapsto \int F_\rho(\Omega,\theta)\,\mathrm{d}\Omega$	$[K_\theta(\Omega)]\rvert_{\Omega=0} = 1$
Marginal condition	$\lvert\psi(x)\rvert^2$ and $\lvert\psi(p)\rvert^2$ are recovered	$[K_\theta(x,p)]\rvert_{p=0} = [K_\theta(x,p)]\rvert_{x=0} = 1$

Table 5.1: Properties of phase-space distribution functions from Definition 5.3.

However, these filter functions were restricted to non-zero, analytic functions. Definition 5.3 extends these cases to the Cohen class via Theorem 5.1 which allows for more general phase spaces. For example, the filter function of the Born-Jordan distribution has zeros (see Theorem 5.3 below), and is therefore not covered by [11].

Most of the well-known distribution functions are elements of the Cohen class. We calculate important special cases in Sec. 5.6.3. The Born-Jordan distribution and its parity operator are detailed in Sec. 5.7. In the following, we detail important properties of $F_\rho(\Omega,\theta)$ and their relation to properties of $K_\theta(\Omega)$ and Π_θ. These properties will guide our discussion of parity operators and this allows us to compare the Born-Jordan distribution to other phase spaces. Table 5.1 provides a summary of these properties and the proofs have been deferred to Appendix D.1.

Property 5.1. Boundedness: The phase-space distribution function $F_\rho(\Omega,\theta)$ is bounded in its absolute value, i.e. $\pi\hbar\,\lvert F_\rho(\Omega,\theta)\rvert \leq \lVert\Pi_\theta\rVert_{\sup} \leq \lVert K_\theta\rVert_{L^2}/\sqrt{8\pi\hbar}$, if the operator Π_θ is bounded, refer to Lemma 5.1. The second inequality ensures that square-integrable filter functions [as for $K_\theta(x,p) \in L^2(\mathbb{R}^2,\mathrm{d}x\,\mathrm{d}p)$] give rise to bounded parity operators. The proof of Property 5.1 in Appendix D.1 implies the even stronger statement that Π_θ is a Hilbert-Schmidt operator if K_θ is square integrable. Expectation values of bounded parity operators Π_θ are well-defined, continuous linear mappings from density operators to distribution functions that are free of singularities. In general, if Π_θ is unbounded, the function value $F_\rho(\Omega,\theta)$ assigned by the trace is not well defined for arbitrary density operators ρ or arbitrary phase-space points Ω.

Property 5.2. Square integrability: The phase-space distribution function $F_\rho(\Omega,\theta)$ is square integrable [i.e. $F_\rho(\Omega,\theta) \in L^2(\mathbb{R}^2)$] for all $\rho \in \mathcal{B}^1(\mathcal{H})$ if the absolute value of the filter function is bounded [i.e. $K_\theta(\Omega) \in L^\infty(\mathbb{R}^2)$].

Property 5.3. Postulate (iv): The phase-space distribution function $F_\rho(\Omega,\theta)$ satisfies by definition the covariance property. In particular, a displaced density operator $\rho' := \mathcal{D}(\Omega')\rho\mathcal{D}^\dagger(\Omega')$ is mapped to the inversely displaced distribution function $F_{\rho'}(\Omega,\theta) = F_\rho(\Omega-\Omega',\theta)$.

Property 5.4. Rotational covariance: Let us denote a rotated density operator $\rho^\phi = U_\phi\rho U_\phi^\dagger$, where the phase-space rotation operator is given by $U_\phi := \exp(-i\phi\hat{a}^\dagger\hat{a})$ in terms of creation and annihilation operators. The phase-space distribution function is covariant under phase-space rotations,[a] i.e. $F_{\rho^\phi}(\Omega,\theta) = F_\rho(\Omega^{-\phi},\theta)$, if the filter function $K_\theta(\Omega)$ (or equivalently the parity operator Π_θ) is invariant under rotations. Here, $\Omega^{-\phi}$ is the inversely rotated phase-space coordinate, e.g., $\alpha^{-\phi} = \exp(i\phi)\alpha$. As a consequence of this symmetry, the corresponding parity operators are diagonal in the number-state representation, i.e. $\langle n|\Pi_\theta|m\rangle \propto \delta_{nm}$.

[a] Note that any physically motivated distribution function must be covariant under $\pi/2$ rotations in phase-space, which correspond to the Fourier transform of pure states and connect coordinate representations $\psi(x)$ to momentum representations $\psi(p)$.

Property 5.5. Postulate (ii): The phase-space distribution function $F_\rho(\Omega,\theta)$ is real if Π_θ is Hermitian. This condition translates to the symmetry $K_\theta^*(-\Omega) = K_\theta(\Omega)$ of the filter function.

Property 5.6. Postulate (iiia): The trace of a trace-class operator $\mathrm{Tr}[\rho]$ is mapped to the phase-space integral $\int F_\rho(\Omega,\theta)\,\mathrm{d}\Omega$ if the corresponding filter function satisfies $K_\theta(0) = 1$. Note that this property also implies that the trace exists, i.e. $\mathrm{Tr}(\Pi_\theta) = K_\theta(0)/2$, in some particular basis, even though Π_θ might not be of trace class.

Property 5.7. Marginals: An even more restrictive subclass of the Cohen class satisfies the marginal properties $\int F_\rho(x,p,\theta)\mathrm{d}x = |\psi(p)|^2$ and $\int F_\rho(x,p,\theta)\mathrm{d}p = |\psi(x)|^2$ if and only if $[K_\theta(x,p)]|_{p=0} = 1$ and $[K_\theta(x,p)]|_{x=0} = 1$. This follows, e.g., directly from Proposition 14 in [111].

5.6.2 Relation to quantization

Recall that the Weyl quantization of a phase-space function (or tempered distribution) $a(\Omega) \in \mathcal{S}'(\mathbb{R}^2)$ yields by definition the operator (cf. [111, Def. 7 & Prop. 9])

$$\mathrm{Op}_{\mathrm{Weyl}}(a) = (\pi\hbar)^{-1}\int a(\Omega)\,\mathcal{D}(\Omega)\Pi\mathcal{D}^\dagger(\Omega)\,\mathrm{d}\Omega = (2\pi\hbar)^{-1}\int a_\sigma(\Omega)\,\mathcal{D}(\Omega)\,\mathrm{d}\Omega, \quad (5.22)$$

where the symplectic Fourier transform $a_\sigma(\Omega) = [F_\sigma a(\cdot)](\Omega)$ is used for the second equality. Recall that quantizations associated with the Cohen class $\mathrm{Op}_\theta(a)$ are essentially Weyl quantizations of convolved phase-space functions (or tempered distributions) up to the coordinate reflection $\theta^\vee(\Omega) = \theta(-\Omega)$, i.e.

$$\mathrm{Op}_\theta(a) = \mathrm{Op}_{\mathrm{Weyl}}(a * \theta^\vee) = (\pi\hbar)^{-1} \int [a * \theta^\vee](\Omega)\, \mathcal{D}(\Omega)\Pi\mathcal{D}^\dagger(\Omega)\, \mathrm{d}\Omega \tag{5.23}$$

$$= (2\pi\hbar)^{-1} \int a_\sigma(\Omega) K_\theta(\Omega)\, \mathcal{D}(\Omega)\, \mathrm{d}\Omega, \tag{5.24}$$

where $a, \theta, a * \theta \in \mathcal{S}'(\mathbb{R}^2)$, cf. [111, Prop. 7.35]. The symplectic Fourier transform $[F_\sigma(a * \theta^\vee)](\Omega) = a_\sigma(\Omega)K_\theta(\Omega)$ from Theorem 5.1 is used for the second equality, refer to §7.2.4 in [111].

Proposition 5.1. *The quantization* $\mathrm{Op}_\theta(a)$ *of a phase-space function (or tempered distribution)* $a(\Omega) \in \mathcal{S}'(\mathbb{R}^2)$ *is associated with the Cohen class via*

$$\mathrm{Op}_\theta(a) = (\pi\hbar)^{-1} \int a(\Omega)\, \mathcal{D}(\Omega)\Pi_\theta\mathcal{D}^\dagger(\Omega)\, \mathrm{d}\Omega,$$

where Π_θ *is the parity operator from Definition 5.3.*

Proof. The Plancherel formula $\int a(\Omega)b(\Omega)\,\mathrm{d}\Omega = \int a_\sigma(\Omega)b_\sigma(-\Omega)\,\mathrm{d}\Omega$ implies that

$$\begin{aligned}\mathrm{Op}_\theta(a) &= (2\pi\hbar)^{-1} \int a_\sigma(\Omega) K_\theta(\Omega)\, \mathcal{D}(\Omega)\, \mathrm{d}\Omega \\ &= (2\pi\hbar)^{-1} \int F_\sigma[a_\sigma(\cdot)](\Omega)\, F_\sigma[K_\theta(\cdot)\, \mathcal{D}(\cdot)](-\Omega)\, \mathrm{d}\Omega,\end{aligned}$$

where the equality $\mathcal{D}(\Omega)\Pi_\theta\mathcal{D}^\dagger(\Omega) = \frac{1}{2}F_\sigma[K(\cdot)\mathcal{D}(\cdot)](-\Omega)$ follows from (5.18) and the square of the symplectic Fourier transform $F_\sigma[a_\sigma(\cdot)](\Omega) = a(\Omega)$ is applied. □

One can consider single Fourier components $e^{i(p_0x - ix_0p)/\hbar} =: f_{\Omega_0}(\Omega)$, for which the Weyl quantization yields the displacement operator $\mathrm{Op}_{\mathrm{Weyl}}(f_{\Omega_0}) = \mathcal{D}(\Omega_0)$ from Sec. 5.5.1, refer to Proposition 11 in [111]. Let us now consider the θ-type quantization of a single Fourier component (cf. Def. 5.3), which results in the displacement operator being multiplied by the corresponding filter function via (5.23)-(5.24). Substituting $a_\sigma(\Omega) = F_\sigma[f_{\Omega_0}](\Omega)$ into (5.23), one obtains

$$\mathrm{Op}_\theta(f_{\Omega_0}) = K_\theta(\Omega_0)\mathcal{D}(\Omega_0) \quad \text{and} \quad \Pi_\theta = (4\pi\hbar)^{-1} \int \mathrm{Op}_\theta(f_{\Omega_0})\, \mathrm{d}\Omega_0.$$

The second equality follows from (5.16) and it specifies the parity operator as a phase-space average of quantizations of single Fourier components.

But it is even more instructive to consider the case of the delta distribution denoted as $\delta^{(2)} := \delta^{(2)}(\Omega)$, the Weyl quantization of which yields the Grossmann-Royer parity operator $\mathrm{Op}_{\mathrm{Weyl}}(\delta^{(2)}) = \pi\hbar\,\Pi$ (as obtained in [119]). Applying (5.23), the Cohen quantization of the delta distribution yields the parity operator from (5.16). In particular, the operator Π_θ from

Ordering	(τ, s)	$K_{\tau s}(\Omega_0)$	$\mathrm{Op}_{\tau s}(f_{\Omega_0})$
Normal	$(\frac{1}{2}, 1)$	$e^{\lvert\alpha_0\rvert^2/2}$	$e^{\alpha_0\hat{a}^\dagger}e^{-\alpha_0^*\hat{a}}$
Antinormal	$(\frac{1}{2}, -1)$	$e^{-\lvert\alpha_0\rvert^2/2}$	$e^{-\alpha_0^*\hat{a}}e^{\alpha_0\hat{a}^\dagger}$
Weyl	$(\frac{1}{2}, 0)$	1	$e^{\alpha_0\hat{a}^\dagger-\alpha_0^*\hat{a}} = e^{\frac{i}{\hbar}p_0\hat{x}-\frac{i}{\hbar}x_0\hat{p}}$
Standard	$(1, 0)$	$e^{\frac{i}{2\hbar}p_0x_0}$	$e^{\frac{i}{\hbar}p_0\hat{x}}e^{-\frac{i}{\hbar}x_0\hat{p}}$
Antistandard	$(0, 0)$	$e^{-\frac{i}{2\hbar}p_0x_0}$	$e^{-\frac{i}{\hbar}x_0\hat{p}}e^{\frac{i}{\hbar}p_0\hat{x}}$
Born-Jordan	$\int_0^1(\tau, 0)\mathrm{d}\tau$	$\mathrm{sinc}(p_0x_0/2)$	refer to Sec. 5.7

Table 5.2: Common operator orderings, their defining filter functions $K_{\tau s}(\Omega_0)$, and the corresponding single Fourier component quantizations $\mathrm{Op}_{\tau s}(f_{\Omega_0})$ as displacement operators with $e^{i(p_0x-ix_0p)/\hbar} =: f_{\Omega_0}(\Omega)$, refer to, e.g., [50, 217, 11, 10, 111]. Coordinates $\Omega_0 \simeq \alpha_0 \simeq (x_0, p_0)$ with subindex 0 are used for clarity.

Definition 5.3 is a θ-type quantization of the delta distribution as

$$\Pi_\theta = (\pi\hbar)^{-1}\,\mathrm{Op}_\theta(\delta^{(2)}) = (\pi\hbar)^{-1}\,\mathrm{Op}_{\mathrm{Weyl}}(\theta^\vee), \tag{5.25}$$

or equivalently, the Weyl quantization of the Cohen kernel, up to the coordinate reflection $\theta^\vee(\Omega) = \theta(-\Omega)$ [which follows from (5.23) via $\Pi_\theta = (\pi\hbar)^{-1}\,\mathrm{Op}_{\mathrm{Weyl}}(\theta^\vee * \delta^{(2)}) = (\pi\hbar)^{-1}\,\mathrm{Op}_{\mathrm{Weyl}}(\theta^\vee)$]. Since Π_θ is the Weyl quantization of the function (or tempered distribution) $\theta^\vee(\Omega) = \theta(-\Omega) \in \mathcal{S}'(\mathbb{R}^2)$, one can adapt results contained in [69] to precisely state conditions on θ, for which bounded operators Π_θ are obtained via their Weyl quantizations, refer also to Property 5.1. For example, square-integrable $\theta \in L^2(\mathbb{R}^2)$ result in Hibert-Schmidt operators Π_θ, absolutely integrable $\theta \in L^1(\mathbb{R}^2)$ result in compact operators Π_θ, and Schwartz functions $\theta \in \mathcal{S}(\mathbb{R}^2)$ result in trace-class operators Π_θ, refer to [69].

We consider now a class of explicit quantization schemes along the lines of [51, 50, 10, 111] and they are motivated by different (τ, s)-orderings of non-commuting operators $\hat{x}$ and $\hat{p}$ or $\hat{a}$ and $\hat{a}^\dagger$ ($-1 \le s \le 1$ and $0 \le \tau \le 1$). This class is obtained via the (τ, s)-parametrized filter function (where the relation $\alpha = (\lambda x + ip/\lambda)/\sqrt{2\hbar}$ from Section 5.5.1 is used)

$$K_{\tau s}(\Omega) := \exp\big[\tfrac{2\tau-1}{4}(\alpha^2-(\alpha^*)^2) + \tfrac{s}{2}|\alpha|^2\big] = \exp\big[\tfrac{i(2\tau-1)px}{2\hbar} + \tfrac{s(\lambda^2x^2+\lambda^{-2}p^2)}{4\hbar}\big], \tag{5.26}$$

which has the symmetry $K_{\tau s}(\Omega) = K_{\tau s}(-\Omega)$. The corresponding (τ, s)-parametrized quantizations of a single Fourier component are given by the operators of the form $\mathrm{Op}_{\tau s}(f_{\Omega_0}) := K_{\tau s}(\Omega)\mathcal{D}(\Omega)$, which are central in ordered expansions into non-commuting operators. Also note that for $s \le 0$, the resulting distribution functions are in the Cohen class with $K_{\tau s}(\Omega) \in \mathcal{S}'(\mathbb{R}^2)$ due to Theorem 5.1. Important, well-known special cases are summarized in Table 5.2, refer also to [50, 11, 10, 111].

Name	(τ, s)	$K_{\tau s}(\Omega)$	$\theta_{\tau s}(\Omega)$
Wigner function	$(1/2, 0)$	1	$\delta^{(2)}(\Omega)$
s-parametrized	$(1/2, s)$	$\exp\left[\frac{s}{2}\lvert\alpha\rvert^2\right]$	$-\frac{1}{\pi s}\exp\left[\frac{2}{s}\lvert\alpha\rvert^2\right]$
Husimi Q function	$(1/2, -1)$	$\exp\left[-\frac{1}{2}\lvert\alpha\rvert^2\right]$	$\frac{1}{\pi}\exp\left[-2\lvert\alpha\rvert^2\right]$
Glauber P function	$(1/2, 1)$	$\exp\left[\frac{1}{2}\lvert\alpha\rvert^2\right]$	$-\frac{1}{\pi}\exp\left[2\lvert\alpha\rvert^2\right]$
Shubin's τ-distribution	$(\tau, 0)$	$\exp\left[\frac{i}{\hbar}\frac{2\tau-1}{2}px\right]$	$\frac{1}{\hbar\pi\lvert 2\tau-1\rvert}\exp\left[\frac{2i}{\hbar(2\tau-1)}px\right]$
Born-Jordan distribution	$\int_0^1(\tau, 0)\,\mathrm{d}\tau$	$\mathrm{sinc}[px/(2\hbar)]$	$F_\sigma\{\mathrm{sinc}[px/(2\hbar)]\}/(2\pi\hbar)$

Table 5.3: Well-known phase-space distribution functions and their corresponding Cohen kernels recovered for particular values of τ or s via expectation values of displaced parity operators from (5.27).

5.6.3 Explicit form of parity operators

Expectation values of displaced parity operators

$$\Pi_{\tau s} = (4\pi\hbar)^{-1}\int K_{\tau s}(\Omega)\mathcal{D}(\Omega)\,\mathrm{d}\Omega = (4\pi\hbar)^{-1}\int \mathrm{Op}_{\tau s}(f_{\Omega_0})\,\mathrm{d}\Omega \tag{5.27}$$

are obtained via the kernel function in (5.26) and recover well-known phase-space distribution functions[5] for particular cases of τ or s, which are motivated by the ordering schemes $\mathrm{Op}_{\tau s}(f_{\Omega_0})$ from Table 5.2. Important special cases of these distribution functions and their corresponding filter functions and Cohen kernels are summarized in Table 5.3.

In particular, the parameters $\tau = 1/2$ and $s = 0$ identify the Wigner function with $K_{1/2,0}(\Omega) \equiv 1$ and (5.27) reduces to (5.11). Note that the corresponding Cohen kernel θ from Theorem 5.1 is the 2-dimensional delta distribution $\delta^{(2)}(\Omega)$ and that convolving with $\delta^{(2)}(\Omega)$ is the identity operation, i.e. $\delta^{(2)} * W_\rho = W_\rho$ [see (5.17)].

The filter function $K_{\tau s}$ from (5.26) results for a fixed parameter of $\tau = 1/2$ in the Gaussian $K_s(\Omega) := K_{1/2,s}(\Omega) = \exp\left[\frac{s}{2}\lvert\alpha\rvert^2\right]$. The corresponding parity operators are diagonal in the number-state representation (refer to Property 5.4), and they can be specified for $-1 \leq s < 1$ in terms of number-state projectors [50, 194, 217] as

$$\Pi_s := \Pi_{1/2,s} = (4\pi\hbar)^{-1}\int e^{s\lvert\alpha\rvert^2/2}\,\mathcal{D}(\Omega)\,\mathrm{d}\Omega = \sum_{n=0}^{\infty}(-1)^n\frac{(1+s)^n}{(1-s)^{n+1}}|n\rangle\langle n|, \tag{5.28}$$

where the second equality specifies Π_s in the form of a spectral decomposition. This form has implicitly appeared in, e.g., [50, 194, 217]. We provide a more compact proof in Appendix D.2. Note that the operator norm of Π_s is equal to $\|\Pi_s\|_{\sup} = 1/(1-s)$ for $s \leq 0$ and the operators are trace class for $s < 0$ (so in particular, they are Hilbert-Schmidt operators). However, distribution functions for $s > 0$ can develop singularities as their parity operators are unbounded, as detailed in Property 5.1. Nevertheless, their symplectic Fourier transform

[5] This family of phase-space representations is related to the one considered in [11, 10] by setting $\lambda = s/2$ and $\mu = -\nu = 2\tau - 1/4$.

always exists and it is related to the Wigner function via $K_s(\Omega)F_\sigma[W_\rho(\cdot)](\Omega)$ by multiplying with the filter function $K_s(\Omega)$. This class of s-parametrized phase-space representations has gained widespread applications in quantum optics and beyond [182, 108, 266, 232, 62], and they correspond to Gaussian convolved Wigner functions

$$F_\rho(\Omega, s) = F_{|0\rangle}(\Omega, s{+}1) * W_\rho(\Omega),$$

for $s < 0$ such as the Husimi Q function for $s = -1$. Note that the Cohen kernel θ_s from Theorem 5.1 corresponds to the vacuum state $F_{|0\rangle}(\Omega, s{+}1)$ of a quantum harmonic oscillator [50]. Gaussian deconvolutions of the Wigner function are formally obtained for $s > 0$, which includes the Glauber P function for $s = 1$ [50]. Due to the rotational symmetry of its filter function $K_s(\Omega)$, the s-parametrized distribution functions are covariant under phase-space rotations, refer to Property 5.4.

Another important special case is obtained for a fixed parameter of $s = 0$, which results in Shubin's τ-distribution, refer to [111, 38, 37, 39]. Its filter function from (5.26) reduces to the chirp function $K_{\tau 0}(\Omega) =: K_\tau(\Omega) = \exp[i(2\tau{-}1)px/(2\hbar)]$ while relying on the parametrization with x and p. The resulting distribution functions $F_\rho(\Omega, \tau)$ are in the Cohen class due to Theorem 5.1 and they are square integrable following Property 5.2 as the absolute value of $K_\tau(\Omega)$ is bounded. We calculate the explicit action of the corresponding parity operator Π_τ.

Theorem 5.2. *The action of the τ-parametrized parity operator $\Pi_\tau := \Pi_{\tau 0}$ on some coordinate representation $\psi(x) \in L^2(\mathbb{R})$ is explicitly given for any $\tau \neq 1$ by*

$$\Pi_\tau \psi(x) = \frac{1}{2|\tau{-}1|}\psi(\tfrac{\tau x}{\tau{-}1}), \tag{5.29}$$

which for the special case $\tau = 1/2$ reduces (as expected) to the usual parity operator Π. It follows that Π_τ is bounded for every $0 < \tau < 1$ (or in general for every real τ that does not equal to 0 or 1) and its operator norm is given by $\|\Pi_\tau\|_{\sup} = 1/\sqrt{4(\tau{-}\tau^2)}$.

Proof. By (5.27), the parity operator Π_τ acts on the coordinate representation $\psi(x)$ via

$$\Pi_\tau \psi(x) = (4\pi\hbar)^{-1} \int K_{\tau 0}(\Omega)\, \mathcal{D}(\Omega)\psi(x)\, \mathrm{d}\Omega.$$

This integral can be evaluated using the explicit form of $K_{\tau 0}(\Omega)$ form (5.26) and the action of $\mathcal{D}$ on coordinate representations $\psi(x)$ from (5.9) yields

$$\int K_{\tau 0}(\Omega)\, \mathcal{D}(\Omega)\psi(x)\, \mathrm{d}\Omega = \int e^{\frac{i}{2\hbar}(2\tau-1)p_0x_0} e^{\frac{i}{\hbar}(p_0x - \frac{1}{2}p_0x_0)} \psi(x{-}x_0)\, \mathrm{d}x_0\, \mathrm{d}p_0$$
$$= \int \left[\int e^{\frac{i}{\hbar}p_0(x+(\tau-1)x_0)}\, \mathrm{d}p_0\right] \psi(x{-}x_0)\, \mathrm{d}x_0 = \frac{1}{|\tau{-}1|}\int \left[\int e^{\frac{i}{\hbar}p_0 y}\, \mathrm{d}p_0\right] \psi(\frac{\tau x - y}{\tau{-}1})\, \mathrm{d}y,$$

where the change of variables $y = x + (\tau-1)x_0$ with the substitutions $x_0 = (y-x)/(\tau-1)$ and $\mathrm{d}y = |\tau-1|\mathrm{d}x_0$ was used. Therefore, the right-hand side is

$$\frac{2\pi\hbar}{|\tau-1|}\int \delta(y)\,\psi\Big(\frac{\tau x-y}{\tau-1}\Big)\,\mathrm{d}y = \frac{2\pi\hbar}{|\tau-1|}\psi(\tfrac{\tau x}{\tau-1}).$$

Now let $\tau \in (0,1)$. Recall that the operator norm is calculated using the following formula $||\Pi_\tau||_{\sup} = \sup_{||\phi(x)||_{L^2}=1}||\Pi_\tau\phi(x)||_{L^2}$. For an arbitrary square-integrable $\phi(x)$ with L^2 norm $||\phi(x)||_{L^2} = 1$ one obtains

$$\begin{aligned}||\Pi_\tau\phi||_{L^2}^2 &= \langle\Pi_\tau\phi|\Pi_\tau\phi\rangle = (2|\tau-1|)^{-2}\int_{\mathbb{R}}\phi^*(\tfrac{\tau x}{\tau-1})\phi(\tfrac{\tau x}{\tau-1})\,\mathrm{d}x\\ &= (2|\tau-1|)^{-2}\tfrac{|\tau-1|}{|\tau|}||\phi(x)||_{L^2} = \tfrac{1}{4|\tau-1||\tau|} = \tfrac{1}{4(\tau-\tau^2)}\end{aligned}$$

by applying a change of variables, which results in $||\Pi_\tau||_{\sup} = [4(\tau-\tau^2)]^{-1/2}$. □

This parity operator is bounded for every $0 < \tau < 1$, and its expectation value gives rise to well-defined distribution functions (Property 5.1), which are also integrable as $K_\tau(0) = 1$ (Property 5.6). Note that this family of distribution functions $F_\rho(\Omega,\tau,0)$ for $\tau \neq 1/2$ does not satisfy Property 5.5, i.e. self-adjoint operators ρ are mapped to complex functions. In particular, the symmetry $K_\tau^*(\Omega) = K_{1-\tau}(\Omega)$ implies that

$$F_{\rho^\dagger}(\Omega,\tau) = F_\rho^*(\Omega,1-\tau).$$

In the following, we will rely on this τ-parametrized family to construct and analyze the parity operator of the Born-Jordan distribution.

5.7 The Born-Jordan distribution

5.7.1 Parity-operator description of the Born-Jordan distribution

The Born-Jordan distribution $F_\rho(\Omega,\mathrm{BJ})$ is an element of the Cohen class [59, 111, 38] and is obtained by averaging over the τ-distributions $F_\rho(\Omega,\tau) \in L^2(\mathbb{R}^2)$:

$$F_\rho(\Omega,\mathrm{BJ}) := \int_0^1 F_\rho(\Omega,\tau)\,\mathrm{d}\tau. \tag{5.30}$$

As in Definition 5.3, this distribution function is also obtained via the expectation value of a parity operator.

Theorem 5.3. *The Born-Jordan distribution $F_\rho(\Omega, \mathrm{BJ})$ of a density operator $\rho \in \mathcal{B}^1(\mathcal{H})$ is an element of the Cohen class, and it is obtained as the expectation value*

$$F_\rho(\Omega, \mathrm{BJ}) = (\pi\hbar)^{-1} \operatorname{Tr}[\,\rho\,\mathcal{D}(\Omega)\Pi_{\mathrm{BJ}}\mathcal{D}^\dagger(\Omega)\,] \tag{5.31}$$

of the displaced parity operator Π_{BJ} that is defined by the relation

$$\Pi_{\mathrm{BJ}} := (4\pi\hbar)^{-1} \int K_{\mathrm{BJ}}(\Omega)\mathcal{D}(\Omega)\,\mathrm{d}\Omega, \tag{5.32}$$

where $K_{\mathrm{BJ}}(\Omega) = \mathrm{sinc}(a) = \sin(a)/a$ is the sinus cardinalis function with the argument $a = (2\hbar)^{-1}px = i[(\alpha^*)^2 - \alpha^2]/4$. Here one applies the substitution $\alpha = (\lambda x + ip/\lambda)/\sqrt{2\hbar}$ from Sec. 5.5.1 and the expression for a is independent of λ.

Proof. Combining Eqs. (5.30) and (5.15), the Born-Jordan distribution is the expectation value

$$F_\rho(\Omega, \mathrm{BJ}) = (\pi\hbar)^{-1} \operatorname{Tr}[\,\rho\,\mathcal{D}(\Omega)(\int_0^1 \Pi_{\tau 0}\,\mathrm{d}\tau)\mathcal{D}^\dagger(\Omega)\,],$$

and the corresponding parity operator can be expanded as

$$\Pi_{\mathrm{BJ}} = (4\pi\hbar)^{-1} \int \left[\int_0^1 K_{\tau 0}(\Omega)\,\mathrm{d}\tau\right]\mathcal{D}(\Omega)\,\mathrm{d}\Omega.$$

Using the explicit form of $K_{\tau 0}(\Omega)$ from (5.26), the evaluation of the integral

$$\int_0^1 K_{\tau 0}(\Omega)\,\mathrm{d}\tau = \int_0^1 \exp\left[\tfrac{i}{2\hbar}(2\tau - 1)px\right]\mathrm{d}\tau = \mathrm{sinc}[(2\hbar)^{-1}px]$$

over τ concludes the proof. □

This confirms that the Born-Jordan distribution is square integrable $F_\rho(\Omega, \mathrm{BJ}) \in L^2(\mathbb{R}^2)$ following Property 5.2 as its filter function is bounded, i.e., $|\mathrm{sinc}[(2\hbar)^{-1}px]| \leq 1$ for all $(x, p) \in \mathbb{R}^2$. The filter function K_{BJ} satisfies $K_{\mathrm{BJ}}(x, 0) = K_{\mathrm{BJ}}(0, p) = 1$, and the Born-Jordan distribution therefore gives rise to the correct marginals as quantum-mechanical probabilities (Property 5.7). In particular, integrating over the Born-Jordan distribution reproduces the quantum mechanical probabilty densities, i.e. $\int F_\rho(x, p, \mathrm{BJ})\mathrm{d}x = |\psi(p)|^2$ and $\int F_\rho(x, p, \mathrm{BJ})\mathrm{d}p = |\psi(x)|^2$. It is well-known that the Born-Jordan distribution is related to the Wigner function via a convolution with the Cohen kernel θ_{BJ}, refer to [111, 113]. However, calculating this kernel, or the corresponding parity operator directly might prove difficult. In the following, we establish a more convenient representation of the Born-Jordan parity operator which is an "average" of Π_τ from Theorem 5.2 via the formal integral transformation

$$\Pi_{\mathrm{BJ}} = \int_0^1 \Pi_\tau\,\mathrm{d}\tau, \tag{5.33}$$

which—as in Sect. 5.5.2—is interpreted as $\Pi_{\mathrm{BJ}}\psi(x) = \int_0^1 \Pi_\tau\psi(x)\,\mathrm{d}\tau$ for all $\psi(x) \in L^2(\mathbb{R})$. Recall that the parity operator Π_τ is well-defined and bounded for every $0 < \tau < 1$.

Remark 5.1. Note that evaluating $\Pi_{\mathrm{BJ}}\psi(x)$ at $x = 0$ for some $\psi(x) \in L^2(\mathbb{R})$ with $\psi(0) \neq 0$ leads to a divergent integral in (5.33). This comes from the singularity at $\tau = 1$ in (5.29). However, we will later see that this is harmless as it only happens on a set of measure zero (so one can define $\Pi_{\mathrm{BJ}}\psi(x)|_{x=0}$ to be 0 or $\psi(0)$ or arbitrary) and, more importantly, that $\psi(x) \in L^2(\mathbb{R})$ implies $\Pi_{\mathrm{BJ}}\psi(x) \in L^2(\mathbb{R})$ (cf. Proposition 5.2).

Let us explicitly specify the squeezing operator

$$S(\xi) := \exp[i\xi/2(\hat{p}\hat{x} + \hat{x}\hat{p})] = \exp[i\xi/2(\hat{a}^2 - (\hat{a}^\dagger)^2)] \tag{5.34}$$

while following [58] and Chapter 2.3 in [171]. It acts on a coordinate representation $\psi(x)$ via $S(\xi)\psi(x) = e^{\xi/2}\psi(e^{\xi}x)$.

Theorem 5.4. *Let us consider the squeezing operator $S(\xi)$ which depends on the real squeezing parameter $\xi \in \mathbb{R}$. The Born-Jordan parity operator*

$$\Pi_{\mathrm{BJ}} = [\, \tfrac{1}{4} \int_{-\infty}^{\infty} \operatorname{sech}(\xi/2) S(\xi) \mathrm{d}\xi \,]\, \Pi \tag{5.35}$$

is a composition of the reflection operator Π followed by a squeezing operator (and the two operations commute), and this expression is integrated with respect to a well-behaved weight function $\operatorname{sech}(\xi/2) = 2/(e^{\xi/2}+e^{-\xi/2})$. Note that here the function $\operatorname{sech}(\xi/2) \in \mathcal{S}(\mathbb{R})$ is fast decreasing and invariant under the Fourier transform (e.g., as Hermite polynomials).

Proof. The explicit action of Π_{BJ} on a coordinate representation $\psi(x) \in L^2(\mathbb{R})$ is given by (see Theorem 5.2)

$$\Pi_{\mathrm{BJ}}\psi(x) = \int_0^1 \Pi_\tau \psi(x)\, \mathrm{d}\tau = \int_0^1 \frac{1}{2|\tau-1|} \psi(\tfrac{\tau x}{\tau-1})\, \mathrm{d}\tau.$$

Applying a change of variables $e^{\xi} = \tau/(1-\tau)$ with $\xi \in \mathbb{R}$ yields the substitutions $\tau = 1/(1+e^{-\xi})$, $1/(2|\tau-1|) = (1+e^{\xi})/2$. and $\mathrm{d}\tau = e^{\xi}/(1+e^{\xi})^2 \mathrm{d}\xi$. One obtains

$$\Pi_{\mathrm{BJ}}\psi(x) = \int_{-\infty}^{\infty} \frac{e^{\xi}}{2(1+e^{\xi})} \psi(-e^{\xi}x) \mathrm{d}\xi.$$

Let us recognize that $\psi(-e^{\xi}x) = e^{-\xi/2} S(\xi)\, \Pi\, \psi(x)$ is the composition of a coordinate reflection and a squeezing of the pure state $\psi(x)$; also the two operations commute. This results in the explicit action

$$\Pi_{\mathrm{BJ}}\psi(x) = \int_{-\infty}^{\infty} \frac{e^{\xi/2}}{2(1+e^{\xi})} S(\xi)\, \Pi\, \psi(x) \mathrm{d}\xi,$$

where $e^{\xi/2}/[2(1+e^{\xi})] = [2(e^{-\xi/2}+e^{\xi/2})]^{-1}$ concludes the proof. □

The expression for the parity operator in Theorem 5.4 is very instructive when compared to Theorem 5.3, and this confirms that the parity operator Π_{BJ} decomposes into the usual parity operator Π followed by a geometric transformation, refer also to Section 5.7.2. This geometric transformation is in the case of the Born-Jordan parity operator an average of squeezing operators.

Remark 5.2. The Born-Jordan distribution is covariant under squeezing, which means that the squeezed density operator $\rho' = S(\xi)\rho S^\dagger(\xi)$ is mapped to the inversely squeezed phase-space representation $F_{\rho'}(x,p,\mathrm{BJ}) = F_\rho(e^{-\xi}x, e^{\xi}p, \mathrm{BJ})$.

The form of Π_{BJ} given in (5.35) allows us to specify a finite upper bound for its operator norm, which then confirms that Born-Jordan distributions are well defined for arbitrary quantum states, refer to Property 5.1. Note that the largest (generalized) eigenvalue of Π_{BJ} is exactly $\pi/2$ as shown in Theorem 5.5 below.

Proposition 5.2. *The operator norm of the Born-Jordan parity operator Π_{BJ} is bounded (cf. Property 5.1) as an upper bound is given by $\|\Pi_{\mathrm{BJ}}\|_{\sup} \leq \pi/2$.*

Proof. Using the definition $\|\Pi_{\mathrm{BJ}}\|_{\sup} = \sup_{\|\phi(x)\|_{L^2}=1} \|\Pi_{\mathrm{BJ}}\phi(x)\|_{L^2}$, the norm of the function $\Pi_{\mathrm{BJ}}\phi(x)$ can be expressed for any $\phi(x)$ with $\|\phi(x)\|_{L^2} = 1$ as

$$\begin{aligned}\|\Pi_{\mathrm{BJ}}\phi(x)\|_{L^2}^2 = \langle\phi|\Pi_{\mathrm{BJ}}^\dagger\Pi_{\mathrm{BJ}}|\phi\rangle &= \tfrac{1}{16}\int\int \operatorname{sech}(\xi/2)\operatorname{sech}(\xi'/2)\langle\phi|S(\xi'-\xi)|\phi\rangle \mathrm{d}\,\xi\,\mathrm{d}\,\xi' \\ &\leq \tfrac{1}{16}\int\int \operatorname{sech}(\xi/2)\operatorname{sech}(\xi'/2)|\langle\phi|S(\xi'-\xi)|\phi\rangle| \mathrm{d}\,\xi\,\mathrm{d}\,\xi',\end{aligned}$$

and it was used that $\Pi^\dagger\Pi = \Pi^2 = 1$ and $S^\dagger(\xi)S(\xi') = S(\xi'-\xi)$. Since $S(\xi'-\xi)$ is unitary, one obtains that $|\langle\phi|S(\xi'-\xi)|\phi\rangle| \leq 1$. Finally,

$$\|\Pi_{\mathrm{BJ}}\phi\|_{L^2}^2 \leq \tfrac{1}{16}\int\int \operatorname{sech}(\xi/2)\operatorname{sech}(\xi'/2)\mathrm{d}\,\xi\,\mathrm{d}\,\xi' = \pi^2/4.$$

□

Remark 5.3. One may also obtain the above result from the Π_τ-representation of Π_{BJ} via

$$\begin{aligned}\|\Pi_{\mathrm{BJ}}\psi(x)\|_{L^2} = \Big\|\int_0^1 \Pi_\tau\psi(x)\,\mathrm{d}\tau\Big\|_{L^2} &\leq \int_0^1 \|\Pi_\tau\psi(x)\|_{L^2}\,\mathrm{d}\tau \\ &\leq \int_0^1 \frac{1}{\sqrt{4(\tau-\tau^2)}}\,\mathrm{d}\tau\,\|\psi(x)\|_{L^2} = \frac{\pi}{2}\|\psi(x)\|_{L^2}\end{aligned}$$

for arbitrary $\psi(x) \in L^2(\mathbb{R})$ where in the second-to-last step we used Proposition 5.2.

5.7.2 Spectral decomposition of the Born-Jordan parity operator

We will now adapt results for generalized spectral decompositions, refer to [57, 58, 187, 100]. This will allow us to solve the generalized eigenvalue equation for parity operators and to determine their spectral decompositions.

We have introduced a distributional pairing for smooth, well-behaved functions $\psi(x) \in \mathcal{S}(\mathbb{R})$ in Section 5.4.2 with respect to functions of slow growth $a(x) \in \mathcal{S}'(\mathbb{R})$. We will use this distributional pairing to construct L^2 scalar products $\langle a, \psi\rangle = \int_{\mathbb{R}} a^*(x)\psi(x)\,dx$, which corresponds to a rigged Hilbert space [100, 57] or the Gelfand triple $\mathcal{S}(\mathbb{R}) \subset L^2(\mathbb{R}) \subset \mathcal{S}'(\mathbb{R})$. This rigged Hilbert space allows us to specify the generalized spectral decomposition of the Born-Jordan parity operator with generalized eigenvectors in $\mathcal{S}'(\mathbb{R})$ as functions of slow growth.

It was shown in the previous section that the Born-Jordan parity operator Π_{BJ} is a composition of a coordinate reflection and a squeezing operator. We now recapitulate results on the spectral decomposition of the squeezing operator from [57, 58, 41], up to minor modifications. Recall that the squeezing operator forms a unitary, strongly continuous one-parameter group $S(\xi) = e^{-i\xi H}$ with $\xi \in \mathbb{R}$ that is generated by the unbounded Hamiltonian

$$H := -\tfrac{1}{2}(\hat{x}\hat{p}+\hat{p}\hat{x}) = -\tfrac{1}{2}[\hat{a}^2-(\hat{a}^\dagger)^2].$$

This Hamiltonian admits a purely continuous spectrum $E \in \mathbb{R}$, and satisfies the generalized eigenvalue equation

$$\langle H\psi|\psi_\pm^E\rangle = \langle\psi|H\psi_\pm^E\rangle = E\langle\psi|\psi_\pm^E\rangle$$

for every $\psi \in \mathcal{S}(\mathbb{R})$, where the last equation is equivalent to $H|\psi_\pm^E\rangle = E|\psi_\pm^E\rangle$. The Gelfand-Maurin spectral theorem [187, 100, 57] results in a spectral resolution of

$$H = \int_{-\infty}^{\infty} E\,|\psi_\pm^E\rangle\langle\psi_\pm^E|\,\mathrm{d}E.$$

The generalized eigenvectors are specified in terms of their coordinate representations as slowly increasing functions from Section 5.4.1, i.e. $\psi_\pm^E(x) := \langle x|\psi_\pm^E\rangle \in S'(\mathbb{R})$ with

$$\psi_+^E(x) = \tfrac{1}{2\sqrt{\pi}}|x|^{-(iE+\frac{1}{2})} \text{ and } \psi_-^E(x) = \tfrac{1}{2\sqrt{\pi}}\mathrm{sgn}(x)|x|^{-(iE+\frac{1}{2})}, \tag{5.36}$$

refer to [57, 58, 187, 100] and Appendix D.3 for more details. Note that $\psi_\pm^E(x)$ are generalized eigenfunctions: they are not square integrable, but the integral $\int_{\mathbb{R}}[\psi_\pm^E(x)]^*\phi(x)\,dx$ exists as a distributional pairing for every $\phi \in \mathcal{S}(\mathbb{R})$. Also note that these generalized eigenvectors can be decomposed into the number-state basis with finite expansion coefficients that decrease to zero for large n, refer to Appendix D.3. The spectral decomposition of the squeezing operator is then given by

$$S(\xi) = \int_{-\infty}^{\infty} e^{-iE\xi}[\,|\psi_+^E\rangle\langle\psi_+^E| + |\psi_-^E\rangle\langle\psi_-^E|\,]\,\mathrm{d}E,$$

refer to Eq. 6.12 in [57] and Eq. 2.14 in [58]. Note that these eigenvectors are also invariant under the Fourier transform (e.g., as Hermite polynomials).

It immediately follows that the squeezing operator satisfies the generalized eigenvalue equation

$$S(\xi)|\psi_{\pm}^{E}\rangle = e^{-i\xi E}\,|\psi_{\pm}^{E}\rangle, \tag{5.37}$$

which can be easily verified using the explicit action of the squeezing operator $S(\xi)\psi_{\pm}^{E}(x) = e^{\xi/2}\psi_{\pm}^{E}(e^{\xi}x) = e^{-iE\xi}\psi_{\pm}^{E}(x)$. One can now specify the Born-Jordan parity operator using its spectral decomposition.

Theorem 5.5. *Generalized eigenvectors $|\psi_{\pm}^{E}\rangle$ of the squeezing operator from* (5.36) *are also generalized eigenvectors of the Born-Jordan parity operator which satisfy*

$$\Pi_{\mathrm{BJ}}\,|\psi_{\pm}^{E}\rangle = \pm\tfrac{\pi}{2}\,\mathrm{sech}(\pi E)\,|\psi_{\pm}^{E}\rangle$$

for all $E \in \mathbb{R}$. The parity operator Π_{BJ} therefore admits the spectral decomposition

$$\Pi_{\mathrm{BJ}} = \tfrac{\pi}{2}\int_{-\infty}^{\infty}\mathrm{sech}(\pi E)\,[\,|\psi_{+}^{E}\rangle\langle\psi_{+}^{E}| - |\psi_{-}^{E}\rangle\langle\psi_{-}^{E}|\,]\,\mathrm{d}E,$$

where $\langle\psi_{\pm}^{E}|\Pi = \pm\langle\psi_{\pm}^{E}|$ has been used.

Proof. The generalized eigenvalues can be computed via

$$\Pi_{\mathrm{BJ}}\,|\psi_{\pm}^{E}\rangle = \tfrac{1}{4}\int_{-\infty}^{\infty}\mathrm{sech}(\xi/2)S(\xi)\mathrm{d}\xi\;\Pi\,|\psi_{\pm}^{E}\rangle,$$

where $\Pi\,|\psi_{\pm}^{E}\rangle = \pm|\psi_{\pm}^{E}\rangle$. Using (5.37), one obtains

$$\Pi_{\mathrm{BJ}}\,|\psi_{\pm}^{E}\rangle = \pm\tfrac{1}{4}\int_{-\infty}^{\infty}\mathrm{sech}(\xi/2)e^{-iE\xi}\mathrm{d}\xi\;|\psi_{\pm}^{E}\rangle = \pm\tfrac{\pi}{2}\,\mathrm{sech}(\pi E)\,|\psi_{\pm}^{E}\rangle.$$

□

Similarly as the previously discussed parity operators in Theorem 5.5, both Π_{τ} and Π_{s} can be decomposed using the above formalism.

Remark 5.4. Applying the substitution $e^{\xi} := \tau/(1-\tau)$, the parity operator Π_{τ} from (5.29) can be decomposed for $0 < \tau < 1$ into $\Pi_{\tau} = \cosh(\xi/2)S(\xi)\,\Pi$ which consists of a coordinate reflection and a squeezing. The parity operator Π_{τ} therefore admits a spectral decomposition

$$\Pi_{\tau} = \cosh(\xi/2)\int e^{-iE\xi}[\,|\psi_{+}^{E}\rangle\langle\psi_{+}^{E}| - |\psi_{-}^{E}\rangle\langle\psi_{-}^{E}|\,]\,\mathrm{d}E,$$

where $\langle\psi_{\pm}^{E}|\Pi = \pm\langle\psi_{\pm}^{E}|$ has been used.

Remark 5.5. The parity operator $\Pi_s = (1-s)^{-1} e^{\kappa_s \hat{a}^\dagger \hat{a}} \Pi$ from (5.28) with $\kappa_s := \ln[(1+s)/(1-s)]$ and $-1 < s < 1$ is the composition of the usual coordinate reflection Π followed by a positive semi-definite operator. In particular, $\Pi_{-1} = \frac{1}{2} |0\rangle\langle 0| \Pi$. Note that the positive semi-definite operator $e^{\kappa_s \hat{a}^\dagger \hat{a}}$ describes the effective phenomenon of photon loss for $s < 0$, refer to [172].

Remark 5.6. Recall from (5.35) that the Born-Jordan parity operator

$$\Pi_{\mathrm{BJ}} = [\, \tfrac{1}{4} \int_{-\infty}^{\infty} \operatorname{sech}(\xi/2) S(\xi) \mathrm{d}\xi \,] \Pi$$

is also a composition of the regular parity operator Π followed by a geometric transformation.

5.8 Matrix representation of the Born-Jordan parity operator

Recall that the s-parametrized parity operators Π_s are diagonal in the Fock basis and their diagonal entries can be computed using the simple expression in (5.28). This enables the experimental reconstruction of distribution functions from photon-count statistics [74, 180, 32, 21] in quantum optics.

Remark 5.7. The Born-Jordan parity operator Π_{BJ} is not diagonal in the number-state basis, as its filter function $K_{\mathrm{BJ}}(\Omega)$ is not invariant under arbitrary phase-space rotations, refer to Property 5.4. The filter function $K_{\mathrm{BJ}}(\Omega)$ is, however, invariant under $\pi/2$ rotations in phase space, and therefore only every fourth off-diagonal is non-zero.

We now discuss the number-state representation of the parity operator Π_{BJ}, which provides a convenient way to calculate (or, more precisely, approximate) Born-Jordan distributions.

Theorem 5.6. *The matrix elements* $[\Pi_{\mathrm{BJ}}]_{mn} := \langle m|\Pi_{\mathrm{BJ}}|n\rangle$ *of the Born-Jordan parity operator in the Fock basis can be calculated in the form of a finite sum*

$$[\Pi_{\mathrm{BJ}}]_{mn} = \sum_{k=0}^{n} \sum_{\substack{\ell=0 \\ \ell \text{ even}}}^{m-n} d_{mn}^{k\ell}\, \Phi^{k}_{(m-n-\ell)/2,\ell/2}\,, \tag{5.38}$$

for $m \in \{n, n+4, n+8, \dots\}$ *and* $[\Pi_{\mathrm{BJ}}]_{mn} = [\Pi_{\mathrm{BJ}}]_{nm}$ *with the coefficients*

$$d_{mn}^{k\ell} := (-1)^{(\ell+m-n)/2}\sqrt{\frac{n!}{m!}}\,2^{(2k+m-n)/2}\binom{m}{n-k}\binom{m-n}{\ell}/k!, \tag{5.39}$$

$$\Phi_{ab}^{k} := [\partial_{\mu}^{k}[\partial_{\lambda}^{a}\partial_{\mu}^{b} f(\lambda,\mu)]|_{\lambda=\mu}]|_{\mu=1}. \tag{5.40}$$

Here, Φ_{ab}^{k} *are the* a*th and* b*th partial derivatives of the two-variate function demoted by* $f(\lambda,\mu) = \operatorname{arcsinh}[1/\sqrt{\lambda\mu}]$ *with respect to its variables* λ *and* μ*, respectively, evaluated at* $\lambda = \mu$*, then differentiated again* k *times and finally its variable is set to* $\mu = 1$*.*

Refer to Appendix D.4 for a proof. The derivatives in (5.40) can be calculated in the form of a finite sum

$$\Phi_{ab}^{k} = \sqrt{2}(-1)^{a+b}\,2^{-2a-2b-k}\sum_{j=0}^{a+b+k-1}\xi_{j}^{abk}, \tag{5.41}$$

where $a+b+k \geq 1$ and ξ_{j}^{abk} are recursively defined integers, refer to (D.6) in Appendix D.5. Substituting ℓ for 2ℓ in (5.38), the matrix elements $[\Pi_{\mathrm{BJ}}]_{mn}$ then depend only on these integers ξ_{j}^{abk} via the finite sum

$$[\Pi_{\mathrm{BJ}}]_{mn} = \gamma_{mn}\sum_{k=0}^{n}\sum_{\ell=0}^{(m-n)/2}[\sum_{j}\xi_{j}^{a\ell k}]\,(-1)^{\ell+m-n}\binom{m}{n-k}\binom{m-n}{2\ell}/k!,$$

where $\gamma_{mn} := 2^{[-(m-n)+1]/2}\sqrt{n!/m!}$ for $m \in \{n, n+4, n+8, \dots\}$ and $a = (m-n-2\ell)/2$.

Figure 5.1(a) shows the first 8×8 entries of $[\Pi_{\mathrm{BJ}}]$. One observes the following structure: only every fourth off-diagonal is non-zero, the matrix is real and symmetric, and the entries along every diagonal and off-diagonal decrease in their absolute value. In particular, the diagonal elements of Π_{BJ} admit the following special property.

Proposition 5.3. *For every* $n \in \{0,1,2,\dots\}$*, the diagonal entries of* Π_{BJ} *in the Fock basis are*

$$[\Pi_{\mathrm{BJ}}]_{nn} = \operatorname{arcsinh}(1) - \sqrt{2}\sum_{k=0}^{n-1}\frac{(-1)^{k}}{k+1}\sum_{m=0}^{\lfloor\frac{k}{2}\rfloor}\binom{2m}{m}\Big(\frac{-1}{4}\Big)^{m}. \tag{5.42}$$

In particular, $[\Pi_{\mathrm{BJ}}]_{nn} \to 0$ *as* $n \to \infty$*. For a proof we refer to Appendix D.6.*

Also note that the sum of these decreasing diagonal entries results in a trace $\mathrm{Tr}[\Pi_{\mathrm{BJ}}] = 1/2$ (Property 5.6) in the number-state basis. However, this trace does not necessarily exist in an arbitrary basis, as Π_{BJ} is not a trace-class operator.

(a)

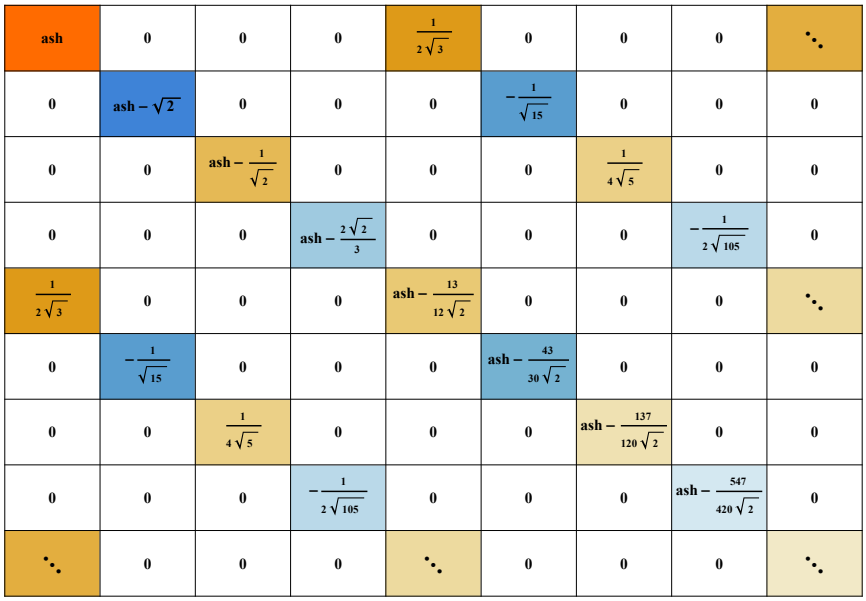

(b)

$M_{0,0}=0$	$M_{0,1}=4$	$M_{0,2}=432$	$M_{0,3}=144960$	$M_{0,4}=100074240$	$M_{0,5}=117361198080$	$\cdots$
$M_{1,0}=-1$	$M_{1,1}=-8$	$M_{1,2}=-1248$	$M_{1,3}=-520320$	$M_{1,4}=-418844160$	$M_{1,5}=-553081374720$	$\cdots$
$M_{2,0}=-\frac{1}{2}$	$M_{2,1}=6$	$M_{2,2}=1320$	$M_{2,3}=682080$	$M_{2,4}=641208960$	$M_{2,5}=955751892480$	$\cdots$
$M_{3,0}=-\frac{2}{3}$	$M_{3,1}=-4$	$M_{3,2}=-1200$	$M_{3,3}=-759360$	$M_{3,4}=-829059840$	$M_{3,5}=-1390797112320$	$\cdots$
$M_{4,0}=-\frac{13}{24}$	$M_{4,1}=\frac{19}{2}$	$M_{4,2}=3330$	$M_{4,3}=2367960$	$M_{4,4}=2838477600$	$M_{4,5}=5147874103680$	$\cdots$
$M_{5,0}=-\frac{43}{60}$	$M_{5,1}=-15$	$M_{5,2}=-6372$	$M_{5,3}=-5199600$	$M_{5,4}=-6938809920$	$M_{5,5}=-13741845384960$	$\cdots$
$\vdots$	$\vdots$	$\vdots$	$\vdots$	$\vdots$	$\vdots$	$\ddots$

Figure 5.1: (a) The first 8×8 matrix elements of the Born-Jordan parity operator from Eq. (5.38) where ash denotes $\operatorname{arcsinh}(1)$. (b) The first 6×6 elements of the recursive sequence that defines the Born-Jordan parity operator via Eq. (5.43). Orange and blue colors represent positive and negative values, respectively, while the color intensity reflects the absolute value of the corresponding numbers.

In the following, we specify a more convenient form for the calculation of these matrix elements, i.e. a direct recursion without summation, which is based on the following conjecture (see Appendix D.7).

Conjecture 5.1. *The non-zero matrix elements*

$$[\Pi_{\mathrm{BJ}}]_{k+4\ell,k} = [\Pi_{\mathrm{BJ}}]_{k,k+4\ell} = \Gamma_{k\ell}\,[M_{k\ell} + \delta_{\ell 0}\,\mathrm{arcsh}(1)/\sqrt{2}], \tag{5.43}$$

of the Born-Jordan parity operator are determined by a set of rational numbers $M_{k\ell}$ where $\Gamma_{k\ell} = 2^{-2\ell+1/2}\sqrt{k!/(k+4\ell)!}$ and $k,\ell \in \{0,1,2,\dots\}$. The indexing is specified relative to the diagonal (where $\ell = 0$) and $\delta_{\ell m}$ is the Kronecker delta. The rational numbers $M_{k\ell}$ can be calculated recursively using only 8 numbers as initial conditions, refer to Appendix D.7 for details. This form does not require a summation.

Figure 5.1(b) shows the first 6×6 elements of the recursive sequence of rational numbers $M_{k\ell}$. The first column of M_{k0} corresponds to the diagonal of the matrix $[\Pi_{\mathrm{BJ}}]_{mn}$ from Figure 5.1(a). For example, for $k = 5$ one obtains $M_{5,0} = -43/60$, which corresponds to $[\Pi_{\mathrm{BJ}}]_{5,5} = \Gamma_{5,0}[M_{5,0} + \delta_{0,0}\,\mathrm{arcsh}(1)/\sqrt{2}]$ and $\Gamma_{5,0} = \sqrt{2}$, and therefore $[\Pi_{\mathrm{BJ}}]_{5,5} = -43\sqrt{2}/60 + \mathrm{arcsh}(1)$ as detailed in Figure 5.1(a).

The direct recursion in Conjecture 5.1 enables us to conveniently and efficiently calculate the matrix elements $[\Pi_{\mathrm{BJ}}]_{mn}$ and we have verified the correctness of this approach for up to 6400 matrix elements, i.e. by calculating a matrix representation of size 80×80. This facilitates an efficient calculation and plotting of Born-Jordan distributions for harmonic oscillator systems, such as in quantum optics [182, 108, 171]. Note that a recursively calculated 80×80 matrix representation, which we have verified with exact calculations, is sufficient for most physical applications, i.e., Figures 5.2 and 5.3 (below) were calculated using 30×30 matrix representations. However, a matrix representation of size 2000×2000 can be easily calculated on a notebook using the recursive method. Numerical evidence shows that the matrix representation of Π_{BJ} can be well-approximated by a low-rank matrix, i.e, diagonalizing the matrix Π_{BJ} reveals only very few significant eigenvalues. In particular, the sum of squares of the first 9 eigenvalues corresponds to approximately 99.97% of the sum of squares of all the eigenvalues of a 2000×2000 matrix representation.

5.9 Example quantum states

Matrix representations of parity operators are used to conveniently calculate phase-space representations for bosonic quantum states via their associated Laguerre polynomial decompositions. The s-parametrized distribution functions of Fock states $|n\rangle$ are sums

$$F_{|n\rangle}(\Omega, s) = \sum_{\mu=0} |[\mathcal{D}(\Omega)]_{n\mu}|^2\,[\Pi_s]_{\mu\mu}$$

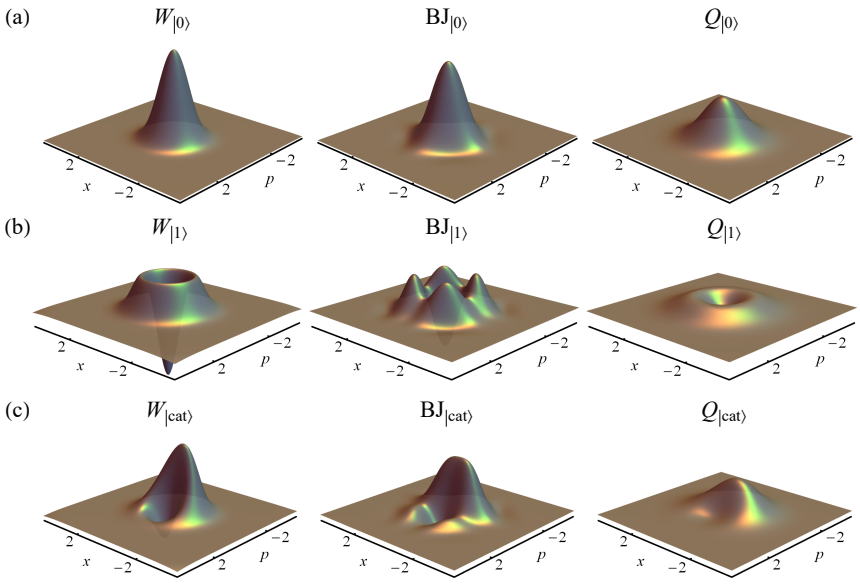

Figure 5.2: (a) and (b) Wigner, Born-Jordan, and Husimi Q phase-space plots of the number states $|0\rangle$ and $|1\rangle$ (which are eigenstates of the quantum harmonic oscillator). (c) Corresponding phase-space plots of the Schrödinger cat state $|\mathrm{cat}\rangle = (|0\rangle+|1\rangle)/\sqrt{2}$ (which is a superposition of the previous states).

of the associated Laguerre polynomials from (5.8), which are weighted by their parity operator elements. The corresponding phase-space functions are radially symmetric as the function $|[\mathcal{D}(\Omega)]_{n\mu}|^2$ depends only on the radial distance x^2+p^2. The Wigner function in Fig. 5.2(a)-(b) is radially symmetric and shows strong oscillations, which are sometimes regarded as a quantum-mechanical feature [171].

In contrast, the Born-Jordan parity operator is not diagonal in the number state representation and it can be written in terms of projectors as $\Pi_{\mathrm{BJ}} = \sum_{\mu=0}[\Pi_{\mathrm{BJ}}]_{\mu\mu}|\mu\rangle\langle\mu| + \sum_{\mu=0}\sum_{\nu=1}[\Pi_{\mathrm{BJ}}]_{\mu,4\nu}\left(|\mu{+}4\nu\rangle\langle\mu| + |\mu\rangle\langle\mu{+}4\nu|\right)$, and the Born-Jordan distribution of number states $|n\rangle$ is given by

$$F_{|n\rangle}(\Omega,\mathrm{BJ}) = \sum_{\mu=0} |[\mathcal{D}]_{n\mu}|^2\,[\Pi_{\mathrm{BJ}}]_{\mu\mu} \tag{5.44}$$

$$+ \sum_{\mu=0}\sum_{\nu=1} 2\,\Re([\mathcal{D}]_{n\mu}([\mathcal{D}]_{n,\mu+4\nu})^*)[\Pi_{\mathrm{BJ}}]_{\mu,\mu+4\nu}. \tag{5.45}$$

The Born-Jordan distribution of coherent states, i.e. the displaced vacuum states, closely matches the Wigner functions, see Fig. 5.2(a). The first part in Eq. (5.44) contains the diagonal elements of the parity operator which correspond to the radially symmetric part of $F_{|n\rangle}(\Omega,\mathrm{BJ})$, see Fig. 5.3(b) (left). The second part in Eq. (5.45) results in a radially non-symmetric function, see Fig. 5.3(b) (right). The radially symmetric parts are quite similar to the Wigner function and have $n+1$ wave fronts enclosed by the Bohr-Sommerfeld band [171, 77], i.e. the ring with radius $\sqrt{2n{+}1}$. The radially non-symmetric functions have $n+1$ local maxima along the outer squares, i.e. along phase-space cuts at the Bohr-Sommerfeld distance $x, p \propto \sqrt{2n{+}1}$. The sum of these two contributions is the Born-Jordan distribution and it is not radially symmetric for number states, see Fig. 5.3(a).

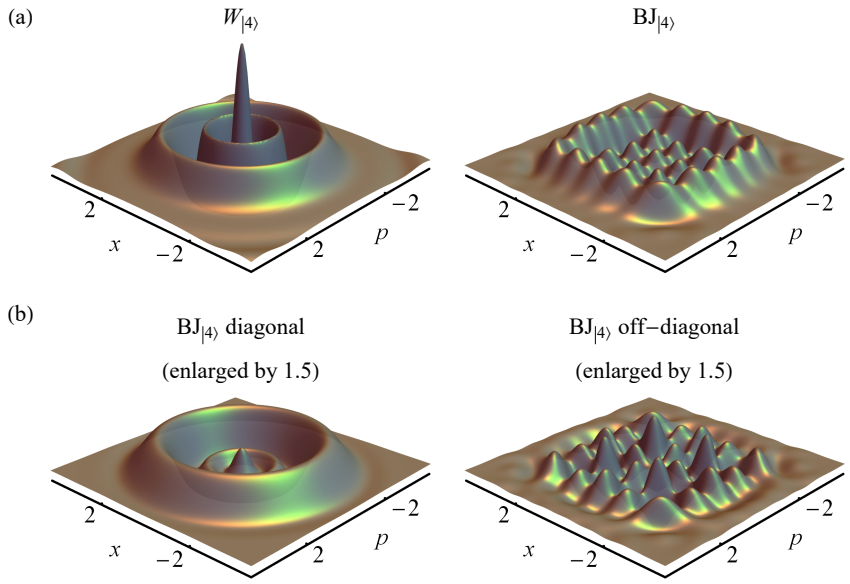

Figure 5.3: (a) Wigner and Born-Jordan phase-space plots of the number state $|4\rangle$. (b) The Born-Jordan distribution is decomposed into functions that correspond to diagonal and off-diagonal entries of the parity operator matrix.

5.10 Conclusion

We have introduced parity operators Π_θ which give rise to a rich family of phase-space distribution functions of quantum states. These phase-space functions have previously been defined in terms of convolutions, integral transformations, or Fourier transformations, and parity operators now allow for direct calculations as quantum-mechanical expectation values. We motivate the name "parity operator" as these are indeed compositions $\Pi_\theta = A_\theta \circ \Pi$ of the usual parity operator and some geometric or physical transformation. We detailed them for various phase spaces and, in particular, for the Born-Jordan distribution. We have also obtained a generalized spectral decomposition of the Born-Jordan parity operator, proved its boundedness, and calculated its explicit matrix representation in the number state basis. The latter will be useful to connect our results with applications in (e.g.) quantum optics, where our approaches relying on squeezing operators and the number-state representation are conceptually important.

APPENDIX A

Appendix of Chapter 2

A.1 Proof of Theorem 2.1

The following proof is based on the technique and results obtained in [16]. In particular[1], a limit of Clebsch-Gordan coefficients was proved in [16] as

$$\lim_{J\to\infty}\sum_{j=0}^{2J}\Delta_{j,n}^{J}=2,\quad\text{with}\quad\Delta_{j,n}^{J}=\sqrt{(2j{+}1)/(2J{+}1)}\,C^{j0}_{J(J-n),J(n-J)}. \tag{A.1}$$

We will use the following partial results up to minor modifications while calculating an explicit rate of convergence. In particular, the Clebsch-Gordan coefficient $\Delta_{j,n}^{J}$ approximately factorizes into a product

$$\Delta_{j,n}^{J}=\Lambda_n(x_j)\Delta_{j,0}^{J}+\mathcal{O}(n^2J^{-1}),\text{where the statring term is} \tag{A.2}$$

$$\Delta_{j,0}^{J}=\tfrac{2j+1}{\sqrt{2J+1}}(2J)!\,[(2J{+}j{+}1)!\,(2J{-}j)!\,]^{-1/2}, \tag{A.3}$$

and the function $\Lambda_n(x_j)=(-1)^nL_n(x_j)$ is the Laguerre polynomial with $x_j:=\frac{j(j+1)}{2J+1}$. We also correct an error in [16] as the correct form of (41) should be as in (A.3).

We now apply these partial results for Clebsch-Gordan coefficients to the parity operators in Result 2.1. Let us expand matrix elements of the parity operator M_s form Result 2.1. In

[1] we harmonize notations with [16] by substituting $S\to J$ and $l\to j$

particular, Clebsch-Gordan coefficients from the text after Result 2.1 can be reindexed via

$$[\mathrm{T}_{j0}]_{mm} = \sqrt{(2j+1)/(2J+1)}\, C^{Jm}_{Jm,j0} = (-1)^{J-m} C^{j0}_{Jm,J(-m)}. \tag{A.4}$$

Matrix elements are then related to $\Delta^J_{j,n}$ with the substitution $m = J - n$

$$[M_s]_{nn} = \frac{1}{R}\sum_{j=0}^{2J}\sqrt{\tfrac{2j+1}{4\pi}}(\gamma_j)^{-s}(-1)^n C^{j0}_{J(J-n),J(-(n-J)} \tag{A.5}$$

$$= \frac{1}{R}\sum_{j=0}^{2J}\sqrt{\tfrac{2j+1}{4\pi}}(\gamma_j)^{-s}(-1)^n \sqrt{(2J+1)/(2j+1)}\Delta^J_{j,n} \tag{A.6}$$

$$= \frac{1}{R}\sqrt{\tfrac{2J+1}{4\pi}}(-1)^n \sum_{j=0}^{2J}(\gamma_j)^{-s}\Delta^J_{j,n} = \sqrt{\tfrac{2J+1}{2J}}(-1)^n \sum_{j=0}^{2J}(\gamma_j)^{-s}\Delta^J_{j,n} \tag{A.7}$$

Recall now the explicit form of γ_j form the text after Result 2.1 with $R := \sqrt{J/(2\pi)}$. One can relate γ_j to $\Delta^J_{j,0}$ using (A.3)

$$\gamma_j = R\sqrt{4\pi}(2J)!\,[(2J+j+1)!\,(2J-j)!\,]^{-1/2} = \sqrt{2J}\tfrac{\sqrt{2J+1}}{2j+1}\,\Delta^J_{j,0}. \tag{A.8}$$

We can now substitute $\Delta^J_{j,0} = \frac{2j+1}{\sqrt{2J(2J+1)}}\gamma_j$ into (A.2), which results in the form

$$\Delta^J_{j,n} = \tfrac{2j+1}{\sqrt{2J(2J+1)}}\Lambda_n(x_j)\gamma_j + \mathcal{O}(n^2J^{-1}), \tag{A.9}$$

which can be substituted back to (A.7) as

$$[M_s]_{nn} = (-1)^n \sum_{j=0}^{2J}(\gamma_j)^{1-s}\sqrt{\tfrac{2J+1}{2J}}\tfrac{2j+1}{\sqrt{2J(2J+1)}}\Lambda_n(x_j) + \mathcal{O}(n^2J^{-1}). \tag{A.10}$$

Let us collect the prefactors in this equation, which finally have the form

$$\sqrt{\tfrac{2J+1}{2J}}\tfrac{2j+1}{\sqrt{2J(2J+1)}} = \tfrac{2j+1}{2J} = \tfrac{2(j+1)}{2J+1} + \mathcal{O}(J^{-1}) = \Delta(x_j) + \mathcal{O}(J^{-1}), \tag{A.11}$$

where the last equality establishes the connection with $\Delta(x_j) := x_{j+1} - x_j$. We therefore obtain the following sum for the matrix elements

$$[M_s]_{nn} = (-1)^n \sum_{j=0}^{2J}(\gamma_j)^{1-s}\Lambda_n(x_j)\Delta(x_j) + \mathcal{O}(n^2J^{-1}). \tag{A.12}$$

We now utilize the asymptotic expansion form (C.8) up to a minor modification, which does not change the order of convergence, i.e.,

$$\gamma_j = \exp\left[-\tfrac{1}{2}j(j+1)/(2J+1)\right] + \mathcal{O}(J^{-1}) = \exp\left[-\tfrac{1}{2}x_j\right] + \mathcal{O}(J^{-1}), \tag{A.13}$$

and leads to the following expression for the matrix elements with $\Lambda_n(x_j) = (-1)^n L_n(x_j)$

$$[M_s]_{nn} = \sum_{j=0}^{2J}\exp\left[-\tfrac{1-s}{2}x_j\right]L_n(x_j)\Delta(x_j) + \mathcal{O}(n^2J^{-1}). \tag{A.14}$$

Let us now calculate the limit of these matrix elements with first fixing $n \in \mathbb{N}$, i.e. it does not depend on J

$$\lim_{J\to\infty} [M_s]_{nn} = \lim_{J\to\infty} \sum_{j=0}^{2J} \Delta(x_j) \exp\left[-\tfrac{1-s}{2} x_j\right] L_n(x_j) \tag{A.15}$$

$$= \int_0^\infty \exp\left[-\tfrac{1-s}{2} x\right] L_n(x) \mathrm{d}x, \tag{A.16}$$

where the second equality is the limiting case of a Riemann sum as an integral, which can be evaluated using Eq. 44 in [16] as

$$\int_0^\infty e^{-x/t} L_n(x) \mathrm{d}x = t(1-t)^n. \tag{A.17}$$

Substituting $t = \frac{2}{1-s}$ finally concludes the proof via

$$\lim_{J\to\infty} [M_s]_{nn} = \tfrac{2}{1-s}(1 - \tfrac{2}{1-s})^n = 2(-1)^n \frac{(1+s)^n}{(1-s)^{n+1}} = [\Pi_s]_{nn}. \tag{A.18}$$

Numerical examples are provided in Figure 2.3.

A.2 Proof of Theorem 2.2

The Q function $Q_{|JJ\rangle} := F_{|JJ\rangle}(\Omega, -1)$ of the spin-up state has the convenient form

$$F_{|JJ\rangle}(\Omega, -1) = |D^J_{JJ}|^2 = \cos(\theta/2)^{4J}. \tag{A.19}$$

Using the definition of $\square(s)$ from (4.41) which translates between different s-parametrized phase-space representations $F_{|JJ\rangle}(\Omega, s)$, one obtains

$$F_{|JJ\rangle}(\Omega, s) = \square(s+2)\, F_{|JJ\rangle}(\Omega, -1) = \square(s+2)\, \cos(\theta/2)^{4J}. \tag{A.20}$$

Let us now substitute $\cos(\theta/2)^{4J} = \exp[4J \ln\cos(\theta/2)]$, where the Taylor expansion of the function $\ln\cos(\theta/2) = -\frac{\theta^2}{8} - \frac{\theta^4}{192} + \mathcal{O}(\theta^6)$, results in the relation

$$\cos(\theta/2)^{4J} = \exp[-J\theta^2/2 - J\theta^4/48 + \dots]. \tag{A.21}$$

This exponential function can be expanded asymptotically via making the change of variables $\alpha = \sqrt{J/2}\,\theta\, e^{-i\phi}$ that results in $\theta^2 = 2/J|\alpha|^2$

$$\begin{aligned}
\exp[-J\theta^2/2 - J\theta^4/48 + \dots] &= \exp[-|\alpha|^2] \exp[-|\alpha|^4/(12J) + \dots] \\
&= \exp[-|\alpha|^2] \left(1 - |\alpha|^4/(12J) + \mathcal{O}(|\alpha|^6/J^2)\right) \\
&= \exp[-|\alpha|^2] - |\alpha|^4/(12J) \exp[-|\alpha|^2] + \mathcal{O}(|\alpha|^6/J^2).
\end{aligned}$$

This is a sum, the first term of which $\exp[-|\alpha|^2]$ does not depend explicitly on J and all other terms depend inversely on J and have the general form $c|\alpha|^m J^{-n} \exp[-|\alpha|^2]$, with

suitable coefficients $m, n \in \mathbb{N}$ and bounded $c \in \mathbb{R}$. The Gaussian function (it is a Schwartz function) has the convenient property that for any $m \in \mathbb{N}$ and bounded $c_k \in \mathbb{R}$, all terms of the form $c_k\,|\alpha|^m \exp[-|\alpha|^2]$ are bounded in absolute value and decay to zero for $|\alpha| \to \infty$. One therefore obtains the limit

$$\lim_{J\to\infty}[\cos(\theta/2)^{4J}] = \exp[-|\alpha|^2] + \lim_{J\to\infty}\sum_{n,m,k=1}^{\infty} c_k\,|\alpha|^m J^{-n}\exp[-|\alpha|^2] = \exp[-|\alpha|^2].$$

We now substitute back the expansion of the spin-up state into (A.20)

$$F_{|JJ\rangle}(\Omega, s) = \Box(s+2)\,\exp[-|\alpha|^2] + \sum_{n,m,k=1}^{\infty} c_k\,|\alpha|^m J^{-n}\,\Box\,(s+2)\exp[-|\alpha|^2], \qquad \text{(A.22)}$$

and note that the operator $\Box(s+2)$ can be applied to $\exp[-|\alpha|^2]$, as all of its derivatives are bounded in absolute value, and let us therefore denote sum as $\mathcal{O}(J^{-1})$. We can now apply the assymptotic expansion (4.45) of the differential operator $\Box(s+2)$ which yields

$$F_{|JJ\rangle}(\Omega, s) = \exp[\tfrac{-(1+s)}{2}\,\partial_{\alpha^*}\partial_\alpha]\exp[-|\alpha|^2] + \mathcal{O}(J^{-1}) = F_{|0\rangle}(\Omega, s) + \mathcal{O}(J^{-1}). \qquad \text{(A.23)}$$

Here the second equality proves the statement of Theorem 2.2 using that

$$\lim_{J\to\infty}[F_{|JJ\rangle}(\Omega, s)] = \exp[\tfrac{-(1+s)}{2}\,\partial_{\alpha^*}\partial_\alpha]\exp[-|\alpha|^2] = F_{|0\rangle}(\Omega, s) \qquad \text{(A.24)}$$

which follows from the well-known differential relation [50, 11, 12]

$$\exp[\tfrac{-(1+s)}{2}\,\partial_{\alpha^*}\partial_\alpha]\exp[-|\alpha|^2] = \tfrac{2}{(1-s)}\exp[\tfrac{2}{(s-1)}|\alpha|^2]. \qquad \text{(A.25)}$$

This differential relation can be shown using the Fourier transform of Gaussian functions

$$\exp[-|\alpha|^2] = \int \exp[-|\beta|^2]\exp[\alpha\beta^* - \alpha^*\beta]\mathrm{d}^2\beta, \qquad \text{(A.26)}$$

which allows for evaluating the derivatives

$$(\partial_{\alpha^*}\partial_\alpha)^n \exp[-|\alpha|^2] = \int \exp[-|\beta|^2](-|\beta|^2)^n \exp[\alpha\beta^* - \alpha^*\beta]\mathrm{d}^2\beta, \qquad \text{(A.27)}$$

and substituting this into the power series of derivatives yields

$$\begin{aligned}
&\exp[\tfrac{-(1+s)}{2}\,\partial_{\alpha^*}\partial_\alpha]\exp[-|\alpha|^2] \\
&= \sum_n \left(\tfrac{-(1+s)}{2}\right)^n /n! \int \exp[-|\beta|^2](-|\beta|^2)^n \exp[\alpha\beta^* - \alpha^*\beta]\mathrm{d}^2\beta \\
&= \int \exp[-|\beta|^2]\exp[\tfrac{(1+s)}{2}|\beta|^2]\exp[\alpha\beta^* - \alpha^*\beta]\mathrm{d}^2\beta \\
&= \int \exp[\tfrac{(s-1)}{2}|\beta|^2]\exp[\alpha\beta^* - \alpha^*\beta]\mathrm{d}^2\beta = \tfrac{2}{(1-s)}\exp[\tfrac{2}{(s-1)}|\alpha|^2].
\end{aligned}$$

This concludes the proof via the Fourier transform in the last equality, which converges for $s < 1$, and yields $\delta^{(2)}(\alpha)$ for $s = 1$, as expected. Numerical examples are provided in Figure 2.4.

APPENDIX B

Appendix of Chapter 3

B.1 Tensor operators, embedded operators, and normalization factors

Here, we provide a short tutorial on tensor operators, embedded operators, and normalization factors as far as they are used in Secs. 3.4, 3.5, and 3.6. The four single-spin tensor operators $\mathrm{T}_{00} = \mathrm{Id}/\sqrt{2}$, $\mathrm{T}_{1,-1}$, T_{10}, and T_{11} from Eq. (3.4) span the space of all 2×2 matrices, and they conform to the defining relation in Eq. (3.5). Any 2×2 matrix A can be expanded in terms of the tensor operators T_{jm} as $A = \sum_{j\in\{0,1\}} \sum_{-j\leq m\leq j} \mathrm{Tr}(\mathrm{T}_{jm}^{\dagger} A)\, \mathrm{T}_{jm}$. This follows since tensor operators are chosen as orthonormal, i.e., the product $\mathrm{T}_{jm}^{\dagger}\mathrm{T}_{j'm'}$ of any two of them has trace one for identical operators with $j = j'$ and $m = m'$, and trace zero otherwise. However, Cartesian product operators, such as I_x are only orthogonal, and not normalized [e.g. $\mathrm{Tr}(I_x^{\dagger} I_x) = 1/2$].

Operators for a two-spin system can be decomposed into sums of tensor products $\mathrm{T}_{j_1 m_1} \otimes \mathrm{T}_{j_2 m_2}$ of two 2×2 matrices. There are sixteen linearly independent tensor product operators of this form, providing an orthonormal basis of 4×4 matrices (cf. Lemma 3.2). The tensor product operators can be divided into four subsets depending on which spins they act on: The normalized identity operator $\mathrm{T}_{00} \otimes \mathrm{T}_{00}$ acts on no spin at all. The normalized linear operators $\mathrm{T}_{1m} \otimes \mathrm{T}_{00}$ with $m \in \{-1, 0, 1\}$ act on the first spin, and $\mathrm{T}_{00} \otimes \mathrm{T}_{1m}$ acts on the second

Table B.1: Cartesian product operators in a coupled two-spin system. Any linear combination of operators in the same column or row remains a product operator.

Id_4	I_{1x}	I_{1y}	I_{1z}
I_{2x}	$I_{1x}I_{2x}$	$I_{1y}I_{2x}$	$I_{1z}I_{2x}$
I_{2y}	$I_{1x}I_{2y}$	$I_{1y}I_{2y}$	$I_{1z}I_{2y}$
I_{2z}	$I_{1x}I_{2z}$	$I_{1y}I_{2z}$	$I_{1z}I_{2z}$

one. Finally, the normalized bilinear operators $\mathrm{T}_{1m_1} \otimes \mathrm{T}_{1m_2}$ act on both spins ($m_1, m_2 \in \{-1, 0, 1\}$).

Similarly, one can also introduce embedded operators $\mathrm{T}^{\{1\}}_{1m} := \mathrm{T}_{1m} \otimes \mathrm{T}_{00}$ and $\mathrm{T}^{\{2\}}_{1m} := \mathrm{T}_{00} \otimes \mathrm{T}_{1m}$ which are single-spin operators embedded into 4×4 matrices (cf. Lemma 3.1). These embedded operators enable a description without (explicit) tensor products. This implies that a bilinear operator $\mathrm{T}_{j_1m_1} \otimes \mathrm{T}_{j_2m_2}$ can written as a matrix product of embedded operators with an additional normalization factor. For example, the tensor product

$$B = \mathrm{T}_{10} \otimes \mathrm{T}_{11} = \begin{pmatrix} \frac{1}{\sqrt{2}} & 0 \\ 0 & \frac{-1}{\sqrt{2}} \end{pmatrix} \otimes \begin{pmatrix} 0 & -1 \\ 0 & 0 \end{pmatrix} = \begin{pmatrix} 0 & \frac{-1}{\sqrt{2}} & 0 & 0 \\ 0 & 0 & 0 & 0 \\ 0 & 0 & 0 & \frac{1}{\sqrt{2}} \\ 0 & 0 & 0 & 0 \end{pmatrix}$$

is normalized. Using the normalized single-spin operators

$$\mathrm{T}^{\{1\}}_{10} = \begin{pmatrix} \frac{1}{2} & 0 & 0 & 0 \\ 0 & \frac{1}{2} & 0 & 0 \\ 0 & 0 & \frac{-1}{2} & 0 \\ 0 & 0 & 0 & \frac{-1}{2} \end{pmatrix} \text{ and } \mathrm{T}^{\{2\}}_{11} = \begin{pmatrix} 0 & \frac{-1}{\sqrt{2}} & 0 & 0 \\ 0 & 0 & 0 & 0 \\ 0 & 0 & 0 & \frac{-1}{\sqrt{2}} \\ 0 & 0 & 0 & 0 \end{pmatrix},$$

we can form the matrix product

$$\mathrm{T}^{\{1\}}_{10}\mathrm{T}^{\{2\}}_{11} = \begin{pmatrix} 0 & \frac{-1}{2\sqrt{2}} & 0 & 0 \\ 0 & 0 & 0 & 0 \\ 0 & 0 & 0 & \frac{1}{2\sqrt{2}} \\ 0 & 0 & 0 & 0 \end{pmatrix} = B/2,$$

which differs from $B = \mathrm{T}_{10} \otimes \mathrm{T}_{11}$ by a factor of 2; $B/2$ has a squared norm of $\mathrm{Tr}(B^\dagger B)/4 = 1/4$. The normalization factors for general spin systems are given in Table 3.4. Products of embedded single-spin operators commute if they act on different spins, e.g. $\mathrm{T}^{\{1\}}_{10}\mathrm{T}^{\{2\}}_{11} = \mathrm{T}^{\{2\}}_{11}\mathrm{T}^{\{1\}}_{10}$.

B.2 Visualization of Wigner functions

In this appendix, we shortly discuss certain properties of the visualization of Wigner functions introduced in Sec. 3.4. The Wigner functions of product operators in a two-spin system are in general of the form $\lambda f(\theta_1, \phi_1) g(\theta_2, \phi_2)$ with $\lambda \in \mathbb{C}$. This is visualized as two overlapping circles to reflect the product nature of the spherical functions. The first circle contains the Wigner function $\sqrt{\lambda} f(\theta_1, \phi_1)$, and the second one contains $\sqrt{\lambda} g(\theta_2, \phi_2)$. The prefactor λ is distributed equally, but different choices are possible, and the size of the visualized objects can vary assuming that λ stays constant.

If the desired operator is a linear combination of product operators, it is represented as a sum of product operators in the PROPS representation. However the decomposition of an operator into sums of product operators is not unique, consequently there are different visualizations possible for the same operator. In a system of N spins 1/2 there are 4^N independent basis operators, and these can be combined in order to minimize the number of product operators in a sum decomposition. We provide a mathematica package for computing with examples of Wigner functions of spin operators, their Poisson brackets, and the time evolution [1].

For a two-spin system there are sixteen independent product operators, but any operator can be decomposed into a sum of at most four product operators. This is verified using Table B.1 where basis operators are grouped such that any linear combination within the same row or column results again in a product operator, for example

$$a I_{2z} + b I_{1x} I_{2z} + c I_{1y} I_{2z} + d I_{1z} I_{2z} = (a\,\mathrm{Id} + b I_{1x} + c I_{1y} + d I_{1z}) I_{2z}. \tag{B.1}$$

B.3 Stratonovich postulates

We summarize the postulates on which the continuous Wigner representation for spins relies. Starting from the original set of postulates defined by Stratonovich [243], which are then generalized to the case of coupled spins.

B.3.1 Stratonovich postulates for a single spin

The Wigner representation for spins is a generalization of the flat phase-space representation (p, q) of quantum mechanics to the phase-space representation $(R\cos\theta, \phi)$ over the sphere. In the generalized Wigner representation, spin operators are mapped onto spherical functions. This mapping is based on the Stratonovich postulates [243], providing four fundamental requirements for pairs of operators and their corresponding Wigner functions. Let us denote

the Wigner function of an arbitrary spin operator A as W_A, then the postulates are given by

$$\begin{aligned}
&\text{(i)} && \text{linearity:} \quad A \to W_A \text{ is one-to-one,}\\
&\text{(ii)} && \text{reality:} \quad \text{if } B = A^\dagger, \text{ then } W_B = W_A^*,\\
&\text{(iiia)} && \text{normalization:} \quad \mathrm{Tr}(\mathrm{Id}A) = \int_{S^2} W_{\mathrm{Id}} W_A \mathrm{d}\Omega,\\
&\text{(iiib)} && \text{traciality:} \quad \mathrm{Tr}(B^\dagger A) = \int_{S^2} W_B^* W_A \mathrm{d}\Omega,\\
&\text{(iv)} && \text{covariance:} \quad W_{\mathcal{R}(A)}(\Omega) = W_A(\mathcal{R}^{-1}\Omega),
\end{aligned}$$

where $\mathrm{d}\Omega$ denotes the surface element $\sin\theta \mathrm{d}\theta\mathrm{d}\phi$ in the spherical phase space. A consequence of the postulate (ii) is that Wigner functions of a hermitian operator are real functions. The postulates (iiia) and (iiib) can be reinterpreted by introducing the scalar products $\langle B|A\rangle = \mathrm{Tr}(B^\dagger A)$ for matrices and $\langle W_B|W_A\rangle = \int_{S^2} W_B^* W_A \mathrm{d}\Omega$ for Wigner functions (by integrating over the unit sphere). Then, the postulates (iiia) and (iiib) can be summarized as $\langle B|A\rangle = \langle W_B|W_A\rangle$. The postulate (iv) determines the Wigner function of an operator A if A is rotated by a unitary conjugation resulting in $\mathcal{R}(A)$, then the arguments of the Wigner function (or equivalently the sphere) are rotated inversely by the same rotation.

B.3.2 Generalization of the Stratonovich postulates

We extend the Wigner formalism to multiple, coupled spins. The postulates (iii) and (iv) are generalized in order to interpret the Stratonovich postulates for the Wigner representation of N coupled spins as mapping operators onto sums of function on N spheres. The condition in postulate (iii) is extended to an integral $\int_{S_1^2}\cdots\int_{S_N^2} W_B^* W_A \mathrm{d}\Omega_1 \ldots \mathrm{d}\Omega_N$ over N spheres. For the PROPS representation, Postulate (iv) is generalized by interpreting $\mathcal{R}$ as an arbitrary rotation in the form of a product of local rotations as $\mathcal{R} = \prod_k^N \mathcal{R}_k$. An arbitrary local rotation $\mathcal{R}_k$ acting on spin k is described in the Wigner space as the inverse rotation of the kth sphere $W_A(\Omega_1, \ldots, \mathcal{R}_k^{-1}\Omega_k, \ldots \Omega_N)$ of the corresponding Wigner representation. The mapping of spin operators onto spherical functions described in [98] satisfies the generalized Stratonovich postulates under simultaneous rotations $\mathcal{R}$ built from equal rotations $\mathcal{R}_k$ of all spheres. Consequently, the current approach generalizes the rotational covariance criterion in [98] to arbitrary local rotations. Finally, the generalized postulates are

$$\begin{aligned}
&\text{(i)} && \text{linearity:} \quad A \to W_A \text{ is one-to-one,}\\
&\text{(ii)} && \text{reality:} \quad \text{if } B = A^\dagger, \text{ then } W_B = W_A^*,\\
&\text{(iiia)} && \text{normalization: } \mathrm{Tr}(\mathrm{Id}A) = \int\limits_{S_1^2 \ldots S_N^2}\!\!\cdots\!\!\int W_{\mathrm{Id}} W_A \prod_k^N \mathrm{d}\Omega_k,\\
&\text{(iiib)} && \text{traciality:} \quad \mathrm{Tr}(B^\dagger A) = \int\limits_{S_1^2 \ldots S_N^2}\!\!\cdots\!\!\int W_B^* W_A \prod_k^N \mathrm{d}\Omega_k,\\
&\text{(iv)} && \text{covariance:} \quad W_{\mathcal{R}(A)}(\Omega_1, \ldots, \Omega_N) = W_A(\mathcal{R}_1^{-1}\Omega_1, \ldots, \mathcal{R}_N^{-1}\Omega_N).
\end{aligned}$$

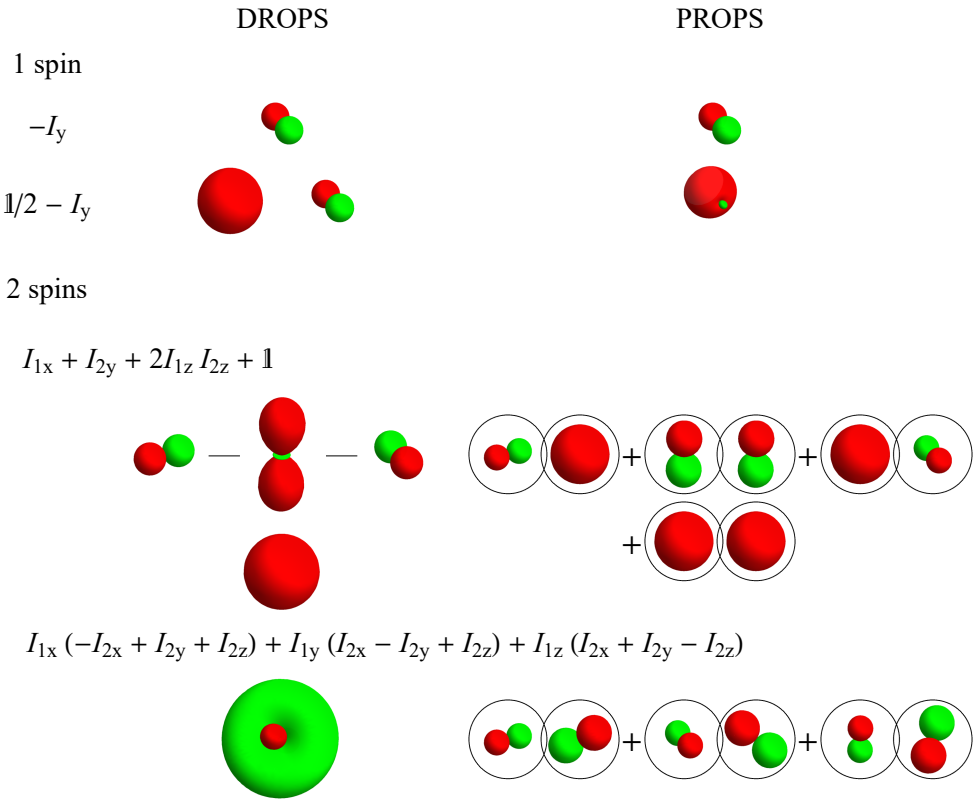

Figure B.1: (Color online) The DROPS representation using the LISA basis is compared to the PROPS representations. For a single spin $1/2$, the DROPS representation consists in general of two spherical function where the first one corresponds to the identity part Id_2 which acts on no spin at all and the second one corresponds in this example to the operator $-I_y$. Both contributions are combined in the PROPS representation. The DROPS representation of two coupled spins $1/2$ consists in general of four spherical functions: the identity part Id_4, linear operators such as I_{2x} and I_{2y} acting on the first and second spin, as well as bilinear operators such as $2I_{1z}I_{2z}$ acting on both spins. The number of product operators in the PROPS representation can be in certain cases reduced by combining some of its components, e.g., $I_{1x} + I_{2y} + 2I_{1z}I_{2z} + \mathrm{Id}_4$ equals to $(I_x{+}\mathrm{Id}_2/2) \otimes \mathrm{Id}_2 + \mathrm{Id}_2 \otimes (I_y{+}\mathrm{Id}_2/2) + 2I_{1z}I_{2z}$.[3]

B.4 Comparison to the DROPS representation

We compare our visualization technique with the so-called DROPS representation from [98] both of which represent operators of coupled spin systems in the form of a collection of spherical functions. A particular case of the DROPS representation is given by the LISA basis [98] which is spanned by a set of tensor operators $T^{(\ell)}_{jm}$ with $\ell \in L$. Each element $T^{(\ell)}_{jm}$ is mapped to a spherical harmonic Y_{jm} and transforms naturally under simultaneous rotations of all spins. The DROPS representation using the LISA basis provides a compact visualization of coupled spin operators by plotting $|L|$ spherical functions. Figure B.1 contains a comparison for spin operators of one and two spins.

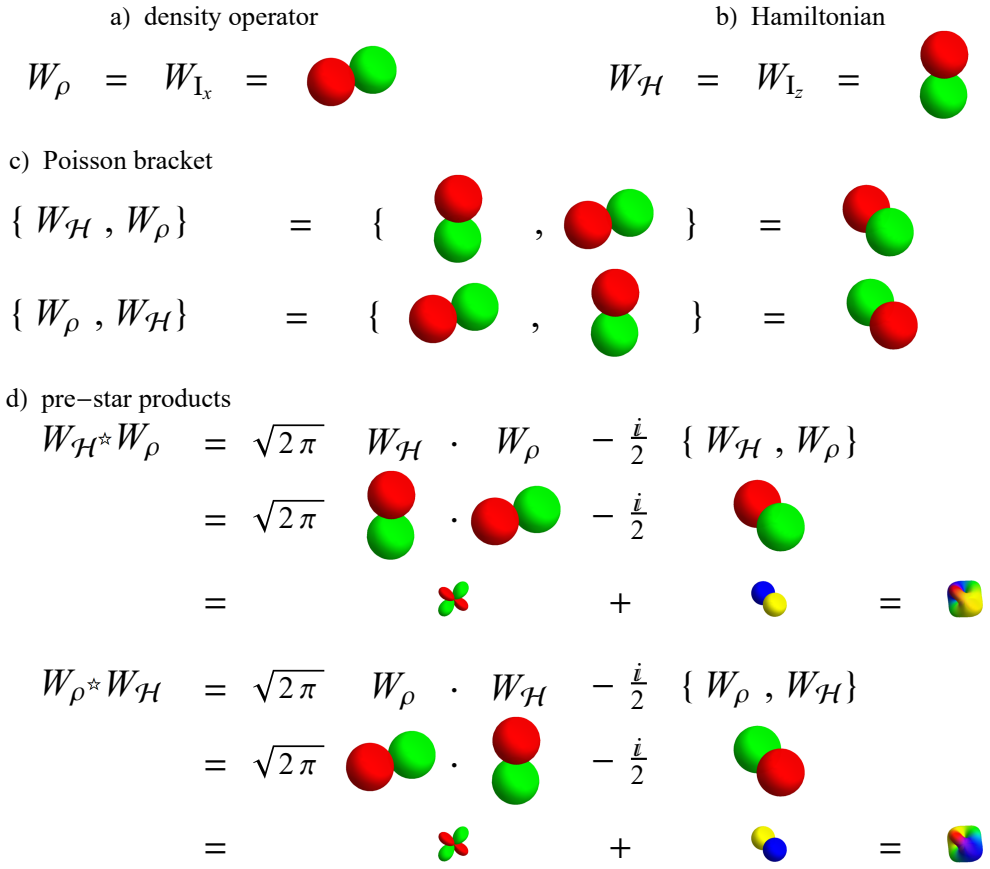

Figure B.2: (Color online) Graphical visualization of the equation of motion for a single spin $1/2$. a) and b) depict the Hamiltonian and deviation density matrix from Eq. (3.8). Individual steps illustrate how the equation of motion for a single spin $1/2$ in Figure B.3 g) [refer to Eq. (3.9)] is derived by specifying c) the Poisson brackets (c.f. Fig 3.1), d) and the pre-star products of the Wigner functions $W_{\mathcal{H}}$ and W_ρ. Refer also to Figure B.3.[3]

B.5 Time evolution of a single spin $1/2$

We further detail the derivation of the equation of motion for a single spin $1/2$ which had been deferred from Sec. 3.4.1.2 to this appendix. The Figures B.2-B.3 illustrate the individual steps required to derive the time evolution of the Wigner function for a single spin $1/2$: Subfigures a) and b) contain graphical representation of the Hamiltonian and density operator from Eq. (3.8). In Subfigure c), the Poisson bracket of $W_{\mathcal{H}}$ and W_ρ is computed following Fig. 3.1; the Poisson bracket is antisymmetric with respect to the order of its two arguments. The pre-star product is decomposed in Subfigure d) into a sum of the pointwise product and the Poisson bracket of $W_{\mathcal{H}}$ and W_ρ, and the summands are weighted by the prefactors $\sqrt{2\pi}$ and $-i/2$, respectively [see Eq. (3.47)]. In Subfigure e), the star product, which is the analog of the matrix product of the two Wigner functions $W_{\mathcal{H}}$ and W_ρ (see Sec. 3.5.2.3), is obtained by projecting the pre-star product onto spherical harmonics of rank-zero and one [refer to Eq. (3.48)]. Subfigure f) shows the star commutator as the star analog of the matrix commutator (see Sec. 3.5.2.3). Finally, Subfigure g) determines the time evolution of the density operator by specifying its time derivative. The result in this particular case conforms

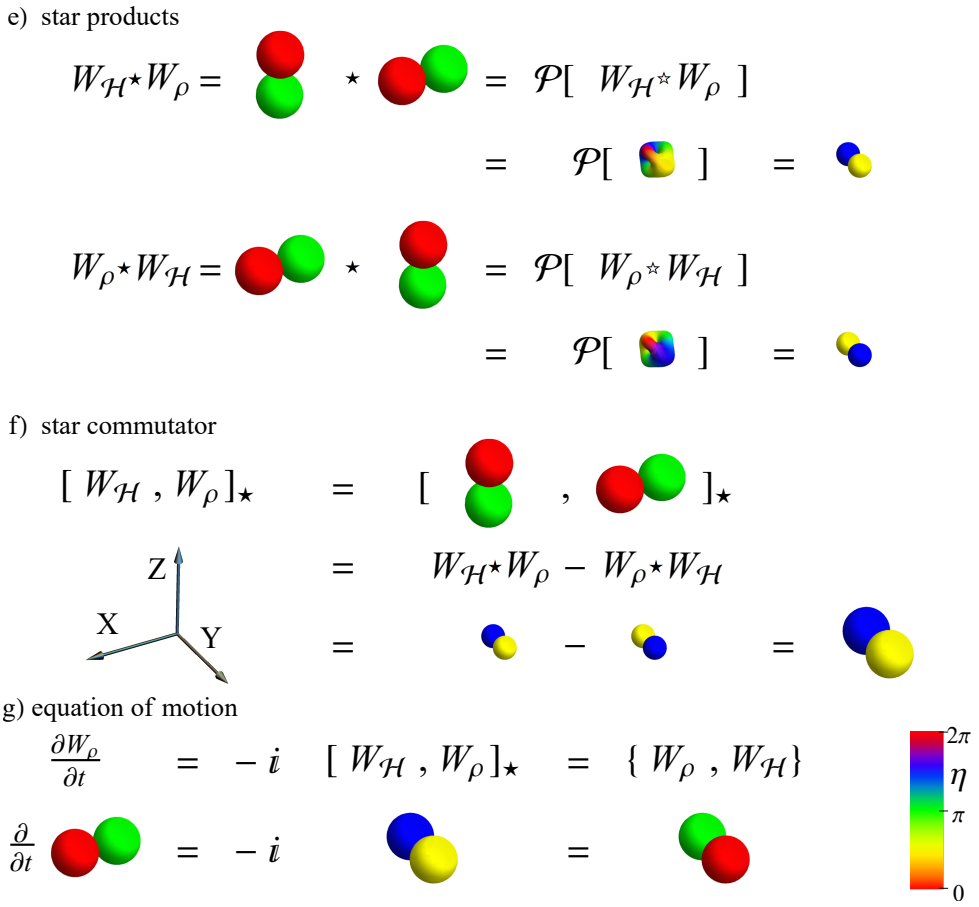

Figure B.3: (Color online) Continuation of Figure B.2. e) star products, f) the star commutator, and g) the equation of motions for the Wigner functions $W_{\mathcal{H}}$ and W_ρ. Refer to the main text for further details.[3]

with the general argument that the time evolution is given by the Poisson bracket of $W_{\mathcal{H}}$ and W_ρ.

B.6 Integral form of the star product

Similarly as in [253], we evaluate the integral form of the star product of Wigner functions corresponding to arbitrary operators A and B acting on a single spin J. Based on the explicit form of the kernel for the Wigner transformation in Eq. (3.25) and the expansion formula of tensor-operator matrix products in Eq. (3.38), we evaluate the explicit form of the trikernel. Let us first consider the matrix product AB of two arbitrary operators A and B of a spin J and the corresponding Wigner function W_{AB}, which is obtained according to Eq. (3.25) as

$$\mathcal{W}(AB) := W_{AB}(\theta,\phi) = \mathrm{Tr}[\Delta_J(\theta,\phi)AB]. \tag{B.2}$$

The definition of the integral star product is derived by substituting A and B in Eq. (B.2) with the formula for the inverse Wigner transform of W_A and W_B from Eq. (3.30). This leads to

$$W_{AB}(\theta,\phi) = W_A(\theta_1,\phi_1) \star W_B(\theta_2,\phi_2) = \int_{\theta_1,\theta_2,\phi_1,\phi_2\geq 0}^{\theta_1,\theta_2\leq\pi,\phi_1,\phi_2\leq 2\pi} \cdots \int \Delta_J^{(T)} W_A W_B \, \sin\theta_1 \sin\theta_2 \, \mathrm{d}\theta_1 \, \mathrm{d}\theta_2 \, \mathrm{d}\phi_1 \, \mathrm{d}\phi_2, \tag{B.3}$$

where $W_A := W_A(\theta_1,\phi_1)$ and $W_B := W_B(\theta_2,\phi_2)$ denote Wigner functions of A and B depending on different variables, and the trikernel is given by

$$\Delta_J^{(T)} = \mathrm{Tr}[\Delta_J(\theta,\phi)\Delta_J(\theta_1,\phi_1)\Delta_J(\theta_2,\phi_2)]. \tag{B.4}$$

Using the expansion formula in Eq. (3.38) to evaluate the explicit form of the trikernel, one obtains

$$\Delta_J^{(T)} = \sum_{\vec{j},\vec{m}} \mathrm{Y}^*_{j_1 m_1}(\theta_1,\phi_1)\mathrm{Y}^*_{j_2 m_2}(\theta_2,\phi_2) \sum_{L=|j_1-j_2|}^{n} Q^{(J)}_{j_1 j_2 L} C^{LM}_{j_1 m_1 j_2 m_2} \mathrm{Y}_{LM}(\theta,\phi), \tag{B.5}$$

where $\vec{j} = (j_1, j_2)$, $\vec{m} = (m_1, m_2)$ and $0 \leq j_1, j_2 \leq 2J$, and the upper limit n given as $n := \min(j_1{+}j_2, 2J)$; note $M = m_1{+}m_2$. With this form of the trikernel, Eq. (B.3) can be interpreted in the following way: Integrating over the product $W_A W_B$ multiplied by the trikernel, one obtains the decomposition of both W_A and W_B into spherical harmonics, and the Wigner transformation of the product ${}^J\mathrm{T}_{j_1,m_1}{}^J\mathrm{T}_{j_2,m_2}$ is obtained for each pair $\mathrm{Y}_{j_1 m_1}$ and $\mathrm{Y}_{j_2 m_2}$ of spherical harmonics.

APPENDIX C

Appendix of Chapter 4

C.1 Expansions of products of tensor operators

Adopting the notation of [159], the product of two irreducible tensor operators can be—similarly as in Equation 4.12—expanded as (see [254])

$$\mathrm{T}_{j_1 m_1}\mathrm{T}_{j_2 m_2} = \sum_{L=|j_1-j_2|}^{n} {}^{J}Q_{j_1 j_2 L}\, C^{LM}_{j_1 m_1 j_2 m_2}\mathrm{T}_{LM}. \tag{C.1}$$

The upper limit $n \coloneqq \min(j_1{+}j_2, 2J)$ of the summation is bounded by $2J$. We have set $M \coloneqq m_1{+}m_2$ and also use the Clebsch-Gordan coefficients $C^{LM}_{j_1 m_1, j_2 m_2}$ [192]. The coefficients ${}^{J}Q_{j_1 j_2 L}$ from [159] are proportional to Wigner 6-j symbols [192] and depend only on j_1, j_2, and L, but are independent of m_1, m_2, and M.

Similarly, the product of any two spin-weighted spherical harmonics can be decomposed into a sum of spin-weighted spherical harmonics (see Eq. 2.54 in [73])

$$\begin{aligned}\mathrm{Y}^{\eta_1}_{j_1 m_1}\mathrm{Y}^{\eta_2}_{j_2 m_2} = \sum_{L=|j_1-j_2|}^{j_1+j_2} (-1)^{M+\eta_3}\sqrt{\tfrac{(2j_1+1)(2j_2+1)(2L+1)}{4\pi}} \\ \times \begin{pmatrix} j_1 & j_2 & L \\ m_1 & m_2 & -M \end{pmatrix}\begin{pmatrix} j_1 & j_2 & L \\ -\eta_1 & -\eta_2 & \eta_3 \end{pmatrix}\mathrm{Y}^{\eta_3}_{LM}\end{aligned} \tag{C.2}$$

where the Wigner 3-j symbols [192] are used. The values of $M = m_1 + m_2$ and $\eta_3 = \eta_1 + \eta_2$ are bounded by $-L \leq M \leq L$ and $-L \leq \eta_3 \leq L$. Substituting the left-hand side of this equation with the definition of spin-weighted spherical harmonics ${}^{\eta_1}\mathrm{Y}_{j_1 m_1}$ and ${}^{\eta_2}\mathrm{Y}_{j_2 m_2}$ from Equation 4.15 while also assuming that $\eta_1 = -\eta_2 =: \eta$, one obtains the relation

$$(\eth^{\eta}\,\mathrm{Y}_{j_1 m_1})(\overline{\eth}^{\eta}\,\mathrm{Y}_{j_2 m_2}) = \sum_{L=|j_1-j_2|}^{j_1+j_2} (-1)^{M+\eta}\sqrt{\tfrac{(2j_1+1)(2j_2+1)(2L+1)}{4\pi}} \tag{C.3}$$

$$\times\, x^{j_2}_{\eta j_1} \begin{pmatrix} j_1 & j_2 & L \\ m_1 & m_2 & -M \end{pmatrix} \begin{pmatrix} j_1 & j_2 & L \\ -\eta & \eta & 0 \end{pmatrix} \mathrm{Y}_{LM}, \tag{C.4}$$

where the factor $x^{j_2}_{\eta j_1}$ can be obtained from Equation 4.15 and is determined by

$$x^{j_2}_{\eta j_1} = \sqrt{\tfrac{(j_2+\eta)!(j_1+\eta)!}{(j_2-\eta)!(j_1-\eta)!}}. \tag{C.5}$$

Finally, the explicit form of the factor κ in Equation 4.20-Equation 4.21 is now given by (with $M = m_1+m_2$)

$$\begin{aligned} {}^{\eta}\kappa^{L}_{j_1 m_1, j_2 m_2} =& (-1)^{M+\eta}\sqrt{\tfrac{(2j_1+1)(2j_2+1)(2L+1)}{4\pi}} \\ & \times\, x^{j_2}_{|\eta| j_1} \begin{pmatrix} j_1 & j_2 & L \\ m_1 & m_2 & -M \end{pmatrix} \begin{pmatrix} j_1 & j_2 & L \\ -\eta & \eta & 0 \end{pmatrix} \mathrm{Y}_{LM}. \end{aligned} \tag{C.6}$$

C.2 Proof of Result 4.1

We prove now Result 4.1. Both formulas in Equation 4.32 must satisfy the defining property Equation 4.14 of the star product. The expansions from Equation 4.20-Equation 4.21 result in the condition

$$K^{L}_{jm,j'm'} = \left[\frac{\gamma_L}{\gamma_j \gamma_{j'}}\right]^{\pm 1} \frac{1}{R} \sum_{\eta=0}^{2J} \lambda^{(\pm 1)}_{\eta}\; {}^{\pm\eta}\kappa^{L}_{j_1 m_1, j_2 m_2}$$

for $\lambda^{(\pm 1)}_{\eta}$ which holds for every j, m, j', m' with $j, j' \leq 2J$. This specifies an overdetermined linear system of equations for $\lambda^{(\pm 1)}_{\eta}$ which can be recognized as the matrix-vector equation $K = \kappa^{(\pm 1)}\,\lambda^{(\pm 1)}$. Here, the vector $\lambda^{(\pm 1)}$ has the entries $\lambda^{(\pm 1)}_{\eta}$ and every entry K_i of the vector K is given by a value of $K^{L_i}_{j_i m_i, j'_i m'_i}$ with $i \in \{1, 2, \ldots, (2J{+}1)^5\}$. The corresponding matrix $\kappa^{(\pm 1)}$ has the dimension $(2J{+}1) \times (2J{+}1)^5$ and rank $(2J{+}1)$. This linear system has a unique, exact solution and one obtains the coefficients in Equation 4.33.

C.3 Asymptotic expansion of weight factors

Detailed expansion formulas for Section 4.8.2 and Section 4.9.2 are computed in the following. The coefficients in Equation 4.33 can be expanded into the form

$$\lambda^{(-1)}_{\eta}\eta! = \frac{(2J-\eta)!}{(2J)!} = \prod_{k=0}^{\eta-1}(2J-k)^{-1} = \prod_{k=0}^{\eta-1}[(2J)^{-1} + k(2J)^{-2} + \mathcal{O}((2J)^{-3})],$$

where the second equality follows from the Taylor expansion of the function $(a+b)^{-1} = 1/a - b/a^2 + b^2/a^3 + \cdots$ with $a := 2J$ and $b := -k$ and $|b| < a$. Collecting the error terms as $(2J)^{-\eta+1} \sum_{k=0}^{\eta-1}[k\,(2J)^{-2}] = (2J)^{-\eta-1}[\eta(\eta-1)]/2$ yields the formula

$$\lambda_\eta^{(-1)}\eta! = (2J)^{-\eta} + (2J)^{-\eta-1}[\eta(\eta-1)] + \mathcal{O}((2J)^{-\eta-2}).$$

This results in the asymptotic expansion in Equation 4.34-Equation 4.35. Similarly, $\lambda_\eta^{(1)}$ is expanded as

$$\lambda_\eta^{(1)}(-1)^\eta\eta! = \frac{2J\,(2J)!}{(2J+\eta+1)!} = 2J\prod_{k=1}^{\eta+1}(2J+k)^{-1} = 2J\prod_{k=1}^{\eta+1}[(2J)^{-1} + k(2J)^{-2} + \mathcal{O}((2J)^{-3})],$$

which simplifies to the asymptotic expansion (which is used in Equation 4.36)

$$\lambda_\eta^{(1)}(-1)^\eta\eta! = (2J)^{-\eta} + (2J)^{-\eta-1}\,\tfrac{(\eta+1)(\eta+2)}{2} + \mathcal{O}((2J)^{-\eta-2}).$$

The coefficients in the definition of spin-weighted spherical harmonics in Equation 4.15 can similarly be expanded as

$$\sqrt{(j-\eta)!/(j+\eta)!} = \prod_{k=-\eta+1}^{\eta}(j+k)^{1/2} = \prod_{k=-\eta+1}^{\eta}[j^{1/2} + \tfrac{k}{2j^{1/2}} + \mathcal{O}(j^{-3/2})]$$

where the second equality is obtained from the Taylor expansion $(a+b)^{1/2} = a^{1/2}+b/(2a^{1/2})-b^2/(8a^{3/2}) + \cdots$ with $a := j$ and $b := k$ and $b < a$. This yields the expansion

$$\sqrt{(j-\eta)!/(j+\eta)!} = j^\eta + \tfrac{\eta}{2j^{1/2}} + \mathcal{O}(j^{-5/2}). \tag{C.7}$$

Following similar arguments, the factor γ_j, which is defined in Equation 4.11, can be in terms of $j(j+1)$ expanded into the exponential function

$$\gamma_j = \exp\left[-j(j+1)/(4J)\right] + \mathcal{O}(J^{-1}) = \sum_n [-j(j+1)/(4J)]^n/n! + \mathcal{O}(J^{-1}). \tag{C.8}$$

This expansion is used in Equation 4.43 to derive an approximation of the operator $\Box(s)$.

C.4 Proof of Result 4.3 and the associated expansion coefficients

We now prove Result 4.3 and determine the corresponding expansion coefficients $c_n(s)$. The coefficients $c_n(s)$ are uniquely determined by the values of γ_j^{1-s} and the condition

$$\gamma_j^{1-s} = \sum_{n=0}^{2J} c_n(s)\,[-j(j+1)]^n \quad \text{for } 0 \le j \le 2J. \tag{C.9}$$

This yields the linear system $V\,c(s) = \gamma(s)$ of equations where V is the Vandermonde matrix with entries $[V]_{nj} := [-j(j+1)]^n$ and its inverse V^{-1} can be computed analytically [35]. The entries of the vectors $c(s)$ and $\gamma(s)$ are given by $c_n(s)$ and γ_j^{1-s}, respectively. The exact, unique solution is determined by $V^{-1}\,\gamma(s) = c(s)$.

Note that simultaneously truncating the spherical-harmonics decomposition can also be achieved by enlarging the summation upper limit in Equation C.9 to $4J$. In that case, one has $\square(s)\mathrm{Y}_{jm} = 0$ for $2J < j \leq 4J$. Alternatively, a projection operator $\mathcal{P}_J$ from Result 2 of [159] can be applied to spin-J phase-space representations, where $\mathcal{P}_J := \sum_{n=0}^{4J} p_n\,(\eth\overline{\eth})^n$ and the coefficients p_n are computed from the linear system of equations

$$\sum_{n=0}^{4J} p_n\,[-j(j+1)]^n = \begin{cases} 1 & \text{for } 0 \leq j \leq 2J \\ 0 & \text{for } 2J < j \leq 4J \end{cases} \tag{C.10}$$

which is determined by the inverse Vandermonde matrix V^{-1}.

C.5 Asymptotic expansion of differential operators

C.5.1 Expansion formulas using polar and arc-length parametrizations

In this section, we show how the operators $\eth$ and $\overline{\eth}$ approach their infinite-dimensional counterparts given by the derivatives ∂_{α^*} and ∂_α. We consider the polar parametrization $\alpha = re^{i\phi}$ of the complex plane with $r = \sqrt{\alpha^*\alpha}$ and $\phi := \arg\alpha$. Using $\partial_\alpha = \frac{\partial r}{\partial\alpha}\partial_r + \frac{\partial\phi}{\partial\alpha}\partial_\phi$, the derivatives ∂_α and ∂_{α^*} can be expressed in the polar parametrization by substituting $\frac{\partial r}{\partial\alpha} = \frac{1}{2}e^{-i\phi}$ and $\frac{\partial\phi}{\partial\alpha} = \frac{-i}{2}e^{-i\phi}/r$ which results in

$$\partial_\alpha = e^{-i\phi}\tfrac{1}{2}[\partial_r - i/r\;\partial_\phi] \;\text{ and }\; \partial_{\alpha^*} = e^{i\phi}\tfrac{1}{2}[\partial_r + i/r\;\partial_\phi]. \tag{C.11}$$

Applying these formulas one obtains formulas for powers of derivatives:

$$[\partial_{\alpha^*}]^\eta = e^{i\eta\phi}\prod_{k=0}^{\eta-1}\tfrac{1}{2}[-k/r + \partial_r + i/r\;\partial_\phi],\; [\partial_\alpha]^\eta = e^{-i\eta\phi}\prod_{k=0}^{\eta-1}\tfrac{1}{2}[-k/r + \partial_r - i/r\;\partial_\phi]. \tag{C.12}$$

For comparison, we apply the spin-weight raising and lowering differential operators from Equation 4.17 and Equation 4.18 and obtain

$$[\eth/\sqrt{2J}]^\eta\,\mathrm{Y}_{jm} = (-1)^\eta\prod_{k=0}^{\eta-1}\tfrac{1}{2}(-k\tfrac{\cos\theta}{\sqrt{J/2}\sin\theta} + \tfrac{\partial_\theta}{\sqrt{J/2}} + \tfrac{i}{\sqrt{J/2}\sin\theta}\,\partial_\phi)\mathrm{Y}_{jm} \tag{C.13}$$

$$[\overline{\eth}/\sqrt{2J}]^\eta\,\mathrm{Y}_{jm} = (-1)^\eta\prod_{k=0}^{\eta-1}\tfrac{1}{2}(-k\tfrac{\cos\theta}{\sqrt{J/2}\sin\theta} + \tfrac{\partial_\theta}{\sqrt{J/2}} - \tfrac{i}{\sqrt{J/2}\sin\theta}\,\partial_\phi)\mathrm{Y}_{jm}. \tag{C.14}$$

The arc-length parametrization $\alpha = \sqrt{J/2}\,\theta\, e^{-i\phi}$ (see, e.g., [160]) implies that $r = \sqrt{\alpha^*\alpha} = \sqrt{J/2}\,\theta$. The following terms from Equation C.13 and Equation C.14 can be expanded by applying their Taylor series and substituting $\theta = r/\sqrt{J/2}$:

$$\frac{i}{\sqrt{J/2}\sin(r/\sqrt{J/2})} = \frac{i}{r} + \frac{ir}{3J} + \mathcal{O}(J^{-3/2}) \text{ and } \frac{\cos(r/\sqrt{J/2})}{\sqrt{J/2}\sin(r/\sqrt{J/2})} = \frac{1}{r} - \frac{2r}{3J} + \mathcal{O}(J^{-3/2}). \quad \text{(C.15)}$$

Substituting these expansions back into Equation C.13 and C.14 results in

$$[\eth/\sqrt{2J}]^\eta \,\mathrm{Y}_{jm} = (-1)^\eta \prod_{k=0}^{\eta-1} \tfrac{1}{2}[-k(\tfrac{1}{r} - \tfrac{2r}{3J}) + \partial_r + (\tfrac{i}{r} + \tfrac{ir}{3J})\partial_\phi + \mathcal{O}(J^{-3/2})]\mathrm{Y}_{jm},$$
$$[\overline{\eth}/\sqrt{2J}]^\eta \,\mathrm{Y}_{jm} = (-1)^\eta \prod_{k=0}^{\eta-1} \tfrac{1}{2}[-k(\tfrac{1}{r} - \tfrac{2r}{3J}) + \partial_r - (\tfrac{i}{r} + \tfrac{ir}{3J})\,\partial_\phi + \mathcal{O}(J^{-3/2})]\mathrm{Y}_{jm}.$$

Note that $\partial_\phi \mathrm{Y}^\eta_{jm} = im\mathrm{Y}^\eta_{jm}$. The expressions in the parentheses can up to an error term $\epsilon := \frac{r}{3J}(2k-m)$ be transformed into terms that are directly comparable to Equation C.12:

$$[\eth/\sqrt{2J}]^\eta \,\mathrm{Y}_{jm} = (-1)^\eta \prod_{k=0}^{\eta-1} \tfrac{1}{2}[-k/r + \partial_r + i/r\partial_\phi + \epsilon + \mathcal{O}(J^{-3/2})]\mathrm{Y}_{jm}, \quad \text{(C.16)}$$
$$[\overline{\eth}/\sqrt{2J}]^\eta \,\mathrm{Y}_{jm} = (-1)^\eta \prod_{k=0}^{\eta-1} \tfrac{1}{2}[-k/r + \partial_r - i/r\,\partial_\phi - \epsilon + \mathcal{O}(J^{-3/2})]\mathrm{Y}_{jm}. \quad \text{(C.17)}$$

We compare Equation C.12 with Equation C.16 and Equation C.17, apply the expression $\sum_{k=0}^{\eta-1} \epsilon/2 = \frac{r}{6J}(1+\eta)(\eta-m)$, and denote the residual error terms the using their abbreviations as $\zeta := \mathcal{O}(J^{-3/2}[\eth/\sqrt{2J}]^{\eta-1})$ and $\bar{\zeta} := \mathcal{O}(J^{-3/2}[\overline{\eth}/\sqrt{2J}]^{\eta-1})$. This leads to

$$[\eth/\sqrt{2J}]^\eta \,\mathrm{Y}_{jm} = [(-1)^\eta e^{-i\eta\phi}(\partial_{\alpha^*})^\eta + \tfrac{r(1+\eta)(\eta-m)}{6J}[\eth/\sqrt{2J}]^{\eta-1} + \zeta]\,\mathrm{Y}_{jm} \quad \text{(C.18)}$$
$$[\overline{\eth}/\sqrt{2J}]^\eta \,\mathrm{Y}_{jm} = [(-1)^\eta e^{i\eta\phi}(\partial_{\alpha})^\eta - \tfrac{r(1+\eta)(\eta-m)}{6J}[\overline{\eth}/\sqrt{2J}]^{\eta-1} + \bar{\zeta}]\,\mathrm{Y}_{jm}. \quad \text{(C.19)}$$

Substituting this expansion into the definition of spin-weighted spherical harmonics in Equation 4.15, one obtains for a fixed arc length α the forms (refer to Equation 4.22-Equation 4.23 and Figure 4.3(a-b))

$$\mathrm{Y}^\eta_{jm} - (-1)^\eta e^{-i\eta\phi}(\partial_{\alpha^*})^\eta \,\mathrm{Y}_{jm} \propto |\alpha|(j\sqrt{J})^{-1}\,\mathrm{Y}^{\eta-1}_{jm} + \mathcal{O}(J^{-1}) \text{ and} \quad \text{(C.20)}$$
$$\mathrm{Y}^{-\eta}_{jm} - e^{i\eta\phi}(\partial_{\alpha})^\eta \,\mathrm{Y}_{jm} \propto |\alpha|(j\sqrt{J})^{-1}\,\mathrm{Y}^{-\eta+1}_{jm} + \mathcal{O}(J^{-1}). \quad \text{(C.21)}$$

The difference on the left-hand side vanishes in the limit of infinite J for every bounded α, as the spin-weighted spherical harmonics $\mathrm{Y}^{-\eta\pm1}_{jm}$ on the right-hand side are bounded, i.e., $|\mathrm{Y}^{-\eta\pm1}_{jm}(\theta,\phi)| < \infty$.

We now describe a general criterion (see Section 4.7) for spherical functions and their differentials to be bounded. Assume now that the spherical function of the form $f = f(\theta,\phi) = \sum f_{jm}\mathrm{Y}_{jm}(\theta,\phi)$ is bounded, i.e., $|f(\theta,\phi)| < \infty$. Note that the expansion coefficients might depend on J. Also, assume that the differentials are bounded, i.e., $|\eth^\eta f(\theta,\phi)| < \infty$ and

$|\overline{\eth}^{\eta} f(\theta,\phi)| < \infty$, which translates to

$$|(\eth/\sqrt{2J})^{\eta} f(\theta,\phi)| = |\sum \sqrt{(2J)^{\eta}(j-\eta)!/(j+\eta)!}^{-1} f_{jm} {}_{\eta}\mathrm{Y}_{jm}(\theta,\phi)| < \infty$$
$$|(\overline{\eth}/\sqrt{2J})^{\eta} f(\theta,\phi)| = |\sum \sqrt{(2J)^{\eta}(j-\eta)!/(j+\eta)!}^{-1} f_{jm} {}_{-\eta}\mathrm{Y}_{jm}(\theta,\phi)| < \infty.$$

We emphasize that f and all of its derivatives are bounded if there are only a finite number of non-zero expansion coefficients f_{jm} or if the expansion coefficients $|f_{jm}|$ decay faster in j than the coefficients $\sqrt{(j-\eta)!/(j+\eta)!} \approx j^{-\eta}$ from Equation C.7. Applying Equation C.16 and Equation C.17 to the spherical function f one gets for a fixed arc length $|\alpha|$ that

$$[(\eth/\sqrt{2J})^{\eta} - (-1)^{\eta} e^{-i\eta\phi} (\partial_{\alpha^*})^{\eta}] f(\alpha) \propto |\alpha| J^{-1} [\eth/\sqrt{2J}]^{\eta-1} f(\alpha)$$
$$[(\overline{\eth}/\sqrt{2J})^{\eta} - (-1)^{\eta} e^{i\eta\phi} (\partial_{\alpha})^{\eta}] f(\alpha) \propto |\alpha| J^{-1} [\overline{\eth}/\sqrt{2J}]^{\eta-1} f(\alpha).$$

This difference clearly vanishes if $g = |\alpha| [\eth/\sqrt{2J}]^{\eta-1} f(\alpha)$ remains bounded in the limit of infinite J. (The assumption could be weakened such that the growth of the absolute value of g in J is slower than $\mathcal{O}(J)$.) For a fixed α, this expansion of the action of spin-weight lowering and raising operators has the convergence rate $\mathcal{O}(J^{-1})$, refer to Proposition 4.1.

We now describe when spherical functions and their differentials are in general bounded in the L^2 norm, and this information is utilized in Section 4.7. The asymptotic behavior of the difference function can be measured in the L^2 norm. Assume that the square-integrable spherical function $f = f(\theta,\phi) = \sum f_{jm} \mathrm{Y}_{jm}(\theta,\phi)$ observes $R^2 \sum |f_{jm}|^2 = 1$. Also asssume that its differentials are square integrable. Applying the orthonormality of spin-weighted spherical harmonics, this translates to

$$\|(\eth/\sqrt{2J})^{\eta} f(\theta,\phi)\|_{L^2} = R^2 \sum ((2J)^{\eta}(j-\eta)!/(j+\eta)!)^{-1} |f_{jm}|^2 < \infty, \quad \text{(C.22)}$$
$$\|(\overline{\eth}/\sqrt{2J})^{\eta} f(\theta,\phi)\|_{L^2} = R^2 \sum ((2J)^{\eta}(j-\eta)!/(j+\eta)!)^{-1} |f_{jm}|^2 < \infty. \quad \text{(C.23)}$$

Note that f and all of its derivatives are square integrable for finite J if there are only a finite number of non-zero expansion coefficients f_{jm} or if the expansion coefficients $|f_{jm}|^2$ decay faster in j than $(j-\eta)!/(j+\eta)! \approx j^{-2\eta}$ from Equation C.7. Applying Equation C.16 and Equation C.17, the norm of the difference is given by

$$\|[(\eth/\sqrt{2J})^{\eta} - (-1)^{\eta} e^{-i\eta\phi} (\partial_{\alpha^*})^{\eta}] f(\theta,\phi)\|_{L^2} \propto J^{-1} \| |\alpha| [\eth/\sqrt{2J}]^{\eta-1} f(\theta,\phi)\|_{L^2}$$
$$\|[(\overline{\eth}/\sqrt{2J})^{\eta} - (-1)^{\eta} e^{i\eta\phi} (\partial_{\alpha})^{\eta}] f(\theta,\phi)\|_{L^2} \propto J^{-1} \| |\alpha| [\overline{\eth}/\sqrt{2J}]^{\eta-1} f(\theta,\phi)\|_{L^2}.$$

This difference clearly vanishes if the norm $\| |\alpha| [\eth/\sqrt{2J}]^{\eta-1} f(\theta,\phi)\|_{L^2}$ remains bounded in the large-spin limit. (This assumption can be weakened such that the growth of this norm in J is slower than $\mathcal{O}(J)$.) Refer to Proposition 4.1.

Alternatively, the following expansions can be derived from Equation C.16 and Equation C.17:

$$[(\eth/\sqrt{2J})^\eta - (-1)^\eta e^{-i\eta\phi}(\partial_{\alpha^*})^\eta]f(\alpha) \propto J^{-1}|\alpha|\frac{\partial^{\eta-1}f(\alpha)}{(\partial_{\alpha^*})^{\eta-1}},$$
$$[(\overline{\eth}/\sqrt{2J})^\eta - (-1)^\eta e^{i\eta\phi}(\partial_{\alpha})^\eta]f(\alpha) \propto J^{-1}|\alpha|\frac{\partial^{\eta-1}f(\alpha)}{(\partial_{\alpha})^{\eta-1}}.$$

These differences vanish in the limit of infinite J if the derivatives remain bounded, i.e.,

$$||\alpha|\frac{\partial^{\eta-1}f(\alpha,\alpha^*)}{(\partial_{\alpha^*})^{\eta-1}}| < \infty \text{ and } ||\alpha|\frac{\partial^{\eta-1}f(\alpha,\alpha^*)}{(\partial_{\alpha^*})^{\eta-1}}| < \infty. \tag{C.24}$$

In addition, the L^2 norm of the differences vanishes if the derivatives remain square integrable, i.e.,

$$||\,|\alpha|\frac{\partial^{\eta-1}f(\alpha,\alpha^*)}{(\partial_{\alpha^*})^{\eta-1}}\|_{L^2} < \infty \text{ and } \|\,|\alpha|\frac{\partial^{\eta-1}f(\alpha,\alpha^*)}{(\partial_{\alpha^*})^{\eta-1}}\|_{L^2} < \infty, \tag{C.25}$$

or if the growth of the norm and the absolute value in J is slower than $\mathcal{O}(J)$. This is used in Proposition 4.1.

Following similar arguments, asymptotic expansions for products of differentials from Proposition 4.2 are obtained in the formulas

$$|f[(\overleftarrow{\eth}^\eta)(\overrightarrow{\overline{\eth}}^\eta)/(2J)^\eta]g - f(\overleftarrow{\partial}_{\alpha^*})^\eta(\overrightarrow{\partial}_{\alpha})^\eta g| \propto J^{-1} \text{ and} \tag{C.26}$$
$$\|\,f[(\overleftarrow{\eth}^\eta)(\overrightarrow{\overline{\eth}}^\eta)/(2J)^\eta - (\overleftarrow{\partial}_{\alpha^*})^\eta(\overrightarrow{\partial}_{\alpha})^\eta]\,g\|_{L^2} \propto J^{-1}, \tag{C.27}$$

and the two formulas are also valid for the conjugate derivatives. Consider two square-integrable functions f and g with the additional constraint that the product fg as well as the products of differentials $|\alpha|(\eth^\eta f)(\overline{\eth}^\eta g)$ are square integrable. The L^2-norm convergence then holds (refer to Proposition 4.2).

C.5.2 The product $\eth\overline{\eth}$ of the spin-weight raising and lowering operators

We now derive the second part of Proposition 4.1. The derivatives $\partial_{\alpha^*}\partial_\alpha$ in the polar parametrization are expanded into

$$\partial_{\alpha^*}\partial_\alpha = [-1/r + \partial_r + i/r\,\partial_\phi][\partial_r - i/r\,\partial_\phi]/4. \tag{C.28}$$

Similarly, the expansion of the operator $\eth\overline{\eth}/(2J)$ is given by

$$\eth\overline{\eth}/(2J)\,{}_{\mathrm{Y}}{}_{jm} = [-\tfrac{\cos\theta}{\sqrt{2J}\sin\theta} + \partial_\theta/\sqrt{2J} + \tfrac{i}{\sqrt{2J}\sin\theta}\,\partial_\phi][\,\partial_\theta/\sqrt{2J} - \tfrac{i}{\sqrt{2J}\sin\theta}\,\partial_\phi]\,{}_{\mathrm{Y}}{}_{jm}. \tag{C.29}$$

Applying the expansions from Equation C.15 and the parametrization $\theta = r/\sqrt{J/2}$ yields

$$\begin{aligned}\eth\overline{\eth}/(2J)\,\mathrm{Y}_{jm} =&[-\tfrac{1}{r} - \tfrac{2r}{3J} + \partial_r + (\tfrac{i}{r}+\tfrac{ir}{3J})\partial_\phi + \mathcal{O}(J^{-3/2})]\\ &\times[\partial_r - (\tfrac{i}{r}+\tfrac{ir}{3J})\partial_\phi + \mathcal{O}(J^{-3/2})]\,\mathrm{Y}_{jm}/4.\end{aligned}$$

Now separating the terms and expanding the action $\partial_\phi \mathrm{Y}_{jm}$ results in

$$\begin{aligned}\eth\overline{\eth}/(2J)\,\mathrm{Y}_{jm} =&[-\tfrac{1}{r} + \partial_r + \tfrac{i}{r}\partial_\phi - \tfrac{(m+2)r}{3J} + \mathcal{O}(J^{-3/2})]\\ &\times[\,\partial_r - \tfrac{i}{r}\,\partial_\phi - \tfrac{mr}{3J} + \mathcal{O}(J^{-3/2})]\,\mathrm{Y}_{jm}/4.\end{aligned}$$

Finally, we obtain for a bounded spherical function f that

$$[\eth\overline{\eth}/(2J) - \partial_{\alpha^*}\partial_\alpha]f \propto |\alpha|J^{-1} \text{ and } \|[\eth\overline{\eth}/(2J) - \partial_{\alpha^*}\partial_\alpha]\,f\|_{L^2} \propto |\alpha|J^{-1}.$$

The norm or the absolute value vanish in the large-spin limit if both the function f and its differentials are bounded or square integrable in the limit, see Proposition 4.1.

C.6 Proof of Result 4.6

We prove Result 4.6. Substituting the approximations of $\Box(s)$ from Equation 4.44 and of $\star^{(-1)}$ form Equation 4.39 into Equation 4.46 yields the formula

$$\begin{aligned}&f\,[\overleftarrow{\Box}(-s)\,\star^{(-1)}\,\overrightarrow{\Box}(-s)]\,g\\ &= f\,\exp[\,\tfrac{1+s}{2}\overleftarrow{\partial}_{\alpha^*}\overleftarrow{\partial}_{\alpha}\,]\exp[\,\overleftarrow{\partial}_{\alpha}\overrightarrow{\partial}_{\alpha^*}\,]\exp[\,\tfrac{1+s}{2}\overrightarrow{\partial}_{\alpha^*}\overrightarrow{\partial}_{\alpha}\,]\,g + \mathcal{O}(J^{-1})\\ &= f\,\exp[\,\tfrac{1+s}{2}\overleftarrow{\partial}_{\alpha^*}\overleftarrow{\partial}_{\alpha} + \overleftarrow{\partial}_{\alpha}\overrightarrow{\partial}_{\alpha^*} + \tfrac{1+s}{2}\overrightarrow{\partial}_{\alpha^*}\overrightarrow{\partial}_{\alpha}\,]\,g + \mathcal{O}(J^{-1}),\end{aligned}$$

where the second equality follows from the commutativity of partial derivatives. Using the Leibniz rule of partial derivatives

$$\partial_{\alpha^*}\partial_\alpha(fg) = (\partial_{\alpha^*}\partial_\alpha f)g + f(\partial_{\alpha^*}\partial_\alpha g) + (\partial_{\alpha^*}f)(\partial_\alpha g) + (\partial_\alpha f)(\partial_{\alpha^*}g) \tag{C.30}$$

results in a convenient description for the action of the approximation of $\Box(s)fg$:

$$\exp[\,-\tfrac{1+s}{2}\partial_{\alpha^*}\partial_\alpha\,]fg = f\exp[\,-\tfrac{1+s}{2}\left(\overleftarrow{\partial}_{\alpha^*}\overleftarrow{\partial}_{\alpha} + \overrightarrow{\partial}_{\alpha^*}\overrightarrow{\partial}_{\alpha} + \overleftarrow{\partial}_{\alpha^*}\overrightarrow{\partial}_{\alpha} + \overleftarrow{\partial}_{\alpha}\overrightarrow{\partial}_{\alpha^*}\right)\,]g. \tag{C.31}$$

Substituting this into $\Box(s+2)\left(f\,[\overleftarrow{\Box}(-s)\,\star^{(-1)}\,\overrightarrow{\Box}(-s)]\,g\right)$, one obtains Equation 4.52 which is expanded as

$$f\,\star^{(s)}\,g = \sum_{n=0}^{\infty}\sum_{m=0}^{n} c_{nm}(s)\,(\partial_\alpha^m\,\partial_{\alpha^*}^{n-m}f)(\partial_{\alpha^*}^m\,\partial_\alpha^{n-m}g) + \mathcal{O}(J^{-1}), \tag{C.32}$$

where $c_{nm}(s)$ are the expansion coefficients of the exponential $\exp[\tfrac{(1-s)}{2}a - \tfrac{(1+s)}{2}b] = \sum_{n=0}^{\infty}\sum_{m=0}^{n} c_{nm}(s)\,a^m b^{n-m}$ for commutative a and b. Using the polar parametrization from

Equation C.12, the derivatives $\partial_\alpha^n \partial_{\alpha^*}^m$ can be represented as

$$\partial_\alpha^n \partial_{\alpha^*}^m = e^{i(m-n)\phi} \prod_{\eta=-m}^{n-m-1} \tfrac{1}{2}[-\eta/r + \partial_r - i/r\, \partial_\phi] \prod_{\eta=0}^{m-1} \tfrac{1}{2}[-\eta/r + \partial_r + i/r\, \partial_\phi]. \quad \text{(C.33)}$$

One applies arguments from C.5 and the expansion

$$(\partial_\alpha^n \partial_{\alpha^*}^m f)(\partial_{\alpha^*}^n \partial_\alpha^m g) = (2J)^{-n-m} (\overline{\eth}^n \eth^m f)(\eth^n \overline{\eth}^m g) + \mathcal{O}(J^{-1}) \quad \text{(C.34)}$$

of the differential operators can be established which finally yields Equation 4.51.

C.7 Details for the example in Section 4.12

We discuss some details for the example in Section 4.12. The normalization factor N in Equation 4.69 can be computed using $1/N^2 = \langle JJ|K^\dagger K|JJ\rangle$ where

$$\begin{aligned} K &= \mathcal{R}^{-1}(\Omega_0)\mathcal{J}_-\mathcal{R}(\Omega_0)/\sqrt{2J} \\ &= [\mathcal{J}_- D^1_{-1,-1}(\Omega') + \mathcal{J}_z D^1_{0,-1}(\Omega')/\sqrt{2} + \mathcal{J}_+ D^1_{1,-1}(\Omega')]/\sqrt{2J}. \end{aligned} \quad \text{(C.35)}$$

Here, $D^j_{m,m'}$ are Wigner D-matrix elements [61]. All the contributions in Equation C.35 vanish except for $\langle JJ|\mathcal{J}_+\mathcal{J}_-|JJ\rangle = 2J$ and $\langle JJ|\mathcal{J}_z\mathcal{J}_z|JJ\rangle = J^2$. Finally, one obtains $1/N^2 = \cos(\theta/2)^2[1 + 2J - (2J-1)\cos(\theta)]/2$.

The phase-space representation $F_{K(\Omega_0)}$ of the operator K from Equation 4.69 can be specified in terms of spherical harmonics as [159]

$$\begin{aligned} F_{K(\Omega_0)} &= c_s \mathcal{R}(\Omega_0) \mathrm{Y}_{1,-1}(\Omega) \\ &= c_s[\mathrm{Y}_{1,-1}(\Omega) D^1_{-1,-1}(\Omega_0) + \mathrm{Y}_{1,0}(\Omega) D^1_{0,-1}(\Omega_0) + \mathrm{Y}_{1,1}(\Omega) D^1_{1,-1}(\Omega_0)], \end{aligned}$$

where the rotation can be written in terms of Wigner D-matrices and the prefactor is given by $c_s = N\sqrt{(J+1)(2J+1)/3}\,\gamma_1^{-s}/R$.

The star product with $F_{K(\Omega_0)}$ in Equation 4.70 and Equation 4.71 can be *approximated* using Equation 4.51. The approximate actions of $\mathcal{K}(\Omega_0)$ and $\overline{\mathcal{K}}(\Omega_0)$ are then given by

$$\mathcal{K}(\Omega_0)\, f = [F_{K(\Omega_0)} + \tfrac{1-s}{4J}(\overline{\eth} F_{K(\Omega_0)})\eth - \tfrac{1+s}{4J}(\eth F_{K(\Omega_0)})\overline{\eth}]\, f + \mathcal{O}(J^{-1}) \quad \text{(C.36)}$$

$$\overline{\mathcal{K}}(\Omega_0)\, f = [(F_{K(\Omega_0)})^* + \tfrac{1-s}{4J}(\eth (F_{K(\Omega_0)})^*)\overline{\eth} - \tfrac{1+s}{4J}(\overline{\eth}(F_{K(\Omega_0)})^*)\eth]\, f + \mathcal{O}(J^{-1}). \quad \text{(C.37)}$$

Using the star-product approximation from Equation 4.52, the actions of $\mathcal{K}(\Omega_0)$ and $\overline{\mathcal{K}}(\Omega_0)$ can be expanded into

$$\mathcal{K}(\Omega_0)\, f = [F_{K(\Omega_0)} + \tfrac{1-s}{4J}(\partial_\alpha F_{K(\Omega_0)})\partial_{\alpha^*} - \tfrac{1+s}{4J}(\partial_{\alpha^*} F_{K(\Omega_0)})\partial_\alpha]\, f + \mathcal{O}(J^{-1}) \quad \text{(C.38)}$$

$$\overline{\mathcal{K}}(\Omega_0)\, f = [(F_{K(\Omega_0)})^* + \tfrac{1-s}{4J}(\partial_{\alpha^*} (F_{K(\Omega_0)})^*)\partial_\alpha - \tfrac{1+s}{4J}(\partial_\alpha (F_{K(\Omega_0)})^*)\partial_{\alpha^*}]\, f + \mathcal{O}(J^{-1}). \quad \text{(C.39)}$$

Knowing that $F_{K(0)} = c_s \mathrm{Y}_{1,-1}(\Omega)$ with $\eth \mathrm{Y}_{1,-1} = \sqrt{2}\mathrm{Y}^{1}_{1,-1}$, $\overline{\eth}\mathrm{Y}_{1,-1} = -\sqrt{2}\mathrm{Y}^{-1}_{1,-1}$, and $(\mathrm{Y}_{1,-1})^* = \mathrm{Y}_{1,1}$, the action of $\mathcal{K}(\Omega_0)$ and $\overline{\mathcal{K}}(\Omega_0)$ at the point $\Omega_0 = 0$ is given by

$$\mathcal{K}(0)\, f = \mathcal{K}\, f = c_s[\mathrm{Y}_{1,-1} - \sqrt{2}\tfrac{1-s}{4J}\mathrm{Y}^{-1}_{1,-1}\eth - \sqrt{2}\tfrac{1+s}{4J}\mathrm{Y}^{1}_{1,-1}\overline{\eth}]\, f + \mathcal{O}(J^{-1}) \text{ and} \quad \text{(C.40)}$$

$$\overline{\mathcal{K}}(0)\, f = \overline{\mathcal{K}}\, f = c_s[\mathrm{Y}_{1,1} + \sqrt{2}\tfrac{1-s}{4J}\mathrm{Y}^{1}_{1,1}\overline{\eth} + \sqrt{2}\tfrac{1+s}{4J}\mathrm{Y}^{-1}_{1,1}\eth]\, f + \mathcal{O}(J^{-1}), \quad \text{(C.41)}$$

which are then used in Equation 4.73-Equation 4.74.

APPENDIX D

Appendix of Chapter 5

D.1 Proofs of the Properties from Section 5.6.1

D.1.1 Proof of Property 5.1

Recall that the Hilbert-Schmidt norm of an operator A is defined as $||A||_{\mathrm{HS}}^2 := \mathrm{Tr}(A^\dagger A)$. One obtains

$$||\Pi_\theta||_{\mathrm{HS}}^2 = \mathrm{Tr}(\Pi_\theta^\dagger \Pi_\theta) = (4\pi\hbar)^{-2} \int \int K_\theta^*(\Omega) K_\theta(\Omega') \,\mathrm{Tr}[\mathcal{D}^\dagger(\Omega)\mathcal{D}(\Omega')]\,\mathrm{d}\Omega\,\mathrm{d}\Omega'$$

by substituting Π_θ with its definition from (5.16). Formally writing [51] $\mathrm{Tr}[\mathcal{D}^\dagger(\Omega)\mathcal{D}(\Omega')] = 2\pi\hbar\,\delta(\Omega{-}\Omega')$, it follows that

$$||\Pi_\theta||_{\mathrm{HS}}^2 = (8\pi\hbar)^{-1} \int K_\theta^*(\Omega) K_\theta(\Omega)\,\mathrm{d}\Omega = (8\pi\hbar)^{-1} ||K_\theta(\Omega)||_{L^2}^2.$$

Here, $||K_\theta(\Omega)||_{L^2}^2$ is the L^2 norm of the filter function. The inequality $||\Pi_\theta||_{\sup} \leq ||\Pi_\theta||_{\mathrm{HS}} = ||K_\theta(\Omega)||_{L^2}/\sqrt{8\pi\hbar}$ (see Thm. VI.22.(d) in [211]) concludes the proof.

D.1.2 Proof of Property 5.2

Recall that the Wigner function is square integrable as $\mathrm{Tr}(\rho_1^\dagger \rho_2) = \int W_{\rho_1}^* W_{\rho_2}\,\mathrm{d}\Omega$ and $|\langle W_{\rho_1} | W_{\rho_2} \rangle_{L^2}| \leq 1$ hold. Similarly, one obtains for elements $F_\rho(\Omega, \theta) = \theta(\Omega) * W_\rho(\Omega)$

of the Cohen class the scalar products

$$\int F^*_{\rho_1}(\Omega,\theta)\, F_{\rho_2}(\Omega,\theta)\,\mathrm{d}\Omega = \int [\theta(\Omega) * W_{\rho_1}(\Omega)]^*[\theta(\Omega) * W_{\rho_2}(\Omega)]\,\mathrm{d}\Omega$$
$$= \int F_\sigma[\theta(\cdot) * W_{\rho_1}(\cdot)]^*(\Omega)\, F_\sigma[\theta(\cdot) * W_{\rho_2}(\cdot)](\Omega)\,\mathrm{d}\Omega$$

using the Plancherel formula $\int a(\Omega)b^*(\Omega)\,\mathrm{d}\Omega = \int a_\sigma(\Omega)b^*_\sigma(\Omega)\,\mathrm{d}\Omega$. One can simplify the integrands to

$$F_\sigma[\theta(\cdot) * W_{\rho_2}(\cdot)](\Omega) = 2\pi\hbar F_\sigma[\theta(\cdot)](\Omega)\, F_\sigma[W_{\rho_2}(\cdot)](\Omega)$$

by applying the convolution formula from (5.14). Theorem 5.1 implies the relation $K_\theta(\Omega) = 2\pi\hbar[F_\sigma\theta(\cdot)](-\Omega)$ which yields the simplified integral

$$\int F^*_{\rho_1}(\Omega,\theta)\, F_{\rho_2}(\Omega,\theta)\,\mathrm{d}\Omega = \int |K_\theta(-\Omega)|^2\, F_\sigma[W_{\rho_1}(\cdot)]^*(\Omega)\, F_\sigma[W_{\rho_2}(\cdot)](\Omega)\,\mathrm{d}\Omega. \quad \text{(D.1)}$$

By assumption, $K_\theta(\Omega) \in L^\infty(\mathbb{R}^2)$, i.e, there exists a constant $C \in \mathbb{R}$ such that $|K_\theta(\Omega)| \leq C$ holds almost everywhere. Applying this bound to Eq. (D.1) after setting $\rho_1 = \rho_2 =: \rho$ yields

$$\int |K_\theta(-\Omega)|^2\, |F_\sigma[W_\rho(\cdot)](\Omega)|^2\,\mathrm{d}\Omega \leq C^2 \int |F_\sigma[W_\rho(\cdot)](\Omega)|^2\,\mathrm{d}\Omega = C^2 \int |W_\rho(\Omega)|^2\,\mathrm{d}\Omega$$

with the help of the Plancherel formula. The above mentioned result for the Wigner function implies the square integrability of $F_\rho(\Omega,\theta)$, which concludes the proof.

D.1.3 Proof of Property 5.3

As in (5.6), one considers the density operators $\rho = \sum_n p_n|\psi_n\rangle\langle\psi_n|$ and $\rho' = \sum_n p_n|\phi_n\rangle\langle\phi_n|$. The orthonormality of $|\phi_n\rangle = \mathcal{D}(\Omega')|\psi_n\rangle$ is used to evaluate the trace and this yields

$$\mathrm{Tr}\,[\,\rho'\,\mathcal{D}(\Omega)\Pi_\theta\mathcal{D}^\dagger(\Omega)] = \sum_n p_n\langle\phi_n|\mathcal{D}(\Omega)\Pi_\theta\mathcal{D}^\dagger(\Omega)|\phi_n\rangle$$
$$= \sum_n p_n\langle\psi_n|\mathcal{D}^\dagger(\Omega')\mathcal{D}(\Omega)\Pi_\theta\mathcal{D}^\dagger(\Omega)\mathcal{D}(\Omega')|\psi_n\rangle.$$

Computing the addition of products $\mathcal{D}(\Omega)\mathcal{D}(\Omega')$ of displacement operators [113, Eq. (1.10)] concludes the proof with the help of $\mathcal{D}^\dagger(\Omega') = \mathcal{D}(-\Omega')$ and $\mathrm{Tr}\,[\,\rho'\,\mathcal{D}(\Omega)\Pi_\theta\mathcal{D}^\dagger(\Omega)] = \mathrm{Tr}\,[\,\rho\,\mathcal{D}(\Omega-\Omega')\Pi_\theta\mathcal{D}^\dagger(\Omega-\Omega')]$.

D.1.4 Proof of Property 5.4

First, we prove that the displacement operator is covariant under rotations, i.e. $U^\dagger_\phi\mathcal{D}(\Omega)U_\phi = \mathcal{D}(\Omega^{-\phi})$. This is conveniently shown in the coherent-state representation as detailed in Eq. (5.7). Note that

$$U^\dagger_\phi\mathcal{D}(\Omega)U_\phi|0\rangle = e^{-|\alpha|^2/2}\sum_{n=0}^{\infty}\tfrac{\alpha^n}{\sqrt{n!}}U^\dagger_\phi|n\rangle = e^{-|\alpha|^2/2}\sum_{n=0}^{\infty}\tfrac{[\exp(i\phi)\alpha]^n}{\sqrt{n!}}|n\rangle = \mathcal{D}(\Omega^{-\phi})|0\rangle,$$

where the eigenvalue equation $U_\phi^\dagger|n\rangle = \exp(in\phi)|n\rangle$ was used together with its special case $U_\phi|0\rangle = |0\rangle$. It follows from (5.16) that

$$U_\phi \Pi_\theta U_\phi^\dagger = (4\pi\hbar)^{-1} \int K_\theta(\Omega) U_\phi \mathcal{D}(\Omega) U_\phi^\dagger \,\mathrm{d}\Omega = (4\pi\hbar)^{-1} \int K_\theta(\Omega) \mathcal{D}(\Omega^\phi) \,\mathrm{d}\Omega = \Pi_\theta$$

and the last equation is a consequence of the invariance $K_\theta(\Omega) = K_\theta(\Omega^\phi)$. Now, writing the density operators as $\rho = \sum_n p_n|\psi_n\rangle\langle\psi_n|$ and $\rho^\phi = \sum_n p_n|\chi_n\rangle\langle\chi_n|$, the traces can be evaluated as

$$\begin{aligned}\mathrm{Tr}\,[\,\rho^\phi\,\mathcal{D}(\Omega)\Pi_\theta\mathcal{D}^\dagger(\Omega)\,] &= \sum_n p_n \langle\chi_n|\mathcal{D}(\Omega)\Pi_\theta\mathcal{D}^\dagger(\Omega)|\chi_n\rangle \\ = \sum_n p_n \langle\chi_n|\mathcal{D}(\Omega)U_\phi\Pi_\theta U_\phi^\dagger\mathcal{D}^\dagger(\Omega)|\chi_n\rangle &= \sum_n p_n \langle\psi_n|U_\phi^\dagger\mathcal{D}(\Omega)U_\phi\Pi_\theta U_\phi^\dagger\mathcal{D}^\dagger(\Omega)U_\phi|\psi_n\rangle \\ &= \mathrm{Tr}\,[\,\rho\,\mathcal{D}(\Omega^{-\phi})\Pi_\theta\mathcal{D}^\dagger(\Omega^{-\phi})\,],\end{aligned}$$

which verifies that the displacement operator is covariant under rotations. The diagonality of Π_θ in the Fock basis can be shown as follows: If $K_\theta(\Omega)$ is invariant under rotations it must be a function of the polar radius in the phase space, i.e. $K_\theta(\Omega) = K_\theta(|\alpha|^2)$. The matrix elements can be calculated via (5.8) as

$$\langle n|\Pi_\theta|m\rangle = (4\pi\hbar)^{-1} \int K_\theta(|\alpha|^2)\,[\mathcal{D}(\alpha)]_{nm}\,\mathrm{d}\Omega \propto \int \alpha^{m-n} f(|\alpha|^2)\,\mathrm{d}\Omega \propto \delta_{nm}$$

with $f(|\alpha|^2) = K_\theta(|\alpha|^2)e^{-|\alpha|^2/2}L_n^{(m-n)}(|\alpha|^2)$, so the integral vanishes unless $n = m$.

D.1.5 Proof of Property 5.5

The expectation value $\langle\psi_n|\mathcal{D}(\Omega)\Pi_\theta\mathcal{D}^\dagger(\Omega)|\psi_n\rangle = \langle\phi_n|\Pi_\theta|\phi_n\rangle$ is real if Π_θ is Hermitian, where the orthonormal bases $\{|\psi_n\rangle\}_{n=0,1,\ldots}$ and $\{|\phi_n\rangle\}_{n=0,1,\ldots}$ of the considered Hilbert space have been applied. Assuming $K_\theta^*(-\Omega) = K_\theta(\Omega)$, this translates to

$$\begin{aligned}\Pi_\theta^\dagger &= \tfrac{1}{4\pi\hbar}\int K_\theta^*(\Omega)\mathcal{D}^\dagger(\Omega)\,\mathrm{d}\Omega = \tfrac{1}{4\pi\hbar}\int K_\theta^*(\Omega)\mathcal{D}(-\Omega)\,\mathrm{d}\Omega = \tfrac{1}{4\pi\hbar}\int K_\theta(\Omega)\mathcal{D}(\Omega)\,\mathrm{d}\Omega \\ &= \Pi_\theta.\end{aligned}$$

D.1.6 Proof of Property 5.6

The phase-space integral

$$\begin{aligned}\int F_\rho(\Omega,\theta)\mathrm{d}\Omega &= (\pi\hbar)^{-1}\mathrm{Tr}\,[\,\rho\int\mathcal{D}(\Omega)\Pi_\theta\mathcal{D}^\dagger(\Omega)\mathrm{d}\Omega] \\ &= 2\,\mathrm{Tr}\{\,\rho\,F_\sigma[\mathcal{D}(\cdot)\Pi_\theta\mathcal{D}^\dagger(\cdot)](\Omega)|_{\Omega=0}\} = \mathrm{Tr}\,[\,\rho\,\mathcal{D}(0)K_\theta(0)\,] = 1\end{aligned}$$

is mapped to the trace of ρ with $\mathcal{D}(0) \equiv \mathrm{Id}$ assuming that $K_\theta(0) = 1$. The second equality applies the symplectic Fourier transform of Eq. (5.18) at the point $\Omega = 0$. The trace of Π_θ is

given by

$$\mathrm{Tr}[\Pi_\theta] = (4\pi\hbar)^{-1} \int K_\theta(\Omega)\mathrm{Tr}[\mathcal{D}(\Omega)]\,\mathrm{d}\Omega = (2)^{-1} \int K_\theta(\Omega)\delta(\Omega)\,\mathrm{d}\Omega,$$

where we have applied that [51] $\mathrm{Tr}[\mathcal{D}^\dagger(\Omega)\mathcal{D}(\Omega')] = 2\pi\hbar\,\delta(\Omega{-}\Omega')$. Alternatively, this also follows from (5.25) by computing the trace

$$\mathrm{Tr}[\Pi_\theta] = (\pi\hbar)^{-1}\mathrm{Tr}[\mathrm{Op}_{\mathrm{Weyl}}(\theta)] = (\pi\hbar)^{-2} \int \theta(\Omega)\,\mathrm{Tr}[\mathcal{D}(\Omega)\Pi\mathcal{D}^\dagger(\Omega)]\,\mathrm{d}\Omega,$$

where the trace of the Grossmann-Royer operator from (5.12) evaluates via the expression $\mathrm{Tr}[\mathcal{D}(\Omega)\Pi\mathcal{D}^\dagger(\Omega)] = \mathrm{Tr}[\Pi] = 1/2$, refer to (6.38) and the following text in [51]. Substituting its definition from (5.16), the trace of Π_θ is computed as $\mathrm{Tr}[\Pi_\theta] = (2\pi^2\hbar^2)^{-1} \int \theta(\Omega)\mathrm{d}\Omega = (\pi\hbar)^{-1}F_\sigma[\theta(\cdot)]|_{\Omega=0} = K(0)/2$.

D.2 Proof of s-parametrized parity operators

Recall that due to Property 5.4, the parity operator is diagonal in the number-state representation $\langle m|\Pi_s|n\rangle \propto \delta_{nm}$. Its diagonal elements can be calculated

$$[\Pi_s]_{nn} = (4\pi\hbar)^{-1} \int e^{s|\alpha|^2/2}\,[\mathcal{D}(\Omega)]_{nn}\,\mathrm{d}\Omega = (4\pi\hbar)^{-1} \int e^{s|\alpha|^2/2}\,e^{-|\alpha|^2/2}L_n(|\alpha|^2)\,\mathrm{d}\Omega$$

where (5.8) was used for $[\mathcal{D}(\Omega)]_{nn}$. One applies the polar parameterization of the complex plane via $\Omega = \alpha = r\exp(i\phi)$ so that $\mathrm{d}\Omega = 2\hbar\,\mathrm{d}\Re(\alpha)\mathrm{d}\Im(\alpha) = 2\hbar\,r\,\mathrm{d}r\,\mathrm{d}\phi$. Then

$$\begin{aligned}[\Pi_s]_{nn} &= (2\pi)^{-1} \int_0^{2\pi} \mathrm{d}\phi \int_0^\infty e^{sr^2/2}\,e^{-r^2/2}L_n(r^2)\,r\,\mathrm{d}r \\ &= \tfrac{1}{2} \int_0^\infty e^{y(s-1)/2}L_n(y)\,\mathrm{d}y = \tfrac{1}{2} \int_0^\infty e^{-y}e^{y(s+1)/2}L_n(y)\,\mathrm{d}y,\end{aligned}$$

where the second equality is due to $r\,\mathrm{d}r = \mathrm{d}y/2$ with $y = r^2$ and the integral with respect to ϕ results in the multiplication by 2π. The Laguerre polynomial decomposition of the exponential function $e^{-\gamma x} = \sum_{m=0}^\infty[\gamma^m/(1{+}\gamma)^{m+1}]L_m(x)$ with $\gamma = -(s{+}1)/2$ [164, p. 90] and the orthogonality relation $\int_0^\infty e^{-x}L_n(x)L_m(x)\,\mathrm{d}x = \delta_{nm}$ finally yields $[\Pi_s]_{nn} = \gamma^n/[2(1{+}\gamma)^{n+1}] = (-1)^n(s{+}1)^n/(1{-}s)^{n+1}$, which concludes the proof.

D.3 Spectral decomposition of the squeezing operator

The eigenvectors from (5.36) are orthogonal and δ-delta normalized as detailed by

$$\langle\psi_\pm^{E_1}|\psi_\pm^{E_2}\rangle = \int [\psi_\pm^{E_1}(x)]^*\,\psi_\pm^{E_2}(x)\,\mathrm{d}x = \delta(E_1{-}E_2).$$

The integral can be calculated using a change of variables $\mathrm{d}x = e^v\mathrm{d}v$ with $v = \ln(|x|)$. One obtains a complete basis

$$\int [\psi_\pm^E(x)]^*\,\psi_\pm^E(x')\,\mathrm{d}E = \delta(x{-}x'),$$

by applying an integral of two different Fourier components indexed by x and x', refer to [57, 58] for more details. The eigenfunctions $\psi_{\pm}^{E}(x)$ are not square integrable, but they can be decomposed into the number-state basis with finite coefficients. The coefficients shrink to zero, but are not square summable. The resulting integrals $\langle n|\psi_{\pm}^{E}\rangle$ can be specified in terms of a finite sum. In particular, $\psi_{+}^{0} = |x|^{-1/2}/(2\sqrt{\pi})$ has the largest eigenvalue. Its number-state representation is given by

$$\langle n|\psi_{+}^{0}\rangle = \tfrac{1}{2\sqrt{\pi}} \sum_{k=0}^{n/2} \frac{\pi 2^{-3k+n+\frac{1}{4}}\sqrt{n!}}{k!(n-2k)!\,\Gamma(k-\frac{n}{2}+\frac{3}{4})} \;\text{ if }\; n \bmod 4 = 0,$$

where every fourth entry is non-zero and the entries decrease to zero for large n.

D.4 Matrix representation of the Born-Jordan parity operator

The matrix elements of the parity operator can be computed via Theorem 5.3 as

$$[\Pi_{\mathrm{BJ}}]_{mn} = (4\pi\hbar)^{-1} \int K_{\mathrm{BJ}}(\Omega)\,[\mathcal{D}(\Omega)]_{mn}\,\mathrm{d}\Omega = (4\pi\hbar)^{-1} \int \mathrm{sinc}(\tfrac{px}{2\hbar})\,[\mathcal{D}(\alpha)]_{mn}\,\mathrm{d}x\,\mathrm{d}p.$$

It was discussed in Section 5.5.1 that one can substitute $\alpha = (\lambda x + i\lambda^{-1}p)/\sqrt{2\hbar}$, which results in the integral

$$[\Pi_{\mathrm{BJ}}]_{mn} = (4\pi\hbar)^{-1} \int \mathrm{sinc}(\tfrac{px}{2\hbar})\,\{\mathcal{D}[(\lambda x + i\lambda^{-1}p)/\sqrt{2\hbar}]\}_{mn}\,\mathrm{d}x\,\mathrm{d}p.$$

Let us now apply a change of variables $x \mapsto \lambda^{-1}\sqrt{\hbar}x$ and $p \mapsto \lambda\sqrt{\hbar}p$ which yields $\mathrm{d}x\,\mathrm{d}p \mapsto \hbar\mathrm{d}x\,\mathrm{d}p$ and the integral

$$[\Pi_{\mathrm{BJ}}]_{mn} = (4\pi)^{-1} \int \mathrm{sinc}(\tfrac{px}{2})\,\{\mathcal{D}[(x+ip)/\sqrt{2}]\}_{mn}\,\mathrm{d}x\,\mathrm{d}p.$$

We now substitute the explicit form of $[\mathcal{D}(\alpha)]_{mn}$ with $\{\mathcal{D}[(x+ip)/\sqrt{2}]\}_{mn}$ from (5.8) and obtain

$$[\Pi_{\mathrm{BJ}}]_{mn} = (4\pi)^{-1} \sum_{k=0}^{n} c_{mn}^{k} \int \mathrm{sinc}(\tfrac{px}{2})\,[\tfrac{x+ip}{\sqrt{2}}]^{m-n} e^{-(x^2+p^2)/4}(x^2+p^2)^k\,\mathrm{d}x\,\mathrm{d}p, \qquad \text{(D.2)}$$

where the Laguerre polynomials are expanded using the new coefficients

$$c_{mn}^{k} := \sqrt{\tfrac{n!}{m!}}(-1)^k 2^{-k}\binom{m}{n-k}/k!.$$

One applies the expansion

$$[\tfrac{x+ip}{\sqrt{2}}]^{m-n} = 2^{-(m-n)/2} \sum_{\ell=0}^{m-n} \binom{m-n}{\ell} x^{m-n-\ell}\,(ip)^{\ell}.$$

and the integral in (D.2) vanishes for odd powers of x and p due to symmetry of the integrand. Therefore, all non-vanishing matrix elements have even $m-n$ values and the summations can be restricted to $\ell \in \{0,2,4,\dots,m-n\}$. The integral is also invariant under a permutation of x and p and certain terms in the sum cancel each other out: every term $x^{m-n-\ell}\,(ip)^{\ell}$ in the sum has a counterpart $(ip)^{m-n-\ell}\,x^{\ell}$ which results in the same integral and these two terms therefore cancel each other out after the integration if the condition $(i)^{\ell} = -(i)^{m-n-\ell}$ holds (which occurs unless $m-n$ is a multiple of four). This elementary argument shows that only matrix elements $[\Pi_{\mathrm{BJ}}]_{mn}$ with $m-n$ multiples of four are non-zero. Recall that we have been using an indexing scheme with $m \geq n$ on account of the Laguerre polynomials in (5.8), but matrix elements with $m < n$ are trivially obtained as $[\Pi_{\mathrm{BJ}}]_{mn} = [\Pi_{\mathrm{BJ}}]_{nm}$. Introducing the coefficient [with $i^{\ell} = (-1)^{\ell/2}$]

$$w^{k}_{mn\ell} := (-1)^{\ell/2} 2^{-(m-n)/2} \binom{m-n}{\ell} c^{k}_{mn}$$

and denoting $a = (m-n-\ell)/2$ and $b = \ell/2$, one obtains

$$[\Pi_{\mathrm{BJ}}]_{mn} = (4\pi)^{-1} \sum_{k=0}^{n} \sum_{\substack{\ell=0 \\ \ell \text{ even}}}^{m-n} w^{k}_{mn\ell} \int \operatorname{sinc}\!\left(\tfrac{px}{2}\right) x^{2a}\, p^{2b}\, (x^2+p^2)^{k}\, e^{-(x^2+p^2)/4}\, \mathrm{d}x\, \mathrm{d}p. \quad \text{(D.3)}$$

The integral in (D.3) is absolutely convergent due to the estimate

$$\left|\operatorname{sinc}\!\left(\tfrac{px}{2}\right) x^{2a}\, p^{2b}\, (x^2+p^2)^{k}\, e^{-(x^2+p^2)/4}\right| \leq x^{2a}\, p^{2b}\, (x^2+p^2)^{k}\, e^{-(x^2+p^2)/4}$$

and integrating over the upper bound yields without a proof that $4\pi\, 4^{a+b+k} (\tfrac{1}{2})_a (\tfrac{1}{2})_b (1+a+b)_k < \infty$, where $(\cdot)_a$ denotes the Pochhammer symbol [4, (6.1.22)]. The integral in (D.3) can then be rewritten using the partial derivatives

$$\begin{aligned} &(4\pi)^{-1} \int \operatorname{sinc}\!\left(\tfrac{px}{2}\right) x^{2a}\, p^{2b}\, (x^2+p^2)^{k}\, e^{-(x^2+p^2)/4}\, \mathrm{d}x\, \mathrm{d}p \\ &= (-1)^{a+b+k} 4^{a+b+k} [(\partial_{\mu}^{k} [\partial_{\lambda}^{a} \partial_{\mu}^{b} f(\lambda,\mu)]|_{\lambda=\mu})]|_{\mu=1}, \end{aligned}$$

where the equality follows from evaluating elementary differentials of the Gaussian function with

$$f(\lambda,\mu) = (4\pi)^{-1} \int \operatorname{sinc}\!\left(\tfrac{px}{2}\right) e^{-(\lambda x^2+\mu p^2)/4}\, \mathrm{d}x\, \mathrm{d}p = \operatorname{arcsinh}[(\lambda\mu)^{-1/2}].$$

Note that λ now denotes the variable of the function $f(\lambda,\mu)$ and should not be confused with the scaling parameter $\alpha = (\lambda x + i\lambda^{-1} p)/\sqrt{2\hbar}$ from Section 5.5.1, which has also been used in the beginning of this section. This results in

$$[\Pi_{\mathrm{BJ}}]_{mn} = \sum_{k=0}^{n} \sum_{\substack{\ell=0 \\ \ell \text{ even}}}^{m-n} w^{k}_{mn\ell} (-1)^{k+(m-n)/2} 4^{k+(m-n)/2} (\partial_{\mu}^{k} \{[\partial_{\lambda}^{a} \partial_{\mu}^{b} f(\lambda,\mu)]|_{\lambda=\mu}\})|_{\mu=1}.$$

D.5 Calculating derivatives for the sum in Theorem 5.6

The derivatives $\Phi^k_{ab} = [\partial^k_\mu[\partial^a_\lambda\partial^b_\mu f(\lambda,\mu)]|_{\lambda=\mu}]|_{\mu=1}$ of the function $f : (0,\infty)\times(0,\infty) \to \mathbb{R}, (\lambda,\mu) \mapsto \operatorname{arcsinh}[1/\sqrt{\lambda\mu}]$, cf. (5.40), can be computed recursively. Note that, obviously, f is smooth. The inner derivatives of Φ^k_{ab} gives rise to the following lemma.

Lemma D.1. *Let any $a,b \in \mathbb{N}_0 := \{0,1,\ldots\}$ with $a+b \geq 1$ (else we are not taking any derivative). Then*

$$\partial^a_\lambda\partial^b_\mu f(\lambda,\mu) = \frac{\sum_{j=0}^{a+b-1} c^{ab}_j \lambda^{j-b}\mu^{j-a}}{(-2)^{a+b}(\sqrt{\lambda\mu+1})^{2(a+b)-1}} \tag{D.4}$$

where the coefficients c^{ab}_j are defined recursively by

$$c^{ab}_j = \begin{cases} c^{ab}_j = 0 \;\; \textit{if} \;\; j<0 \;\; \textit{or} \;\; j \geq a+b \\ c^{1\,0}_0 = 1 \\ c^{a+1,b}_j = c^{ab}_{j-1}(4a+2b+1-2j) - 2\,c^{ab}_j(j-a) \end{cases}$$

and have the symmetry $c^{ab}_j = c^{ba}_j$.

Proof. Note that the symmetry of the c^{ab}_j holds due to Schwarz's theorem [220, pp. 235-236] as f is smooth. Then this statement is readily verified via induction over $n = a+b$. First, $n=1$ corresponds to $a=1, b=0$ so $\partial_\mu \operatorname{arcsinh}[(\lambda\mu)^{-1/2}] = 1/(-2\mu\sqrt{\lambda\mu+1})$ which reproduces (D.4). For $n \mapsto n+1$ it is enough to consider $(a,b) \mapsto (a+1,b)$ due to the stated symmetry. The key result here is that

$$\partial_\mu \frac{\mu^{j-a}}{(\sqrt{\lambda\mu+1})^{2(a+b)-1}} = \frac{\mu^{j-a-1}}{2(\sqrt{\lambda\mu+1})^{2(a+b)+1}}[\lambda\mu(2j-4a-2b+1)+2(j-a)]$$

which is readily verified. Straightforward calculations conclude the proof. □

For $a+b \geq 1$, the above result immediatly yields

$$\Phi^k_{ab} = \partial^k_\mu[\,\frac{\sum_{j=0}^{a+b-1} c^{ab}_j \mu^{2j-b-a}}{(-2)^{a+b}(\sqrt{\mu^2+1})^{2(a+b)-1}}\,]|_{\mu=1}\,.$$

Now the c^{ab}_j are used to initialize the recursion of the coefficients ξ^{abk}_j for $a+b \geq 1$, the sum of which determines the resulting derivatives as we will see now.

Lemma D.2. *Let any $a, b, k \in \mathbb{N}_0$ with $a + b + k \geq 1$. Then*

$$\partial_\mu^k [\partial_\lambda^a \partial_\mu^b f(\lambda, \mu)]|_{\lambda=\mu}] = \frac{\sum_{j=0}^{a+b+k-1} \xi_j^{abk} \mu^{2j}}{(-2)^{a+b} \mu^{a+b+k} (\sqrt{\mu^2+1})^{2(a+b+k)-1}} \tag{D.5}$$

where the coefficients ξ_j^{abk} have the symmetry $\xi_j^{abk} = \xi_j^{bak}$ and are defined by

$$\xi_j^{abk} = \begin{cases} \xi_j^{abk} = 0 \;\; \textit{if} \;\; j < 0 \;\; \textit{or} \;\; j \geq a + b + k \\ \xi_0^{0\,0\,1} = -1 \\ \xi_j^{ab\,0} = c_j^{ab} \;\; \textit{if} \;\; a + b \geq 1 \\ \xi_j^{ab,k+1} = \xi_{j-1}^{abk}(2j - 1 - 3a - 3b - 3k) + \xi_j^{abk}(2j - a - b - k). \end{cases} \tag{D.6}$$

Proof. The key result here is

$$\partial_\mu \frac{\mu^{2j-\beta}}{(\sqrt{1+\mu^2})^{2\beta-1}} = \frac{\mu^{2j-\beta-1}}{(\sqrt{1+\mu^2})^{2\beta+1}} [\mu^2(2j - 3\beta + 1) + (2j - \beta)] \tag{D.7}$$

for any $\beta, j \in \mathbb{N}$ which can be easily seen. We have to distinguish the cases $a + b = 0$ and $a + b \geq 1$. First, let $a + b = 0$ so $a = 0, b = 0$ and the expression in question boils down to

$$\partial_\mu^k f(\mu, \mu) = \partial_\mu^k \mathrm{arcsinh}[\mu^{-1}] = \frac{\sum_{j=0}^{k-1} \xi_j^{00k} \mu^{2j-k}}{(\sqrt{1+\mu^2})^{2k-1}}$$

as can be shown via induction over $k \in \mathbb{N}$. Here, setting $\beta = k$ in (D.7) yields

$$\xi_j^{00,k+1} = \xi_{j-1}^{00k}(2j - 1 - 3k) + \xi_j^{00k}(2j - k)$$

which recovers the recursion formula of ξ_j^{abk} for $a = 0$ and $b = 0$. Now assume $a + b \geq 1$ such that we can carry out the proof via induction over $k \in \mathbb{N}_0$ (where $k = 0$ is obvious as it is simply Lemma D.1). Using (D.7) in the inductive step for $\beta = a + b + k$ recovers the recursion formula of the ξ_j^{abk} by straightforward computations. □

Finally, evaluating (D.5) at $\mu = 1$ for any $a, b, k \in \mathbb{N}_0$ with $a + b + k \geq 1$ readily implies Eq. (5.41).

D.6 Proof of Proposition 5.3

The proof which is given below was informed by a discussion on MathOverflow[84] and its idea was provided GH and M. Alekseyev. We consider the generating function of the entries $[\Pi_{\mathrm{BJ}}]_{nn}$.

Lemma D.3. *For all $|t| < 1$ one has*

$$\sum_{n=0}^{\infty} [\Pi_{\mathrm{BJ}}]_{nn} t^n = \frac{1}{1-t} \operatorname{arcsinh}\Big(\frac{1-t}{1+t}\Big)$$

where

$$[\Pi_{\mathrm{BJ}}]_{nn} = \sum_{k=0}^{n} \binom{n}{k} \frac{2^k c_k}{k!} \quad \textit{and} \quad c_n = \frac{d^n}{dx^n} \operatorname{arcsinh}\Big(\frac{1}{x}\Big)\Big|_{x=1}$$

for all $n \in \mathbb{N}_0$.

Proof. Obviously, $\operatorname{arcsinh}(1/w) = \sum_{n=0}^{\infty} (c_k/k!)(w-1)^k$ for all $|w-1| < 1$, so changing w to $1 + 2w$ yields

$$\operatorname{arcsinh}\Big(\frac{1}{1+2w}\Big) = \sum_{n=0}^{\infty} \frac{2^k c_k}{k!} w^k \tag{D.8}$$

for all $|w| < 1/2$. By the generalized Leibniz rule,

$$\begin{aligned} [w^n](1+w)^n \operatorname{arcsinh}\Big(\frac{1}{1+2w}\Big) &= \frac{1}{n!} \frac{d^n}{dw^n} (1+w)^n \operatorname{arcsinh}\Big(\frac{1}{1+2w}\Big)\Big|_{w=0} \\ = \frac{1}{n!} \sum_{k=0}^{n} \binom{n}{k} \underbrace{\frac{d^k}{dw^k} \operatorname{arcsinh}\Big(\frac{1}{1+2w}\Big)\Big|_{w=0}}_{=2^k c_k \text{ by (D.8)}} \underbrace{\frac{d^{n-k}}{dw^{n-k}} (1+w)^n\Big|_{w=0}}_{=n!/k!} &= \sum_{k=0}^{n} \binom{n}{k} \frac{2^k c_k}{k!} = [\Pi_{\mathrm{BJ}}]_{nn} \end{aligned} \tag{D.9}$$

for all $n \in \mathbb{N}_0$. Here, $[t^n]g(t) = g^{(n)}(0)/n!$ denotes the nth coefficient in the Taylor series of $g(t)$ around 0. Now we apply the Lagrange–Bürmann formula [4, 3.6.6] to $\phi(w) = 1 + w$ [so $w/\phi(w) = t$ for $|t| < 1$ has the unique solution $w = t/(1-t)$] and $H(w) = (1+w)\operatorname{arcsinh}[1/(1+2w)]$ which concludes the proof via

$$\begin{aligned} [t^n] \frac{1}{1-t} \operatorname{arcsinh}\Big(\frac{1-t}{1+t}\Big) = [t^n] H\Big(\frac{t}{1-t}\Big) &= [w^n] H(w) \phi(w)^{n-1} [\phi(w) - w\phi'(w)] \\ &= [w^n](1+w)^n \operatorname{arcsinh}\Big(\frac{1}{1+2w}\Big) \overset{\text{(D.9)}}{=} [\Pi_{\mathrm{BJ}}]_{nn}. \end{aligned}$$

□

Lemma D.4. *The following sum converges:*

$$\sum_{k=0}^{\infty} \frac{(-1)^k}{k+1} \sum_{m=0}^{\lfloor \frac{k}{2} \rfloor} \binom{2m}{m} \Big(\frac{-1}{4}\Big)^m \tag{D.10}$$

Proof. For arbitrary $k \in \{0,1,2,\dots\}$ we define

$$b_k := (-1)^k \sum_{m=0}^{\lfloor \frac{k}{2} \rfloor} \binom{2m}{m} \Big(\frac{-1}{4}\Big)^m .$$

Due to the summation limit $\lfloor \frac{k}{2} \rfloor$, one has $b_{2k} = -b_{2k+1}$ for all $k \in \{0,1,2,\dots\}$ and thus

$$\Big(\sum_{k=0}^{n} b_k \Big)_{n=0,1,2,\dots} = (b_0, 0, b_2, 0, b_4, 0, \dots) . \tag{D.11}$$

Therefore $(\sum_{k=0}^{n} b_k)_{n=0,1,2,\dots}$ consists of the null sequence and $(b_{2n})_{n=0,1,2,\dots}$, and it is therefore bounded due to

$$\lim_{n\to\infty} b_{2n} = \sum_{m=0}^{\infty} \binom{2m}{m} (-1/4)^m = 1/\sqrt{2} .$$

In total, (D.10) then converges due to Dirichlet's test [127, p. 328]. □

With these intermediate results we can finally prove the proposition in question.

Proof. Again using the generalized Leibniz rule, Lemma D.3 yields that

$$\begin{aligned}
[\Pi_{\mathrm{BJ}}]_{nn} &= [t^n] \frac{1}{1-t} \operatorname{arcsinh}\Big(\frac{1-t}{1+t}\Big) = \frac{1}{n!} \frac{d^n}{dt^n} \frac{1}{1-t} \operatorname{arcsinh}\Big(\frac{1-t}{1+t}\Big)\Big|_{t=0} \\
&= \frac{1}{n!} \sum_{k=0}^{n} \binom{n}{k} \frac{d^k}{dt^k} \operatorname{arcsinh}\Big(\frac{1-t}{1+t}\Big)\Big|_{t=0} \underbrace{\frac{d^{n-k}}{dt^{n-k}} \frac{1}{1-t}\Big|_{t=0}}_{=(n-k)!} \\
&= \operatorname{arcsinh}(1) + \sum_{k=1}^{n} \frac{1}{k!} \frac{d^k}{dt^k} \operatorname{arcsinh}\Big(\frac{1-t}{1+t}\Big)\Big|_{t=0}
\end{aligned}$$

holds for any $n \in \mathbb{N}_0$. It follows that

$$\begin{aligned}
\frac{d}{dt} \operatorname{arcsinh}\Big(\frac{1-t}{1+t}\Big) &= \frac{-\sqrt{2}}{(1+t)\sqrt{1+t^2}} = -\sqrt{2}\Big[\sum_{m=0}^{\infty} (-t)^m\Big]\Big[\sum_{m=0}^{\infty} \underbrace{\binom{-1/2}{m}}_{=\left(\frac{-1}{4}\right)^m \binom{2m}{m}} t^{2m}\Big] \\
&= -\sqrt{2} \sum_{m=0}^{\infty} \Big[\sum_{n=0}^{m} (-t)^{m-n} \binom{2n}{n} \Big(\frac{-1}{4}\Big)^n t^{2n} \Big] = -\sqrt{2} \sum_{m=0}^{\infty} (-1)^m t^m \sum_{n=0}^{m} \binom{2n}{n} \Big(\frac{t}{4}\Big)^n
\end{aligned}$$

for any $|t| < 1$ by taking the Cauchy product. Thus the kth derivative of $\operatorname{arcsinh}[(1-t)/(1+t)]$ at $t = 0$ only consists of the coefficients with exponent $n + m = k - 1$ of t. Explicitly,

$$\frac{d^k}{dt^k} \operatorname{arcsinh}\Big(\frac{1-t}{1+t}\Big)\Big|_{t=0} = -\sqrt{2} \underbrace{\frac{d^{k-1}}{dt^{k-1}} t^{k-1}\Big|_{t=0}}_{=(k-1)!} \sum_{\substack{m=0 \\ 0\le k-m-1\le m}}^{\infty} (-1)^m \binom{2k-2m-2}{k-m-1} \Big(\frac{1}{4}\Big)^{k-m-1}$$

for all $k \in \mathbb{N}$ as $n \in \{0, \dots, m\}$. The condition $0 \le k-m-1 \le m$ translates to $m \le k-1 \le 2m$, so $(k-1)/2 \le m \le k-1$ and thus

$$\begin{aligned}\frac{d^k}{dt^k}\operatorname{arcsinh}\Big(\frac{1-t}{1+t}\Big)\Big|_{t=0} &= -\sqrt{2}(k-1)!\sum_{m=\lceil\frac{1}{2}(k-1)\rceil}^{k-1}(-1)^m\binom{2k-2m-2}{k-m-1}\Big(\frac{1}{4}\Big)^{k-m-1}\\ &= \sqrt{2}(-1)^k(k-1)!\sum_{m=0}^{\lfloor\frac{1}{2}(k-1)\rfloor}(-1)^m\binom{2m}{m}\Big(\frac{1}{4}\Big)^m,\end{aligned}$$

where the second equality follows by substituting m with $k-1-m$. One then obtains

$$\begin{aligned}[\Pi_{\mathrm{BJ}}]_{nn} &= \operatorname{arcsinh}(1) + \sum_{k=1}^{n}\frac{1}{k!}\frac{d^k}{dt^k}\operatorname{arcsinh}\Big(\frac{1-t}{1+t}\Big)\Big|_{t=0}\\ &= \operatorname{arcsinh}(1) + \sqrt{2}\sum_{k=1}^{n}\frac{(-1)^k}{k}\sum_{m=0}^{\lfloor\frac{1}{2}(k-1)\rfloor}\binom{2m}{m}\Big(\frac{-1}{4}\Big)^m.\end{aligned}$$

To get (5.42) we shift k to $k+1$. Due to (5.42) and Lemma D.4, the limit $\lim_{n\to\infty}[\Pi_{\mathrm{BJ}}]_{nn}$ exists. Now consider $\operatorname{arcsinh}[(1-t)/(1+t)]$ and its Taylor series $\sum_{k=0}^{\infty}a_k t^k$ around $t_0 = 0$ for any $|t| < 1$. By Lemma D.3,

$$\begin{aligned}\sum_{k=0}^{\infty}a_k t^k = \operatorname{arcsinh}\Big(\frac{1-t}{1+t}\Big) = (1-t)\frac{1}{1-t}\operatorname{arcsinh}\Big(\frac{1-t}{1+t}\Big) &= \sum_{n=0}^{\infty}[\Pi_{\mathrm{BJ}}]_{nn}(1-t)t^n\\ &= [\Pi_{\mathrm{BJ}}]_{00} + \sum_{n=1}^{\infty}([\Pi_{\mathrm{BJ}}]_{nn} - [\Pi_{\mathrm{BJ}}]_{(n-1)(n-1)})t^n,\end{aligned}$$

thus $\sum_{k=0}^{n}a_k = [\Pi_{\mathrm{BJ}}]_{nn}$ for any $n \in \mathbb{N}_0$. By Lemma D.4, $\sum_{k=0}^{\infty}a_k = \lim_{n\to\infty}[\Pi_{\mathrm{BJ}}]_{nn}$ exists so Abel's theorem [127, Th. 8.2] yields the following limit as $\lim_{n\to\infty}[\Pi_{\mathrm{BJ}}]_{nn} = \sum_{k=0}^{\infty}a_k = \lim_{t\to 1^-}\operatorname{arcsinh}[(1-t)/(1+t)] = \operatorname{arcsinh}(0) = 0$ as claimed. □

D.7 Direct recursive calculation of the matrix elements

The non-zero matrix elements are defined by a set of rational numbers

$$M_{k\ell} := [\Pi_{\mathrm{BJ}}]_{k+4\ell,k}/(\Gamma_{k\ell}) - \delta_{\ell 0}\operatorname{arcsh}(1)/\sqrt{2}, \tag{D.12}$$

where the indexing $k, \ell \in \{0, 1, 2, \dots\}$ is now relative to the diagonal (where $\ell = 0$) and $\Gamma_{k\ell} := \gamma_{k+4\ell,k} = 2^{-2\ell+1/2}\sqrt{k!/(k+4\ell)!}$. Here, δ_{nm} is the Kronecker delta and note the symmetry $[\Pi_{\mathrm{BJ}}]_{k,k+4\ell} = [\Pi_{\mathrm{BJ}}]_{k+4\ell,k}$. For example, the values M_{k0} define the diagonal of the Born-Jordan parity operator $[\Pi_{\mathrm{BJ}}]_{kk}$ up to the constants $\Gamma_{k0} = \sqrt{2}$ and $\operatorname{arcsh}(1)/\sqrt{2}$, compare to Fig. 5.1. These rational numbers appear to satisfy the following recursive relations

$$M_{k+4,\ell} = \tfrac{1}{k+4}M_{k+3,\ell} + \tfrac{4\ell+2k+5}{(k+3)(k+4)}M_{k+2,\ell} + \tfrac{4\ell+k+2}{(k+3)(k+4)}M_{k+1,\ell} + \tfrac{(4\ell+k+1)(4\ell+k+2)}{(k+3)(k+4)}M_{k\ell},$$

i.e., each element in a column is determined by the previous four values. Calculating a column requires, however, the first four elements $M_{0\ell}, M_{1\ell}, M_{2\ell}, M_{3\ell}$ as initial conditions.

Surprisingly, the first four rows appear to satisfy the following recursive relations

$$
\begin{aligned}
M_{0,\ell+2} &= 4\big[(27+56\ell+32\ell^2)M_{0,\ell+1} - 16\ell(1{+}4\ell)(2{+}4\ell)(3{+}4\ell)M_{0\ell}\big]\\
M_{1,\ell+2} &= 4\big[(39+72\ell+32\ell^2)M_{1,\ell+1} - 16\ell(2{+}4\ell)(3{+}4\ell)(5{+}4\ell)M_{1\ell}\big]\\
M_{2,\ell+2} &= 4\big[(55+88\ell+32\ell^2)M_{2,\ell+1} - 16\ell(3{+}4\ell)(5{+}4\ell)(6{+}4\ell)M_{2\ell}\big]\\
M_{3,\ell+2} &= 4\big[(75+104\ell+32\ell^2)M_{3,\ell+1} - 16\ell(5{+}4\ell)(6{+}4\ell)(7{+}4\ell)M_{3\ell}\big].
\end{aligned}
$$

Ultimately, eight initial values $M_{0,0} = 0$, $M_{0,1} = 4$, $M_{1,0} = -1$, $M_{1,1} = -8$, $M_{2,0} = -1/2$, $M_{2,1} = 6$, $M_{3,0} = -2/3$, and $M_{3,1} = -4$ appear to determine the Born-Jordan parity operator via the above recursion relations for the elements $M_{k\ell}$.

References

[1] See Ancillary files at arxiv.org/abs/1612.06777 for the Mathematica files.

[2] Abadie, J., Abbott, B., Abbott, R., Abbott, T., Abernathy, M., Adams, C., Adhikari, R., Affeldt, C., Allen, B., Allen, G., et al.: A gravitational wave observatory operating beyond the quantum shot-noise limit. Nat. Phys. **7**(12), 962 (2011)

[3] Abragam, A., Carr, H.Y.: The principles of nuclear magnetism. Clarendon Press, Oxford (1961)

[4] Abramowitz, M., Stegun, I.A.: Handbook of Mathematical Functions: with Formulas, Graphs, and Mathematical Tables. Dover, New York (1965)

[5] Acevedo, O., Safavi-Naini, A., Schachenmayer, J., Wall, M., Nandkishore, R., Rey, A.: Exploring many-body localization and thermalization using semiclassical methods. Phys. Rev. A **96**(3), 033604 (2017)

[6] Agarwal, G., Tara, K.: Nonclassical properties of states generated by the excitations on a coherent state. Phys. Rev. A **43**(1), 492 (1991)

[7] Agarwal, G.S.: Relation between atomic coherent-state representation, state multipoles, and generalized phase-space distributions. Phys. Rev. A **24**, 2889–2896 (1981)

[8] Agarwal, G.S.: State reconstruction for a collection of two-level systems. Phys. Rev. A **57**, 671–673 (1998)

[9] Agarwal, G.S., Puri, R.R., Singh, R.P.: Atomic Schrödinger cat states. Phys. Rev. A **56**, 2249–2254 (1997)

[10] Agarwal, G.S., Wolf, E.: Quantum Dynamics in Phase Space. Phys. Rev. Lett. **21**, 180–183 (1968)

[11] Agarwal, G.S., Wolf, E.: Calculus for functions of noncommuting operators and general phase-space methods in quantum mechanics. I. Mapping theorems and ordering of functions of noncommuting operators. Phys. Rev. D **2**(10), 2161 (1970)

[12] Agarwal, G.S., Wolf, E.: Calculus for functions of noncommuting operators and general phase-space methods in quantum mechanics. II. Quantum mechanics in phase space. Phys. Rev. D **2**(10), 2187 (1970)

[13] Ali, S.T., Antoine, J.P., Gazeau, J.P.: Coherent states, wavelets and their generalizations. Springer, New York (2000)

[14] Altmann, S.L.: Rotations, quaternions, and double groups. Dover, Mineola (2005)

[15] Amiet, J.P., Weigert, S.: Reconstructing the density matrix of a spin s through Stern-Gerlach measurements. J. Phys. A **31**(31), L543 (1998)

[16] Amiet, J.P., Weigert, S.: Contracting the Wigner kernel of a spin to the Wigner kernel of a particle. Phys. Rev. A **63**(1), 012102 (2000)

[17] Anderson, M.H., Ensher, J.R., Matthews, M.R., Wieman, C.E., Cornell, E.A.: Observation of Bose-Einstein condensation in a dilute atomic vapor. Science **269**(5221), 198–201 (1995)

[18] Arecchi, F., Courtens, E., Gilmore, R., Thomas, H.: Atomic coherent states in quantum optics. Phys. Rev. A **6**(6), 2211 (1972)

[19] Arfken, G.B., Weber, H.J.: Mathematical methods for physicists, 6. edn. Academic Press, Amsterdam (2005)

[20] Arnol'd, V.I.: Mathematical methods of classical mechanics. Springer Science & Business Media, New York (2013)

[21] Banaszek, K., Radzewicz, C., Wódkiewicz, K., Krasiński, J.S.: Direct measurement of the Wigner function by photon counting. Phys. Rev. A **60**, 674–677 (1999)

[22] Banaszek, K., Wódkiewicz, K.: Nonlocality of the Einstein-Podolsky-Rosen state in the Wigner representation. Phys. Rev. A **58**, 4345–4347 (1998)

[23] Banaszek, K., Wódkiewicz, K.: Testing quantum nonlocality in phase space. Phys. Rev. Lett. **82**, 2009–2013 (1999)

[24] Barbieri, M., Spagnolo, N., Genoni, M.G., Ferreyrol, F., Blandino, R., Paris, M.G., Grangier, P., Tualle-Brouri, R.: Non-Gaussianity of quantum states: an experimental test on single-photon-added coherent states. Phys. Rev. A **82**(6), 063833 (2010)

[25] Bayen, F., Flato, M., Fronsdal, C., Lichnerowicz, A., Sternheimer, D.: Deformation theory and quantization. I. Deformations of symplectic structures. Ann. Phys. **111**(1), 61–110 (1978)

[26] Bayen, F., Flato, M., Fronsdal, C., Lichnerowicz, A., Sternheimer, D.: Deformation theory and quantization. II. Physical applications. Ann. Phys. **111**(1), 111–151 (1978)

[27] Benedict, M.G., Czirják, A.: Wigner functions, squeezing properties, and slow decoherence of mesoscopic superposition of two-level atoms. Phys. Rev. A **60**, 4034–4044 (1999)

[28] Berezin, F.A.: Quantization. Mathematics of the USSR-Izvestiya **8**(5), 1109 (1974)

[29] Berezin, F.A.: General concept of quantization. Comm. Math. Phys. **40**(2), 153–174 (1975)

[30] Bergeron, H., Gazeau, J., Youssef, A.: Are the Weyl and coherent state descriptions physically equivalent? Phys. Lett. A **377**(8), 598 – 605 (2013)

[31] Bernstein, M.A., King, K.F., Zhou, X.J.: Handbook of MRI pulse sequences. Elsevier, London (2004)

[32] Bertet, P., Auffeves, A., Maioli, P., Osnaghi, S., Meunier, T., Brune, M., Raimond, J.M., Haroche, S.: Direct measurement of the Wigner function of a one-photon Fock state in a cavity. Phys. Rev. Lett. **89**, 200402 (2002)

[33] Biedenharn, L.C., Louck, J.D.: Angular Momentum in Quantum Physics. Addison-Wesley, Reading, MA (1981)

[34] Bishop, R.F., Vourdas, A.: Displaced and squeezed parity operator: its role in classical mappings of quantum theories. Phys. Rev. A **50**(6), 4488 (1994)

[35] Björck, À., Pereyra, V.: Solution of Vandermonde systems of equations. Math. Comp. **24**(112), 893–903 (1970)

[36] Björk, G., Klimov, A.B., de la Hoz, P., Grassl, M., Leuchs, G., Sánchez-Soto, L.L.: Extremal quantum states and their Majorana constellations. Physical Review A **92**(3), 031801 (2015)

[37] Boggiatto, P., Cuong, B.K., De Donno, G., Oliaro, A.: Weighted integrals of Wigner representations. J. Pseudo-Differ. Oper. Appl. **1**(4), 401–415 (2010)

[38] Boggiatto, P., De Donno, G., Oliaro, A.: Time-frequency representations of Wigner type and pseudo-differential operators. Trans. Amer. Math. Soc. **362**(9), 4955–4981 (2010)

[39] Boggiatto, P., De Donno, G., Oliaro, A.: Hudson's theorem for τ-Wigner transforms. B. Lond. Math. Soc. **45**(6), 1131–1147 (2013)

[40] Bohnet, J.G., Sawyer, B.C., Britton, J.W., Wall, M.L., Rey, A.M., Foss-Feig, M., Bollinger, J.J.: Quantum spin dynamics and entanglement generation with hundreds of trapped ions. Science **352**(6291), 1297–1301 (2016)

[41] Bollini, C.G., Oxman, L.E.: Shannon entropy and the eigenstates of the single-mode squeeze operator. Phys. Rev. A **47**(3), 2339–2343 (1993)

[42] Bopp, F.: La méchanique quantique est-elle une méchanique statistique classique particuliere? Ann. Inst. H. Poincaré **15**, 81–112 (1956)

[43] Born, M., Jordan, P.: Zur Quantenmechanik. Zeitschr. Phys. **34**(1), 858–888 (1925)

[44] Bouchard, F., de la Hoz, P., Bjork, G., Boyd, R.W., Grassl, M., Hradil, Z., Karimi, E., Klimov, A.B., Leuchs, G., Rehacek, J., Sanchez-Soto, L.L.: Quantum metrology at the limit with extremal Majorana constellations. Optica **4**(11), 1429–1432 (2017)

[45] Bransden, B.H., Joachain, C.J.: Quantum mechanics. Pearson Education (2000)

[46] Brif, C., Mann, A.: A general theory of phase-space quasiprobability distributions. J. Phys. A **31**, L9–L17 (1997)

[47] Brif, C., Mann, A.: Phase-space formulation of quantum mechanics and quantum-state reconstruction for physical systems with Lie-group symmetries. Phys. Rev. A **59**(2), 971–987 (1999)

[48] Bužek, V., Keitel, C.H., Knight, P.L.: Sampling entropies and operational phase-space measurement. II. Detection of quantum coherences. Phys. Rev. A **51**(3), 2594–2601 (1995)

[49] Cabrera, R., Bondar, D.I., Jacobs, K., Rabitz, H.A.: Efficient method to generate time evolution of the Wigner function for open quantum systems. Phys. Rev. A **92**(4), 042122 (2015)

[50] Cahill, K.E., Glauber, R.: Density operators and quasiprobability distributions. Phys. Rev. **177**(5), 1882 (1969)

[51] Cahill, K.E., Glauber, R.J.: Ordered Expansions in Boson Amplitude Operators. Phys. Rev. **177**(5), 1857–1881 (1969)

[52] Carrington, A., McLachlan, A.D.: Introduction to magnetic resonance with applications to chemistry and chemical physics. Harper & Row, New York (1967)

[53] Carruthers, P., Zachariasen, F.: Quantum collision theory with phase-space distributions. Rev. Mod. Phys. **55**(1), 245–285 (1983)

[54] Cavanagh, J., Fairbrother, W.J., Palmer, A.G., Skelton, N.J.: Protein NMR spectroscopy: principles and practice. Academic Press, San Diego (1996)

[55] Chaturvedi, S., Marmo, G., Mukunda, N., Simon, R., Zampini, A.: The Schwinger representation of a group: concept and applications. Rev. Math. Phys. **18**(08), 887–912 (2006)

[56] Chountasis, S., Vourdas, A., Bendjaballah, C.: Fractional Fourier operators and generalized Wigner functions. Physical Review A **60**(5), 3467 (1999)

[57] Chruściński, D.: Quantum mechanics of damped systems. J. Math. Phys. **44**(9), 3718–3733 (2003)

[58] Chruściński, D.: Spectral properties of the squeeze operator. Phys. Lett. A **327**(4), 290–295 (2004)

[59] Cohen, L.: Generalized phase-space distribution functions. J. Math. Phys. **7**(5), 781–786 (1966)

[60] Cohen, L.: Time-Frequency Analysis. Prentice-Hall, Englewood Cliffs, NJ (1995)

[61] Cohen-Tannoudji, C., Diu, B., Laloe, F.: Quantum Mechanics, Vol. 1. Wiley, New York (1991)

[62] Curtright, T.L., Fairlie, D.B., Zachos, C.K.: A Concise Treatise on Quantum Mechanics in Phase Space. World Scientific, Singapore (2014)

[63] Dahl, J.P.: On the group of translations and inversions of phase space and the Wigner functions. Phys. Script. **25**(4), 499 (1982)

[64] Dahl, J.P., Mack, H., Wolf, A., Schleich, W.P.: Entanglement versus negative domains of Wigner functions. Phys. Rev. A **74**, 042323 (2006)

[65] Dahl, J.P., Schleich, W.P.: Concepts of radial and angular kinetic energies. Phys. Rev. A **65**(2), 022109 (2002)

[66] Dahl, J.P., Springborg, M.: Wigner's phase space function and atomic structure: I. The hydrogen atom ground state. Mol. Phys. **47**(5), 1001–1019 (1982)

[67] Dahl, J.P., Springborg, M.: The Morse oscillator in position space, momentum space, and phase space. J. Chem. Phys. **88**(7), 4535–4547 (1988)

[68] Daubechies, I.: Coherent states and projective representation of the linear canonical transformations. J. Math. Phys. **21**(6), 1377–1389 (1980)

[69] Daubechies, I.: On the distributions corresponding to bounded operators in the Weyl quantization. Comm. Math. Phys. **75**(3), 229–238 (1980)

[70] Daubechies, I., Grossmann, A.: An integral transform related to quantization. J. Math. Phys. **21**(8), 2080–2090 (1980)

[71] Daubechies, I., Grossmann, A., Reignier, J.: An integral transform related to quantization. II. Some mathematical properties. J. Math. Phys. **24**(2), 239–254 (1983)

[72] Davidson, S.M., Polkovnikov, A.: SU(3) semiclassical representation of quantum dynamics of interacting spins. Phys. Rev. Lett. **114**(4), 045701 (2015)

[73] Del Castillo, G.F.T.: 3-D Spinors, Spin-Weighted Functions and Their Applications. Springer, New York (2012)

[74] Deleglise, S., Dotsenko, I., Sayrin, C., Bernu, J., Brune, M., Raimond, J.M., Haroche, S.: Reconstruction of non-classical cavity field states with snapshots of their decoherence. Nature **455**, 510–514 (2008)

[75] Dicke, R.H.: Coherence in spontaneous radiation processes. Phys. Rev. **93**(1), 99–110 (1954)

[76] Dirac, P.A.M.: The principles of quantum mechanics. Oxford university press, Oxford (1930)

[77] Dowling, J., Schleich, W., Wheeler, J.: Interference in phase space. Ann. Phys. (Berl.) **503**(7), 423–478 (1991)

[78] Dowling, J.P., Agarwal, G.S., Schleich, W.P.: Wigner distribution of a general angular-momentum state: applications to a collection of two-level atoms. Phys. Rev. A **49**(5), 4101–4109 (1994)

[79] Dür, W., Vidal, G., Cirac, J.I.: Three qubits can be entangled in two inequivalent ways. Phys. Rev. A **62**, 062314 (2000)

[80] D'Ariano, G., Maccone, L., Paini, M.: Spin tomography. J. Opt. B **5**(1), 77 (2003)

[81] Ehrenfest, P., Ehrenfest, T.: Begriffliche Grundlagen der statistischen Auffassung in der Mechanik. B. G. Teubner, Liepzig (1911)

[82] Eichler, C., Bozyigit, D., Lang, C., Steffen, L., Fink, J., Wallraff, A.: Experimental state tomography of itinerant single microwave photons. Phys. Rev. Lett. **106**, 220503 (2011)

[83] Eltschka, C., Siewert, J.: Quantifying entanglement resources. J. Phys. A **47**, 424005 (2014)

[84] vom Ende, F.: Closed, sum-free form for the n-th derivative of $\mathrm{arcsinh}(1/x)$ in $x = 1$. MathOverflow. https://mathoverflow.net/q/295019 (2018-03-12)

[85] Ernst, R.R., Bodenhausen, G., Wokaun, A.: Principles of nuclear magnetic resonance in one and two dimensions. Clarendon Press, Oxford (1987)

[86] Faist, P., Renner, R.: Practical and reliable error bars in quantum tomography. Phys. Rev. Lett. **117**(1), 010404 (2016)

[87] Fano, U.: Geometrical characterization of nuclear states and the theory of angular correlations. Phys. Rev. **90**(4), 577–579 (1953)

[88] Farrar, T.C.: Density matrices in NMR spectroscopy: part I. Concepts Magn. Reson. A **2**(1), 1–12 (1990)

[89] Feng, X.M., Wang, P., Yang, W., Jin, G.R.: High-precision evaluation of Wigner's d matrix by exact diagonalization. Phys. Rev. E **92**, 043307 (2015)

[90] Ferrie, C.: Quasi-probability representations of quantum theory with applications to quantum information science. Rep. Prog. Phys. **74**, 116001 (2011)

[91] Ferrie, C., Emerson, J.: Frame representations of quantum mechanics and the necessity of negativity in quasi-probability representations. J. Phys. A **41**, 352001 (2008)

[92] Ferrie, C., Emerson, J.: Framed Hilbert space: hanging the quasi-probability pictures of quantum theory. New J. Phys. **11**(6), 063040 (2009)

[93] Feynman, R.P., Hibbs, A.R.: Quantum Mechanics and Path Integrals. McGraw-Hill, New York (1965)

[94] Feynman, R.P., Vernon Jr., F.L., Hellwarth, R.W.: Geometrical representation of the Schrödinger equation for solving maser problems. J. Appl. Phys. **28**, 49–52 (1957)

[95] Freidel, L., Krasnov, K.: The fuzzy sphere star product and spin networks. J. Math. Phys. **43**, 1737

[96] Freude, D.: Quadrupolar Nuclei in Solid-State Nuclear Magnetic Resonance. In: R.A. Meyers, C. Dybowski (eds.) Encyclopedia of Analytical Chemistry (2006)

[97] Gadella, M.: Moyal formulation of quantum mechanics. Fortschr. Phys. **43**(3), 229 (1995)

[98] Garon, A., Zeier, R., Glaser, S.J.: Visualizing operators of coupled spin systems. Phys. Rev. A **91**, 042122 (2015)

[99] Gazeau, J.P.: Coherent States in Quantum Physics. Wiley-VCH, Weinheim (2009)

[100] Gelfand, I.M., Vilenkin, N.Y.: Generalized Functions, Vol. IV. Academic Press, New York (1964)

[101] Gibbons, K.S., Hoffman, M.J., Wootters, W.K.: Discrete phase space based on finite fields. Phys. Rev. A **70**(6), 062101 (2004)

[102] Gieres, F.: Mathematical surprises and Dirac's formalism in quantum mechanics. Rep. Prog. Phys. **63**(12), 1893–1931 (2000)

[103] Giraud, O., Braun, P., Braun, D.: Classicality of spin states. Phys. Rev. A **78**(4), 042112 (2008)

[104] Glaser, S.J., Boscain, U., Calarco, T., Koch, C.P., Köckenberger, W., Kosloff, R., Kuprov, I., Luy, B., Schirmer, S., Schulte-Herbüggen, T., Sugny, D., Wilhelm, F.K.: Training Schrödinger's Cat: Quantum Optimal Control. Eur. Phys. J. D **69**, 279 (2015)

[105] Glaser, S.J., Schulte-Herbrüggen, T., Sieveking, M., Schedletzky, O., Nielsen, N.C., Sørensen, O.W., Griesinger, C.: Unitary control in quantum ensembles: maximizing signal intensity in coherent spectroscopy. Science **280**(5362), 421–424 (1998)

[106] Glauber, R.J.: Coherent and Incoherent States of the Radiation Field. Phys. Rev. **131**(6), 2766–2788 (1963)

[107] Glauber, R.J.: Nobel Lecture: One hundred years of light quanta. Rev. Mod. Phys. **78**(4), 1267–1278 (2006)

[108] Glauber, R.J.: Quantum theory of optical coherence: selected papers and lectures. John Wiley & Sons, Weinheim (2007)

[109] Gleick, J.: Chaos: Making a New Science. Viking, New York (1987)

[110] de Gosson, M.A.: Born–Jordan quantization and the equivalence of the Schrödinger and Heisenberg pictures. Found. Phys. **44**(10), 1096–1106 (2014)

[111] de Gosson, M.A.: Born–Jordan Quantization. Springer, Switzerland (2016)

[112] de Gosson, M.A.: The Angular Momentum Dilemma and Born–Jordan Quantization. Found. Phys. **47**(1), 61–70 (2017)

[113] de Gosson, M.A.: The Wigner Transform. World Scientific, London (2017)

[114] Grangier, P., Slusher, R.E., Yurke, B., LaPorta, A.: Squeezed-light–enhanced polarization interferometer. Phys. Rev. Lett. **59**, 2153–2156 (1987)

[115] Gratus, J.: A natural basis of states for the noncommutative sphere and its Moyal bracket. J. Math. Phys. **38**, 4283 (1997)

[116] Gröchenig, K.: Foundations of Time-Frequency Analysis. Birkhäuser, Boston (2001)

[117] Groemer, H.: Geometric Applications of Fourier Series and Spherical Harmonics. Cambridge University Press, Cambridge (1996)

[118] Groenewold, H.: On the principles of elementary quantum mechanics. Physica **12**, 405–460 (1946)

[119] Grossmann, A.: Parity operator and quantization of δ-functions. Comm. Math. Phys. **48**(3), 191–194 (1976)

[120] Grote, H., Danzmann, K., Dooley, K.L., Schnabel, R., Slutsky, J., Vahlbruch, H.: First long-term application of squeezed states of light in a gravitational-wave observatory. Phys. Rev. Lett. **110**, 181101 (2013)

[121] Gühne, O., Tóth, G.: Entanglement detection. Phys. Rep. **474**, 1–75 (2009)

[122] Haas, F., Volz, J., Gehr, R., Reichel, J., Estève, J.: Entangled states of more than 40 atoms in an optical fiber cavity. Science **344**(6180), 180–183 (2014)

[123] Hall, B.C.: Quantum theory for mathematicians. Springer, New York (2013)

[124] Halstead, T.K., Osment, P.A.: Multipole NMR. IX. Polar graphical representation of nuclear spin polarizations. J. Magn. Reson. **60**, 382–396 (1984)

[125] Hamilton, W.R.: On a general method in dynamics. Philos. Trans. R. Soc. London **124**, 247–308 (1834)

[126] Hamley, C.D., Gerving, C.S., Hoang, T.M., Bookjans, E.M., Chapman, M.S.: Spin-nematic squeezed vacuum in a quantum gas. Nat. Phys. **8**(4), 305–308 (2012)

[127] Hardy, G.H.: Course of Pure Mathematics. Cambridge University Press, Cambridge (2015)

[128] Harland, D., Everitt, M.J., Nemoto, K., Tilma, T., Spiller, T.P.: Towards a complete and continious Wigner function for an ensemble of spins or qubits. Phys. Rev. A **86**, 062117 (2012)

[129] Heisenberg, W.: Über quantentheoretische Umdeutung kinematischer und mechanischer Beziehungen. Z. Phys. **33**, 879–893 (1925)

[130] Heiss, S., Weigert, S.: Discrete Moyal-type representations for a spin. Phys. Rev. A **63**(1), 012105 (2000)

[131] Hillery, M., O'Connell, R.F., Scully, M.O., Wigner, E.P.: Distribution functions in physics: fundamentals. Phys. Rep. **106**(3), 121–167 (1984)

[132] Ho, T.L.: Spinor Bose condensates in optical traps. Phys. Rev. Lett. **81**(4), 742–745 (1998)

[133] Horodecki, R., Horodecki, P., Horodecki, M., Horodecki, K.: Quantum entanglement. Rev. Mod. Phys. **81**(2), 865–942 (2009)

[134] Howard, M., Wallman, J., Veitch, V., Emerson, J.: Contextuality supplies the 'magic' for quantum computation. Nature **510**(7505), 351–355 (2014)

[135] Husimi, K.: Some formal properties of the density matrix. Proc. Phys. Math. Soc. Japan **22**(4), 264–314 (1940)

[136] Jackson, J.D.: Classical electrodynamics, third edn. John Wiley & Sons, New York (1999)

[137] Jacobi, C.G.J.: Vorlesungen über dynamik. Georg Reimer, Berlin (1866)

[138] Jessen, P.S., Haycock, D.L., Klose, G., Smith, G.A., Deutsch, I.H., Brennen, G.K.: Quantum control and information processing in optical lattices. Quant. Inf. Comp. **1**, 20–32 (2001)

[139] Johansen, L.M.: EPR correlations and EPW distributions revisited. Phys. Lett. A **236**, 173–176 (1997)

[140] Kalev, A., Mann, A., Mello, P.A., Revzen, M.: Inadequacy of a classical interpretation of quantum projective measurements via Wigner functions. Phys. Rev. A **79**, 014104 (2009)

[141] Kanem, J., Maneshi, S., Myrskog, S., Steinberg, A.: Phase space tomography of classical and nonclassical vibrational states of atoms in an optical lattice. J. Opt. B **7**(12), S705 (2005)

[142] Kanwal, R.P.: Generalized functions: Theory and Technique. Springer, Boston (2012)

[143] Kasperkovitz, P.: Quasiclassical descriptions of quantum systems based on coherent states: Product formulae. J. Phys. A **23**(23), 5493 (1990)

[144] Keeler, J.: Understanding NMR spectroscopy, 2nd edn. John Wiley & Sons, Chichester (2011)

[145] Keihänen, E., Reinecke, M.: ArtDeco: a beam-deconvolution code for absolute cosmic microwave background measurements. Astron. Astrophys. **548**, A110 (2012)

[146] Kenfack, A., Życzkowski, K.: Negativity of the Wigner function as an indicator of non-classicality. J. Opt. B **6**, 396–404 (2004)

[147] Kennedy, R.A., Sadeghi, P.: Hilbert Space Methods in Signal Processing. Cambridge University Press, Cambridge (2013)

[148] Keyl, M., Kiukas, J., Werner, R.F.: Schwartz operators. Rev. Math. Phys. **28**(03), 1630001 (2016)

[149] Kim, Y.S., Noz, M.E.: Phase Space Picture of Quantum Mechanics: Group Theoretical Approach. World Scientific, Singapore (1991)

[150] Klimov, A.B.: Exact evolution equations for $\mathrm{SU}(2)$ quasidistribution functions. J. Math. Phys. **43**(5), 2202–2213 (2002)

[151] Klimov, A.B., Espinoza, P.: Moyal-like form of the star product for generalized $\mathrm{SU}(2)$ Stratonovich-Weyl symbols. J. Phys. A **35**, 8435 (2002)

[152] Klimov, A.B., Espinoza, P.: Classical evolution of quantum fluctuations in spin-like systems: squeezing and entanglement. J. Opt. B **7**(6), 183 (2005)

[153] Klimov, A.B., de Guise, H.: General approach to $\mathfrak{SU}(n)$ quasi-distribution functions. J. Phys. A **43**, 402001 (2010)

[154] Klimov, A.B., Romero, J.: A generalized Wigner function for quantum systems with the $\mathrm{SU}(2)$ dynamical symmetry group. J. Phys. A **41**(5), 055303 (2008)

[155] Klimov, A.B., Romero, J.L., de Guise, H.: Generalized SU(2) covariant Wigner functions and some of their applications. J. Phys. A **50**, 1–54 (2017)

[156] Klimov, A.B., Zwierz, M., Wallentowitz, S., Jarzyna, M., Banaszek, K.: Optimal lossy quantum interferometry in phase space. New J. Phys **19**(08), 073013 (2017)

[157] Knips, L., Schwemmer, C., Klein, N., Reuter, J., Tóth, G., Weinfurter, H.: How long does it take to obtain a physical density matrix? (2015). (*Preprint* `arXiv:1512.06866v1`)

[158] Koczor, B., vom Ende, F., de Gosson, M.A., Glaser, S.J., Zeier, R.: Phase Spaces, Parity Operators, and the Born-Jordan Distribution (2018). (*Preprint* `arXiv:1811.05872`)

[159] Koczor, B., Zeier, R., Glaser, S.J.: Time evolution of coupled spin systems in a generalized Wigner representation (2016). (*Preprint* `arXiv:1612.06777`)

[160] Koczor, B., Zeier, R., Glaser, S.J.: Continuous phase-space representations for finite-dimensional quantum states and their tomography (2017). (*Preprint* `arXiv:1711.07994`)

[161] Koczor, B., Zeier, R., Glaser, S.J.: Continuous phase spaces and the time evolution of spins: star products and spin-weighted spherical harmonics. J. Phys. A. **52**(5), 055302 (2019)

[162] Kumar, R., Barrios, E., Kupchak, C., Lvovsky, A.: Experimental characterization of bosonic creation and annihilation operators. Phys. Rev. Lett. **110**(13), 130403 (2013)

[163] Landau, L.D., Lifshitz, E.M.: Course on theoretical physics. Pergamon Press, Oxford (1976)

[164] Lebedev, N.N., Silverman, R.A.: Special Functions and Their Applications. Dover, New York (1972)

[165] Lee, H.W.: Theory and application of the quantum phase-space distribution functions. Phys. Rep. **259**(3), 147–211 (1995)

[166] Leibfried, D., Knill, E., Seidelin, S., Britton, J., Blakestad, R.B., Chiaverini, J., Hume, D.B., Itano, W.M., Jost, J.D., Langer, C., Reichle, R., Wineland, D.J.: Creation of a six-atom 'Schrödinger cat'state. Nature **438**(7068), 639–642 (2005)

[167] Leiner, D., Glaser, S.J.: Wigner process tomography and visualization of spin propagators and their spinor properties. Phys. Rev. A **96**(6), 063413 (2018)

[168] Leiner, D., Zeier, R., Glaser, S.J.: Wigner tomography of multispin quantum states. Phys. Rev. A **96**, 063413 (2017)

[169] Leiner, D., Zeier, R., Glaser, S.J.: Symmetry-adapted decomposition of tensor operators and the visualization of coupled spin systems (2018). Preprint `arXiv:1809.09006`

[170] Leonhardt, U.: Discrete Wigner function and quantum-state tomography. Phys. Rev. A **53**(5), 2998–3013 (1996)

[171] Leonhardt, U.: Measuring the Quantum State of Light. Cambridge Univ. Press, Cambridge (1997)

[172] Leonhardt, U., Paul, H.: Realistic optical homodyne measurements and quasiprobability distributions. Phys. Rev. A **48**, 4598–4604 (1993)

[173] Levitt, M.H.: Spin dynamics: basics of nuclear magnetic resonance. John Wiley & Sons, Chichester (2001)

[174] Li, H.: Group-theoretical derivation of the Wigner distribution function. Phys. Lett. A **188**(2), 107 – 109 (1994)

[175] Li, H.: Wigner function and the parity operator. Phys. Lett. A **190**(5), 370 – 372 (1994)

[176] Lin, Y.J., Jiménez-García, K., Spielman, I.: A spin-orbit coupled Bose-Einstein condensate. Nature **471**, 83–86 (2011)

[177] Liouville, J.: Note on the Theory of the Variation of Arbitrary Constants. J. Math. Pure. Appl. **3**, 342–349 (1838)

[178] Lücke, B., Peise, J., Vitagliano, G., Arlt, J., Santos, L., Tóth, G., Klempt, C.: Detecting multiparticle entanglement of Dicke states. Phys. Rev. Lett. **112**(15), 155304 (2014)

[179] Lugiato, L., Gatti, A., Brambilla, E.: Quantum imaging. J. Opt. B. **4**(3), S176 (2002)

[180] Lutterbach, L.G., Davidovich, L.: Method for direct measurement of the Wigner function in cavity QED and ion traps. Phys. Rev. Lett. **78**, 2547–2550 (1997)

[181] Ma, J., Wang, X., Sun, C.P., Nori, F.: Quantum spin squeezing. Phys. Rep. **509**(2-3), 89–165 (2011)

[182] Mandel, L., Wolf, E.: Optical coherence and quantum optics. Cambridge university press, Cambridge (1995)

[183] Mandilara, A., Karpov, E., Cerf, N.J.: Extending Hudson's theorem to mixed states. Phys. Rev. A **79**, 062302 (2009)

[184] Man'ko, V.I., Man'ko, O.V.: Spin state tomography. J. Exp. Theor. Phys. **85**(3), 430–434 (1997)

[185] Marchiolli, M.A., Galetti, D., Debarba, T.: Spin squeezing and entanglement via finite-dimensional discrete phase-space description. Int. J. Quantum Inf. **11**(01), 1330001 (2013)

[186] Marzlin, K.P., Osborn, T.A.: Quantum-collapse Bell inequalities. Phys. Rev. A **89**, 032123 (2014)

[187] Maurin, K.: General Eigenfunction Expansions and Unitary Representations of Topological Groups. PWN-Polish Scientific Publishers, Warsaw (1968)

[188] McConnell, R., Zhang, H., Hu, J., Ćuk, S., Vuletić, V.: Entanglement with negative Wigner function of almost 3,000 atoms heralded by one photon. Nature **519**(7544), 439–442 (2015)

[189] McKenzie, K., Shaddock, D.A., McClelland, D.E., Buchler, B.C., Lam, P.K.: Experimental Demonstration of a Squeezing-Enhanced Power-Recycled Michelson Interferometer for Gravitational Wave Detection. Phys. Rev. Lett. **88**, 231102 (2002)

[190] Meise, R., Vogt, D.: Introduction to Functional Analysis. Oxford University Press, Oxford (1997)

[191] Merkel, S.T., Jessen, P.S., Deutsch, I.H.: Quantum control of the hyperfine-coupled electron and nuclear spins in alkali-metal atoms. Phys. Rev. A **78**, 023404 (2008)

[192] Messiah, A.: Quantum mechanics, vol. I. North-Holland, Amsterdam (1961)

[193] Monz, T., Schindler, P., Barreiro, J.T., Chwalla, M., Nigg, D., Coish, W.A., Harlander, M., Hänsel, W., Hennrich, M., Blatt, R.: 14-qubit entanglement: Creation and coherence. Phys. Rev. Lett. **106**(13), 130506 (2011)

[194] Moya-Cessa, H., Knight, P.L.: Series representation of quantum-field quasiprobabilities. Phys. Rev. A **48**(3), 2479 (1993)

[195] Moyal, J.E.: Quantum mechanics as a statistical theory. Proc. Camb. Phil. Soc. **45**, 99–124 (1949)

[196] Newman, E.T., Penrose, R.: Note on the Bondi-Metzner-Sachs group. J. Math. Phys. **7**(5), 863–870 (1966)

[197] Nielsen, M.A., Chuang, I.L.: Quantum computation and quantum information. Cambridge University Press, Cambridge, UK (2000)

[198] Nolte, D.D.: The tangled tale of phase space. Phys. Today **63**(4), 33–38 (2010)

[199] Ohmi, T., Machida, K.: Bose-Einstein condensation with internal degrees of freedom in alkali atom gases. J. Phys. Soc. Jpn. **67**(6), 1822–1825 (1998)

[200] Okamoto, T., Hu, W.: Cosmic microwave background lensing reconstruction on the full sky. Phys. Rev. D **67**(8), 083002 (2003)

[201] Oliveira, I., Sarthour Jr, R., Bonagamba, T., Azevedo, E., Freitas, J.C.: NMR quantum information processing. Elsevier, Amsterdam (2011)

[202] Opatrnỳ, T., Bužek, V., Bajer, J., Drobnỳ, G.: Propensities in discrete phase spaces: Q function of a state in a finite-dimensional Hilbert space. Phys. Rev. A **52**(3), 2419–2428 (1995)

[203] Orús, R.: A practical introduction to tensor networks: Matrix product states and projected entangled pair states. Ann. Phys. **349**, 117–158 (2014)

[204] Paris, M., Řeháček, J. (eds.): Quantum State Estimation. Springer, Berlin (2004)

[205] Perelomov, A.: Generalized Coherent States and Their Applications. Springer, Berlin (2012)

[206] Philp, D.J., Kuchel, P.W.: A way of visualizing NMR experiments on quadrupolar nuclei. Concepts Magn. Reso. A **25A**, 40–52 (2005)

[207] Pines, A., Vega, S., Ruben, D.J., Shattuck, T.W., Wemmer, D.E.: Double quantum NMR in solids. In: R. Blinc, G. Lahajnar (eds.) Magnetic resonance in condensed matter: recent developments, proceedings of the IVth Ampere international summer school, Pula, Yugoslavia, pp. 127–179. University of Ljubljana (1976)

[208] Plancherel, M.: Beweis der Unmöglichkeit ergodischer mechanischer Systeme. Annalen der Physik **347**(15), 1061–1063 (1913)

[209] Racah, G.: Theory of Complex Spectra II. Phys. Rev. **62**, 438–462 (1942)

[210] Rae, A.: Quantum mechanics, 5th edn. Taylor & Francis, Boca Raton, FL (2008)

[211] Reed, M., Simon, B.: Methods of Modern Mathematical Physics I: Functional Analysis. Academic Press, San Diego (1980)

[212] Reinecke, M., Seljebotn, D. S.: Libsharp - spherical harmonic transforms revisited. Astron. Astrophys. **554**, A112 (2013)

[213] Revzen, M., Mello, P.A., Mann, A., Johansen, L.M.: Bell's inequality violation with non-negative Wigner functions. Phys. Rev. A **71**, 022103 (2005)

[214] Riedel, M.F., Böhi, P., Li, Y., Hänsch, T.W., Sinatra, A., Treutlein, P.: Atom-chip-based generation of entanglement for quantum metrology. Nature **464**, 1170–1173 (2010)

[215] Riofrí, C.A., Gross, D., Flammia, S.T., Monz, T., Nigg, D., Blatt, R., Eisert, J.: Experimental quantum compressed sensing for a seven-qubit system. Nat. Commun. **8**, 15305 (2017)

[216] Rosenthal, A.: Beweis der Unmöglichkeit ergodischer Gassysteme. Ann. Phys. **347**(14), 796–806 (1913)

[217] Royer, A.: Wigner function as the expectation value of a parity operator. Phys. Rev. A **15**(2), 449–450 (1977)

[218] Royer, A.: Measurement of quantum states and the Wigner function. Found. Phys. **19**(1), 3–32 (1989)

[219] Royer, A.: Phase states and phase operators for the quantum harmonic oscillator. Phys. Rev. A **53**, 70–108 (1996)

[220] Rudin, W.: Principles of Mathematical Analysis. McGraw-Hill, New York (1976)

[221] Rundle, R.P., Mills, P.W., Tilma, T., Samson, J.H., Everitt, M.J.: Simple procedure for phase-space measurement and entanglement validation. Phys. Rev. A **96**(2), 022117 (2017)

[222] Rundle, R.P., Tilma, T., Samson, J.H., Dwyer, V.M., Bishop, R.F., Everitt, M.J.: A general approach to quantum mechanics as a statistical theory (2017)

[223] Sakurai, J.J.: Modern Quantum Mechanics, rev. edn. Addison-Wesley, Reading (1994)

[224] Sanctuary, B.C., Halstead, T.K.: Multipole NMR. Adv. Opt. NMR Reson. **15**, 97–161 (1991)

[225] Schachenmayer, J., Pikovski, A., Rey, A.M.: Many-body quantum spin dynamics with Monte Carlo trajectories on a discrete phase space. Phys. Rev. X **5**(1), 011022 (2015)

[226] Schervish, M.J.: Theory of Statistics. Springer, New York (1995)

[227] Schleich, W.P.: Quantum Optics in Phase Space. Wiley-VCH, Berlin (2001)

[228] Schmied, R., Treutlein, P.: Tomographic reconstruction of the Wigner function on the Bloch sphere. New J. Phys. **13**, 065019 (2011)

[229] Schnabel, R.: Squeezed states of light and their applications in laser interferometers. Phys. Rep. **684**, 1–51 (2017)

[230] Schollwöck, U.: The density-matrix renormalization group in the age of matrix product states. Ann. Phys. **326**(1), 96–192 (2011)

[231] Schrödinger, E.: Quantisierung als eigenwertproblem. Ann. Phys. **385**(13), 437–490 (1926)

[232] Schroeck Jr, F.E.: Quantum mechanics on phase space. Springer, Dordrecht (2013)

[233] Schwemmer, C., Knips, L., Richart, D., Weinfurter, H., Moroder, T., Kleinmann, M., Gühne, O.: Systematic errors in current quantum state tomography tools. Phys. Rev. Lett. **114**(8), 080403 (2015)

[234] Schwinger, J.: On Angular Momentum. In: L.C. Biedenharn, H. Van Dam (eds.) Quantum Theory of Angular Momentum, pp. 229–279. Academic Press, New York (1965)

[235] Seljak, U., Zaldarriaga, M.: Signature of gravity waves in the polarization of the microwave background. Phys. Rev. Lett. **78**(11), 2054 (1997)

[236] Silva, G.B., Glancy, S., Vasconcelos, H.M.: Investigating bias in maximum-likelihood quantum-state tomography. Phys. Rev. A **95**(2), 022107 (2017)

[237] Smithey, D.T., Beck, M., Raymer, M.G., Faridani, A.: Measurement of the Wigner distribution and the density matrix of a light mode using optical homodyne tomography: Application to squeezed states and the vacuum. Phys. Rev. Lett. **70**, 1244–1247 (1993)

[238] Spekkens, R.W.: Negativity and contextuality and equivalent notions of nonclassicality. Phys. Rev. Lett. **101**, 020401 (2008)

[239] Steffens, A., Riofrí, C.A., McCutcheon, W., Roth, I., Bell, B.A., McMillan, A., Tame, M.S., Rarity, J.G., Eisert, J.: Experimentally exploring compressed sensing quantum tomography. Quantum Sci. Technol. **2**, 025005 (2017)

[240] Stenger, J., Inouye, S., Stamper-Kurn, D., Miesner, H.J., Chikkatur, A., Ketterle, W.: Spin domains in ground state spinor Bose-Einstein condensates. Nature **396**, 345–348 (1998)

[241] Stockton, J.K., Geremia, J.M., Doherty, A.C., Mabuchi, H.: Characterizing the entanglement of symmetric many-particle spin-1/2 systems. Phys. Rev. A **67**(2), 022112 (2003)

[242] Stratonovich, R.: A gauge invariant analog of the Wigner distribution. Sov. Phys. D **1**, 414–418 (1956)

[243] Stratonovich, R.L.: On distributions in representation space. J. Exptl. Theoret. Phys. (U.S.S.R.) **31**, 1012–1020 (1956)

[244] Strobel, H., Muessel, W., Linnemann, D., Zibold, T., Hume, D.B., Pezzè, L., Smerzi, A., Oberthaler, M.K.: Fisher information and entanglement of non-Gaussian spin states. Science **345**(6195), 424–427 (2014)

[245] Suess, D., Rudnicki, Ł., Gross, D., Maciel, T.O.: Error regions in quantum state tomography: computational complexity caused by geometry of quantum states. New J. Phys. **19**, 093013 (2017)

[246] Tajima, N.: Analytical formula for numerical evaluations of the Wigner rotation matrices at high spins. Phys. Rev. C **91**, 014320 (2015)

[247] Thorne, K.S.: Multipole expansions of gravitational radiation. Rev. Mod. Phys. **52**(2), 299 (1980)

[248] Tilma, T., Everitt, M.J., Samson, J.H., Munro, W.J., Nemoto, K.: Wigner functions for arbitrary quantum systems. Phys. Rev. Lett. **117**(18), 180401 (2016)

[249] Tilma, T., Nemoto, K.: $SU(N)$-symmetric quasi-probability distribution functions. J. Phys. A **45**, 015302 (2012)

[250] Tóth, G., Wieczorek, W., Gross, D., Krischek, R., Schwemmer, C., Weinfurter, H.: Permutationally invariant quantum tomography. Phys. Rev. Lett. **105**(25), 250403 (2010)

[251] Treps, N., Grosse, N., Bowen, W.P., Fabre, C., Bachor, H.A., Lam, P.K.: A quantum laser pointer. Science **301**(5635), 940–943 (2003)

[252] Usha Devi, A.R., Shudha, Rajagopal, A.K.: Majorana representation of symmetric multiqubit states. Quantum Inf. Process. **11**(3), 685–710 (2012)

[253] Várilly, J.C., Garcia-Bondía, J.M.: The Moyal representation for spin. Ann. Phys. **190**, 107–148 (1989)

[254] Varshalovich, D.A., Moskalev, A.N., Khersonskii, V.K.: Quantum Theory of Angular Momentum. World Scientific, Singapore (1988)

[255] Von Neumann, J.: Wahrscheinlichkeitstheoretischer Aufbau der Quantenmechanik. Nachrichten von der Gesellschaft der Wissenschaften zu Göttingen, Mathematisch-Physikalische Klasse **1927**, 245–272 (1927)

[256] Wallman, J.J., Bartlett, S.D.: Non-negative subtheories and quasiprobability representations of qubits. Phys. Rev. A **85**, 062121 (2012)

[257] Wandelt, B.D., Górski, K.M.: Fast convolution on the sphere. Phys. Rev. D **63**, 123002 (2001)

[258] Werner, R.: Quantum harmonic analysis on phase space. J. Math. Phys. **25**(5), 1404–1411 (1984)

[259] Weyl, H.: Quantenmechanik und Gruppentheorie. Z. Phys. **46**, 1–33 (1927)

[260] Weyl, H.: Gruppentheorie und Quantenmechanik, 2nd edn. Hirzel, Leipzig (1931). English translation in [261]

[261] Weyl, H.: The theory of groups & quantum mechanics, 2nd edn. Dover Publ., New York (1950)

[262] Wigner, E.: On the quantum correction for thermodynamic equilibrium. Phys. Rev. **40**(5), 749 (1932)

[263] Wootters, W.K.: A Wigner-function formulation of finite-state quantum mechanics. Ann. Phys. **176**(1), 1–21 (1987)

[264] Wurtz, J., Polkovnikov, A., Sels, D.: Cluster truncated Wigner approximation in strongly interacting systems. Ann. Phys. **395**, 341–365 (2018)

[265] Xiao, M., Wu, L.A., Kimble, H.J.: Precision measurement beyond the shot-noise limit. Phys. Rev. Lett. **59**, 278–281 (1987)

[266] Zachos, C.K., Fairlie, D.B., Curtright, T.L.: Quantum Mechanics in Phase Space: An Overview with Selected Papers. World Scientific, Singapore (2005)

[267] Zaldarriaga, M., Seljak, U.: All-sky analysis of polarization in the microwave background. Phys. Rev. D **55**(4), 1830 (1997)

[268] Zavatta, A., Parigi, V., Bellini, M.: Experimental nonclassicality of single-photon-added thermal light states. Phys. Rev. A **75**(5), 052106 (2007)

[269] Zavatta, A., Viciani, S., Bellini, M.: Quantum-to-classical transition with single-photon-added coherent states of light. Science **306**(5696), 660–662 (2004)

[270] Zavatta, A., Viciani, S., Bellini, M.: Single-photon excitation of a coherent state: catching the elementary step of stimulated light emission. Phys. Rev. A **72**(2), 023820 (2005)

[271] Zueco, D., Calvo, I.: Bopp operators and phase-space spin dynamics: application to rotational quantum Brownian motion. J. Phys. A **40**(17), 4635 (2007)